UNIVERSITA' DEGLI STUDI DI PARMA

Dottorato di ricerca in Scienze della Terra

Ciclo XXIII

Eocene-Oligocene paleoceanography of the subantarctic South Atlantic: Calcareous Nannofossil reconstructions of temperature, nutrient, and dissolution history

Coordinatore:
Chiar.mo Prof. Renzo Valloni

Tutor:
Chiar.ma Prof. ssa Giuliana Villa

Dottoranda: Laura Pea

Ai miei genitori e alla nonna Teresa

Contents

Abstract (English)

Extremely warm 'Greenhouse' climates of the early Eocene came to a gradual end during a prolonged interval of global climatic deterioration in the middle-to-late Eocene (~49 to 34 Ma), resulting in the eventual initiation of an 'Icehouse' climate state in the early Oligocene. This global climatic transition represents one of the most significant climate changes of the Cenozoic and is punctuated both by prominent cooling steps and by several transient warming and cooling phases superimposed on the long-term cooling trend. This dissertation focuses on two key periods of accelerated climatic change during this interval: the Middle Eocene Climatic Optimum (MECO) (~40 Ma) and the Eocene-Oligocene Transition (EOT) (~34 Ma). The MECO is a transient (500 kyr) warming event recorded worldwide by foraminiferal oxygen isotopes and is associated with deep-ocean acidification. In contrast, the EOT is associated with expansion of Antarctic ice sheets, global cooling, sea level fall, marine and terrestrial biotic turnover, and deepening of the calcite compensation depth (CCD). Calcareous nannofossil assemblages are used to investigate both surface-water environments and deep-sea dissolution across these events at drill sites in the South Atlantic Ocean. Paleoecological study of the nannofossil assemblages is employed to reconstruct temperature and nutrient changes at the sea surface, and analysis of preservation state of individual nannofossil taxa is used to constrain the history of CCD fluctuations.

In Chapter 2, the MECO interval was studied at Ocean Drilling Program (ODP) Site 702 (50°S; Islas Orcadas Rise) using quantitative analysis of calcareous nannofossil assemblages in the time interval between 43.5 and 39.5 Ma. Biostratigraphic analysis shows that the MECO event corresponds to significant nannofossil turnover, with five biostratigraphic events occurring in conjunction with warming. Paleoecological interpretation of the assemblages also indicate that temperature and nutrient conditions of surface waters at this site varied frequently and rapidly during the MECO, and a shift from oligotrophic to eutrophic conditions occurred in correspondence to peak warming. Cooling at the termination of the MECO marks the return to oligotrophic conditions following the warming event. In the long-term record prior to the MECO, nannofossil assemblages also record a marked sea-surface warming between 41.5 and 42.5 Ma (designated as the *'C19r warming event'*), which is not identified in the bulk oxygen isotope record. To verify that assemblages were not biased by dissolution within the studied section at Site 702, selected taxa were used to calculate dissolution and preservation indices. This analysis suggests that strong sea-floor dissolution did not affect the assemblages which therefore faithfully record surface-water changes at this site.

In Chapter 3, high-resolution quantitative nannofossil assemblage analysis was carried out on late Eocene–late Oligocene (35.5–26.5 Ma) sediments at ODP Site 1090 (42°S; Agulhas Ridge), with the primary goal of reconstructing paleoceanographic changes through the Eocene-Oligocene transition. Eleven biostratigraphic events and several distinct climatic phases are recognized within the study interval. Surface waters initially cooled between 35.5 and 34.25 Ma and then warmed between 34.15 and 33.8 Ma. Following this warming interval, marked changes in nannofossil assemblages are recorded both at 33.6 Ma, interpreted to indicate an increase in nutrient availability, and at ~30 Ma, when the opportunist species *Cyclicargolithus floridanus*

became dominant. Throughout the study interval at Site 1090, climatic variations recorded by nannofossil are interpreted as a response to changes in the influence of different water masses sourced from the Indian Ocean or the Pacific Ocean, or to the influence of latitudinal movements of frontal positions. An intense dissolution level, previously identified at other Southern Ocean sites, is interpreted between 28.0 and 28.8 Ma, which is may be related to a regional shoaling of the CCD in the South Atlantic.

One of the primary characteristics of the EOT interval is a worldwide deepening of the CCD, interpreted based on the increase in carbonate accumulation at deep-sea sites. In the South Atlantic, the CCD is interpreted to have deepened by ~1 km, but a detailed CCD history has not been developed across the EOT interval in this region. For this reason, quantitative analysis of calcareous nannofossil assemblages was carried out across the EOT at ODP Site 1090 (42°S). These results are reported in Chapter 4. The goals of this work were to: (1) to assess the degree of dissolution affecting nannofossil assemblages; (2) to use the nannofossil dissolution signal as proxy for CCD variation; and (3) to characterize surface-water temperature and nutrient changes. Indices of dissolution were calculated using the preservation state of two common taxa (*Coccolithus pelagicus* and *Reticulofenestra umbilicus* group) and the characteristics of the entire assemblage. Comparison between these indices and carbonate content shows a striking correspondence, indicating that dissolution was a major factor controlling carbonate sedimentation and assemblage composition in the EOT interval at this site. Additionally, a good correspondence is noted between carbonate content and *Blackites* and *Clausicoccus* abundance, suggesting that dissolution is also determinant in controlling the stratigraphic distribution of these taxa. Variation in the calculated indices and carbonate content are interpreted to reflect CCD fluctuations. Several high-magnitude CCD oscillations are recorded in the latest Eocene, which are followed by a CCD deepening in the earliest Oligocene in correspondence with oxygen isotope Step 2. An intense dissolution interval is observed in the latest Eocene immediately prior to oxygen isotope Step 1, and an interval of carbonate dilution is interpreted just prior to oxygen isotope Step 2. A selection of well-preserved samples was used for the paleoecological interpretation of the assemblages, and a major change is observed near the E/O boundary (~33.6 Ma), which most likely reflects an increase in sea-surface nutrient availability. This event is followed by a gradual increase in fertility associated with cooling that culminates at Step 2 in the earliest Oligocene.

Chapter 5 of this dissertation reports the preliminary results of Integrated Ocean Drilling Program (IODP) Expedition 317, *'Canterbury Basin Sea Level (New Zealand), Global and Local Controls on Continental Margin Stratigraphy'*, in which I participated as a nannofossil micropaleontologist. One of the central objectives of the expedition was to understand the Eocene to Recent climatic evolution of the southern Pacific Ocean – a theme that complements the general topic of paleoclimatology in the high southern latitudes treated in my other doctoral projects. Shipboard biostratigraphic analysis of nannofossil assemblages enabled the construction of detailed age models for the drilled sequences, and changes in assemblage characteristics, such as abundance and preservation, provide new information for interpreting the sedimentary records and sequence stratigraphy of the New Zealand continental margin.

Abstract (Italiano)

Il regime climatico estremamente caldo che caratterizza l'Eocene inferiore (*Greenhouse*) termina nell'Eocene medio-superiore (~49-34 Ma) ad opera di un lungo trend di raffreddamento che culmina, nell'Oligocene inferiore, nella transizione ad un regime di *Icehouse*. Questa transizione climatica globale è punteggiata sia da intense fasi di deterioramento climatico a carattere più permanente, sia da temporanei eventi di riscaldamento/raffreddamento sovraimposti al lungo trend di raffreddamento. Questa tesi di dottorato è focalizzata su due periodi ritenuti particolarmente critici di questa transizione climatica: l'optimum climatico dell'Eocene medio (MECO) (~40) Ma, e la Transizione Eocene-Oligocene (EOT) (~34 Ma). Il MECO rappresenta un periodo di temporaneo riscaldamento globale (500 kyr) registrato nei record isotopici dell'ossigeno misurato sui gusci dei foraminiferi, ed è associato ad acidificazione degli oceani. Al contrario, la EOT è associata all'espansione della calotta polare antartica, ad un raffreddamento globale, alla caduta del livello del mare, a forti variazioni nella flora e fauna sia terrestre che marina ed all' abbassamento della profondità di compensazione del carbonato (CCD).

Il MECO è stato studiato al Site Ocean Drilling Program (ODP) 702 (50°S) (Capitolo 2) attraverso un'analisi quantitativa delle associazioni a nannofossili calcarei in un intervallo di tempo che va da ~43.5 a 39.5 Ma. L'analisi biostratigrafica ha messo in luce che il MECO corrisponde ad un turnover dei nannofossili calcarei, con cinque eventi biostratigrafici riconosciuti. Inoltre, l'analisi paleoecologica delle associazioni ha rivelato che, durante il MECO, le caratteristiche delle acque superficiali variano frequentemente e rapidamente, ed un passaggio da condizioni oligotrofiche ad eutrofiche avviene in corrispondenza del massimo riscaldamento. Il raffreddamento che segna la fine del MECO vede il ritorno ad acque oligotrofiche. Oltre al MECO, le associazioni a nannofossili hanno individuato un evento di riscaldamento delle acque superficiali tra 41.5 e 42.5 Ma (evento denominato qui '*C19r warming event'*). Per verificare che, lungo la sezione studiata, le associazioni non fossero state impoverite dalla dissoluzione, alcuni taxa selezionati sono stati utilizzati per calcolare degli indici di dissoluzione/preservazione, il cui confronto ha confermato che una debole dissoluzione può aver agito sulle associazioni, ma senza comprometterne la composizione e le caratteristiche.

Nel Capitolo 3 sono discussi i risultati dell'analisi quantitativa delle associazioni a nannofossili calcarei svolta su sedimenti datati 35.5-26.5 Ma (Eocene superiore-Oligocene superiore) provenienti dal Site ODP 1090 (42°S). Questa analisi ha avuto come obiettivo principale la ricostruzione delle variazioni paleoceanografiche durante la transizione Eocene-Oligocene. Attraverso l'analisi biostratigrafica sono stati riconosciuti undici eventi e attraverso l'analisi paleoecologica sono state identificate diverse fasi climatiche. Acque superficiali fresche dominano tra 35.5 e 34.15 Ma, sostituite poi da acque più calde e eutrofiche da 34.15 a 33.8 Ma. Un sensibile aumento nella disponibilità di nutrienti è registrato a 33.6 Ma (in prossimità del limite Eocene/Oligocene), ed è seguito a circa 30 Ma (Oligocene inferiore) da un evento di completa riorganizzazione delle associazioni, in corrispondenza del quale *Cyclicargolithus floridanus* diventa dominante. Le variazioni delle associazioni a nannofossili al Site 1090 sono state interpretate come risposta all'influsso di diverse masse d'acqua provenienti dall'Oceano

Indiano o dal Pacifico, o come risposta al movimento latitudinale dei fronti oceanici. Un livello a dissoluzione molto intensa è stato identificato tra 28.8 e 28.0 Ma, prodotto o da un temporaneo innalzamento della CCD o dall'effetto di masse d'acqua oceaniche sottosature in carbonato.

Una delle principali caratteristiche dalla EOT è il marcato approfondimento della CCD, identificato a livello globale dall'aumento della deposizione di carbonato nei sites oceanici profondi. Nonostante l'abbassamento della CCD sia stimato essere di circa 1 km nell'Oceano Atlantico, l'evoluzione della CCD in questa regione è ancora poco chiara. Per questo motivo, un'analisi quantitativa delle associazioni a nannofossili calcarei è stata svolta al Site 1090 (42°S) (Capitolo 4), con gli obiettivi di: 1) valutare il grado di dissoluzione che ha agito sulle associazioni; 2) usare il segnale di dissoluzione dei nannofossili come indicatori delle variazioni della CCD; 3) capire le variazioni delle caratteristiche delle acque superficiali durante la EOT. A tal fine, sono stati calcolati indici di dissoluzione basati sullo stato di preservazione di due comuni taxa (*Coccolithus pelagicus* e *Reticulofenestra umbilicus* group) e sulle caratteristiche dell'intera associazione. Il confronto tra questi indici e il contenuto di carbonato mostra una straordinaria corrispondenza, dimostrando come la dissoluzione sia il fattore che, a questo site, controlla la sedimentazione carbonatica e lo stato di preservazione delle associazioni. Inoltre, il contenuto di carbonato e le abbondanze relative di *Blackites* e *Clausicoccus* mostrano una ottima corrispondenza, suggerendo che la dissoluzione è il fattore di controllo nella distribuzione dei due taxa. Le variazione degli indici di dissoluzione e del contenuto di carbonato sono state interpretate come risposta alle fluttuazioni della CCD: la CCD oscilla marcatamente nell'Eocene superiore e si approfondisce nell'Oligocene inferiore in corrispondenza dello shift isotopico ($\delta^{18}O$) Step 2. Gli indici di dissoluzione hanno inoltre identificato un intervallo di forte dissoluzione appena prima dello shift isotopico Step 1 (Eocene superiore) e un intervallo di diluizione carbonatica appena prima dello Step 2 (Oligocene inferiore). Una selezione di campioni ben preservati è stata usata per l'interpretazione paleoecologica delle associazioni la quale ha identificato un momento di forte cambiamento in prossimità del limite Eocene/Oligocene (~33.6 Ma), interpretato come una risposta all'aumento della fertilità delle acque. Questo evento è seguito da un graduale aumento della fertilità e da raffreddamento che culmina allo Step 2, a seguito del quale, nell'Oligocene inferiore, le associazioni indicano acque fredde e ricche di nutrienti.

Un capitolo di questa tesi di dottorato è dedicato ai risultati preliminari della spedizione Integrated Ocean Drilling Program (IODP) 317, *Canterbury Basin Sea Level (New Zealand), Global and Local Controls on Continental Margin Stratigraphy*, a cui ho partecipato come Micropaleontologa per i Nannofossili Calcarei tra novembre 2009 e gennaio 2010. Uno degli obiettivi della spedizione è stato di capire l'evoluzione climatica dell'Oceano Pacifico meridionale dall'Eocene al Recente, argomento che ben si inquadra nel generale tema di paleoclimatologia delle alte latitudini meridionali trattato nel mio dottorato. L'analisi biostratigrafica tramite i nannofossili calcarei ha permesso un ottimo controllo dell'età delle sequenze carotate e l'analisi paleoecologica preliminare ha fornito informazioni utili all'interpretazione del record sedimentario del margine della Nuova Zelanda.

Chapter 1

Introduction

This work belongs to a series of studies aimed to understand the climatic evolution of the Southern Ocean during the Paleogene.
Analyses of calcareous nannofossil assemblages showed to be a precious tool for the comprehension of sea surface characteristic changes since the Mesozoic (e.g. Aubry, 1992; Haq and Lohmann, 1976; Haq et al., 1977; Wei and Wise, 1990a; Wise et al., 1982) and now nannofossils are considered reliable paleo-climatic proxies.
The importance of studying climatic changes in the Paleogene is twofold: first of all, the Paleogene is a generally warmer period compared to today and can be considered as the equivalent of the future greenhouse conditions, if the process of human-induced global warming will not show a reversal. Knowing the climatic conditions and factors determining past warm climates may help to provide data for modeling of future scenario and thus to face better the future climatic regime. Furthermore, during the Paleogene, the passage from the Greenhouse to the Icehouse worlds (Miller et al., 1991) (Fig. 1), occurs, and is characterized by a shift from a generally warmer climate to globally cooler conditions, controlled by the presence of an Antarctic ice-sheet.

Calcareous nannofossil assemblage studies can contribute significantly to paleoclimatic analysis for several reasons: they play a determinant role in the carbon cycle and in the sedimentation of marine carbonates, ultimately controlling the amount of atmospheric CO_2; they are optimal paleoecological indicators, especially in terms of temperature and fertility variations; their descendants (coccolithophores) represent one of the most abundant phytoplankton group in the oceans, and the comparison between ancient and current nannoplankton characteristics can work as a link between past and present climatic conditions. As a consequence, studying nannofossil assemblage characteristics in a past greenhouse world could help to predict the reactions of living coccolithophores to the gradual increase in atmospheric CO_2, the associated temperature increase and ocean acidification. Predictions for modern global warming include the establishment of

more oligotrophic conditions and the increase of nannoplankton compared to diatom productivity (Cermeno et al., 2008). On the other hand, sea water acidification could strongly affect the ability of carbonate organisms to calcify their tests (Doney et al., 2009; Feely et al., 2004). If this happened, the global carbon cycle, the sedimentation pattern in the oceans, and current chemical oceanic conditions would be disrupted (Feely et al., 2009).

The analysis of Paleogene climatic variations is particularly important in the Southern Ocean (Fig. 2), within the oceanic belt surrounding Antarctic continent. Such a relevance comes from the fact that global cooling, started in the early Paleogene and continued during the Cenozoic (e.g. Zachos et al., 2001) (Fig. 1), is controlled by tectonic and paleoceanographic changes involving Antarctica and nearby continents (e.g. Lawver and Gahagan, 2003). Even if the triggering mechanisms of the global cooling are still debated between opening of the circumpolar passages (e.g. Lagabrielle et al., 2009; Lawver and Gahagan, 2003) and atmospheric CO_2 decrease (Pagani et al., 2005; Pearson and Palmer, 2000a), certainly the onset of a permanent ice-sheet in Antarctica in the late Eocene- early Oligocene had a major role in the reorganization of the global oceanographic setting and global climate (e.g. Zachos et al., 2001).

Several studies have shown that the transition between the Greenhouse and the Icehouse was not linear, but punctuated by transient warming phases, the so-called *hyperthermals* (e.g. Bohaty et al., 2009; Lourens et al., 2005; Sluijs et al., 2007a; Sluijs et al., 2007b; Zachos et al., 2008; Zachos et al., 2006), occurring the in the early-middle Eocene (Fig. 1). The Paleogene cooling has its major expression during the Eocene-Oligocene Transition (EOT) (~34 Ma) (Coxall and Pearson, 2007; Lear et al., 2008), which includes the early Oligocene isotopic Oi-1 event (Miller et al., 1991; Zachos et al., 2001), accordingly interpreted as linked to the formation of a permanent ice-sheet in Antarctica (Kennett et al., 1975; e.g. Liu et al., 2004; Miller et al., 2009; Zachos et al., 2001). The EOT is a period of global climatic reorganization associated to marine biotic turnover (Aubry, 1992; Dunkley Jones et al., 2008; Funakawa and Nishi, 2008; Pearson et al., 2008; Suto, 2006; Villa et al., 2008; Wade and Pearson, 2008), terrestrial faunal and floral changes (e.g. Francis, 1999; Hooker et al., 2004; Jaramillo et al., 2006),

global cooling (Lear et al., 2008; Liu et al., 2009; Miller et al., 2009; Zachos et al., 2001), reorganization of the carbon cycle (Coxall et al., 2005; Diester-Haass and Zahn, 1996; Merico et al., 2008; Shackleton and Kennett, 1975; Zachos et al., 2001), increase of productivity (Anderson and Delaney, 2005; Diester-Haass and Zachos, 2003; Diester-Haass and Zahn, 1996; Salamy and Zachos, 1999), CCD deepening (Coxall et al., 2005; Rea and Lyle, 2005; Van Andel, 1975) and sea-level fall (e.g. Miller et al., 2008; Miller et al., 1991; Pekar et al., 2002).

This Ph.D. dissertation focuses on two important climatic phases characterizing the Paleogene global climatic evolution: the Middle Eocene Climatic Optimum (MECO) (~40 Ma) (Bohaty and Zachos, 2003; Bohaty et al., 2009) and the Eocene-Oligocene Transition (EOT) (~34 Ma) (Coxall and Pearson, 2007) (Figs. 1, 3).
The two studied ODP Sites, 702 and 1090, are both located in the Subantartic sector of the South Atlantic, at 50 and 42°S, respectively (Fig. 2). Considering the geographic vicinity of the two locations, the Paleogene (paleo-) oceanographic setting of the two sites was similar, and the climatic evolution interpreted from the late middle Eocene to the late Oligocene can be thought as representative of the history of the surface waters of the subantarctic South Atlantic in this time interval.

Besides the introduction (this chapter), this dissertation includes 4 Chapters: Chapter 2 pertains to the sea surface history of the late middle Eocene at Site 702 (Islas Orcadas Rise, 50°S), as recorded by calcareous nannofossils. Chapter 3 deals with the analysis of calcareous nannofossil assemblage changes from the late Eocene to the late Oligocene, at ODP Site 1090 (Agulhas Ridge, 50°S). In Chapter 4 we tested and confirmed the reliability of calcareous nannofossil fragmentation as a dissolution and CCD proxy. Chapter 5 pertains to the preliminary results of IODP Expedition 317- Canterbury Basin Sea Level- Local and Global Controls on Continental margin stratigraphy. Despite the participation on this cruise is not strictly part of my Ph.D. program, I have decided to include in this dissertation a short chapter about background, goals, preliminary results and some personal remarks about the expedition. The reasons for this choice were several: first of all, being involved in a scientific expedition as a nannofossil paleontologist and being part of an international Science Party was a beautiful and

useful experience both professionally and personally. Secondly, this experience allowed me to work in a high profile scientific environment, not strictly academic. Thirdly, working as an Italian participant onboard R/V *Joides Resolution* is nowadays an unique opportunity, as only rarely IODP projects are open to the Italian research community (due to the cuts of funding). Furthermore, I spent considerable time to get ready for the Expedition, without compromising the development of my Ph.D. projects. However, the main reason why I decided to include a chapter about my participation in Expedition 317 is that I want to share it with anyone will read this dissertation: it was a really striking scientific experience because doing frontline research is not comparable to anything else, and I consider this Expeditions as an outstanding component of my growth as a young scientist.

Conclusive remarks are discussed in Chapter 6.

Hereinafter, a more detailed introduction about themes involved in this dissertation is given, including 1) the global climatic evolution of the Paleogene, 2) Calcareous Nannofossils and their importance in biostratigraphic and paleoceanographic studies, and 3) the Southern Ocean and its role in driving global climate.

1. Paleogene climatic evolution

The very first oxygen isotope record was compiled by Emiliani and Edwards (1953) from Pleistocene marine sediments. The first isotopic compilation that aimed to provide a global climatic picture was proposed by Shackleton and Kennett (1975); later, Miller and Katz (1987) reported Oligocene to Miocene records from the Atlantic Ocean. Afterwards, other isotopic compilations followed (Matthews and Poore, 1981; Savin et al., 1975; Shackleton and Kennett, 1975) until the *Zachos et al.* compilation was published in 2001 (Zachos et al., 2001) and improved in 2008 (Zachos et al., 2008) (Fig. 1) which is now considered the reference point for Cenozoic paleoclimatic studies and tends to be a global representation of climatic changes. Clearly, other studies at different locations are absolutely necessary to highlight all the numerous paleoclimatic and paleoceanographic factors that isotopic records cannot provide. The last mentioned compilation (Fig. 1) shows that Paleogene climate, as well as all Cenozoic climate, is characterized by a strong variability, which is expressed, based on their duration, by

events occurring in a long-term period (10^6-10^7 years), short-term or orbital-scale (10^4-10^5 years), or as aberrations (10^4-10^5 years), as defined by Zachos et al. (2001). The compilation (Fig. 1) is based on oxygen isotopes measured on benthic foraminifera tests from numerous deep sea sites. As deep ocean waters originate at high southern latitudes, temperatures provided by benthic foraminifera in deep oceans, also represent high latitude sea surface temperature. The isotopic record is interpreted exclusively as controlled by temperature from the Paleocene to the late Eocene because no ice sheets were present at poles, and thus no ice-volume effect is recorded in the isotopic signal. Differently, starting from the late Eocene, the isotope record also contains ice-volume effect. The relative importance of temperature and ice volume in controlling isotope record and its variations is still debated, especially through the EOT (e.g. Coxall and Pearson, 2007). Although it is difficult to quantitatively determine temperature and ice volume print, it is widely accepted that the EOT marks a global cooling and the beginning of glaciation in Antarctica (Coxall et al., 2005; DeConto and Pollard, 2003; Kennett, 1977; Lear et al., 2008; Zachos et al., 2001), which has its maximum expression in the Early Oligocene Glacial Maximum (EOGM) (e.g. Liu et al., 2004). Besides the oxygen isotope record, the global compilation of carbon isotope records (Zachos et al., 2001) provides information about carbon cycle, organic and inorganic carbon burial, oceanic circulation and productivity changes (Coxall et al., 2005; Diester-Haass and Zachos, 2003; Peck et al., 2010; Zachos et al., 2008).

As possible causes of the Cenozoic cooling, several hypothesis have been proposed, pertaining different disciplines such as astronomy, plate tectonics, atmosphere and ocean chemistry. Orbital parameter oscillations (Milankovitch parameters: eccentricity, precession and obliquity) affect the amount and the distribution of solar energy on the Earth surface, that acts as external climatic regulator (Mead et al., 1986; Zachos et al., 2001). For years, the most popular theory used to explain the Cenozoic cooling involved the opening of the circumpolar passages, which allowed the formation of the Antarctic Circumpolar Current (AACC) (Kennett, 1977) and the geographical and thermal isolation of the continent, which caused the cooling and the build-up of the ice-sheet on Antarctica (Lagabrielle et al., 2009; Lawver and Gahagan, 2003). This hypothesis suffers from the lack of a precise timing for the opening of the circumpolar passages,

especially of the Drake Passage, between Antarctica and South America. The age of this tectonic event is, as a matter of fact, still uncertain and has been dated middle or late Eocene (Eagles et al., 2006; Livermore et al., 2007; Livermore et al., 2005; Scher and Martin, 2006), Oligocene (Lawver and Gahagan, 2003), or Miocene (Barker, 2001; Barker and Burrell, 1977). The opening of the Tasmanian Seaway to deep water circulation is dated more consistently at ~35.5 Ma (e.g. Kennett and Exon, 2004; Stickley et al., 2004). In addition to the difficulty in timing, a further problem concerns the role that circumpolar passages had in driving the climatic changes during the EOT. In fact, a recent combined sedimentological, geochemical, micropaleontological and magnetostratigraphic work (Stickley et al., 2004) on the East Tasman Plateau highlighted that the opening of the Tasmanian Seaway was accompanied by flowing of warm, and not cold, waters, implying that this tectonic event did not induce cooling in Antarctica, and that, at the EOT, there was no formation of the AACC. Similar results were obtained by modeling simulations (Huber et al., 2004; Huber and Nof, 2006).

The other factor invoked as cause of the Cenozoic cooling is the decrease of atmospheric CO_2 (DeConto and Pollard, 2003; Pagani et al., 2005; Pearson and Palmer, 2000a; Zachos and Kump, 2005). Also this hypothesis suffers from some inconsistencies and limits. First of all, available CO_2 proxies have been found only recently, and high resolution datasets are still limited. Secondly, CO_2 estimates derived from Alkenones show high values also in the early Oligocene (Pagani et al., 2005), which opens doubts about the reliability of this proxy even if discrepancies might derive from the use of different age models. Nevertheless, the climatic picture given by CO_2 variations is in general agreement with other paleoclimatic proxies, such as the oxygen isotope record, supporting gradual diminishing values in the Paleogene (Pagani et al., 2005). Causes of CO_2 decrease can be a reduction of global spreading rates (Berner et al., 1990), an increase in silicate weathering (Raymo et al., 1988) or increased organic carbon burial (Diester-Haass and Zachos, 2003). It is possible that atmospheric carbon dioxide decrease worked either as a trigger for cooling/glaciation or as a positive feedback for the ongoing cooling. Other than gateway opening and atmospheric CO_2 variations, other factors may have played important roles in driving Cenozoic climatic changes, especially at local scale: various types of tectonic mechanisms, such as the Himalayan horogenesis (influencing weathering and the carbon cycle), opening/closing

of other gateway and oceans (e.g. Thetys) (Oberhansli, 1992), affecting ocean circulation and heat distribution on Earth, terrestrial or marine volcanism (hot spots or along plate margin) (e.g. Jicha et al., 2009), usually associated to release of gases, hydrothermal activity, or extraterrestrial impacts (e.g. Vonhof et al., 2000), etc.
Clearly, some or all of these factors may have acted together, being so closely linked one another. For this reason, new paleoclimatic proxies and high-resolution datasets are needed to separate the single signals.

1.1. Eocene climatic variability and the hyperthermals

Global climate in the early Paleogene was much warmer than today and a long warm interval (~51-58 Ma) occurred between about the late Paleocene and the early Eocene (Zachos et al., 2008; Zachos et al., 2001) (Fig. 1). This warm phase is punctuated by several short (<200.000 years) and intense warmer events (Fig. 1), the so called *hyperthermals*: the Paleocene Eocene Thermal Maximum (PETM or Eocene Thermal Maximum 1, ETM1) (~55 Ma) (Dickens, 2000), the Eocene Thermal Maximum 2 (ETM2 or ELMO) (~53.5 Ma) (Lourens et al., 2005; Sluijs et al., 2009), and the Early Eocene Climatic Optimum (EECO) (51-53 Ma) (Lowenstein and Demicco, 2006; Zachos et al., 2001). After the EECO, a cooling trend started, and was interrupted at ~40 Ma by the Middle Eocene Climatic Optimum (MECO) (Bohaty and Zachos, 2003; Bohaty et al., 2009). Beyond these well-known events, other less studied hyperthermals were found at 53.6 Ma (H-2), at 53.3 (I-1), 53.2 Ma (I-2) and at 52.8 Ma (K, X or ETM-3 event). All hyperthermals, belonging to the *aberrations* of Zachos et al (2001), are superimposed on a long-term gradual climatic trend toward the same direction, i.e. these transient warming events occur within a period characterized by a long-term warming tendency. Differently, the MECO event occurs in the middle of a gradual cooling, it is therefore a short-lived climatic reversal (Bohaty and Zachos, 2003; Bohaty et al., 2009).

In this Section my attention focuses on the PETM and on the MECO (object of study of part of this dissertation) and on their comparison. The PETM is the most widely studied among all hyperthermals. The MECO was discovered only seven years ago (Bohaty and Zachos, 2003) and after that, a few studies followed (Bijl et al., 2010; Bohaty et al.,

2009; Edgar et al., 2010; Jovane et al., 2007; Jovane et al., 2010; Luciani et al., 2010; Spofforth et al., 2010).

During the PETM, ocean surface water temperatures increased of 5°C at low latitudes and of 9°C at high latitudes (Kennett and Stott, 1991; Zachos et al., 2003), while deep water temperatures increased of 4-5°C (Thomas and Shackleton, 1996), as indicated by a negative shift of the oxygen isotopes. One of the major characteristics of the PETM is the negative carbon isotope excursion (CIE) (~3 ‰) indicating the release/s of ^{13}C-depleted carbon to the atmosphere and to the ocean, occurring right before the oxygen shift. As source of this light carbon, methane from marine clathrates (Dickens, 2000; Dickens et al., 1997; Dickens et al., 1995) or CO_2 from volcanic activity (Dickens et al., 1998) have been proposed. The PETM is associated with a dissolution event of marine carbonates (Zachos et al., 2005). Possible triggering mechanisms for the release of greenhouse gases (methane or CO_2) is still debated, and it is not clear if the gas release was a cause or a consequence of the warming occurring at the PETM. In fact, it is possible that warming triggered the release of methane or that the methane release (started by some unknown process), triggered the temperature increase. As suggested by Lourens et al. (2005) and Bowen et al. (2006), the fact that hyperthermals occur in phase with orbital cycles, debases the importance of single paleoceanographic or tectonic mechanisms in driving these extreme climatic events.

Terrestrial and marine flora and fauna strongly responded to the PETM: terrestrial mammals straggled among the Northern Hemisphere continents (Bowen et al., 2002; Clyde and Gingerich, 1998), dwarfism of mammals occurred in North America (Smith et al., 2009), terrestrial flora experienced a dispersal toward higher northern latitudes (Wing et al., 2005), a great number of deep-sea benthic foraminifera went extinct (Thomas, 1998; Thomas and Shackleton, 1996), planktonic foraminifera diversified (Kelly et al., 1998; Kelly et al., 1996), and an acme of dinoflagellate cyst *Apectodinium* occurred worldwide (Crouch and Brinkhuis, 2005; Crouch et al., 2003; Crouch et al., 2001).

Calcareous nannofossils revealed that a shift to warmer and more oligotrophic conditions occurred during the PETM at southern high latitudes (Bralower, 2002), that productivity gradient increased between shelf areas and open oceans, with enhanced oligotrophy and eutrophism in the two settings, respectively (Gibbs et al., 2006), that

fertility increased in the Thetys, accompanied by the temporary occurrence of malformed species, the so-called *excursion taxa* (Agnini et al., 2006). Malformed nannofossils were also found at other locations in the Tethys (Kahn and Aubry, 2004), in the South Atlantic (Raffi et al., 2009; Raffi and De Bernardi, 2008) and in the equatorial Pacific (Raffi et al., 2005) and they have been interpreted by the authors as caused by a strong perturbation of the carbon cycle and CO_2 increase.

The MECO is a transient (~500 krs) warming event occurring at ~40 Ma at the base of magnetochron C18n.2n (Bohaty et al., 2009). It was first documented at southern high latitudes (Bohaty and Zachos, 2003) and then identified worldwide at all latitudes (Bohaty et al., 2009; Edgar et al., 2010; Jovane et al., 2007; Luciani et al., 2010; Spofforth et al., 2010). This warming event, interrupting the long-term Paleogene cooling trend (Fig. 1), was recorded by oxygen isotopes measured on benthic foraminifera (Bohaty and Zachos, 2003; Bohaty et al., 2009; Edgar et al., 2010), fine fraction (Bohaty and Zachos, 2003; Bohaty et al., 2009) and bulk sediment (Bohaty et al., 2009; Spofforth et al., 2010) which show a gradual decrease of ~ 1‰ during a period lasting about 500 krs. Peak negative values, corresponding to the maximum warming phase, were reached at ~40 Ma, and were followed by a rapid increase, initiating the *post-MECO cooling phase* (Bohaty et al., 2009). Considering that in the late middle Eocene there were no ice-sheets at poles, the oxygen isotope excursion occurring at the MECO have been interpreted exclusively as a temperature signal, and a warming of ~ 4-6°C of surface and bottom waters was estimated (Bohaty et al., 2009).
The MECO is related to a global water acidification event and CCD shallowing, as interpreted by carbonate content records (Bohaty et al., 2009; Lyle et al., 2005; Tripati et al., 2005). According to Bohaty et al. (2009), acidification only affected sites deeper than 3000 meters in the Atlantic and also shallower sites in the Pacific, indicating that CCD shallowing was more pronounced in the Pacific compared to the Atlantic. As possible cause of the warming and the acidification, Bohaty and Zachos (2003) and Bohaty et al. (2009) proposed a transient increase of atmospheric CO_2, whose origins may be found in an enhanced volcanic activity linked to the North Atlantic rifting or to metamorphic decarbonation processes associated to the formation of the Himalayan chain. The possibility that the warming occurring at the MECO was caused by methane

release and gas hydrates dissociation (proposed for the PETM) has to be ruled out because no significant negative carbon isotope excursion occurs during or prior to this event (Bohaty and Zachos, 2003; Bohaty et al., 2009). The hypothesis of atmospheric pCO_2 increase during this time period as a possible trigger for the warming, has been recently confirmed by the application of organic proxies (the alkenone unsaturation index, UK37′, and the index of tetraethers, TEX86) on sediments from the south-west Pacific (Bijl et al., 2010), partially filling the lack of high-resolution CO_2 records and adding an important contribution to previous lower resolution works for the Eocene (Pagani et al., 2005; Pearson and Palmer, 2000b). In the Bijl et al. work, an increase of 2000 to 3000 ppmv in atmospheric CO_2 was estimated for the middle Eocene. As possible source of CO_2, the metamorphic decarbonation of carbonates, perhaps caused by Himalayan orogenic processes, has been proposed (Bijl et al., 2010), as previously suggested by Bohaty et al. (2009).

Few works are currently available on the marine biotic response to the MECO, also because the middle Eocene has been considered in the past, as a climatically uneventful time interval, and works mainly focused on other periods. As said, the Middle Eocene has lately become matter of interest, and a few works have been published (see references above), concerning mainly planktonic foraminifera (Edgar, 2008; Edgar et al., 2010; Luciani et al., 2010) and dinoflagellate assemblage changes (Bijl et al., 2010). Planktonic foraminifera from the subtropical Atlantic revealed, during the MECO, a shift from warm and oligotrophic waters to warmer and more mesotrophic conditions (Edgar, 2008). A similar climatic change was recorded in the Thetys, where foraminifera assemblage changes indicate an increase in fertility and productivity (Luciani et al., 2010). No calcareous nannofossil *excursion taxa* have been found at the MECO (Chapter 2 of this dissertation).

2. Coccolithophores and Calcareous Nannofossils

Coccolitophores (Calcareous nannoplankton) are a group of marine singled-cell protista of nanometric dimensions. They first appeared, with few species, in the early Triassic and are currently very abundant in surface waters of all oceans. They belong to regnum *Protista*, phylum *Haptophyta*, class *Coccolitophyceae* and order *Coccolitophorales.*

Coccolithophores derive their food supply from photosynthesis and they are at the base of the food chain. Coccolithophores cells, with a size from ~15 to 100 µm, secretes coccoliths, little calcareous plates which cover all of the cell surface, forming the *Coccosphaera*. Coccoliths are ~2-15 µm in dimension, and their shape and size are the base for their taxonomic classification. Coccoliths are the only remains of Coccolithophores in the geologic records because organic parts are easily dissolved by disaggregation by bacterial activity. Coccoliths are usually composed by micro-crystalline calcite, more rarely by aragonite or vaterite. The function of coccoliths is still debated but it may be linked to protection of the cell against the light or from predatory organisms, or to the concentration of ray lights toward the cell. The most accredited interpretation is the role of coccoliths as buoyancy structures.

A pioneer work about coccolithophores biogeography was published by McIntyre and Bé (1967) who recognized, in the Atlantic Ocean, 5 different coccolithophore assemblages corresponding to the 5 climatic zone: tropical, subtropical, transitional, subartic and subantarctic. Similarly, Okada and Honjo (1973) recognized 6 types of assemblage in the Pacific Ocean. These works remarked the link between coccolithophore distribution and surface water conditions, paving the way for paleoecological studies of coccolithophore (calcareous nannofossil) assemblages for climatic reconstructions at all latitudes and in all oceans.

Today diatoms are more abundant than coccolithophores in coastal areas and in polar and subpolar regions. On the contrary, coccolithophores dominate in temperate, warm and oligotrophic regions. Coccolithophore oceanic forms are commonly oligotrophic and tolerate better low nutrient availability compared to coastal species. Differently, subtropical species do not show significant abundance variations when fertility increases. Coccolitophores, as a whole, can tolerate a wide range of temperature between 2°C, lower boundary for carbonate precipitation, and 31°C; the tolerance of single taxa is limited to more restricted ranges. Being coccolithophores photosynthetizing organisms, they need sunlight to survive and reproduce; for this reason, most of the species live in the upper photic zone (0-50 m) and they move within the water column using two flagella.

Besides responding to climatic changes, they also contribute in the global climatic evolution. In fact, Coccolithophores have played an important role in the global carbon cycle since they appeared in the early Triassic, supplying organic carbon and carbonate to the deep sea, and subtracting CO_2 to the water to perform the photosynthesis. Also, Coccolithophore seasonal blooms strongly affect the albedo and thus the amount of solar energy retained by the planet. Albedo is one of the factors that plausibly acted as a positive feedback for the cooling when ice sheet was forming in Antarctica in the early Oligocene (e.g. Huber and Sloan, 2001). Furthermore, Coccolithophores influence the global climate through the formation of dimetilsufide, a gaseous compound that acts as a condensation nucleus around which humidity condenses, forming clouds. The effect of clouds is similar to albedo, reflecting the sunlight back to the atmosphere. This group of phytoplankton therefore affects global climate in several different ways, directly or indirectly.

Fossil remains of coccolithophores are called *Calcareous Nannofossils* and they have a significant lithogenetic role, being the major constituents of deep sea carbonates. It has been estimated that today, the 80% of carbon buried in open ocean sediments is in the form of $CaCO_3$, most of which of biogenic origin. The 20-40 % of this biogenic carbonate is produced by coccolithophores. The preservation of nannofossils in the geological record depends mainly on the modality they sink in the water column and reach the bottom. Phytoplankton, including coccolithophores, is food for bigger organisms such as copepods which, after ingestion, expel them within fecal pellets. This way, fecal pellets act as a protective barrier for coccolithophores against disaggregation and dissolution.

The use of calcareous nannofossils as paleoclimatic indicators is twofold and both organic and inorganic components are useful to reconstruct past climate. Past surface water temperatures are reconstructed by using alkenones (Brassell et al., 1987), organic chains, whose characteristics are influenced by temperature, and which are produced by some forms of coccolithophores and by their ancient relatives, and that can be found in ocean sediments. Furthermore, nannofossil assemblage characteristics, such as abundance and diversity, depend mainly on sea surface temperature and fertility (e.g.

Haq and Lohmann, 1976; McIntyre and Bé, 1967; Wei and Wise, 1990a) and can be used, together with other proxies, to reconstruct past oceanic conditions.

The importance of calcareous nannofossil as biostratigraphic tools is undoubted (e.g. Haq, 1984) and derives mainly from their wide geographic distribution and high abundance in ocean sediments.

Several works have focused on calcareous nannofossil biostratigraphy and paleoecology at southern high latitudes (Persico and Villa, 2004; Villa et al., 2008; Villa and Persico, 2006; Villa et al., 2003; Wei et al., 2004; Wei and Thierstein, 1991; Wei et al., 1992; Wei and Wise, 1990b; Wei, 2004; Wise et al., 1992; Wise and Mostajo, 1984) and they all highlighted the great potential and reliability of this group of phytoplankton as paleoclimatic tools. This Ph.D. dissertation is also based on the wide knowledge acquired and transmitted from those previous works.

3. The Southern Ocean

The Southern Ocean is constituted by the southern sectors of the Atlantic, Pacific and Indian oceans and it surrounds the Antarctic continent (Fig. 2). The location of its northern boundary is still debated as some authors proposed the southern 60^{th} parallel (e.g. Lazarus and Caulet, 1993) or the Subtropical Front (e.g. Nelson and Cooke, 2001); its southern boundary is the Antarctic continent. Beyond problems related to its definition, the Southern Ocean has a very important role in driving climate at global scale, being the regulator of global oceanic current system. In fact, cold and deep waters originate in the Southern Ocean, flow northward and determine the global thermoaline circulation (Fig. 5). The system of currents in the Southern Ocean is very complicated and only the most important components and characteristics are described hereinafter.

The surface current characterizing the Southern Ocean is the Antarctic Circumpolar Current (AACC) (Fig. 4) which flows eastward around the Antarctic continent and is triggered by strong westerly winds blowing on the Southern Ocean. The AACC connects the southern sectors of all oceans and allows an exchange between water masses. At the same time, it prevents warm surface currents from law latitude to flow southward. The existence of the AACC maintains cold conditions in the Southern Ocean and allows the ice-sheet in Antarctica to endure. The AACC flows around

Antarctica in the southern sector of the Pacific, it crosses the Drake Passage and it flows into the South Atlantic where part of it moves northward as the Falkland Current. The main body of the AACC then flows through the southern Indian Ocean, where, in correspondence of the Kerguelen Plateau, it splits in two branches, one deviating northward. Its main path continues in the in the southern Pacific, where part of it flows northward affecting lower latitudes. The AACC has a complex structure (Fig. 4), where several fronts, separating different water masses, can be distinguished, from the North to the South: the Subtropical Front (STF), separating subtropical warmer and saltier waters from cooler and fresher subpolar waters, the Subantarctic Front (SAF), where a thick layer of Subantarctic Mode Water is present at the surface, the Polar Front, which marks the passage to cooler and fresher Antarctic Surface Water, and the Southern Boundary Front, whose position is controlled by topographic features (Orsi et al., 1995).

The two ODP Sites (1090 and 702) studied during this Ph.D. are located in a position influenced mainly by the movement of the Polar Front (PF) (Fig. 2). The Polar Front, or Antarctic Convergence, is the place where cold Antarctic waters flowing northward encounter the relatively warmer subantarctic waters. Antarctic waters usually sink beneath the subantarctic waters, and the contact between these two water masses creates mixing and upwelling/downwelling which support high primary productivity at the surface. North of the Polar Front, water temperature is usually between 2.8 °C and 5.6°C, and south of it lower than 2 °C. This front is thus a well defined climatic boundary and this explain why the Southern Ocean is considered a separated mass from other oceans, despite the AACC is not interrupted by land masses. The position of the Polar Front varies seasonally between 45° and 65°S and this variability clarify why the 60^{th} parallel has been chosen as conventional northern boundary for the Southern Ocean.

Both studied sites are located in the South Atlantic sector of the Southern Ocean (Fig. 2). A short description of the water masses and currents flowing through the Atlantic Ocean is given hereinafter (Fig. 5). The deep and bottom waters of the Atlantic Ocean are dominated by cold and dense waters. The Antarctic Bottom Water (AABW) is very cold and saline and is produced at the surface essentially in the Weddell Sea and in the Ross Sea during the winter. The Antarctic Deep Water (AADW) is produced off

Antarctica and is slightly warmer and fresher than the AABW. Being saline and cold, the AABW sinks to the bottom of the Atlantic ocean and flows northward reaching low latitudes. The AADW flows at the ocean surface until the Antarctic Convergence where it is forced to sink beneath the warmer subantartic waters, and its flow is confined between the AABW and the North Atlantic Deep Water (NADW), a moderately salty and cold current originated by cooling and evaporation in the North Atlantic. The NADW is produced in a very large area and it is the most common water mass found in the Atlantic, but intermediate waters are also present: the Antarctic Intermediate Water (AAIW), the Arctic Intermediate Water (AIW), and the Mediterranean Intermediate Water (MIW) (Fig. 5). The AAIW is formed in the subantarctic region and the AIW in the subarctic, and their characteristics in terms of temperature and salinity are not as extreme as bottom and deep waters. These waters, after being produced at high latitudes, flow toward lower latitudes above the NADW. A third intermediate current is produced by evaporation in the Mediterranean Sea and, after crossing the Gibraltar straight, it reaches the Atlantic, where it sinks to intermediate depths and forms a tongue of warm and salty water.

Because of its position, near the south tip of Africa, Site 1090 was also affected by the Agulhas Current, a western boundary current flowing from the south Indian Ocean (Fig. 6) which has as major sources the Mozambique current and the East Madagascar Current (Bryden et al., 2005). This narrow, fast and strong current flows south-westward, down the east coast of Africa from 27°S to ~45°S. After reaching the tip of Africa, most of the Agulhas Current retroflects and, following a counter-clockwise path, it goes back to the Indian Ocean as Agulhas Retroflection. This retroflection is caused by the interaction between the Agulhas Current and the AACC. The remaining current flows to the South Atlantic as Agulhas Leakage. As Indian Ocean waters are markedly warmer and saltier than South Atlantic waters, the Agulhas Leakage is a source of salt and heat for the South Atlantic gyre.

References

Agnini, C. et al., 2006. Responses of calcareous nannofossil assemblages, mineralogy and geochemistry to the environmental perturbations across the Paleocene/Eocene boundary in the Venetian Pre-Alps. Marine Micropaleontology, 63: 19-38.

Anderson, L.D. and Delaney, M.L., 2005. Middle Eocene to early Oligocene paleoceanography from Agulhas Ridge, Southern Ocean (Ocean Drilling Program Leg 177, Site 1090). Paleoceanography, 20(1).

Aubry, M.P., 1992. Late Paleogene nannoplankton evolution: a tale of climatic deterioration. In: D.R. Prothero and W.A. Berggren (Editors), Eocene-Oligocene Climatic and Biotic Evolution. Princeton University Press, Princeton.

Barker, P.F., 2001. Scotia Sea regional tectonic evolution; implications for mantle flow and palaeocirculation. Earth-Sci. Rev., 55: 1-39.

Barker, P.F. and Burrell, J., 1977. The opening of Drake Passage. Marine Geology, 25(1-3): 15-34.

Berner, R.A., Arthur, M.A. and Anonymous, 1990. An evaluation of factors affecting atmospheric CO (sub 2) over the past 140 million years.

Bijl, P. et al., 2010. Transient Middle Eocene Atmospheric CO_2 and Temperature Variations. Science, 330: 819-821.

Bohaty, S.M. and Zachos, J.C., 2003. Significant Southern Ocean warming event in the late middle Eocene. Geology, 31(11): 1017-1020.

Bohaty, S.M., Zachos, J.C., Florindo, F. and Delaney, M.L., 2009. Coupled greenhouse warming and deep sea acidification in the middle Eocene. Paleoceanography, 24(PA2207).

Bowen, G.J. et al., 2006. Eocene Hyperthermal Events Offers Insight Into Greenhouse Warmings. EOS, 87(17).

Bowen, G.J. et al., 2002. Mammalian dispersal at the Paleocene/Eocene boundary. Science, 295(5562): 2062-2065.

Bralower, T.J., 2002. Evidence of surface water oligotrophy during the Paleocene-Eocene thermal maximum: Nannofossil assemblage data from Ocean Drilling Program Site 690, Maud Rise, Weddell Sea (vol 17, pg 1023, 2002) - art. no. 1060. Paleoceanography, 17(4): 1060.

Brassell, S.C., Eglinton, G. and Howell, V.J., 1987. Palaeoenvironmental assessment for marine organic-rich sediments using molecular organic geochemistry. Geological Society Special Publications, 26: 79-98.

Bryden, H.L., Beal, L.M. and Duncan, M.N., 2005. Structure and Transport of the Agulhas Current and Its Temporal Variability. Journal of Oceanography, 61: 479-492.

Cermeno, P. et al., 2008. The role of the nutricline depth in regulating the ocean carbon cycle. PNSA, 105(51): 20344-20349.

Clyde, W.C. and Gingerich, P.D., 1998. Mammalian community response to the latest Paleocene themal maximum: An isotaphonomic study in the northern Bighorn Basin, Wyoming. Geology, 26: 1011-1014.

Coxall, H.K. and Pearson, P.N., 2007. The Eocene-Oligocene Transition. In: M. Williams, A.M. Haywood, F.J. Gregory and D.N. Schmidt (Editors), Deep-time Perspectives on Climate Change: Marrying the Signal from Computer Models

and Biological Proxies. Special Publication. The Micropaleontological Society, London, pp. 351-387.

Coxall, H.K., Wilson, P.A., Pälike, H., Lear, C.H. and Backman, J., 2005. Rapid stepwise onset of Antarctic glaciation and deeper calcite compensation in the Pacific Ocean. Nature, 433(7021): 53-57.

Crouch, E.M. and Brinkhuis, H., 2005. Environmental change across the Paleocene-Eocene transition from eastern New Zealand: A marine palynological approach. Marine Micropaleontology, 56(3-4): 138-160.

Crouch, E.M. et al., 2003. The Apectodinium acme and terrestrial discharge during the Paleocene-Eocene thermal maximum: new palynological, geochemical and calcareous nannoplankton observations at Tawanui, New Zealand. Palaeogeography Palaeoclimatology Palaeoecology, 194(4): 387-403.

Crouch, E.M. et al., 2001. Global dinoflagellate event associated with the late Paleocene thermal maximum. Geology, 29(4): 315-318.

DeConto, R.M. and Pollard, D., 2003. Rapid Cenozoic glaciation of Antarctica induced by declining atmospheric CO2. Nature, 421(6920): 245-249.

Dickens, G.R., 2000. Methane oxidation during the Late Palaeocene Thermal Maximum. Bull. Soc. Géol. France, 171(1): 37-49.

Dickens, G.R., Bralower, T.J., Thomas, D.J., Thomas, E. and Zachos, J.C., 1998. High-resolution records of the late Paleocene thermal maximum and circum-Caribbean volcanism; is there a causal link?; discussion and reply. Geology, 26(7): 670-671.

Dickens, G.R., Castillo, M.M. and Walker, J.C.G., 1997. A blast of gas in the latest Paleocene: Simulating first-order effects of massive dissociation of oceanic methane hydrate. Geology, 25(3): 259-262.

Dickens, G.R., O'Neil, J.R., Rea, D.K. and Owen, R.M., 1995. Dissociation of oceanic methane hydrate as a cause of the carbon isotope excursion at the end of the Paleocene. Paleoceanography, 10(6): 965-971.

Diester-Haass, L. and Zachos, J., 2003. The Eocene-Oligocene transition in the Equatorial Atlantic (ODP Site 925); paleoproductivity increase and positive delta (super 13) C excursion. In: D.R. Prothero, L.C. Ivany and E.A. Nesbitt (Editors). Columbia University Press, New York.

Diester-Haass, L. and Zahn, R., 1996. Eocene-Oligocene transition in the Southern Ocean: History of water mass circulation and biological productivity. Geology, 24(2): 163-166.

Doney, S.C., Balch, W.M., Fabry, V.J. and Feely, R.A., 2009. Ocean acidification: a critical emerging problem for the ocean sciences. Oceanography, 22(4): 16-25.

Dunkley Jones, T., Bown, P.R., Pearson, P.N., Wade, B.S. and Coxall, H.K., 2008. Major shifts in calcareous phytoplankton assemblages through the Eocene-Oligocene transition of Tanzania and their implications for low-latitude primary production. Paleoceanography, 23: PA4204.

Eagles, G., Livermore, R. and Morris, P., 2006. Small basins in the Scotia Sea: the Eocene Drake Passage gateway. Earth Planet. Sci. Lett., 242: 343-353.

Edgar, K.M., 2008. Paleoclimatology, stratigraphy and biotic responses in the middle Eocene, University of Southampton, Southampton.

Edgar, K.M. et al., 2010. New biostratigraphic, magnetostratigraphic and isotopic insights into the Middle Eocene Climatic Optimum in low latitudes. Palaeogeography, Palaeoeclimatology, Palaeoecology, 297: 670-682.

Emiliani, C. and Edwards, G., 1953. Tertiary ocean bottom tempertaures. Nature, 171: 887-888.

Feely, R.A., Doeny, S.C. and Cooley, S.R., 2009. Ocean Acidification: Present Conditions and Future Changes in a High-CO_2 world. Oceanography, 22(4).

Feely, R.A. et al., 2004. Impact of anthropogenic CO2 on the CaCO3 system in the oceans. Science, 305: 362-366.

Francis, J.E., 1999. Evidence from fossil plants for Antarctica paleoclimates over the past 100 million years. Terra Antartica, 3: 43-52.

Funakawa, S. and Nishi, H., 2008. Radiolarian faunal changes during the Eocene-Oligocene transition in the Southern Ocean (Maud Rise, ODP Leg 113, Site 689) and its significance in paleoceanographic change. Micropaleontology, 54(1): 15-26.

Gibbs, S.J., Bralower, T.J., Bown, P.R., Zachos, J.C. and Bybell, L.M., 2006. Shelf and open-ocean calcareous phytoplankton assemblages across the Paleocene-Eocene Thermal Maximum: implications for global productivity gradients. Geology, 34(4): 233-236.

Haq, B.U., 1984. Nannofossil Biostratigraphy. Benchmark Papers in Geology. Hutchinson Ross Publishing Company, Stroudsburg, Pennsylvania.

Haq, B.U. and Lohmann, G.P., 1976. Early Cenozoic calcareous nannoplankton biogeography of the Atlantic Ocean. Marine Micropaleontology, 1: 119-194.

Haq, B.U., Premoli-Silva, I. and Lohmann, G.P., 1977. Calcareous Plankton Paleobiogeographic Evidence for Major Climatic Fluctuations in the Early Cenozoic Atlantic Ocean. Jour. Geophys. Research, 82: 3861-3876.

Hooker, J.J., Collinson, M.E. and Sille, N.P., 2004. Eocene-Oligocene mammalian faunal turnover in the Hampshire Basin, UK; calibration to the global time scale and the global major event. Journal of the Geological Society of London, 161: 161-172.

Huber, M. et al., 2004. Eocene circulation of the Southern Ocean: Was Antarctica kept warm by subtropical waters? Paleoceanography, 19(4).

Huber, M. and Nof, D., 2006. The ocean circulation in the Southern Hemisphere and its climatic impacts in the Eocene. Palaeogeography, Palaeoclimatology, Palaeoecology, 231(1-2): 9-28.

Huber, M. and Sloan, L.C., 2001. Heat transport, deep waters, and thermal gradients; coupled simulation of an Eocene greenhouse climate. Geophysical Research Letters, 28(18): 3481-3484.

Jaramillo, C., Rueda, M.J. and Mora, G., 2006. Cenozoic plant diversity in the Neotropics. Science, 311: 1893-1896.

Jicha, B.R., Scholl, D.W. and Rea, D.K., 2009. Circum-Pacific arc flare-ups and global cooling near the Eocene-Oligocene boundary Geology, 37(4): 303-306.

Jovane, L. et al., 2007. The middle Eocene climatic optimum event in the Contessa section, Umbrian Apennines, Italy. Geological Society of America Bulletin, 119(3/4): 413-417.

Jovane, L. et al., 2010. Astronomical calibration of the middle Eocene Contessa Highway section (Gubbio, Italy). Earth and Planetary Science Letters, 298: 77-88.

Kahn, A. and Aubry, M.P., 2004. Provincialism associated with the Paleocene/Eocene Thermal maximum: temporal constrain. Marine Micropaleontology, 52: 117-131.

Kelly, D.C., Bralower, T.J. and Zachos, J.C., 1998. Evolutionary consequences of the latest Paleocene thermal maximum for tropical planktonic Foraminifera. Palaeogeography, Palaeoclimatology, Palaeoecology, 141(1-2): 139-161.

Kelly, D.C., Bralower, T.J., Zachos, J.C., Premoli-Silva, I. and Thomas, E., 1996. Rapid diversification of planktonic foraminifera in the tropical Pacific (ODP Site 865) during the late Paleocene thermal maximum. Geology, 24(5): 423-426.

Kennett, J.P., 1977. Cenozoic evolution of Antarctic glaciation, circum-Antarctic ocean, and their impact on global paleoceanography. Journal of Geophysical Research-Oceans and Atmospheres, 82(27): 3843-3860.

Kennett, J.P. and Exon, N.F., 2004. Paleoceanographic evolution of the Tasmanian Seaway and its climatic implications. In: N.F. Exon, J.P. Kennett and M.J. Malone (Editors), The Cenozoic Southern Ocean: Tectonics, Sedimentation, and Climate Change Between Australia and Antarctica. Geophysical Monograph 151. American Geophysical Union, pp. 345-367.

Kennett, J.P. et al., 1975. Cenozoic paleoceanography in the Southwest Pacific Ocean, Antarctic glaciation, and the development of the Circum-Antarctic Current. Initial Reports of the Deep Sea Drilling Project, 29: 1155-1169.

Kennett, J.P. and Stott, L.D., 1991. Abrupt deep-Sea warming, palaeoceanographic changes and benthic extinctions at the end of the Palaeocene. Nature, 353: 225-229.

Lagabrielle, Y., Goddéris, Y., Donnadieu, Y., Malavieille, J. and Suarez, M., 2009. The tectonic history of Drake Passage and its possible impacts on global climate. Earth and Planetary Science Letters, 279: 197-211.

Lawver, L.A. and Gahagan, L.M., 2003. Evolution of Cenozoic seaways in the circum-Antarctic region. Palaeogeography, Palaeoclimatology, Palaeoecology, 198(1-2): 11-37.

Lazarus, D. and Caulet, J.P., 1993. Cenozoic Southern Ocean reconstructions from sedimentologic, radiolarian, and other microfossil data. In: J.P. Kennett and D.A. Warnke (Editors), The Antarctic paleoenvironment; a perspective on global change; Part two. Antarctic Research Series, pp. 145-174.

Lear, C.H., Bailey, T.R., Pearson, P.N., Coxall, H.K. and Rosenthal, Y., 2008. Cooling and ice growth across the Eocene-Oligocene transition. Geology, 36(3): 251-254.

Liu, Z. et al., 2009. Global Cooling During the Eocene-Oligocene Climate Transition. Science, 323.

Liu, Z., Tuo, S., Zhao, Q., Cheng, X. and Huang, W., 2004. Deep-water earliest Oligocene glacial maximum (EOGM) in South Atlantic. Chinese Science Bulletin, 49(20): 2190-2197.

Livermore, R., Hillenbrand, C.-D., Meredith., M. and Eagles, G., 2007. Drake Passage and Cenozoic climate: An open and shut case? Geochem. Geophys. Geosyst., 8.

Livermore, R., Nankivell, A., Eagles, G. and Morris, P., 2005. Paleogene opening of Drake Passage. Earth and Planetary Science Letters, 236(1-2): 459-470.

Lourens, L.J. et al., 2005. Astronomical pacing of late Palaeocene to early Eocene global warming events. Nature, 435(7045): 1083-1087.

Lowenstein, T.K. and Demicco, R.V., 2006. Elevated eocene atmospheric CO2 and its subsequent decline. Science, 313(5795): 1928-1928.

Luciani, V. et al., 2010. Ecological and evolutionary response of Thethyan planktonic foraminifera to the Middle Eocene Climatic Optimum (MECO) from the Alano

Section (NE Italy). Palaeogeography, Palaeoclimatology, Palaeoecology, 292(1-2): 82-95.

Lyle, M., Lyle, A.O., Backman, J. and Tripati, A., 2005. Biogenic sedimentation in the Eocene equatorial Pacific -- the stuttering greenhouse and Eocene carbonate compensation depth. In: P.A.M.L.a.J.V.F. Wilson (Editor), Proc. ODP, Sci. Results, 199. Ocean Drilling Program, College Station, TX, pp. 1-35.

Matthews, R.K. and Poore, R.Z., 1981. Oxygen isotope record of ice volume history: 100 m.y. of glacio-eustatic sea level fluctuation. AAPG Bulletin, 65(5): 954.

McIntyre, A. and Bé, W.H., 1967. Modern coccolitophoridae of the Atlantic Ocean-I. Placoliths and Cyroliths. Deep-Sea Research, 14: 561-597.

Mead, G.A., Tauxe, L. and LaBrecque, J.L., 1986. Oligocene paleoceanography of the South Atlantic; paleoclimatic implications of sediment accumulation rates and magnetic susceptibility measurements. Paleoceanography, 1(3): 273-284.

Merico, A., Tyrrell, T. and Wilson, P.A., 2008. Eocene/Oligocene ocean de-acidification linked to Antarctic glaciation by sea-level fall. Letters to Nature, 452: 979-982.

Miller, K.G. et al., 2008. Eocene-Oligocene global climate and sea-level change changes: St. Stephens Quarry, Alabama. Geological Society of America Bulletin, 120(1/2): 34-53.

Miller, K.G. and Katz, M.E., 1987. Oligocene to Miocene benthic foraminiferal and abyssal circulation changes in the North Atlantic. Micropaleontology, 33(2): 97-149.

Miller, K.G., Wright, J.D. and Fairbanks, R.G., 1991. Unlocking the ice house: Oligocene-Miocene oxygen isotopes, eustasy, and margin erosion. Journal of Geophysical Research, B, Solid Earth and Planets, 96: 6829-6848.

Miller, K.G. et al., 2009. Climate threshold at the Eocene-Oligocene transition: Antarctic ice sheet influence on ocean circulation. In: C. Koeberl, and Montanari, A., eds. (Editor), The Late Eocene Earth-Hothouse, Icehouse, and Impacts: Geological Society of America Special Paper, pp. 169-178.

Nelson, C.S. and Cooke, P.J., 2001. History of oceanic front development in the New Zealand sector of the Southern Ocean during the Cenozoic -- a synthesis. New Zealand Journal of Geology and Geophysics, 44(4): 535-553.

Oberhansli, H., 1992. The influence of the Thetys on the bottom waters of the early Tertiary ocean. In: J.P. Kennet and D.A. Warnke (Editors), The Antarctic Paleoenvironment: A Perspective on Global Change. Anatrct. Res. Ser., pp. 167-184.

Okada, H. and Honjo, S., 1973. The Distribution of Oceanic Coccolithoporids in the Pacific. Deep-sea research, 20: 355-374.

Orsi, A.H., Whitworth III, T. and Nowlin, W., 1995. On the meridional extent and fronts of the Antarctic Circumpolar Current. Deep-sea Research, 42: 641-673.

Pagani, M., Zachos, J.C., Freeman, K.H., Tipple, B. and Bohaty, S., 2005. Marked decline in atmospheric carbon dioxide concentrations during the Paleogene. Science, 309(5734): 600-603.

Pearson, P.N. et al., 2008. Extinction and environmental change across the Eocene-Oligocene boundary in Tanzania. Geology, 36(2): 179-182.

Pearson, P.N. and Palmer, M.R., 2000a. Atmospheric carbon dioxide concentrations over the past 60 million years. Nature, 406(6797): 695-699.

Pearson, P.N. and Palmer, M.R., 2000b. Estimating Paleogene atmospheric pCO (sub 2) using boron isotope analysis of Foraminifera. In: B. Schmitz, B. Sundquist and F.P. Andreasson (Editors), Gff, pp. 127-128.

Peck, V.L., Yu, J., Kender, S. and Riesselman, C.R., 2010. Shifting ocean carbonate chemistry during the Eocene-Oligocene climate transition: implications for deep ocean Ma/Ca-paleotermometry. Paleoceanography, 25.

Pekar, S.F., Christie-Blick, N., Kominz, M.A. and Miller, K.G., 2002. Calibration between eustatic estimates from backstripping and oxygen isotopic records for the Oligocene. Geology, 30(10): 903-906.

Persico, D. and Villa, G., 2004. Eocene-Oligocene calcareous nannofossils from Maud Rise and Kerguelen Plateau (Antarctica): Paleoecological and paleoceanographic implications. Marine Micropaleontology, 52: 153-179.

Raffi, I., Backman, J. and Palike, H., 2005. Changes in calcareous Nannofossil assemblages across the Paleocene-Eocene transition from the Plaeo-Equatorial Pacific Ocean. Palaeogeography, Palaeoclimatology, Palaeoecology, 226: 93-126.

Raffi, I., Backman, J., Zachos, J.C. and Sluijs, A., 2009. The response of calcareous nannofossil assemblages to the Paleocene Eocene Thermal Maximum at the Walvis Ridge in the South Atlantic. Marine Micropaleontology, 70(3-4): 201-212.

Raffi, I. and De Bernardi, B., 2008. Response of calcareous nannofossils to the Paleocene-Eocene Thermal Maximum: observations on composition, preservation and calcification in sediments from ODP Site 1263 (Walvis Ridge-SW Atlantic) Marine Micropaleontology, 69(2): 119-138.

Raymo, M.E., Ruddiman, W.F. and Froelich, P.N., 1988. Influence of Late Cenozoic Mountain Building on Ocean Geochemical Cycles. Geology, 16(7): 649-653.

Rea, D.K. and Lyle, M.W., 2005. Paleogene calcite compensation depth in the eastern subtropical Pacific: Answers and questions. Paleoceanography, 20.

Salamy, K.A. and Zachos, J.C., 1999. Latest Eocene-early Oligocene climate change and Southern Ocean fertility; inferences from sediment accumulation and stable isotope data. Palaeogeography, Palaeoclimatology, Palaeoecology, 145(1-3): 61-77.

Savin, S.M., Douglas, R.G. and Stehli, F.G., 1975. Tertiary marine paleotemperatures. Geological Society of America Bulletin, 86(11): 1499-1510.

Scher, H.D. and Martin, E.E., 2006. Timing and climatic consequences of the opening of Drake Passage. Science, 312(5772): 428-30.

Shackleton, N.J. and Kennett, J.P., 1975. Paleotemperature history of the Cenozoic and the initiation of Antarctic glaciation: Oxygen and carbon isotope analyses in DSDP sites 277, 279, and 281. Initial Reports of the Deep Sea Drilling Project, 29: 743-755.

Sluijs, A., Bowen, G.J., Brinkhuis, H., Lourens, L.J. and Thomas, E., 2007a. The Palaeocene-Eocene thermal maximum super greenhouse: biotic and geochemical signatures, age models and mechanisms of global change. In: M. Williams and et al. (Editors), Deep time perspectives on Climate Change: Marrying the Signal from Computer Models and Biological Proxies. The Micropalaeontological Society, Special Publications. The Geological Society, London, pp. 323-347.

Sluijs, A. et al., 2007b. Environmental precursors to rapid light carbon injection at the Palaeocene/Eocene boundary. Nature, 450: 1218-U5.

Sluijs, A. et al., 2009. Warm and wet conditions in the Artic refion during the Eocene Thermal Maximum 2. Nature Geoscience, 2: 777-780.

Smith, J.J., Hasiotis, S.T., Kraus, M.J. and Woody, T.D., 2009. Transient dwarfing of soil fauna during the Paleocene-Eocene Thermal Maximum. PNAS, 106(42).

Spofforth, D. et al., 2010. Organic carbon burial following the middle Eocene climatic optimum in the central western Thetys. Paleoceanography, 25.

Stickley, C.E. et al., 2004. Timing and nature of the deepening of the Tasmanian Gateway. Paleoceanography, 19(4).

Suto, I., 2006. The explosive diversification of the diatom genus Chaetoceros across the Eocene-Oligocene and Oligocene-Miocene boundaries in the Norwegian Sea. Marine Geology, 58: 259-269.

Thomas, E., 1998. Biogeography of the late Paleocene benthic foraminiferal extinction. In: S.G.e. Lucas and W.A.e. Berggren (Editors), Late Paleocene early Eocene climatic and biotic events in the marine and terrestrial records.

Thomas, E. and Shackleton, N.J., 1996. The Paleocene-Eocene benthic foraminiferal extinction and stable isotope anomalies. In: R.W.O.B. Knox, R.M. Corfield and R.E. Dunay (Editors), Correlation of the early Paleogene in Northwest Europe. Geoligical Society Special Publication, London, pp. 401-441.

Tripati, A., Backman, J., Elderfield, H. and Ferretti, P., 2005. Eocene bipolar glaciation associated with global carbon cycle changes. Nature, 436(7049): 341-346.

Van Andel, T.H., 1975. Mesozoic/Cenozoic calcite compensation depth and the global distribution of calcareous sediments. Earth and Planetary Science Letters, 26(2): 187-194.

Villa, G., Fioroni, C., Pea, L., Bohaty, S. and Persico, D., 2008. Middle Eocene-late Oligocene climate variability: Calcareous nannofossil response at Kerguelen Plateau, Site 748. Marine Micropaleontology, 69: 173-192.

Villa, G. and Persico, D., 2006. Late Oligocene climatic changes: Evidence from calcareous nannofossils at Kerguelen Plateau Site 748 (Southern Ocean). Palaeogeography, Palaeoclimatology, Palaeoecology, 231: 110-119.

Villa, G. et al., 2003. Biostratigraphic characterization and Quaternary microfossil palaeoecology in sediment drifts west of the Antarctic Peninsula; implications for cyclic glacial-interglacial deposition. In: F. Florindo, A.K. Cooper and P.E. O'Brien (Editors), Palaeogeography, Palaeoclimatology, Palaeoecology, pp. 237-263.

Vonhof, H.B., Smit, J., Brinkhuis, H., Montanari, A. and Nederbragt, A.J., 2000. Global cooling accelerated by early late Eocene impacts? Geology, 28(8): 687-690.

Wade, B.S. and Pearson, P.N., 2008. Planktonic foraminiferal turnover, diversity fluctuations and geochemical signals across the Eocene/Oligocene boundary in Tanzania. Marine Micropaleontology, 68: 244-255.

Wei, W. et al., 2004. Paleogene calcareous nannofossil biostratigraphy of ODP Leg 189 (Australia-Antarctica Gateway). Proceedings of the Ocean Drilling Program, Scientific Results (CD-ROM), 189: 14.

Wei, W. and Thierstein, H.R., 1991. Upper Cretaceous and Cenozoic calcareous nannofossils of the Kerguelen Plateau (southern Indian Ocean) and Prydz Bay (East Antarctica). Proc. ODP, Sci. Results, 119: 467-493.

Wei, W., Villa, G. and Wise, S.W., Jr., 1992. Paleoceanographic implications of Eocene-Oligocene calcareous nannofossils from sites 711 and 748 in the Indian Ocean. Proc. ODP, Sci. Results, 120: 979-999.

Wei, W. and Wise, S.W., Jr., 1990a. Biogeographic gradients of middle Eocene-Oligocene calcareous nannoplankton in the South Atlantic Ocean. Palaeogeography, Palaeoclimatology, Palaeoecology, 79(1-2): 29-61.

Wei, W. and Wise, S.W., Jr., 1990b. Middle Eocene to Pleistocene calcareous nannofossils recovered by Ocean Drilling Program Leg 113 in the Weddell Sea. Proc. ODP, Sci. Results, 113: 639-666.

Wei, W.C., 2004. Opening of the Australia-Antarctica gateway as dated by nannofossils. Marine Micropaleontology, 52(1-4): 133-152.

Wing, S.L. et al., 2005. Transient floral change and rapid global warming at the Paleocene-Eocene boundary. Science, 310(5750): 993-996.

Wise, S.W. et al., 1982. Paleontologic and paleoenvironmental synthesis for the southwest Atlantic Ocean based on Jurassic to Holocene faunas and floras from the Falkland Plateau. In: C. Craddock (Editor), International Union of Geological Sciences. Series B, vol.4, pp. 155-163.

Wise, S.W., Jr., Breza, J.R., Harwood, D.M., Wei, W. and Zachos, J.C., 1992. Paleogene glacial history of Antarctica in light of Leg 120 drilling results. Proceedings of the Ocean Drilling Program, Scientific Results, 120: 1001-1030.

Wise, S.W., Jr. and Mostajo, E.L., 1984. Eocene-Oligocene calcareous nannofossil assemblages from piston cores taken in the vicinity of Deep Sea Drilling sites 511 and 512, Falkland Plateau. Antarctic Journal of the United States, 18(5): 155-156.

Zachos, J. et al., 2003. Coupled isotopic and trace metal evidence for a significant rise in tropical sea surface temperature during the Paleocene-Eocene thermal maximum, Abstracts with Programs - Geological Society of America, pp. 584.

Zachos, J.C., Dickens, G.R. and Zeebe, R.E., 2008. An early Cenozoic perspective on greenhouse warming and carbon-cycle dynamics. Nature, 45: 279-283.

Zachos, J.C. and Kump, L.R., 2005. Carbon cycle feedbacks and the initiation of Antarctic glaciation in the earliest Oligocene. Global and Planetary Change, 47(1): 51-66.

Zachos, J.C., Pagani, M., Sloan, L., Thomas, E. and Billups, K., 2001. Trends, rhythms, and aberrations in global climate 65 Ma to present. Science, 292(5517): 686-693.

Zachos, J.C. et al., 2005. Rapid acidification of the ocean during the Paleocene-Eocene Thermal Maximum. Science, 308(5728): 1611-1615.

Zachos, J.C. et al., 2006. Extreme warming of mid-latitude coastal ocean during the Paleocene-Eocene Thermal Maximum; inferences from TEX86 and isotope data. Geology, 34(9): 737-740.

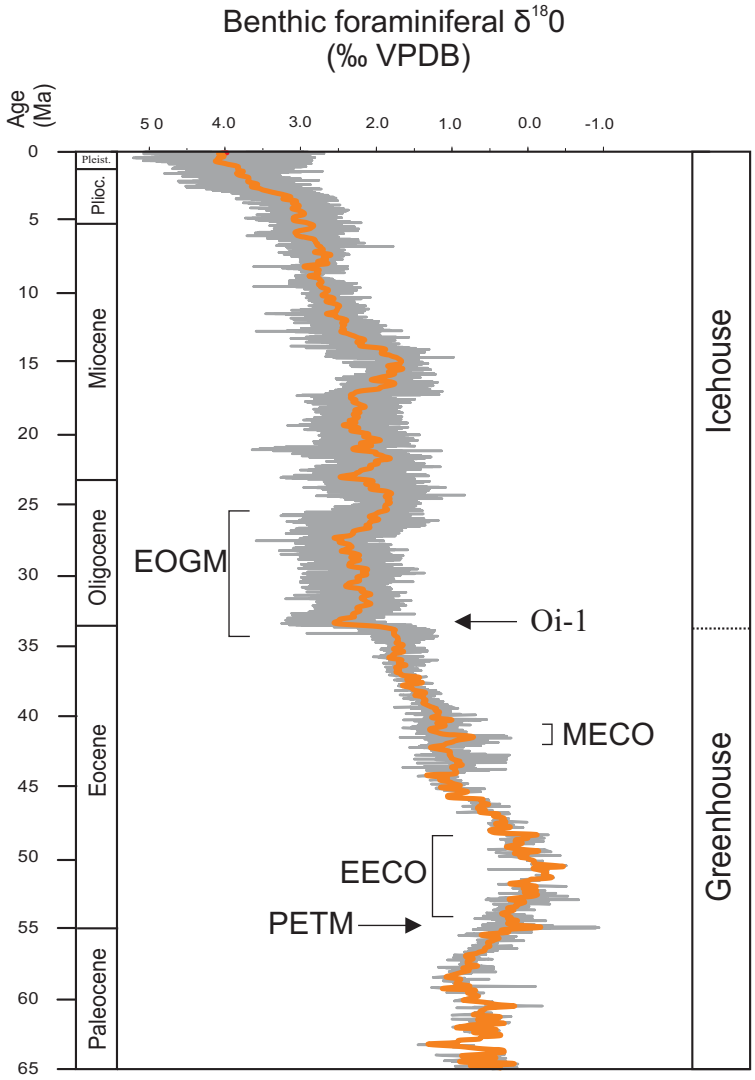

Figure 1: Composite deep-sea benthic foraminiferal $\delta^{18}0$ record for the Paleogene-Recent (Zachos et al. 2008). The temperature decrease shown by the isotope record corresponds to the passage between Greenhouse to Icehouse conditions. PETM: Paleocene-Eocene Thermal Maximum, EECO: Early Eocene Climatic Optimum, MECO: Middle Eocene Climatic Optimum, EOGM: Early Oligocene Glacial Maximum.

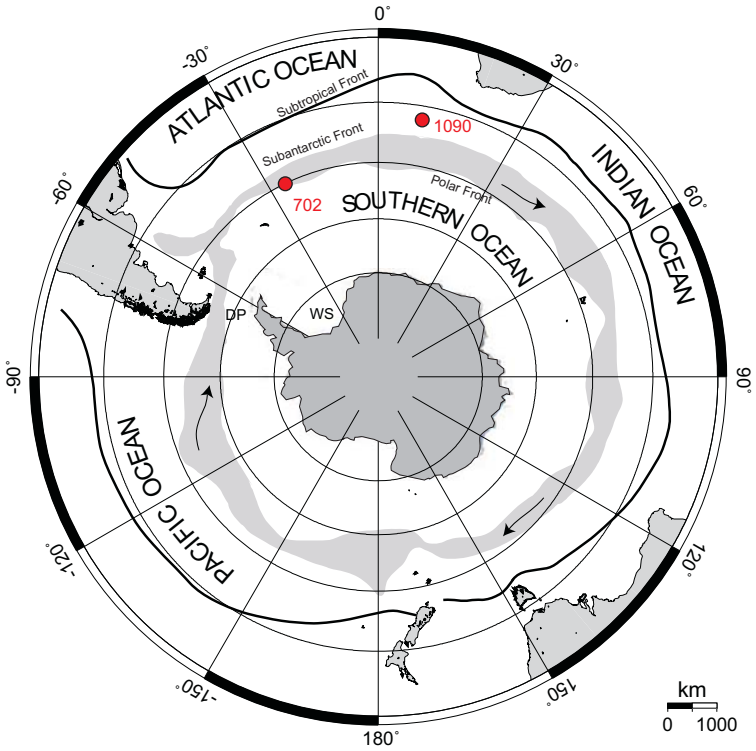

Figure 2: Polar stereographic projection to 30°S showing major oceanic fronts and ODP Sites studied in this work: Site 702 (Islas Orcadas Rise, 50°S, 26°W) and Site 1090 (Agulhas Ridge, 42°S, 8°E); DP- Drake Passage, WS- Weddell Sea. After Florindo et al. (2008), modified.

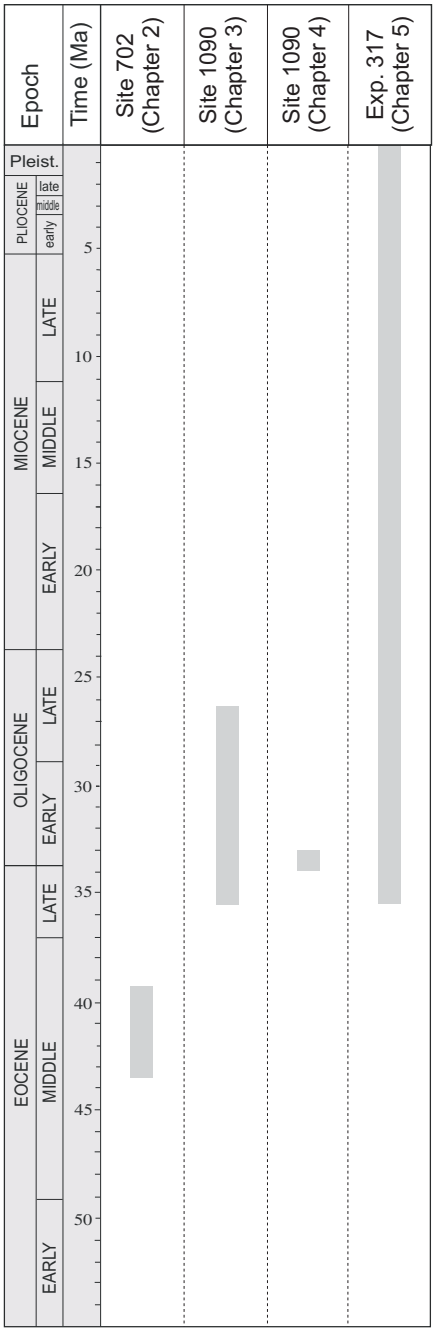

Figure 3: Time intervals discussed in this dissertation.

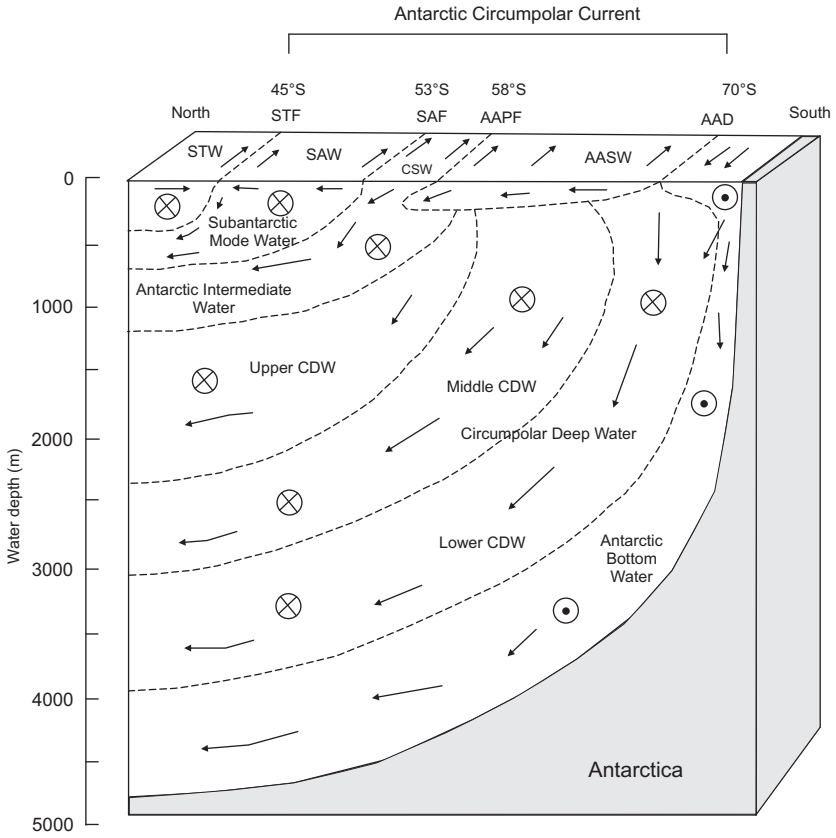

Figure 4: Schematic block diagram showing water masses and fronts in the Southern Ocean. STW- Subtropical Water, STF- Subtropical Front, SAW- Subantarctic Water, SAF- Subantarctic Front, CSW- Circumpolar Surface Water, AAPF, Antarctic Polar Front, AASW- Antarctic Surface Water, AAD- Antarctic Divergence, CDW- Circumpolar Deep Water.

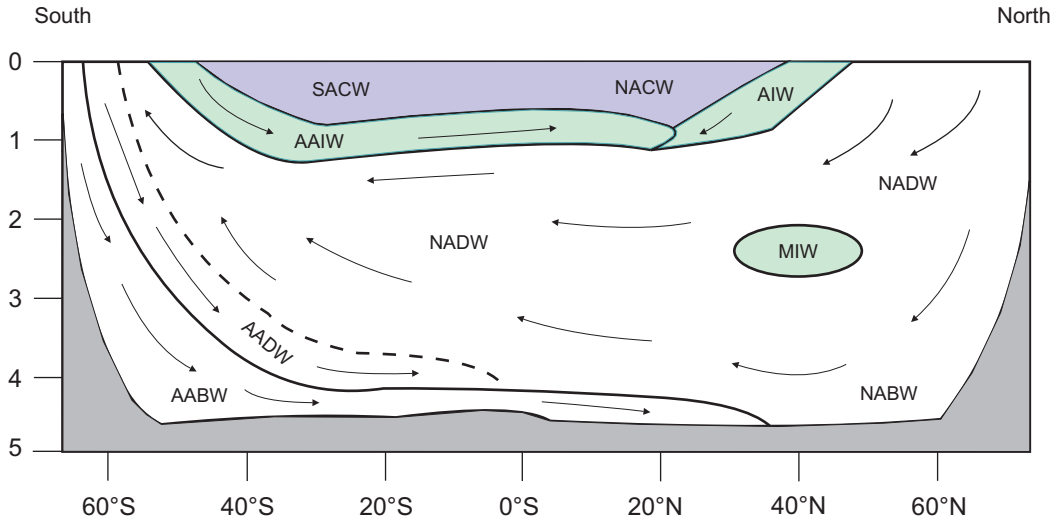

Figure 5: Simplified water mass structure of the Atlantic Ocean. SACW- South Atlantic Central Water, NACW- North Atlantic Central Water, AAIW- Antarctic Intermediate Water, AIW- Arctic Intermediate Water, NADW- North Atlantic Deep Water, MIW- Mediterrenean Intermediate Water, AADW- Antarctic Deep Water, AABW- Antarctic Bottom Water, NABW- North Atlantic Bottom Water. Purple: central waters, Green: Intermediate waters.

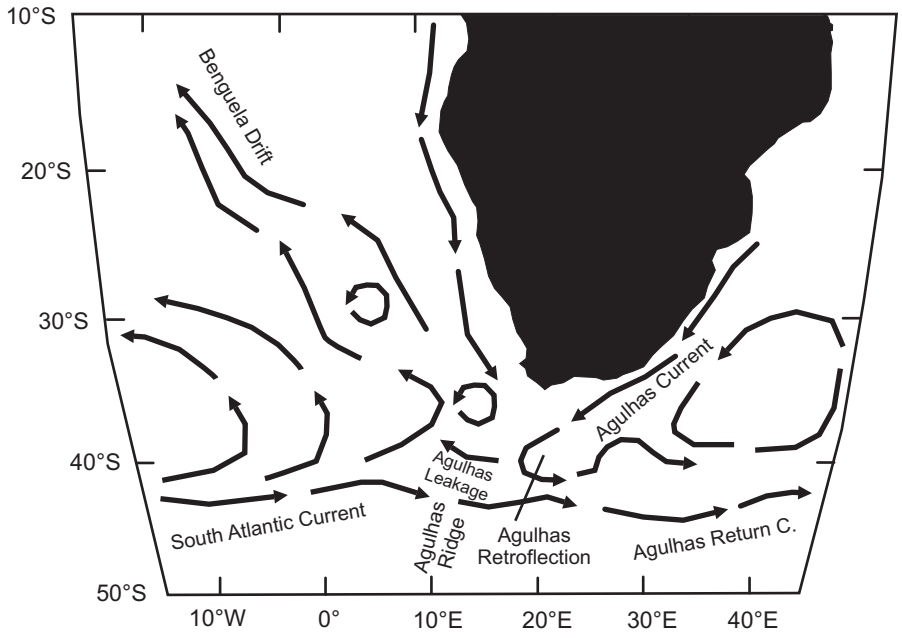

Figure 6: Schematic diagram of intermediate currents in the vicinity of South Africa.

Chapter 2

Calcareous Nannofossil record of temperature variation, nutrient availability and dissolution intensity during the Middle Eocene Climatic Optimum (MECO) at South Atlantic ODP Site 702

1. Introduction

The Eocene is an epoch still little known from a climatic and paleoceanographic point of view, in particular in the Southern Ocean, where Eocene records are scarce, and many of the available sedimentary successions are incomplete, due to the presence of hiatuses, or represented by non-carbonatic lithologies, preventing the study of calcareous microfossils as foraminifera (either assemblages and isotopes) and nannofossils.

In the past, the Eocene was considered a generally warm period, with stable climatic conditions; more recently, some authors (e.g. Zachos et al., 2001) highlighted the climatic variability of this period, characterized by a long term cooling trend starting right after the Early Eocene Climatic Optimum (EECO) (Zachos et al., 2001) (~53-51 Ma), one of the early Eocene hyperthermals. The cooling trend lasts up to the base of the Oligocene where it culminates in the Oi-1 event (Miller et al., 1991; Zachos et al., 2001) and is interrupted by a major warming phase, the Middle Eocene Climatic Optimum (MECO) (Bohaty and Zachos, 2003; Bohaty et al., 2009) at about 40 Ma.

Nannofossil assemblage analyses obtained in this work revealed that the Eocene cooling trend was actually interrupted, at least at ODP Site 702, by another significant warming phase occurring during Chron C19r (~42.5-41.5 Ma), which origin, characteristics and magnitude are still unknown.

The Eocene cooling has been associated to a gradual atmospheric CO_2 decrease (Pagani et al., 2005). However, a recent work (Bijl et al., 2009) questioned this hypothesis showing that the Eocene temperature decrease was not global but restricted to high latitudes.

The MECO represents a transient period of surface and deep ocean warming: global deep-sea foraminiferal $\delta^{18}O$ records indicate that warming was gradual, occurring over a ~500 kyr period, with peak temperatures reached near the base of Chron C18n.2n at ~40.1 Ma (Bohaty et al., 2009; Villa et al., 2008). Assuming no ice storage at poles during the middle Eocene, the negative $\delta^{18}O$ excursion at the MECO indicates a total increase of 4-6 °C in surface and deep water temperatures. The peak of the MECO has been coupled with a dissolution event involving all deep sea Sites (>3000 meters) (Bohaty et al., 2009), likely caused by a shoaling of the Carbonate Compensation Depth (CCD). The coupling of warming and CCD shoaling indicates that the cause of this event might be an increase in pCO_2 (Bohaty and Zachos, 2003; Bohaty et al., 2009), the origin of which is still unknown.
The Middle Eocene is considered a key period in the transition from the Greenhouse to the Icehouse. So far, only a few high resolution works have focused on the middle Eocene of the southern high latitudes (Bohaty et al., 2009). Some recent micropaleontological records spanning the MECO event are however available from the Tethys Ocean (Jovane et al., 2007; Luciani et al., 2010; Spofforth et al., 2010), the Atlantic Ocean (Edgar et al., 2010), and Indian Ocean (Villa et al., 2008).

In this work, we studied calcareous nannofossil assemblages from ODP Site 702 Hole B in the time interval between 43.6 and 39.3 Ma in order to 1) identify changes in the characteristics of sea surface waters, 2) to evaluate if dissolution affected the assemblages 3) at the light of the results of point 2, infer a paleoecological interpretation.The question related to dissolution are discussed first, followed by the paleoecological interpretation.

2. Materials and methods

Ocean Drilling Program (ODP) Site 702 Hole B was drilled during Leg 114. The site is located on the central part of the Islas Orcadas Rise in the Antarctic Sector of the South Atlantic Ocean (50°56' S, 26°22'W) (Fig. 1) at a water depth of 3083 m (~2300 m is the middle Eocene paleodepth).

The studied section spans the time interval between 43.6 and 39.3 Ma (late Middle Eocene) based on the time scale of Cande and Kent (1995).

A quantitative analysis of nannofossil assemblages was carried out on samples from Core 702B-8X to 2X, with a resolution interval of 40 cm, increased to 20 cm in correspondence of major paleoclimatic events or where relevant nannofossil assemblage changes were noted. Samples were prepared as smear slides and analyzed by optical microscope in cross-polarized light and in phase contrast, at 1250X magnification.

The carbonate content at Site 702 is persistently very high, with values from 85 to 90% (Ciesielski et al., 1988b). Nannofossil preservation at this site varies from good to moderate. In general, less etching and fragmentation and better preservation were noted in Cores 702B-10X, 11X and 12X, and a slightly more intense nannofossil fragmentation was seen in Cores 702B-8X and 9X.

At least 550 specimens/sample were counted, with additional traverses to find rare species and to refine the position of biostratigraphic events. Data and metadata were collected and processed using BugWin software. Taxa relative abundances were plotted as percentages except for plots used to show biostratigraphic events where abundances are shown as number of specimens/mm^2. In Fig. 2, the Highest Occurrence (HO) of *Reticulofenestra clatrata* and the Lowest Occurrences (LOs) of *Cribocentrum reticulatum* and *Dyctiococcites bisectus* are not evident in the graphs as those bioevents were identified by further scanning on traverses, so taxa abundance is extremely low and cannot be visualized in plots.

Bulk oxygen stable isotope record was used as proxy for temperature variations (Bohaty et al., 2009). A good and reliable magnetostratigraphy for Hole 702B is available (Ciesielski et al., 1988b; Clement and Hailwood, 1991) and ages of Chron boundaries were assigned using the timescale of Cande and Kent (1995).

In this study, the standard nannofossil zonation schemes (Martini, 1971; Okada and Bukry, 1980) were used, together with the high-latitude zonal scheme of Wei and Wise (1990b). The studied section spans nannofossil Zones NP15 *pars* to NP16 *pars* of Martini (1971), Zones CP13 *pars* to CP14a *pars* of Okada and Bukry (1980) and zones *Nannotetrina fulgens pars* to *Reticulofenestra reticulata pars* of Wei and Wise (1990b) (Fig. 2).

3. Results

3.1. Biostratigraphic events

At Site 702, five nannofossil events were recognized: three Lowest Occurrences (LO), one Highest Occurrence (HO) and one Highest Common Occurrence (HCO), all taking place between 42.48 and 40.00 Ma (Fig. 2, Tabs. 1, 2), identifying the time including the MECO, as a period of biotic turnover. These bioevents, in stratigraphic order, are the LO of *Reticulofenestra umbilicus* (98.05 mbsf, 42.48 Ma), the HO of *Reticulofenestra clatrata* (74.65 mbsf, 40.37 Ma), the LO of *Cribrocentrum reticulatum* (74.20 mbsf, 40.33 Ma), the LO of *Dictyococcites bisectus* (73.15 mbsf, 40.24 Ma) and the HCO of *Discoaster* spp. (71.15 mbsf, 40.06 Ma).

The **LO** of ***Reticulofenestra umbilicus*** (Fig. 2, Tab. 1) occurs between Samples 702B-11X-5-45 (98.25 mbsf) and 11X-5-5 (97.85 mbsf) (average depth: 98.05 mbsf). This event occurs at the base of Chron 19r, with an age of 42.48 Ma, and represents the zonal marker for the base of the NP16 (Martini, 1971), the CP14a (Okada and Bukry, 1980) and the *R. umbilicus* Zone (Wei and Wise, 1990b) .

The **HO** of ***R. clatrata*** (Fig. 2, Tab. 1) was found between Samples 702B-9X-2-65 (74.95 mbsf) and 9X-2-5 (74.35 mbsf) (average depth: 74.65 mbsf). This event was dated here at 40.37 Ma. At Site 748 (Kerguelen Plateau, southern Indian Ocean) this event was dated at 40.55 Ma (Villa et al., 2008) and was found in the same stratigraphic position at Site 738 (Maud Rise, south Atlantic Ocean) (Fioroni et al., 2010) (Tab. 2).

Following Villa et al. (2008), we suggest that species labeled *R. clatrata* represents the *Reticulofenestra onusta* reported in Wei et al. (1992) at Site 748.

The **LO** of ***Cribocentrum reticulatum*** (Fig. 2, Tab. 1) was identified between Samples 702B-9X-2-5 (74.35 mbsf) and 9X-1-125 (74.05 mbsf) (average depth: 74.20 mbsf), corresponding to an age of 40.33 Ma. This event is used as a zonal boundary marker by Wei and Wise (1990b), defining the base of *R. reticulata* Zone. The position of this event must be considered with caution since many *Reticulofenestra* specimens, showing the same characteristics in size and shape of *C. reticulatum*, but lacking the central cross, could not be indisputably identified. For this reason, some specimens of *C. reticulatum* might not have been recognized and, as a consequence, the real position of this bioevent could be slightly older. This event was dated at 42 Ma (Berggren et al., 1995) and at 41.2 Ma in some Southern Ocean sites (Marino and Flores, 2002; Wei, 2004; Wei and Wise, 1992). Villa et al. (2008) at Site 748 found this event at 40.67 Ma, but the presence of a hiatus makes it uncertain (Tab. 2).

The **LO** of ***Dictyococcites bisectus*** (Fig. 2, Tab. 1) was seen between Samples 702B-9X-2-125 (75.55 mbsf) and 9X-3-25 (76.05 mbsf) (average depth: 75.80 mbsf) with an age of 40.475 Ma but only one specimens was detected in this sample, and no specimens were found in the next seven samples. A continuous distribution of this species starts in Sample 702B-9X-1-25 (73.05 mbsf). This event, between Samples 702B-9X-1-45 (73.25 mbsf) and 9X-1-25 (73.05 mbsf) represents the Lowest Consistent Occurrence (LCO) of this species at Site 702 and is dated at 40.241 Ma.
Berggren et al. (1995) dated the LO of *D. bisectus* at 38 Ma, consistently with other results (Arney and Wise, 2003; Mc Gonigal and Di Stefano, 2002) but this event is most likely time-transgressive with latitude. The age assigned at Site 702 is comparable with results from Marino and Flores (2002) who dated this event at 40.13-41.257 at Site 1090 (South Atlantic), despite they identified it at the base of Chron C18r and not in the upper part of this Chron as seen at Site 702.
From the base of the studied section up to Sample 702-11X-6-45 (99.75 mbsf) many specimens similar to *D. bisectus* were found and were labeled here *Dyctiococcites* cf. *bisectus.* The two forms show a slight different proportion between the central area and

the rim and a subtle different birefringence. To avoid confusion, we preferred to consider them separately. Starting from Sample 702-11X-6-5 (99.35 mbsf) up to 9X-3-25 (76.05 mbsf) *D.* cf *bisectus* is absent. In the next upper sample, 702-9X-2-125 (75.55 mbsf) the first unmistakable specimen of *D. bisectus* was found. Studying nannofossil assemblages at Hole 702B, Crux et al. (1991) found similar results and identified the LO of *R. bisecta*/*R.* aff. *R. bisecta* in Chron C19r-C18r. If we consider our *D.* cf. *bisectus* equivalent to the *R.* aff. *bisecta* of Crux et al. (1991), our LO results older, being this taxon present from the base of the study section, corresponding to Chron C20n, with an age older than 43.57 Ma. The possible link between *D. bisectus* and *D. cf. bisectus* is unknown and seen their strong similarity they could represent morphotypes of the same species, but this would lead to some problems in correlating this event with previous works. Also, the absence of both *D. bisectus* and *D.* cf. *bisectus* from Samples 702-11X-6-5 (99.35 mbsf) to 9X-1-45 (73.25 mbsf) is some way unexplainable.

The **HCO** of ***Discoaster*** spp. (Fig. 2, Tab. 1) was found between Samples 702B-8X-6-45 (71.25 mbsf) and 8X-6-25 (71.05 mbsf) (average depth: 71.15 mbsf). The assigned age is 40.063 Ma. This event was proposed at ODP Site 748 (Villa et al., 2008) where it was dated 40.13 Ma. This event occurs in both sites at the same stratigraphic position, just before the peak of the MECO event. This correspondence highlights the paleoecological significance of this event, which seems to be linked to a change in surface water conditions occurring during the MECO. The interpretation of these biotic changes is given in Section 5.1.1..

3.2. The dissolution effect on nannoplankton and proposed dissolution proxies

Carbonate dissolution in the deep ocean can strongly modify original nannoplankton assemblages. The effect of dissolution on single nannofossil specimens can be at times obvious to the operator, but usually it is difficult to estimate only by optical evaluation. Analyzing two closely located ocean sites at different depth, Gibbs et al. (2004) demonstrated that visual evaluation at the optical microscope is not sufficient to correctly estimate the preservation state of nannofossil assemblages. The question

related to the effect of carbonate dissolution is of primary importance when nannofossil assemblages are used for paleoecological and paleoceanographic reconstructions. Dissolution can in fact alter the original assemblages and lead to mis-interpretations of species abundances and, as a consequence, of paleoecological preference. Furthermore, carbonate dissolution has been considered a proxy for surface water productivity (Diester-Haass et al., 1993; Diester-Haass et al., 1996) because dissolution in deep waters can be caused either by changes in water mass properties, or by production of CO_2 from disaggregation of the organic matter. Widely used dissolution proxies involve fragmentation of foraminifera tests (Diester-Haass et al., 1996) and the ratio between benthic and planktic foraminifera (Diester-Haass et al., 1996; Hooper et al., 1991). Other dissolution proxies are based on relative abundance between micropaleontological group, such as the ratio radiolarian/foraminifera (e.g. Peterson and Prell, 1985), the ratio pteropods/foraminifera (e.g. Berner, 1977) or the ratio nannofossils/foraminifera (e.g. Hay, 1970). Dissolution proxies based exclusively on calcareous nannofossil assemblages have also been proposed, mainly established on ranking of delicate and resistant species (Gibbs et al., 2004; Jiang and Wise, 2009; Roth and Thierstein, 1972) or on preservation state of selected taxa (Blaj et al., 2009; Hay, 1970; Matsouoka et al., 1991; Roth and W.H., 1975).

A detailed study of effects of dissolution on calcareous nannofossils was carried out by Jiang and Wise (2009) on a section spanning the Paleocene-Eocene Thermal Maximum from Kerguelen Plateau (southern Indian Ocean). Using nannofossil absolute abundances, Pearson correlation coefficients and stable isotope records, they estimated the degree of dissolution affecting assemblages during this major warming phase.

What it is needed to evaluate dissolution affecting carbonate within the sediment is 1) an *external* dissolution indicator; usually the carbonate content is used as a dissolution proxy but carbonate content itself depends on the balance between carbonate productivity and preservation, and by dilution with other sedimentary components. This implies that carbonate content is not sufficient to understand if nannofossil assemblages were affected by dissolution; 2) a dissolution indicator *within* the assemblage.

Taking into account all intrinsic limits of our approach, we tried to evaluate the degree of dissolution affecting nannofossil assemblages at Site 702 using the assemblage

components, by calculating ratios involving taxa more/less prone to dissolution. This approach is qualitative but it enabled to assess if fossil assemblages were impoverished or biased by dissolution, and to evaluate their use for paleoecological and paleoceanographic studies.

The visual evaluation of nannofossil preservation state at Site 702 indicates that etching and overgrowth affected assemblages, with different intensity, all along the section, but, at this stage, a quantitative evaluation of dissolution is not possible and a fragmentation index would be necessary. Nevertheless, we tried to assess the intensity of dissolution by using collected micropaleontological data, i.e. assemblage composition and taxa relative abundance.

A quantitative method to estimate dissolution intensity was used on sediments spanning the Eocene-Oligocene transition at Site 1090 (Agulhas Ridge, South Atlantic) and is described in Chapter 4 of this dissertation.

Dissolution is usually selective on calcareous flora/fauna in two different ways: it acts 1) at species level and/or 2) on single specimens. The first type of dissolution generally affects the smallest and/or the most delicate species, the second one affects specimen morphology by altering/eroding the shields or the central areas (Roth and Thierstein, 1972; Thierstein, 1980). Commonly, when dissolution acts on the most delicate specimens (e.g. holococcoliths, small specimens), dissolved carbonate overgrows on the most resistant forms (e.g. Discoasters). Major causes of dissolution can be the corrosiveness of intermediate waters and diagenesis. When calcareous nannofossils are sinking from the surface to the sea floor, and are not well protected by fecal pellets or marine snow, water under-saturated of carbonate attacks their calcite structure and carbonate goes dissolved into the water. During this process, intermediate waters play a major role in dissolving the carbonate. Diagenesis occurs once nannofossils are deposited on the sea floor and covered by sediment particles. Dissolution acting at this stage is related to the corrosiveness of bottom and interstitial waters and mostly derive from production of CO_2 by organic matter disaggregation. The final effect on nannofossil assemblages produced by the two processes is essentially the same, even if dissolution occurring within the sediment is usually coupled with overgrowth.

Some nannofossil species are particularly prone to dissolution, others are very resistant. This response depends mainly on the crystalline structure of coccoliths and on the ratio between volume and exposed area. Holococcoliths, i.e. coccoliths composed by tiny elements (<0.1 μm) having the same size and shape, are very susceptible to dissolution (Jiang and Wise, 2009; Thierstein, 1980; Wind and Wise, 1978).
An attempt to rank the species response to dissolution have been made by Gibbs et al. (2004), Jiang and Wise (2009) and Roth and Thierstein (1972).

3.2.1. Dissolution indices calculated by using calcareous nannofossil assemblage components

To separate the paleoceanographic signal given by nannofossils from the dissolution print on calcareous floral assemblages at Site 702, we calculated and tested indices of dissolution (Fig. 3). These dissolution indices are 1) The distribution of the holococcolith *Z. bijugatus*; 2) Ratio (*Chiasmolithu*s sp./ *Chiasmolithus* spp.)*100; 3) Ratio Unidentified rim/(unidentified rims+*R. daviesii*)*100; 4) the distribution of *Blackites* spp. These indices are described hereinafter.

a) Holococcolith *Z. bijugatus* distribution

Z. bijugatus is temperate (Villa et al., 2008) or warm (Bralower, 2002; Gibbs et al., 2006; Kahn and Aubry, 2004), oligotrophic (Agnini et al., 2006; Bralower, 2002; Kahn and Aubry, 2004; Wei and Wise, 1990b) or eutrophic (Tremolada and Bralower, 2004; Villa et al., 2008). As said, *Z. bijugatus* is an holococcolith, and as such is easily affected by dissolution (Jiang and Wise, 2009; Roth and Thierstein, 1972; Wind and Wise, 1978); as a consequence, it is not usually preserved at deep water sites. Despite being not as delicate as modern holococcoliths, *Z. bijugatus* is relatively prone to being dissolved because of its crystalline structure.
As general approach adopted at Site 702, the presence of *Z. bijugatus*, even in low abundances, indicates weak or null dissolution. Its absence might be explained by: 1) paleoecological factors, environmental conditions not favorable to this species. In this case its distribution pattern is pristine and reflects a response to paleoceanographic changes; 2) dissolution effect: *Z. bijugatus* was originally present but went dissolved.

Z. bijugatus distribution (Fig. 3b) shows three major phases of increase: from 111 to 100 mbsf, from 96 to 88 mbsf and from 71 to 63 mbsf. An absence interval (88-71 mbsf) within a higher abundance distribution, makes this species proper to discriminate between dissolution and paleoecological print.

b) Partially dissolved *Chiasmolithus*

Chiasmoliths are elliptical nannofossils composed by an oval rim of variable size with a X-shaped cross in the central area. The size of the rim, together with the shape of the central cross is the base of *Chiasmolithus* classification at species level.
Jiang and Wise (2009) demonstrated that the paleoecological signal of r-selective group *Chiasmolithus* is reliable and pristine even in assemblages strongly affected by dissolution. At Site 702, *Chiasmolithus* spp. are therefore taken into special account. Also, the analysis of the differential preservation state of the central crosses allows some further observations. The central cross of Chiasmoliths is very delicate and is only present in well preserved material; on the contrary, *Chiasmolithus* rims are very resistant. At Site 702 the great majority of genus *Chiasmolithus* are represented by specimens lacking the central cross, here labeled *Chiasmolithus* sp., demonstrating the delicacy of this structural part. Most likely, all unidentified specimens (*Chiasmolithus* sp.) are rims of *Chiasmolithus solitus* and *Chiasmolithus expansus*, two common middle Eocene species identified all throughout the section. *Chiasmolithus* spp. include all specimens belonging to genus *Chiasmolithus*.
The loss of the central cross is plausibly caused by dissolution and, a consequence, the ratio (*Chiasmolithus* sp./*Chiasmolithus* spp.) *100 can be considered as a rough indicator of dissolution (Fig. 3b). This ratio is high all along the section, reaching in some samples values as high as 98%, indicating that *Chiasmolithus* central cross is very delicate and goes easily dissolved or detached from the rim.

c) Unidentified rim relative abundance

At Site 702, many unidentified nannofossil elliptical or subelliptical rims were found all throughout the section, in variable abundance. The identification at species level of

these forms was impossible because of the lack of the central area, whose features are necessary for their taxonomic identification. Originally, all these rims were probably coccolith rims belonging to *Reticulofenestra daviesii* which were affected by selective dissolution, as shown by the mirroring patter of the abundances of *R. daviesii* and of unidentified rims (Fig. 3a). This result is not unexpected as small size species, such as *R. daviesii*, are more easily affected by dissolution compared to bigger species.

It was therefore assumed that the relative abundance of these rims is directly proportional to the intensity of dissolution. This new index was calculated as: unidentified rims/(Unidentified rims+*R. daviesii*)*100 (Fig. 3b).

It is possible that a small number of unidentified rims are remains of *C. reticulatum* and not *R. daviesii* group*;* this species was not considered within the index as *C. reticulatum* remains would certainly represent only a minor component of the unidentified rims. Specimens similar to *C. reticulatum,* but lacking the central cross, were in fact classified in a separated category, labeled *Cribrocentrum* cf. *reticulatum*.

The new index shows a strong variability throughout the section, reaching percentages as high as 57%. Values are high from 108 to 101 mbsf, from 94 to 90 mbsf, from 76 to 69 mbsf, and from 65 mbsf up to the top of the section, separated by intervals with very low values (Fig. 3b).

d) *Blackites* distribution

Blackites belongs to the Rhabdosphaeraceae family and are composed by a prominent central process and a basal ring constituted by one or two shields around a central area with one or more cycles of elements. In Site 702 samples, *Blackites* are only represented by *B. spinosus* and most of the specimens lack the base of the process.

Quantitative analysis of nannofossil assemblage distribution from lower Oligocene sediments at ODP Site 1090 (South Atlantic), described in Chapter 4 of this dissertation, unmistakably shows that *Blackites* distribution is mainly driven, at least at that site, by dissolution intensity, as shown by the perfect parallelism between *Blackites* relative abundance and the carbonate record (Fig. 2, Chapter 4). This confirms that the distribution pattern of this taxon is a reliable dissolution indicator.

The distribution pattern of *Blackites* is similar to *Z. bijugatus*', being both completely absent from ~88 to 74 mbsf (Fig. 3). This resemblance can derive from either an analogous paleoecological preference, or from a comparable response to dissolution.
Based on the comparison between these four indices successive phases were distinguished, in which nannofossil assemblages were differently affected by dissolution, as described in the Section 4.1.

4. Discussion

4.1. Effect of dissolution on nannofossil assemblages

From the base of the studied section up to 101 mbsf (Phase a in Fig. 3) all indices show high values. High ratios of unidentified rims are unexpected, considering the relatively high abundances of *Z. bijugatus* which suggest that no strong dissolution acted. In fact, if dissolution acted strongly on small *Reticulofenestra*e and *Chiasmolithus*, low abundances of *Z. bijugatus* would be expected. This can be explained by a different behavior of these groups with respect to dissolution: most likely the central crosses of *Chiasmolithus* and the central area of small *Reticulofenestra* go dissolved extremely easily, even in conditions of very low carbonate under-saturation. *Z. bijugatus*, despite its is a holococcolith, shows here to be quite resistant to dissolution, or, however, to be more resistant than the other taxa used to calculate the other indices. Based on these considerations, we deem *Z. bijugatus* as the best dissolution indicator among those used here. We infer that in this interval (111-101 mbsf), a moderate dissolution affected nannofossils, as indicated by high values of indices involving *Chiasmolithus* and unidentified rims. The presence of *Z. bijugatus* guaranties that no strong dissolution acted. At 101 mbsf, *Chiasmolithus* and unidentified rim indices, as well as *Z. bijugatus* abundance, decrease. On the contrary, *B. spinosus* increases in abundance.

Between 101 and 94 mbsf (Phase b in Fig. 3), *Chiasmolithus* index values gradually increases, unidentified rim ratio shows low and constant values, and *Z. bijugatus* and *Blackites* are present with variable abundances. The interpretation of this interval is based mainly on the signal given by *Blackites* and *Z. bijugatus*. Being both present,

even if in low abundances, at most a weak dissolution must have affected the assemblages. The fact that *Chiasmolithus* index has high values when other dissolution indices suggest a weak dissolution, confirms that *Chiasmolithus* central crosses are extremely delicate.

Between 94 and 88 mbsf (Phase c in Fig. 3), *Z. bijugatus* is relatively abundant, with two peaks at ~ 93 and 90 mbsf; *Blackites* is relatively abundant, too. Notably, both peaks in *Z. bijugatus* abundance (at 93 and 90 mbsf) correspond to negative peaks of unidentified rim and *Chiasmolithus* indices, and all nannofossil indices undoubtedly give a very consistent dissolution signal, indicating well-preserved material.

The interval between 88 and 74 mbsf (Phase d in Fig. 3) is characterized by the almost complete absence of *Z. bijugatus* and *Blackites*. This confirms the link between these taxa, whose distribution may be related to either a similar response to environmental conditions or to the same response to dissolution. During this phase, unidentified rim index is low compared to the previous interval, and *Chiasmolithus* index is highly variable. Therefore, if we are consistent with our interpretation of *R. daviesii* as prone to dissolution, the low abundances of unidentified rim index suggest for this phase weak dissolution, but this is contrast with the indication provided by high values of *Chiasmolithus* index. We rely on *R. daviesii* index, and the absence of *Z. bijugatus* and *Blackites* is interpreted as a response to unfavorable paleoclimatic conditions (see Section 4.3.).

Between 74 and 71 mbsf (Phase e in Fig. 3), *Z. bijugatus* is almost completely absent and *Blackites* reach relatively high values. Unidentified rim ratio increases compared to the previous phase. The presence of *Blackites* suggests here that the absence of *Z. bijugatus* is not caused by dissolution, but rather by climatic conditions that favored *Blackites* and not *Z. bijugatus*. This implies that their ecological preference is similar but not identical. High values of both unidentified rim and *Chiasmolithus* indices indicate that some dissolution acted here, but it was not strong enough to dissolve *Blackites* and most likely neither the rest of the assemblage. Our interpretation of weak or null dissolution acting within the phase is confirmed by the presence in relatively

high abundance of *Clausicoccus fenestratus* (Fig. 4a) which, similarly to *Blackites*, is strongly controlled by dissolution, as described in Chapter 4 of this dissertation. Furthermore, *Helicosphaera* (Fig. 8a) are basically absent along most of the section but a few specimens are present within this interval, suggesting very week or null dissolution.

At 71 mbsf, *Z. bijugatus* reappears in the assemblages with relatively high percentage values. Its distribution pattern from 71 mbsf to the top of the section (Fig. 3b) shows two phases of high abundance, interrupted by a short interval where this species is rare (~ 67-68 mbsf). In this interval (71-64 mbsf) (Phase f in Fig. 3b), unidentified rim and *Chiasmolithus* indices have similar characteristics and both show a trend of decrease. The high values of *Z. bijugatus* suggest that at most a weak dissolution acted within this interval. Possibly, a stronger dissolution might have affected the assemblages between the short interval from 67 to 68 mbsf, where *Z. bijugatus* and *Blackites* spp. abundances are very low, but this is not supported by low values of *Chiasmolithus* and unidentified rings indices, suggesting that no strong dissolution acted. We therefore interpret this interval (71-64 mbsf) as only affected by weak dissolution, and *Z. bijugatus* and *Blackites* low abundances between 67 and 68 mbsf represent a response to unfavorable climatic condition, as described in Section 5.1.1..

Ratios calculated using calcareous nannofossil taxa allowed us to evaluate if assemblages were moderately, weakly or not affected by dissolution. Nannofossil assemblage analysis revealed that no intense dissolution acted at Site 702. The simultaneous analysis of indices, also permitted to test their reliability and independence. Certainly, *Z. bijugatus* and *Blakites* are the most reliable indicators used in this work, guaranteeing, by their presence, that no strong dissolution acted. Differently, their absence does not ensure that dissolution did not act and, therefore, other dissolution indices are needed to distinguish the print of dissolution from the ecological signal. Both *R. daviesii* and *Chiasmolithus* showed to have an easily-dissoluble central area; unidentified rims index is useful and reliable in most cases, but the use of a comparison factor is advisable. Ratio involving *Chiasmolithus* is almost completely unreliable.

The contemporaneous use of several indices provided a better understanding of behavior of certain taxa toward dissolution. Based on this comparison, we infer that nannofossil assemblages along the studied section were not biased by dissolution effect. Seen that no strong dissolution affected nannofossil communities, their relative abundances are considered pristine and reliable, and are used here for paleoecologiacal and paleoclimatic reconstructions, as described in the following Section.

Bohaty et al. (2009) associated the MECO event with a global acidification of the ocean waters, attributed to a temporary shoaling of the CCD, probably caused by an increase of atmospheric CO_2. This ocean acidification affected Sites deeper than 3000 meters in all oceans, leaving untouched shallower sites (Bohaty et al., 2009). The middle Eocene paleo-depth of sea floor at Site 702 has been estimated to be around ~2300 m. No strong dissolution intervals were found in the studied section, not even at the peak of the MECO event. Our findings support Bohaty et al. (2009) interpretation, who showed that the position of the CCD was about 3000 m.

To be able to evaluate precisely the degree of dissolution affecting nannofossil assemblages, a quantitative analysis of nannofossil fragmentation would be required, similar to the one we carried out at ODP Site 1090 (Chapter 4 of this dissertation), where we demonstrated that nannofossil assemblage fragmentation is a very reliable dissolution proxy.

4.2. Paleoecological interpretation of the assemblages

Species recognized at Site 702 are classified following paleoecological interpretations given in the literature (Aubry, 1992; Bralower, 2002; Monechi et al., 2000; Tremolada and Bralower, 2004; Villa et al., 2008; Wei and Wise, 1990b) and by comparison between nannofossil abundance distribution curves with the oxygen and carbon stable isotope records from Site 702 (Bohaty et al., 2009).

To calculate paleoecological indices we only used species or groups of species with a well defined and confirmed paleoecological interpretation. Even if species with very low abundances are not usually considered because of their low statistical significance, some of them are used here. In fact, for the paleoecological interpretation of the entire

section, even distribution patterns of some minor components are found to be relevant, and their paleoecological signal, together with major paleoecological group characteristics, provides a more complete and consistent paleoclimatic frame of the studied period.
Hereinafter, paleoecological interpretations found in the literature are given, together with the discussion about species/group of species distribution seen at Site 702.

Coccolithus pelagicus

C. pelagicus abundance is around 25% of the total assemblages along most of the section. Two phases of more pronounced increase are present between 92 and 88 mbsf, and between 76 and 74 mbsf, where abundances reach almost 50% (Fig. 4a).
This species has been considered warm (Wei and Wise, 1990a; Wei and Wise, 1990b) or temperate (Villa et al., 2008), but it has changed its ecological preference through time since Pleistocene, and living *C. pelagicus* prefer cold (Haq and Lohmann, 1976) or cold and mesotrophic (Holmes et al., 2004) and/or eutrophic waters (Cachao and Moita, 2000). We interpret *C. pelagicus* as a temperate form, in agreement with Villa et al. (2008).

Reticulofenestra umbilicus group

R. umbilicus group (composed by *R. umbilicus*, *R. hillae*, *R. samodurovi* and *R. dictyoda*) shows a higher variability compared to *C. pelagicus*, with abundances varying from about 5 to 40% (Fig. 4a). Average values of ~18% are maintained from the base of the section up to 88 mbsf; a significant increase is shown between 88 and 76, followed by a short drop between 73 and 74 mbsf. Between 73 and 71 mbsf an increase in abundance is recorded, followed by a return to mean values.
R. umbilicus group has been considered temperate (Persico and Villa, 2004; Villa et al., 2008; Wei and Wise, 1990b), warm and oligotrophic-mesotrophic (Aubry, 1992), and warm and mesotrophic (Monechi et al., 2000). *C. pelagicus* and *R. umbilicus* group have similar paleoecological preferences, as shown by their similar distribution (Fig. 4a). A mirroring patter between these two groups is evident from about 88 mbsf up to

the top of the section. In general, *C. pelagicus* is slightly more abundant where also Discoasters are more abundant and this may indicate a slender preference or a better tolerance of *C. pelagicus* toward oligotrophic waters, compared to *R. umbilicus* group.

Chiasmolithus spp.

Chiasmolithus spp. (*C. solitus*, *C. expansus* and *Chiasmolithus* sp.) (Fig. 4a) have a distribution pattern similar to *R. umbilicus* group, but the maximum abundance reached by this group is around 15%. A slight decrease in abundance occurs from the base of the section up to 100 mbsf. Between 100 and 82 mbsf, abundances are more constant, being around 8%. Between 82 and 76, an increase in abundance occurs and *Chiasmolithus* spp. reaches their highest values (~18%). This is then followed by a gradual decrease from 76 until 70 mbsf. From 70 up to the top of the section, another increase in abundance occurs.

Chiasmolithus are considered cool/cold (Bralower, 2002; Firth and Wise, 1992; Tremolada and Bralower, 2004; Villa et al., 2008; Villa and Persico, 2006; Wei and Wise, 1990a; Wei and Wise, 1990b). We interpret *Chiasmolithus* as mainly controlled by temperature, but a dependence from other ecological factors is suggested by the strong similarity between this taxon and *R. umbilicus* group; this may be related to a similar preference for eutrophic conditions. The paleoecological preference of *R. umbilicus* group for temperate waters is well established, so we suggest that its similarity with *Chiasmolithus* distribution may derive from the same preference for higher nutrient availability.

R. daviesii group extended

R. daviesii group extended (*R. daviesii*+ *Reticulosfenestra* sp. (3-5 μm)+unidentified rims) is the most abundant component of the assemblages, and varies from ~20% to almost 50% (Fig. 4a). Two phases of decrease occur between about 100 and 88 mbsf and between about 74 and 71 mbsf.

R. daviesii is considered as cold (Wei and Thierstein, 1991) or cool (Monechi et al., 2000; Persico and Villa, 2004; Villa et al., 2008; Villa and Persico, 2006; Wei et al.,

1992). At Site 702, *R. daviesii* group *extended* is regarded as cool. A slightly less pronounced decrease is shown by this group in correspondence of the other warming event occurring in correspondence of the isotopic MECO. To emphasize the paleoecological signal in terms of temperature variation, *R. daviesii* group *extended* and *Chiasmolithus* spp. have been grouped in *Cool-water taxa* (Fig. 5). A similar approach is also followed for species with a different preference (warm, temperate, oligotrophic and eutrophic).

***Discoaster* spp.**

At Site 702, *Discoaster* spp. are scarce (Fig. 4b), with maximum values never higher than 5%, but two well-defined phases of higher abundances occur between 98 and 88 mbsf, and between 75 and 72 mbsf. Discoasters are consistently considered warm and oligotrophic (Aubry, 1992; Bralower, 2002; Gibbs et al., 2006; Kahn and Aubry, 2004; Kelly et al., 1996; Tremolada and Bralower, 2004; Villa et al., 2008). The paleoecological significance of Discoasters is considered here extremely reliable thanks to the strong preference of this group for warm and oligotrophic waters and to their strong resistance to dissolution (e.g. Blaj et al., 2009; Gibbs et al., 2004; Jiang and Wise, 2009). We therefore associate the two phases of higher *Discoaster* abundance to warming phases, almost certainly associated to oligotrophic conditions. The oldest warming phase occurs between about 42.5 and 41.5 Ma, in correspondence of Chron C19r (labeled here *C19r warming event*). The youngest warming phase as recorded by Discoasters occurs between 40.5 and 40.1 Ma, in general correspondence with the isotopic MECO event (Fig. 4). A focus on the time interval spanning the MECO event is described in Section 5.1.1. and is shown in Fig. 8. This closer look and the detailed analysis of nannofossil assemblage variations, revealed that *Discoaster* distribution during the MECO event is most likely driven by fertility change, rather than temperature.

Ericsonia formosa

E. formosa (Fig. 4b) has quite constant and low abundances (~1%) along most of the section, but with two major phases of enhanced abundance, between 93 and 87 mbsf, and between 75 and 70 mbsf. The similarity between the distribution of *E. formosa* and *Discoaster* spp. suggests a similar paleoenvironmental preference towards warm waters. The increase in abundance of *E. formosa* during the *C19r warming event*, occurs when *Discoaster* spp. abundance is gradually decreasing and this may suggest a preference of *E. formosa* for more eutrophic waters compared to Discoasters, as previously suggested Agnini et al. (2009). This species has been interpreted as a warm (Monechi et al., 2000; Villa et al., 2008; Wei et al., 1992; Wei and Wise, 1990b) and oligotrophic (Bralower, 2002; Tremolada and Bralower, 2004; Villa et al., 2008) or warm/eutrophic (Agnini et al., 2009). At Site 702, *E. formosa* is interpreted as a warm water taxon with a preference for mesotrophic/eutrophic waters.

Blackites spp.

Blackites spp. (Fig. 4b) are rare at the base of the section up to 100 mbsf. A well-defined increase in abundance occurs between 100 and 88 mbsf. Between 88 and 74 *Blackites* are very rare, only showing a little pulse at ~78 mbsf. At 74 mbsf, they "reappear" in relatively high abundance up to 69 mbsf. From 69 mbsf, their abundance decrease again. No paleoecological interpretations are available in the literature about this taxon. Wei and Wise (1990a) suggest that *Blackites* distribution is not temperature controlled.

Sphenolithus spp.

Most of *Sphenolithus* found at Site 702 consist of *S. moriformis* and are constantly present all throughout the section even if in low abundances (Fig. 4b). *Sphenolithus* distribution at Site 702 confirms their preference for warm waters, as shown by generally higher abundances where Discoasters and *E. formosa* are also abundant, but opens some questions about their interpretation with respect to nutrient conditions.

Sphenoliths have been considered warm and oligotrophic (Bralower, 2002; Gibbs et al., 2006; Villa et al., 2008) but several studies have recently pointed out a species-dependant preference towards nutrients availability (Agnini et al., 2006; Dunkley Jones et al., 2008; Gibbs et al., 2006). The general more pronounced similarity of *Sphenolithus* distribution to *E. formosa* compared to Discoasters could suggest a preference or a better tolerance for this taxa toward nutrient enriched waters.

Neococcolithes dubius

Neococcolithes dubius (Fig. 4b) is another minor component of the assemblages, with values spanning from 0 to about 3%. Abundances are around 3% in the lower part of the section up to 98 mbsf, then they are slightly higher from 98 to 92 mbsf. From 92 to 74, *N. dubius* is almost absent. A distinct abundance increase is then shown from 74 mbsf to the top of the section. The paleoecological preference of this species is not well constrained. It has been interpreted as a near-shore taxon (Mikes et al., 2008) and as a temperate form with some preference for eutrophic conditions (Villa et al., 2008). Here we interpret *N. dubius* as a temperate form because its distribution is similar to *Discoaster* and *E. formosa* distribution (Fig. 4b). The interval of highest abundance of this species occurs during the C19r *warming event*, when Discoasters are also abundant. Therefore, a preference of *N. dubius* for oligotrophic waters is proposed.

Zygrablithus bijugatus

Holococcolith *Z. bijugatus* (Fig. 4b) is extremely variable in abundance; higher abundances are reached from the base up to 88 mbsf, and from 71 mbsf up to 63 mbsf. This interval of higher abundance in the upper part of the section is interrupted, between 67 and 69 mbsf, by an interval of lower abundance. Between 87 and 71 mbsf, this species is almost completely absent. This species is temperate (Villa et al., 2008) or warm (Bralower, 2002; Gibbs et al., 2006; Kahn and Aubry, 2004), oligotrophic (Agnini et al., 2006; Bralower, 2002; Kahn and Aubry, 2004; Wei and Wise, 1990b) or eutrophic (Tremolada and Bralower, 2004; Villa et al., 2008). We interpret *Z. bijugatus* as temperate and oligotrophic.

Cyclicargolithus floridanus

At site 702, *C. floridanus* does not show a clear paleoecological preference (Fig. 4a). It is present along the section with very variable abundances and there is no clear similarity with other nannofossil distributions. Contrasting interpretations are present in the literature: some authors proposed a preference for eutrophic waters (Dunkley Jones et al., 2008; Monechi et al., 2000), for temperate waters (Wei and Wise, 1990a), for temperate-cool waters (Bukry, 1973), for eutrophic/temperate-cold waters (Aubry, 1992); other authors suggested no temperature dependence (Persico and Villa, 2004). The interpretation of *C. floridanus* as eutrophic is not confirmed at Site 702 as it is present in high abundances when also Discoasters are abundant. At Site 702, *C. floridanus* acts as an opportunistic species, able to adapt to different climatic conditions. For these reasons, *C. floridanus* is not considered here in any paleoecological group.

Reticulofenestra clatrata

The interval of highest abundance of this species (97-83 mbsf) coincides with the *C19r warming event* recorded by Discoasters and *E. formosa* (Fig. 4b) and therefore, it is considered as a temperate/warm water taxon. Despite the preference of this species toward warm waters is patent, we decided not to include *R. clatrata* in any paleoecological group because of the lack in the literature of comparative paleoecological interpretations.

Markalius inversus

Markalius inversus is very rare and its abundance reaches at most 1% of the total assemblage (Fig. 4b). Similarly to several other taxa, this species is basically absent in the middle part of the section, between 87 and 74 mbsf. Below 97 mbsf, its presence is very changeable. From 74 to 71 mbsf, *M. inversus* abundance is higher, and this phase is followed by an interval of absence up to the top of the section. The paleoecological preference of *M. inversus* is quite uncertain. Gibbs et al. (2006) suggested that this species thrives in stressed environments. Even if *M. inversus* abundance at Site 702 is

constantly very low (<1%), an ecological preference is however evident, having its highest abundances when other warm species such as *Discoasters*, *E. formosa* or *Sphenolithus* are abundant, indicating a preference for warm waters.

Clausicoccus fenestratus

C. fenestratus abundance varies from 0 to 4% (Fig. 4a). Wei and Wise (1990a) suggested that *C. fenestratus* prefers temperate waters, based on the study of an Eocene to Oligocene latitudinal transect along the South Atlantic, where this species decreases in abundance from lower to higher latitudes. An acme of *Clausicoccus* was found in the lower Oligocene at high southern latitudes (e.g. Chapter 1 of this dissertation, Marino and Flores, 2002; McGonigal and Di Stefano, 2002; Wei and Wise, 1990a), suggesting a preference for cold waters. At Site 702, the paleoecological preference of this species is not apparent and for this reason it was not to included in any paleoecological group.

Further indices to evaluate dissolution effect on nannofossil assemblages

As described in Section 4.1., we think that weak or at most moderate dissolution acted at Site 702 in the late middle Eocene. To test these conclusions and to verify that dissolution did not bias nannofossil assemblage paleoecological interpretation, we compared paleoecological indices (Fig. 6) obtained by using: 1) species having both a well defined paleoecological interpretation *and* a strong resistance to dissolution; 2) species with a well defined paleoecological interpretation, but regardless of their sensitivity to dissolution. This way, if both indices provide a similar paleoecological picture, this would confirm that dissolution did not strongly affect the assemblages and did not change assemblage characteristics in a way to modify their paleoeclimatic signal. For the paleoecological interpretation, we used ratios between species abundances expressed as the pristine numbers. This way, single species abundances are independent from other species variations.

The first index (Fig. 6) was calculated only using dissolution-resistant taxa:

1A) (*Discoaster* spp.+ *Sphenolithus* spp.+ *E. formosa*)/ (*Discoaster* spp.+ *Sphenolithus* spp.+ *E. formosa*+ *Chiasmolithus* spp.)*100.

A similar index (Fig. 6), but also involving species dissolution prone was calculated as:

1B) (*Discoaster* spp.+ *Sphenolithus* spp.+ *E. formosa*)/(*Discoaster* spp. + *Sphenolithus* spp. +*E. formosa*+ *Chiasmolithus* spp.+ *R. daviesii* group)*100.

As discusses above, *Discoaster* spp., *Sphenolithus* spp. and *E. formosa* are warm water taxa, *Chiasmolithus* spp., and *R. daviesii* group are cool forms, so both of these ratios also represent temperature indices, with higher values corresponding to warmer temperatures.

Comparison between 1A) and 1B)

The two calculated indices are very similar (Fig. 6) and give a similar paleoclimatic signal. This confirms that dissolution has not significantly modified nannofossil assemblages. Two major phases of increase, confirm the presence of two warming phases, one corresponding to the *C19r warming event*, and the other one to the isotopic MECO.

Additional indices were calculated, the first one composed only by dissolution resistant taxa:

2A) (*C. pelagicus*+ *R. umbilicus group*)/(*C. pelagicus*+ *R. umbilicus* group+ *Chiasmolithus* spp.)*100

As discussed above, *C. pelagicus* and *R. umbilicus* group are temperate, *Chiasmolithus* spp. are cool. The second comparison index, also involving species sensitive to dissolution, was calculated as:

2B) (*C. pelagicus*+ *R. umbilicus group*)/(*C. pelagicus*+ *R. umbilicus* group+ *Chiasmolithus* spp.+ *R. daviesii* group)*100

Comparison between 2A) and 2B)

The comparison between indices 2A and 2B provides the same general paleoecological picture even if differences between these two indices are slightly more pronounced than between indices 1A and 1B.

Evidence provided by these indices (1A, 1B and 2A, 2B) confirm that nannofossil assemblages at Site 702 are not significantly affected by dissolution during the studied time interval and therefore they can be used for paleoceanographic reconstructions (Section 4.3).

4.3. Paleoecological groups

Species with the same paleoecological preferences were grouped together in *cool*, *warm* and *temperate* water taxa, following an approach proposed by Wei and Wise (1990a) and also used by Villa et al. (2008) (Fig. 5a) in order to stress the paleoecological signal and to compare it with the oxygen stable isotope record. Also, species with the same preference toward nutrient conditions were grouped together, even if in this case the interpretation is less robust because of the lack of comparative proxies (Fig. 5b).
Also, a temperature index (Fig. 5a, top right), representative of the relative abundance between cool, warm and temperate taxa was calculated as:
*(Temperate water taxa+ Warm water taxa)/ (Temperate water taxa+ Warm water taxa+ Cool water taxa)*100*, following the approach of Villa et al. (2008).

R. umbilicus group, *C. pelagicus*, *Z. bijug*atus and *N. dubius* are considered as temperate water taxa, *Discoaster* spp., *Sphenolithus* spp., *E. formosa* and *M. inversus* as warm-water taxa, *Chiasmolithus* spp. and *R. daviesii* group *expanded* as cool-water taxa. Based on the comparison between these three paleoecological groups and the calculated temperature index (Fig. 5a, 7a), several paleoclimatic phases are recognized and interpreted as a response to surface water temperature changes. In addition to these temperature indices, the ratio *R. umbilicus*/*R. umbilicus* group (%) is used, as, being *R. umbilicus* the largest representative of the group (≥14 μm), it probably has a stronger preference for warmer waters. To try to assess variations in surface water nutrient conditions, also taxa with the same preference for oligotrophic or mesotrophic/eutrophic waters, were grouped. *Z. bijugatus*, *Discoaster* spp., *C. reticulatum* and *C.* cf. *reticulatum* are considered as oligotrophic; *R. daviesii* group, *Chiasmolithus* spp., *E. formosa*, *Sphenolithus* spp., *M. inversus*, *Helicosphaera* spp., *C. pelagicus* and *R. umbilicus* group are considered as mesotrophic/eutrophic. Similarly to the temperature

index, the ratio oligotrophic taxa/(oligotrophic+ mesotrophic/eutrophic taxa)*100 (nutrient index) was calculated: higher values of this index indicate enhanced oligotrophic conditions

All paleoecological groups are shown in Fig. 5 (against depth) and in Fig.7 (against age).

***R. umbilicus*/*R. umbilicus* group**

Because of its bigger size (> 14 μm), *R. umbilicus* might prefer higher temperature compared to other medium sized *Reticulofenestrae*. To test this hypothesis and to use this as a potential temperature indicator, the ratio *R. umbilicus*/(*R. umbilicus*+ *R. samodurovi*+ *R. hillae*+ *R. dictyoda*)*100 was calculated (Figs. 5, 7). At 98.05 mbsf (42.48 Ma), *R. umbilicus* has its Lowest Occurrence (Figs. 2, 5). *R. umbilicus*/*R. umbilicus* group (%) ratio is highly variable but average values are higher in correspondence of the two major warming phases previously recognized, the *C19r warming event* and the MECO interval. Thus, these data suggest that all species belonging to the *R. umbilicus* group thrives in temperate waters but *R. umbilicus* has a slight stronger preference for warmer waters.

Warm forms show the most pronounced variations, with two major phases of increase between ~42.5 and 41.5 Ma and between ~40.5 and 40.0 Ma. Warm-water taxa signal is mainly controlled by *Discoaster* abundance, and in a minor way, by other warm forms. Cool water taxa also show a marked variability, with abundances spanning from ~25% and 60%. Temperate-water taxa are the less variable in abundance, showing only two significant wanes, at ~41.6 and at 40.0 Ma.

Because temperate forms are the most abundant within the assemblages, the temperature index signal (Fig. 7b) is mainly controlled by temperate taxa relative abundance. For this reason, the print of warm water taxa, which are present constantly in low abundances, is hidden within the index. As a consequence, the calculated temperature index only roughly represents the variations of the paleoecological groups, but separated signals of cool, warm and temperate taxa have to be preferred for a more complete and detailed interpretation.

Thanks to paleoecological group variations, several climatic phases have been recognized which are indicated in Fig. 7 as colored bands. Two major warming events characterize the studied time interval at site 702. The oldest warming phase (42.5- 41.5 Ma) (*C19 warming event*), is also characterized by oligotrophic conditions, as indicated by the strong increase of *Discoaster* spp. The second one, corresponding to the isotopic MECO event (~40.5-40.0 Ma), can be divided in different paleoclimatic phases (Fig. 8), mainly interpreted by using abundance variations of minor components of nannofossil assemblages. Section 4.3.1. focuses on the interpretation of the MECO warming event as recognized by nannofossils. These two major warming phases (*C19r warming* and the MECO events) are separated by a period (41.5-40.5 Ma) characterized by temperate and mesotrophic/eutrophic waters (Fig. 7) which corresponds to the Pre-MECO cooling phase of Bohaty et al. (2009).

4.4. Paleoclimatology

4.4.1. The MECO warming event and the Post-MECO cooling phase

To better characterize in term of temperature and fertility the MECO event, we focused on sediments from 78.5 to 63.5 mbsf, corresponding to the time interval between ~43.6 and ~39.5 (Fig. 8).

Within this interval shows a decrease of cool *Chiasmolithus* spp. from the base up to about 69.5 mbsf, followed by an increase up to the top of the section.

R. daviesiii group shows a broad mirror pattern, high remarking how these two groups, *Chiasmolithus* spp. and *R. daviesii* group, are complementary and compete for the same niche within the assemblage. In this interval, as well as all along the section, *C. pelagicus* and *R. umbilicus* group constitute the other major components of nannofossil assemblages, and show a mirroring pattern, indicating a mutual relation similar to the one existing between *Chiasmolithus* and *R. daviesii* group.

The interpretation of the MECO event by the point of view of nannofossils was carried out considering, together with these major groups, also minor components, as shown in the Fig. 8a. Despite these species only represent a small part of the assemblages, their

distribution provides important paleoecological information, when compared with signal given by major groups.

From 78 to 74.5 mbsf (Fig. 8b), temperate forms are slightly more abundant than cool forms, and warm taxa are rare. This interval is likely characterized by temperate waters. The fertility level is difficult to evaluate even if low abundance of *Discoaster* spp. and the slightly higher abundance of *R. umbilicus* group compared to *C. pelagicus* suggests that waters have some eutrophic character. Within this interval, *R. umbilicus* group abundance is slightly decreasing and *C. pelagicus* abundance is increasing (Fig. 4a). The gradual switch in distribution of these temperate taxa may be related to variations in nutrient conditions.

At 74.5 mbsf, warm-water taxa abundance starts to increase (Fig. 8b) and minor components of the assemblages show subsequent peaks in abundance (arrow in Fig. 8a): *E. formosa* and *Blackites* spp. are the first taxa giving evidence of the beginning of the warming phase (Phase A in Fig. 8), with an increase in abundance between 74.5 and 73.5 mbsf. This phase is followed between 73.5 and 72.75 mbsf by a strong increase in abundance of Discoasters (Phase B in Fig. 8). At 72.5 mbsf *Sphenolithus* win the day on Discoasters (Phase C in Fig. 8). Phase C corresponds to the peak of the isotopic MECO. From ~71.5 to ~70.5 mbsf, interval where oxygen isotopes identify the latest phase of the MECO event, none of the mentioned taxa dominates compared to the other ones and all of the minor components are equally present (Phase D in Fig. 8). At 70.5 mbsf, the cooling phase begins as warm taxa decrease significantly in abundance.
Interestingly, all of the taxa switching in abundance during the MECO event belong to warm water taxa. This behavior reflects environmental changes that we interpret as being related to nutrient availability changes, coupled with temperature variations.

Phase A (Fig. 8) represents the beginning of the main warming phase associated with the MECO as recorded by nannofossils. During this phase, *Blackites* shows a sudden increase in abundance, followed by an increase of *E. formosa*. Temperate and cool forms do not show significant variations, with only a slight increase and decrease,

respectively. Warm water taxa shows a marked increase, giving evidence of a warming phase.

During **Phase B** (Fig. 8), Discoasters show a positive peak in abundance, temperate forms show a slight decrease, and cold water an increase. The paleoecological signal provided by Discoasters is considered reliable, indicating warm and oligotrophic waters.

The following **phase** (**C**) starts at the switching in abundance between *Discoaster* spp. and Sphenoliths (Fig. 8a). This phase corresponds to the main part of the isotopic MECO where the lowest oxygen isotope values are reached. The decrease in abundance of warm Discoasters (at 72.5 mbsf), right during the warmest period, occurs simultaneously with an increase in abundance of Sphenoliths. During phase C, cool taxa show a negative abundance peak (Fig. 8b). Phase C is also characterized by the presence of rare eutrophic *Helicosphaera* (Fig. 8a). We interpret the decrease of oligotrophic Discoasters, together with the increase of Sphenoliths, Helicosphaerae and *R. umbilicus* group, as a signal of nutrient availability change, from oligotrophic to mesotrophic/ eutrophic conditions.

During **phase D** (71.5-70.5 mbsf) (Fig. 8), warm and temperate forms have lower values compared to the previous phase and identified a gradual cooling, confirmed also by the increase in abundance of cool-water taxa.

During **phase E** (67.75-67.25 mbsf) (Fig. 8), *Z. bijugatus* shows a particular distribution pattern: after being almost completely absent for a long part of the section, it reappears relatively abundant, right in correspondence of the cooling phase recorded by nannofossils at 70.5 mbsf. Within this interval, also *C. reticulatum* is much more abundant compared to the previous phase. Both *Z. bijugatus* and *C. reticulatum* distribution indicate that phase E is likely oligotrophic. The lack of oligotrophic Discoasters is caused by cool conditions, unfavorable for this taxon.

Within **phase F** (67.75 and 67.25 mbsf) (Fig. 8), warm taxa *E. formosa* and *Sphenolithus* spp. are relatively abundant, temperate species show a general increase,

and cool taxa a decrease (Fig. 8). The fact that the two eutrophic species *E. formosa* and *Helicosphaera* spp. experience an increase in abundance at this level suggests waters rich in nutrients, supported also by the drop of oligotrophic *Z. bijugatus* and *C. reticulatum*. The interpretation of this interval as a transient warming phase is supported by oxygen isotope record which shows a decrease in values (Fig. 8a).

Nannofossil assemblage variations confirm that the isotopic MECO corresponds to a sea surface temperature increase also at Site 702, as shown by abundance fluctuations of nannofossil paleoecological groups (Fig. 8). The causes of this warming are still uncertain but several hypothesis have been proposed, such as a release of methane and/or CO_2 into the atmosphere (Bohaty and Zachos, 2003; Bohaty et al., 2009). A release of methane seems unlikely because the MECO is not associated to a decrease of $\delta^{13}C$ values, differently for example from the Paleocene-Eocene Thermal Maximum (e.g. Bice and Marotzke, 2002). It is possible that the warming occurring at the MECO was caused by a transient increase in atmospheric CO_2, whose origins are still unknown. Using new molecular paleothermometry at a southwest Pacific ODP Site 1172, Bijl et al. (2010) found that the MECO corresponds to a 3-6°C warming of the sea surface waters and was accompanied by an increase in pCO_2.

Volcanic activity (hot spots and/or ocean ridge), metamorphic decarbonation and increased carbonatite magmatism have been proposed as possible causes of the warming and acidification (involving only at sites deeper than 3000 meters) occurring at the MECO (Bohaty and Zachos, 2003; Bohaty et al., 2009). Indication of intensified volcanic activity has been found along the Pacific rim (Cambray and Cadet, 1996) but there is no other evidence of strong volcanism in the late middle Eocene. Furthermore, to cause a 500 kyrs warming, like the one associated to the MECO, a continuous and sustained activity would be necessary to guarantee constant and high CO_2 levels in the atmosphere. Metamorphic decarbonation seems a more plausible cause: enhanced metamorphism of carbonate rocks, perhaps in the Himalayan region (Kerrick and Caldeira, 1994), can have caused a prolonged release of CO_2 in the atmosphere.

4.4.1.1. Possible causes of increased nutrient availability at the peak of the MECO

The initial part of the MECO is characterized by warm and oligotrophic waters, followed by a switch to more eutrophic conditions at the peak of the event (Fig. 8). This eutrophic phase has a very short duration (~10 krs) and is delimited by the decrease in abundance of *Discoaster* spp. and the marked increase in abundance of *Z. bijugatus* and *C. reticulatum* at ~40.0 Ma. The almost complete disappearance of *Discoaster* spp. after 40.0 Ma is interpreted as caused by the cold temperatures following the MECO event, (cooling B of Villa et al. (2008) or *post-MECO cooling phase* of Bohaty et al. (2009)), as shown by the decrease in abundance of warm and temperate forms and by the recovery of cool taxa (Fig. 8b).

The increase in nutrient availability seen at the peak of the MECO might be caused by increased upwelling but the location of Site 702, in the central part of a oceanic rise, seems not to facilitate vertical movements of deep waters to the surface. Also, the South Atlantic Ocean during the middle Eocene was probably stratified (Scher and Martin, 2006) and vertical mixing was limited (Mead et al., 1993).

Another possible explanation for the increased fertility is that during the peak of the warming event, continental runoff and weathering increased, discharging nutrients to the ocean. This is plausible but there is no further evidence for such a mechanism, and the location of Site 702 in the middle of the South Atlantic, far away from continents, does not support this hypothesis.

A third possible cause can be enhanced volcanic activity in the South Atlantic, which might have released nutrients such as phosphorous and iron. New spreading centers and a large basin formed in the Paleogene between the Islas Orcadas Rise and the Meteor Rise and it is possible that the new tectonic activity was accompanied by release of nutrients. This theory suffers from the lack of a precise timing of the spreading event.

Being the warming at the MECO global in character, the possible enhanced volcanism occurring in the South Atlantic did not work as a major cause but as a positive feedback which might have strengthened the warming and triggered nutrient release into the ocean waters. However, if warming and eutrophication also derived from local submarine volcanic activity, CO_2 would have been released, together with nutrients, inducing carbonate dissolution, either in the water column or at the sea floor, which did not happen at Site 702, as demonstrated in Section 4.1..

Also, the very short duration (10 krs) of the eutrophic phase during the peak of the event, would correspond to a extremely limited volcanic event. A switch from oligotrophic to eutrophic conditions during the MECO was also found by Edgar (2008) studying foraminifera assemblages from the central-North Atlantic and was explained as caused by an increase in continental runoff, or upwelling or nutrient release from volcanic activity.

4.4.2. The C19r warming event

Nannofossil assemblages clearly show a significant warming event affecting sea surface waters between 42.5 and 41.5 Ma (Fig. 7). This event is also accompanied by oligotrophic conditions as shown by high abundances of Discoasters.

This event lasts about 1 m.y. at this site and spans most of Chron C19r (Fig. 7). A warming phase in the upper part of Chron C19r was also recognized in the equatorial Atlantic (Edgar et al., 2007), but it was of a much shorter duration (<100 krs) compared to the event seen at Site 702. The event recognized by Edgar and co-authors was also associated to a marked shift of both oxygen and carbon isotopes, and to a dissolution event, differently from what seen at Site 702, where no significant dissolution acted and no marked variation of the isotopic values is recorded. A relation between the equatorial and subantarctic Atlantic event cannot be established at this stage, and further studies on other Atlantic sites are necessary to establish their local or wider character. In the literature, there are not other indications of warming events in the Southern Ocean occurring during this time interval, most likely because of the lack of middle Eocene available records.

Two mechanisms are proposed as possible causes of the *C19r warming event* at Site 702: CO_2 increase or the effect of some warm water masses.

Carbon dioxide is released, in the oceanic realm, from spreading centers or from volcanic or hydrothermal activity. There are several reasons why this explanation is considered unlikely: 1) if CO_2 caused the warming, it would have also caused dissolution, and no strong dissolution acted on calcareous nannofossil assemblages at Site 702, as demonstrated by the calculated nannofossil indices; 2) hydrothermal

activity is usually characterized by the release of nutrients; on the contrary, the C19r warming event shows oligotrophic conditions.

An alternative explanation is that Site 702 was affected by water masses of different origin, coming from either the Tethys or the Indo-Pacific Ocean.

Diester-Haass et al. (1996) suggested that in the middle Eocene, a warm saline deep water (WSDW) (Brass et al., 1982), oversaturated in carbonate (Kennett and Stott, 1990; Mead et al., 1993) and coming from the western Tethys (Oberhansli, 1992), bathed Site 690 (Maud Rise, South Atlantic) and protected carbonate from dissolution incraesed by high productivity. If this is true, the same water may have bathed Site 702, (that lies north of Site 689) and caused the warming.

Similarly, Kennett and Stott (1990) proposed, in their Proteus Ocean model, that the Southern Ocean was divided in two-layers, with warm saline deep waters coming from the Tethys, overlain by cooler waters from high southern latitudes. This Eocene ocean was therefore halothermal and strongly stratified. Also Scher and Martin (2004), based on neodymium isotope record analysis, supported the effect of the WSDW on southern Atlantic Site 689 (Maud Rise). Despite several works (e.g. Kennett and Stott, 1990; Pak and Miller, 1992; Zachos et al., 1992) supported an Eocene production of warm deep waters in low latitudes affecting the Southern Ocean (included its south Atlantic sector), there is no certain evidence of its existence, as also found by modeling by Bice and Marotzke (2001).

A similar oceanographic interpretation was proposed by Diekmann et al. (2004), who suggested that the South Atlantic was affected in the middle and late Eocene by waters flowing from the equatorial Indian Ocean. This transport of warm waters to the south Atlantic was triggered by the progressive restriction of the Tethys which started in the early Eocene, and interrupted the circum-equatorial circulation, originating a new system of currents flowing around the tip of Africa and toward southern latitudes (e.g. Baldauf and Barron, 1990; Oberhansli, 1992). As shown by nannofossil assemblages at Site 702, sea-surface conditions were temperate for most of the late middle Eocene, interrupted by two significant warming events (the MECO and the C19r warming event). If a current flowing either from the Indian Ocean or from the Tethys affected the South Atlantic in the late middle Eocene, it would have probably brought its warm and saline waters on Site 702. If waters from lower latitudes were nutrient depleted, the

involvement of such currents in determining the *C19r warming event* would be in agreement with nannofossil record which shows marked oligotrophy. Otherwise, an alternative explanation has to be searched.

In possible agreement with nannofossil record, Diester-Haass et al. (1996) noticed a decrease in productivity starting at ~42 Ma, that was interpreted as caused by the retreat of the warm saline deep water and by the onset of another, unspecified water mass.

Several recent models claim firmly that Eocene climate at high southern latitudes was not maintained by intensified warm currents from lower latitudes or by a strong heat transport (Huber et al., 2004; Huber and Nof, 2006; Huber and Sloan, 2001). Nevertheless, Huber and Sloan (2001) model indicates that Eocene currents produced at low-latitudes could generate high-latitude warming phases of regional character.

Site 702 is located at 50°S, in a position probably ideal to record paleoceanographic changes associated to the opening of the Drake Passage (Fig. 1). Despite the timing of the opening of circum-Antarctic gateways is still widely debated, recent works show that the Drake Passage opened earlier than previously suggested (Lagabrielle et al., 2009; Livermore et al., 2007; Livermore et al., 2005; Scher and Martin, 2006), i.e. in the middle Eocene. Analyzing variations on neodymium isotopes on fossil fish teeth from the south Atlantic, Scher and Martin (2006) recognized the onset of more radiogenic values at ~41 Ma. This radiogenic shift was interpreted as caused by the first influx of Pacific waters trough the Drake Passage. Scher and Martin's work represents the first direct evidence of the early opening of the Drake Passage in the middle Eocene. Also, the authors noticed that another more southern Atlantic site (Site 689, Maud Rise) was not as strongly affected by Pacific waters as Site 1090 (South Atlantic, 42°S) and the difference was explained by the pronounced stratification of the Eocene southern Atlantic, as also suggested by Mead et al. (1993). Livermore et al. (2005) dated the opening of the Drake Passage to surface waters back to 50 Ma, and they associated this tectonic event to the beginning of the cooling trend seen worldwide in the middle Eocene (e.g. Zachos et al., 2001).

We think that it is unlikely that the opening of the Drake Passage could cause the warming event seen between 42.5 and 41.5 Ma at Site 702. Commonly, the opening of the circumpolar passages is associated to flowing of cold and not warm waters. In fact,

the tectonic opening of the Drake and Tasmanian gateways has been claimed for decades as the major cause of Antarctic cooling (e.g. Kennett, 1977; Lagabrielle et al., 2009; Lawver and Gahagan, 2003; Livermore et al., 2007). An alternative possible explanation is proposed by Kennett and Stott (1990) who suggested that, within their Proteus ocean model, a warming in the upper part of the water column, can be caused by a thickening of the cool deeper layer. In their reconstruction, the enhanced flow of deep and cold waters- coming from the Pacific and flowing through the Drake Passage- could have pushed upward the warm saline deep waters, causing a warming in the upper layers. We think that the opening of Drake passage would better explain the cooling phase *after* the *C19r warming event*.

Interestingly, bulk oxygen isotope record do not show evidence of warming during the *C19r warming event* as recorded by nannofossil assemblages (Figs. 4, 5). This would imply that one of the two temperature proxies are not providing a correct information. Possible causes of this mismatching are proposed hereinafter.

Abundance changes recorded by nannofossil assemblage characteristic seem reliable. The increase in abundance of warm-water taxa recorded during the *C19r warming event* is mainly driven by Discoasters, whose paleoecological interpretation as warm and oligotrophic taxa is considered extremely reliable among Paleogene nannofossil specialist community (see references in Section 4.2.). It can be argued that taxa relative abundance changes were biased by the closed-sum approach (derived by the use of percentage relative abundances), and that the increase in abundance of Discoasters was caused by the decrease in abundance of some other taxa. It has to be pointed out that *not* all taxa composing the assemblages were used to calculated the paleoecological groups (warm, temperate, and cool) in a way that the abundance changes of one group are not driven by the abundance changes of the other groups (avoiding the closed-sum problem). To provide a further evidence of the independence of Discoaster paleoecological signal, Discoaster percentage abundances were compared with the abundance/ mm_2, and the correspondence between the two records was verified.

Excluding the possibility of a closed-sum problem, it has to be noticed that the increase of warm water taxa is accompanied by a decrease of cool water taxa and by the increase in temperate taxa (Figs. 5, 7), indicating that the warming phase is recorded by all of the

assemblage components and is interpreted based on the paleoecological preference of numerous taxa, not only Discoasters, which record the signal more strongly.

Another possibility is that nannofossil relative abundances were biased by dissolution, but this hypothesis has to be ruled out considered the results obtained by the analysis described in Section 4.1..

A further hypothesis is that the increase in warm- and temperate-water taxa and the decrease in cool water taxa occurring during the *C19r warming event* is controlled by fertility (or other ecological factors) and not by temperature variations. This means that the increase in abundance of Discoasters and the decrease of cool water taxa would not be a response to temperature increase and decrease, respectively, but to a shift toward lower nutrient availability. In fact, usually, warm water taxa are associated with oligotrophic conditions, and cool taxa with more eutrophic conditions even if this relation is a broad assumption. However, we think that this possibility is extremely unlikely, first of all because Discoasters like oligotrophic *and* warm waters. If the paleoclimatic event recorded during C19r was characterized by oligotrophic and cool waters, *Discoaster* would not thrive anyway. Also, if low nutrient levels determine nannofossil assemblage changes, temperate forms, especially *C. pelagicus* and *R. umbilicus* group, would probably show a decrease, being these taxa associated to a preference for mesotrophic-eutrophic waters.

The other possibility is that the oxygen isotope record was biased by some processes that hid the temperature signal. A mismatch between micropaleontological temperature signal and oxygen isotope record was also found at Site 748 (Indian Ocean), where nannofossil assemblages gave indication of a marked cooling event (labeled *cooling B*) in the middle Eocene but which was not identified by isotopic records (Villa et al., 2008). This apparent discrepancy was then denied by further isotopic records coming from other sites, where the cooling event was found (Bohaty et al., 2009).

The reliability of isotopic measurements on bulk carbonate is still debated as bulk isotopic values can be controlled by several different processes, occurring in the water column or within the sediment, during or after deposition. One of these processes is diagenesis. There is no direct evidence of diagenetic processes occurring in Cores 702B-10X and 11X. However, both nannofossil and planktonic foraminifera assemblages show increasing etching and overgrowth going downward along the

section and foraminifera are constantly recrystallized (Ciesielski et al., 1988a). Also, nannofossil chalk at Site 702 shows increasing micrite content going downhole (Ciesielski et al., 1988a) which, together with the associated increase in diagenetic effect, can explain the fact that the oxygen isotope record in the upper part of the studied section is preserved and pristine, and the isotopic MECO is recorded with characteristic similar to those seen at several other ocean sites (Bohaty et al., 2009). Differently, the isotopic signal in the lower part of the section would be biased by diagenetic effects. A further possibility is that the bulk oxygen isotope record was determined and compromised by nannofossil assemblage changes. In fact, vital effects of calcareous nannofossils show an inter-specific variability in oxygen and carbon isotope vital effect that can alter isotopic measurements on coccoliths-dominated sediments (Stoll, 2005). Nannofossil assemblages change significantly along the studied section, especially in terms of taxa relative abundances and, therefore, the possibility that, at this site, bulk isotope data were controlled by nannofossil assemblage changes cannot be ruled out.

It is also possible that water masses with a different isotopic composition affected the bulk oxygen isotope record and undermined the temperature signal. As said above, recent works show that the Drake Passage opened to surface waters in the middle Eocene (e.g. Scher and Martin, 2006) allowing Pacific waters to flow into the Atlantic. It is possible that these waters affected Site 702 and hid the isotopic temperature signal. If these waters also determined the warming and oligotrophic phase recorded by nannofossils or only biased isotopic record, is unknown, even if it is more likely that cool, and not warm, waters would have come from the Pacific after the opening of the circumpolar passage.

5. Conclusions

In this work we carried out a quantitative analysis on nannofossil assemblages at ODP Site 702 Hole B, located at 50°S on the Islas Orcadas Rise, in the subantarctic sector of the South Atlantic ocean.

The goal of this study was to determine sea-surface and nutrient availability changes from ~39.3 to 43.5 Ma, period also spanning the Middle Eocene Climatic Optimum

event (~40.5- 40.0 Ma), a global and transient warming event which interrupts the long-term Eocene cooling trend.

Also, indices of dissolution calculated by nannofossil assemblage composition were tested and used to evaluate if assemblages were significantly affected and biased by dissolution. Calculated indices show significant variations along the study section and indicate that no strong dissolution affected the assemblages and relative taxa abundances are not considered biased by dissolution.

The biostratigraphic analysis of the assemblage shows that a nannofossil turnover occurs in conjunction with the MECO event, with 4 nannofossil bioevents recognized between 40.3 and 40.0 Ma. A further bioevent occurs at the base of a marked warming event recognized by nannofossils between 41.5 and 42.5 Ma (labeled here *C19r warming event*).

The overall patter of nannofossil assemblages changes documented through the studied section agrees well with relative temperature changes inferred from the bulk oxygen isotope record. Thanks to nannofossil assemblage changes, several paleoclimatic phases were recognized: a temperate/ mesotrophic phase from 43.5 to 42.5 Ma, a warming/ oligotrophic phase between 42.5 and 41.5 Ma, followed by a cool phase between 41.5 and 40.5 Ma. Between 40.5 and 40 Ma, in correspondence of the isotopic MECO, nannofossil assemblages record a sea surface warming, accompanied by generally oligotrophic conditions during and after the event, but with a temporary switch to more eutrophic conditions at the peak of the event (40.15-40.0 Ma).

References

Agnini, C. et al., 2006. Responses of calcareous nannofossil assemblages, mineralogy and geochemistry to the environmental perturbations across the Paleocene/Eocene boundary in the Venetian Pre-Alps. Marine Micropaleontology, 63: 19-38.

Agnini, C. et al., 2009. An Early Eocene carbon cycle perturbation at ~52.5 Ma in the Southern Alps: Chronology and Biotic Response Paleoceanography, 24.

Arney, J.E. and Wise, S.W., 2003. Paleocene-Eocene nannofossil biostratigraphy of ODP Leg 183, Kerguelen Plateau. In: F.A. Frey, M.F. Coffin, P.J. Wallace and P.G.E. Quilty (Editors), Proc. ODP Sci. Results.

Aubry, M.P., 1992. Late Paleogene nannoplankton evolution: a tale of climatic deterioration. In: D.R. Prothero and W.A. Berggren (Editors), Eocene-Oligocene Climatic and Biotic Evolution. Princeton University Press, Princeton.

Baldauf, J.G. and Barron, J.A., 1990. Evolution of biosiliceous sedimentation pattern-Eocene through Quaternary: paleoceanographic response to polar cooling. In: U. Bleil and J. Thiede (Editors), Geological History of the Polar Ocean: Arctic vs. Antarctic. Kluwer Academic Publiching, Dordrecht, pp. 575-607.

Berggren, W.A., Kent, D.V., Swisher, C.C., III and Aubry, M.-P., 1995. A revised Cenozoic geochronology and chronostratigraphy. Special Publication - SEPM (Society for Sedimentary Geology), 54: 129-212.

Berner, R.A., 1977. Sedimentation and dissolution of pteropods in the ocean. In: N.R. Andersen and A. Malahoff (Editors), The Fate of Fossil Fuel CO_2 in the Oceans. Plenum Press, New York, pp. 243-260.

Bice, K.L. and Marotzke, J., 2001. Numerical evidence against reversed thermohaline circulation in the warm Paleocene/Eocene ocean. Journal of Geophysical Research-Oceans, 106(C6): 11529-11542.

Bice, K.L. and Marotzke, J., 2002. Could changing ocean circulation have destabilized methane hydrate at the Paleocene/Eocene boundary? Paleoceanography, 17(2).

Bijl, P. et al., 2010. Transient Middle Eocene Atmospheric CO_2 and Temperature Variations. Science, 330.

Bijl, P. et al., 2009. Early Paleogene temperature evolution of the southwest Pacific Ocean. Letters to Nature, 461: 776-779.

Blaj, T., Backman, J. and Raffi, I., 2009. Late Eocene to Oligocene preservation history and biochronology of calcareous nannofossils from paleo-equatorial Pacific Ocean sediments. Rivista Italiana di Paleontologia e Stratigrafia, 115(1): 67-85.

Bohaty, S.M. and Zachos, J.C., 2003. Significant Southern Ocean warming event in the late middle Eocene. Geology, 31(11): 1017-1020.

Bohaty, S.M., Zachos, J.C., Florindo, F. and Delaney, M.L., 2009. Coupled greenhouse warming and deep sea acidification in the middle Eocene. Paleoceanography, 24(PA2207).

Bralower, T.J., 2002. Evidence of surface water oligotrophy during the Paleocene-Eocene thermal maximum: Nannofossil assemblage data from Ocean Drilling Program Site 690, Maud Rise, Weddell Sea (vol 17, pg 1023, 2002) - art. no. 1060. Paleoceanography, 17(4): 1060.

Brass, G.W., Southam, J.R. and Peterson, W.H., 1982. Warm saline bottom water in the ancient ocean. Nature, 296(5858): 620-623.

Bukry, D., 1973. Low-latitude coccolith biostratigraphic zonation. In: N.T. Edgar and J.B. Saunders (Editors), *Initial Reports* of the DSDP, pp. 685-704.

Cachao, M. and Moita, M.T., 2000. *Coccolithus pelagicus*, a prductivity proxy related to moderate fronts off Western Iberia. Marine Micropaleontology, 39: 131-155.

Cambray, H. and Cadet, J.P., 1996. Synchronisme de l'activite volcanique d'arc: Mythe ou realite? Comptes Rendus de l'Academie des Sciences, Serie II. Sciences de la Terre et des Planetes, 322(3): 237-244.

Cande, S.C. and Kent, D.V., 1995. Revised calibration of the geomagnetic polarity timescale for the Late Cretaceous and Cenozoic. Journal of Geophysical Research, 100(4): 6093-6095.

Ciesielski, P.F. et al., 1988a. Site 702. Proceedings of the Ocean Drilling Program, Part A: Initial Reports, 114: 483-548.

Ciesielski, P.F., Y. Kristoffersen, et al., 1988b. Proc. ODP, Init. Repts., 114. Ocean Drilling Program, College Station, TX.

Clement, B.M. and Hailwood, E.A., 1991. Magnetostratigraphy of sediments from sites 701 and 702. Proc. ODP, Sci. Results, 114: 359-366.

Crux, J.A. et al., 1991. Calcareous nannofossils recovered by Leg 114 in the subantarctic South Atlantic Ocean. Proceedings of the Ocean Drilling Program, Scientific Results, 114: 155-177.

Diekmann, B., Kuhn, G., Gersonde, R. and Mackensen, A., 2004. Middle Eocene to early Miocene environmental changes in the sub-Antarctic Southern Ocean: evidence from biogenic and terrigenous depositional patterns at ODP Site 1090. Global and Planetary Change, 40(3-4): 295-313.

Diester-Haass, L., Robert, C. and Chamley, H., 1993. Paleoceanographic and paleoclimatic evolution in the Weddell Sea (Antarctica) during the middle Eocene-late Oligocene, from a coarse sediment fraction and clay mineral data (ODP Site 689). Marine Geology, 114(3-4): 233-250.

Diester-Haass, L., Robert, C. and Chamley, H., 1996. The Eocene-Oligocene preglacial-glacial transition in the Atlantic sector of the Southern Ocean (ODP Site 690). Marine Geology, 131: 123-149.

Diester-Haass, L. and Zahn, R., 1996. Eocene-Oligocene transition in the Southern Ocean: History of water mass circulation and biological productivity. Geology, 24(2): 163-166.

Dunkley Jones, T., Bown, P.R., Pearson, P.N., Wade, B.S. and Coxall, H.K., 2008. Major shifts in calcareous phytoplankton assemblages through the Eocene-Oligocene transition of Tanzania and their implications for low-latitude primary production. Paleoceanography, 23: PA4204.

Edgar, K.M., 2008. Paleoclimatology, stratigraphy and biotic responses in the middle Eocene, University of Southampton, Southampton.

Edgar, K.M. et al., 2010. New biostratigraphic, magnetostratigraphic and isotopic insights into the Middle Eocene Climatic Optimum in low latitudes. Palaeogeography, Palaeoeclimatology, Palaeoecology, 297: 670-682.

Edgar, K.M., Wilson, P.A., Sexton, P.F. and Suganuma, Y., 2007. No extreme bipolar glaciation during the main Eocene calcite compensation shift. Nature, 448: 908-911.

Fioroni, C., Villa, G., Persico, D., Wise, S.S. and Pea, L., 2010. Revised Eocene-Oligocene calcareous nannofossil biozonation for the Southern Ocean, 13th International Nannoplankton Association Conference, Yamagata.

Firth, J.V. and Wise, S.W., 1992. A preliminary study of the evolution of Chiasmolithus in the middle Eocene to Oligocene of Sites 647 and 748, Proceedings of the Ocean Drilling Program, Scientific Results.

Gibbs, S.J., Bralower, T.J., Bown, P.R., Zachos, J.C. and Bybell, L.M., 2006. Shelf and open-ocean calcareous phytoplankton assemblages across the Paleocene-Eocene Thermal Maximum: implications for global productivity gradients. Geology, 34(4): 233-236.

Gibbs, S.J., Shackleton, N.J. and Young, J.R., 2004. Identification of dissolution pattern in nannofossil assemblages: A high resolution comparison of synchronous records from Ceara Rise, ODP Leg 154. Paleoceanography, 19: PA1029.

Haq, B.U. and Lohmann, G.P., 1976. Early Cenozoic calcareous nannoplankton biogeography of the Atlantic Ocean. Marine Micropaleontology, 1: 119-194.

Hay, W.W., 1970. Calcareous nannofossils from cores recovered on Leg 4. In: U.G.P. Office (Editor), Initial Reports Deep Sea Drilling Project, 4, Washington DC, pp. 455-501.

Holmes, M.A., Watkins, D.K. and Norris, R.D., 2004. Paleocene cyclic sedimentation in the Western North Atlantic, ODP Site 1051, Blake Nose. Marine Geology, 209: 31-43.

Hooper, P.W.P., Funnell, B.M. and Weaver, P.P.E., 1991. Late Miocene-Earli Pliocene planktonic foraminifera and paleoceanography of the North Atlantic. Journal of Micropaleontology, 9: 145-152.

Huber, M. et al., 2004. Eocene circulation of the Southern Ocean: Was Antarctica kept warm by subtropical waters? Paleoceanography, 19(4).

Huber, M. and Nof, D., 2006. The ocean circulation in the Southern Hemisphere and its climatic impacts in the Eocene. Palaeogeography, Palaeoclimatology, Palaeoecology, 231(1-2): 9-28.

Huber, M. and Sloan, L.C., 2001. Heat transport, deep waters, and thermal gradients; coupled simulation of an Eocene greenhouse climate. Geophysical Research Letters, 28(18): 3481-3484.

Jiang, S. and Wise, S.W., 2009. Distinguishing the influence of diagenesis on the paleoecological reconstruction of nannoplankton across the Paleocene/Eocene Thermal Maximum: An example from the Kerguelen Plateau, southern Indian Ocean. Marine Micropaleontology, 72: 49-59.

Jovane, L. et al., 2007. The middle Eocene climatic optimum event in the Contessa section, Umbrian Apennines, Italy. Geological Society of America Bulletin, 119(3/4): 413-417.

Kahn, A. and Aubry, M.P., 2004. Provincialism associated with the Paleocene/Eocene Thermal maximum: temporal constrain. Marine Micropaleontology, 52: 117-131.

Kelly, D.C., Bralower, T.J., Zachos, J.C., Premoli-Silva, I. and Thomas, E., 1996. Rapid diversification of planktonic foraminifera in the tropical Pacific (ODP Site 865) during the late Paleocene thermal maximum. Geology, 24(5): 423-426.

Kennett, J.P., 1977. Cenozoic evolution of Antarctic glaciation, circum-Antarctic ocean, and their impact on global paleoceanography. Journal of Geophysical Research-Oceans and Atmospheres, 82(27): 3843-3860.

Kennett, J.P. and Stott, L.D., 1990. Proteus and Proto-oceanus: Ancestral Paleogene oceans as revealed from Antarctic stable isotopic results; ODP Leg 113. Proc. ODP, Sci. Results, 113: 865-880.

Kerrick, D.M. and Caldeira, K., 1994. Metamorphic CO_2 degassing and early Cenozoic paleoclimate. GSA Today, 4(3): 57.

Lagabrielle, Y., Goddéris, Y., Donnadieu, Y., Malavieille, J. and Suarez, M., 2009. The tectonic history of Drake Passage and its possible impacts on global climate. Earth and Planetary Science Letters, 279: 197-211.

Lawver, L.A. and Gahagan, L.M., 2003. Evolution of Cenozoic seaways in the circum-Antarctic region. Palaeogeography, Palaeoclimatology, Palaeoecology, 198(1-2): 11-37.

Livermore, R., Hillenbrand, C.-D., Meredith., M. and Eagles, G., 2007. Drake Passage and Cenozoic climate: An open and shut case? Geochem. Geophys. Geosyst., 8.

Livermore, R., Nankivell, A., Eagles, G. and Morris, P., 2005. Paleogene opening of Drake Passage. Earth and Planetary Science Letters, 236(1-2): 459-470.

Luciani, V. et al., 2010. Ecological and evolutionary response of Thethyan planktonic foraminifera to the Middle Eocene Climatic Optimum (MECO) from the Alano Section (NE Italy). Palaeogeography, Palaeoclimatology, Palaeoecology, 292(1-2): 82-95.

Marino, M. and Flores, J.A., 2002. Middle Eocene to Early Oligocene calcareous nannofossil stratigraphy at Leg 177 Site 1090. Marine Micropaleontology, 45: 383-398.

Martini, E., 1971. Standart Tertiary and Quaternary calcareous nannoplankton zonation. In: A. Farinacci (Editor), Second Planktonic Conference. Edizioni Tecnoscienza, Rome, pp. 739-785.

Matsouoka, H., McIntyre, A. and Verardo, B., 1991. A sensitive dissolution indicator *Calcidiscus leptoporus*: Concordance with climate-forced dissolution at orbital time scales. EOS, 72(44): 271.

Mc Gonigal, K. and Di Stefano, A., 2002. Calcareous Nannofossil Biostratigraphy of the Eocene- Oligocene transition, ODP Sites 1123 and 1124., Proc. ODP, Sci. Results, pp. 1-22.

McGonigal, K. and Di Stefano, A., 2002. Calcareous Nannofossil Biostratigraphy of the Eocene-Oligocene Transition, ODP Sites 1123 and 1124. In: C. Richter (Editor), Proc. ODP, Sci. Results, pp. 1-22.

Mead, G.A., Hodell, D.A. and Ciesielski, P.F., 1993. Late Eocene to Oligocene vertical oxygen isotopic gradients in the South Atlantic: Implications for warm saline deep water. In: J.P. Kennett and D.A. Warnke (Editors), The Antarctic Paleoenvironment: A Perspective on Global Change, Part Two. Antarctic Research Series. American Geophysical Union, pp. 27-48.

Mikes, T., Baldi-Beke, M., Kazmer, M., Dunkl, I. and von Eynatten, H., 2008. Calcareous nannofossil age constraints on Miocene flysch sedimentation in the Outer Dinarides (Slovenia, Croatia, Bosnia-Herzegovina and Montenegro) In: S. SIEGESMUND, FU¨ GENSCHUH, B. & FROITZHEIM, N. (eds) (Editor), Tectonic Aspects of the Alpine-Dinaride-Carpathian System. Special Publications. Geological Society, London, pp. 335–363.

Miller, K.G., Wright, J.D. and Fairbanks, R.G., 1991. Unlocking the ice house: Oligocene-Miocene oxygen isotopes, eustasy, and margin erosion. Journal of Geophysical Research, B, Solid Earth and Planets, 96: 6829-6848.

Monechi, S., Buccianti, A. and Gardin, S., 2000. Biotic signals from nannoflora across the iridium anomaly in the upper Eocene of the Massignano section: evidence from statistical analysis. Marine Micropaleontology, 39: 219-237.

Oberhansli, H., 1992. The influence of the Thetys on the bottom waters of the early Tertiary ocean. In: J.P. Kennet and D.A. Warnke (Editors), The Antarctic Paleoenvironment: A Perspective on Global Change. Anatrct. Res. Ser., pp. 167-184.

Okada, H. and Bukry, D., 1980. Supplementary modification and introduction of code numbers to the low-latitude coccolith biostratigraphic zonation (Bukry, 1973; 1975). Marine Micropaleontology, 5(3): 321-325.

Pagani, M., Zachos, J.C., Freeman, K.H., Tipple, B. and Bohaty, S., 2005. Marked decline in atmospheric carbon dioxide concentrations during the Paleogene. Science, 309(5734): 600-603.

Pak, D.K. and Miller, K.G., 1992. Paleocene to Eocene benthic foraminiferal isotopes and assemblages; implications for deepwater circulation. Paleoceanography, 7(4): 405-422.

Persico, D. and Villa, G., 2004. Eocene-Oligocene calcareous nannofossils from Maud Rise and Kerguelen Plateau (Antarctica): Paleoecological and paleoceanographic implications. Marine Micropaleontology, 52: 153-179.

Peterson, L.C. and Prell, W.L., 1985. Carbonate dissolution in recent sediments of the eastern equatorial Indian Ocean: Preservation patterns and carbonate loss above the lysocline. Marine Geology, 64: 259-290.

Roth, P.H. and Thierstein, H.R., 1972. Calcareous nannoplankton: Leg 14 of the DSDP. Init. Reports, DSDP, 14: 421-485.

Roth, P.H. and W.H., B., 1975. Distribution and dissolution of coccoliths in the South and Central Pacific. Cushman Foundation, Foram. Res., Spec. Publ., 13: 87-113.

Scher, H.D. and Martin, E.E., 2004. Circulation in the Southern Ocean during the Paleogene inferred from neodymium isotopes. Earth and Planetary Science Letters, 228(3-4): 391-405.

Scher, H.D. and Martin, E.E., 2006. Timing and climatic consequences of the opening of Drake Passage. Science, 312(5772): 428-30.

Spofforth, D. et al., 2010. Organic carbon burial following the middle Eocene climatic optimum in the central western Thetys. Paleoceanography, 25.

Stoll, H.M., 2005. Limited range of interspecific in vital effects of coccolith stable isotopic records during the Paleocene-Eocene thermal maximum. Paleoceanography, 20.

Thierstein, H.R., 1980. Selective Dissolution of Late Cretaceous and Earliest Tertiary Calcareous Nannofossils: Experimental Evidence. Cretaceous Reserach, 2: 165-176.

Tremolada, F. and Bralower, T.J., 2004. Nannofossil assemblage fluctuations during the Paleocene-Eocene Thermal Maximum at Site 213 (Indian Ocean) and 401 (North Atlantic Ocean): paleoceanographic implications. 52: 107-116.

Villa, G., Fioroni, C., Pea, L., Bohaty, S. and Persico, D., 2008. Middle Eocene-late Oligocene climate variability: Calcareous nannofossil response at Kerguelen Plateau, Site 748. Marine Micropaleontology, 69: 173-192.

Villa, G. and Persico, D., 2006. Late Oligocene climatic changes: Evidence from calcareous nannofossils at Kerguelen Plateau Site 748 (Southern Ocean). Palaeogeography, Palaeoclimatology, Palaeoecology, 231: 110-119.

Wei, W. and Thierstein, H.R., 1991. Upper Cretaceous and Cenozoic calcareous nannofossils of the Kerguelen Plateau (southern Indian Ocean) and Prydz Bay (East Antarctica). Proc. ODP, Sci. Results, 119: 467-493.

Wei, W., Villa, G. and Wise, S.W., Jr., 1992. Paleoceanographic implications of Eocene-Oligocene calcareous nannofossils from sites 711 and 748 in the Indian Ocean. Proc. ODP, Sci. Results, 120: 979-999.

Wei, W. and Wise, S.W., Jr., 1990a. Biogeographic gradients of middle Eocene-Oligocene calcareous nannoplankton in the South Atlantic Ocean. Palaeogeography, Palaeoclimatology, Palaeoecology, 79(1-2): 29-61.

Wei, W. and Wise, S.W., Jr., 1990b. Middle Eocene to Pleistocene calcareous nannofossils recovered by Ocean Drilling Program Leg 113 in the Weddell Sea. Proc. ODP, Sci. Results, 113: 639-666.

Wei, W.C., 2004. Opening of the Australia-Antarctica gateway as dated by nannofossils. Marine Micropaleontology, 52(1-4): 133-152.

Wei, W.C. and Wise, S.W., 1992. Eocene-Oligocene calcareous nannofossils magnetobiochronology of the Southern Ocean. Newsl. Stratigr., 26: 119-132.

Wind, F.H. and Wise, S.W., 1978. Mesozoic holococcoliths. Geology, 6: 140-142.

Zachos, J.C., Pagani, M., Sloan, L., Thomas, E. and Billups, K., 2001. Trends, rhythms, and aberrations in global climate 65 Ma to present. Science, 292(5517): 686-693.

Zachos, J.C., Rea, D.K., Seto, K., Nomura, R. and Niitsuma, N., 1992. Paleogene and early Neogene deep water paleoceanography of the Indian Ocean as determined from benthic foraminifer stable carbon and oxygen records. In: R.A. Duncan, D.K. Rea, R.B. Kidd, U. von Rad and J.K. Weissel (Editors), Synthesis of Results from Scientific Drilling in the Indian Ocean. Geophysical Monograph. American Geophysical Union, pp. 351-385.

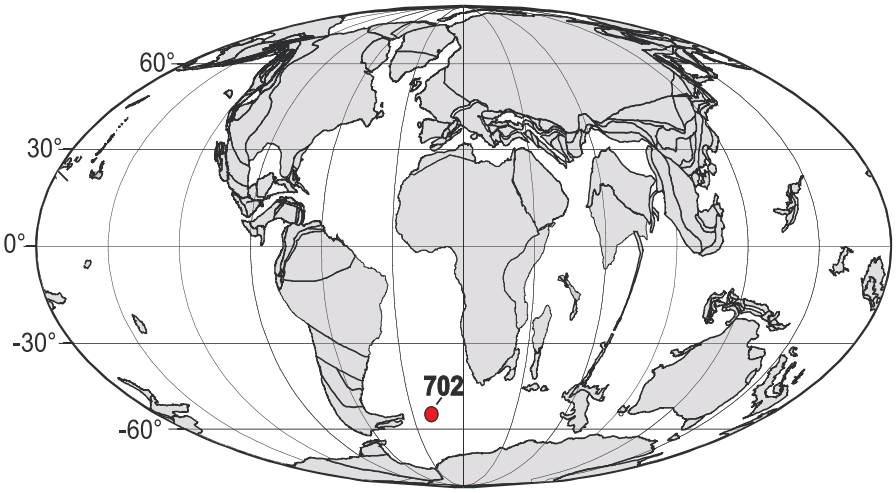

Figure 1: Location of ODP Site 702 (Islas Orcadas Rise, South Atlantic Ocean) on a middle Eocene (40 Ma) paleogeographic reconstruction. From Bohaty et al. (2009), modified.

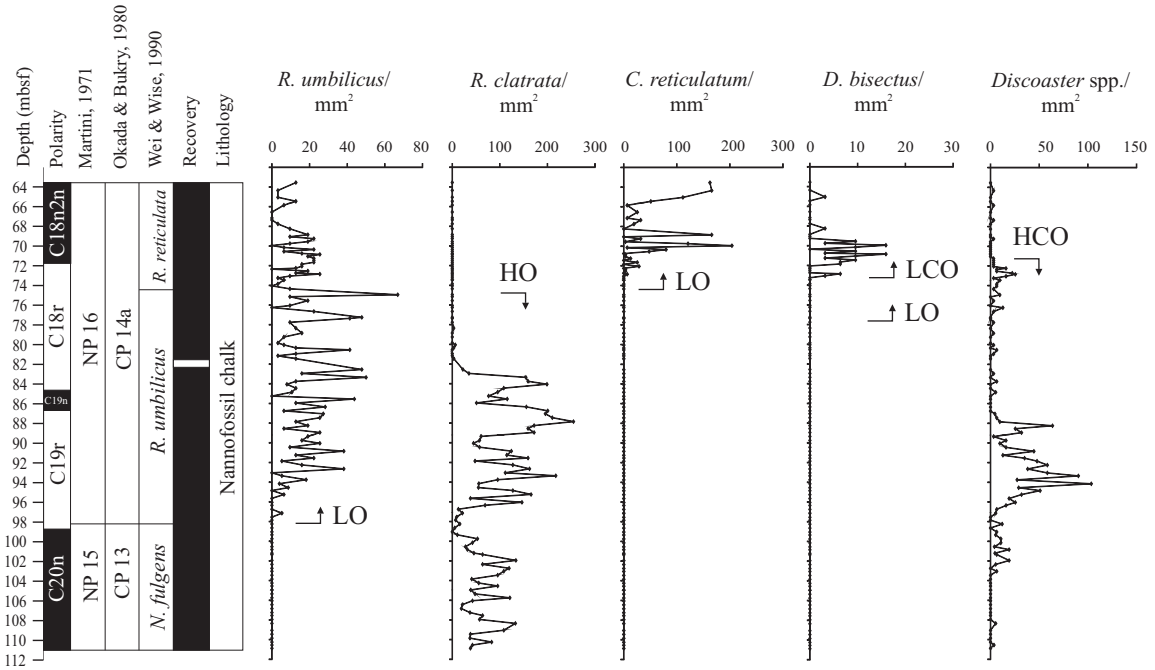

Figure 2: Nannofossil biostratigraphic events recognized at Site 702. LO: Lowest Occurrence, HO: Highest Occurrence, HCO: Highest Common Occurrence, LCO: Lowest Common Occurrence.

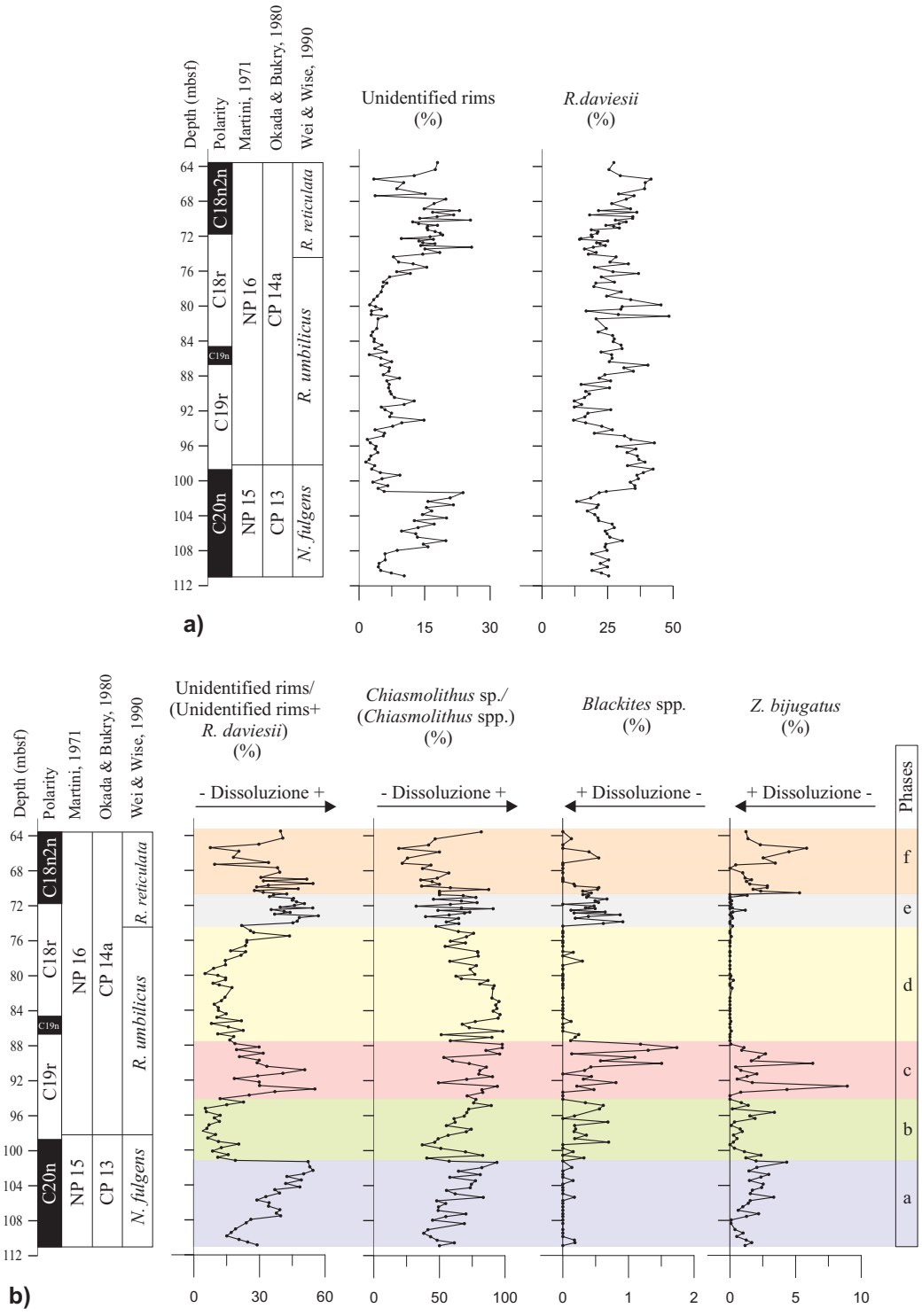

Figure 3: (a) comparison between the relative abundance (%) of unidentified rims and *R. daviesii* distribution. The similarity between the two records reveals that most of the unidentified rims represent remains of *R. daviesii;* (b) comparison between calculated nannofossil dissolution indices (two left plots) and relative abundance of *Blackites* spp. and *Z. bijugatus* (two right plots). Coloured bands and associated phases (a, b, c, d, e and f) are described in the text.

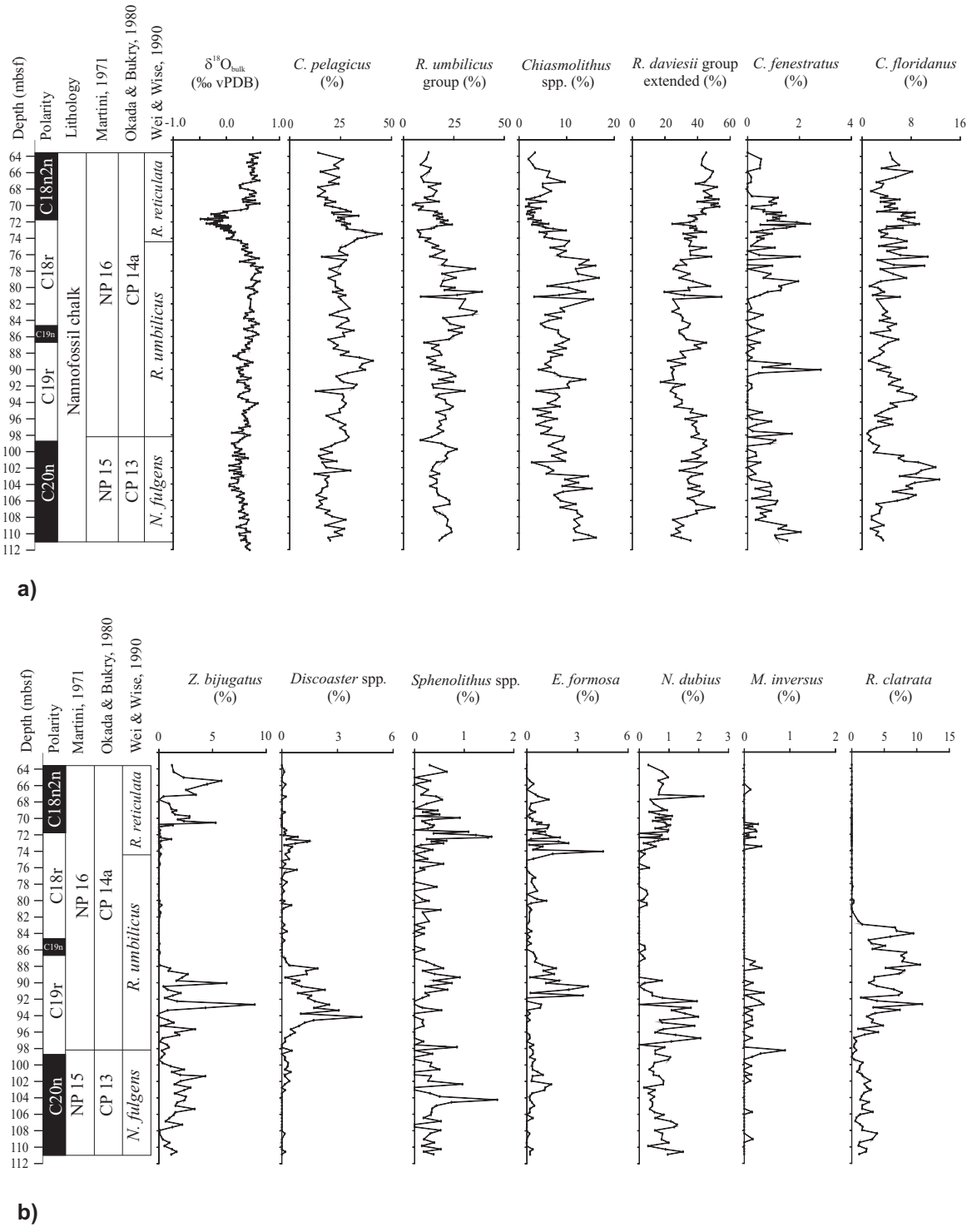

Figure 4: Taxa relative abundance and oxygen istope record.

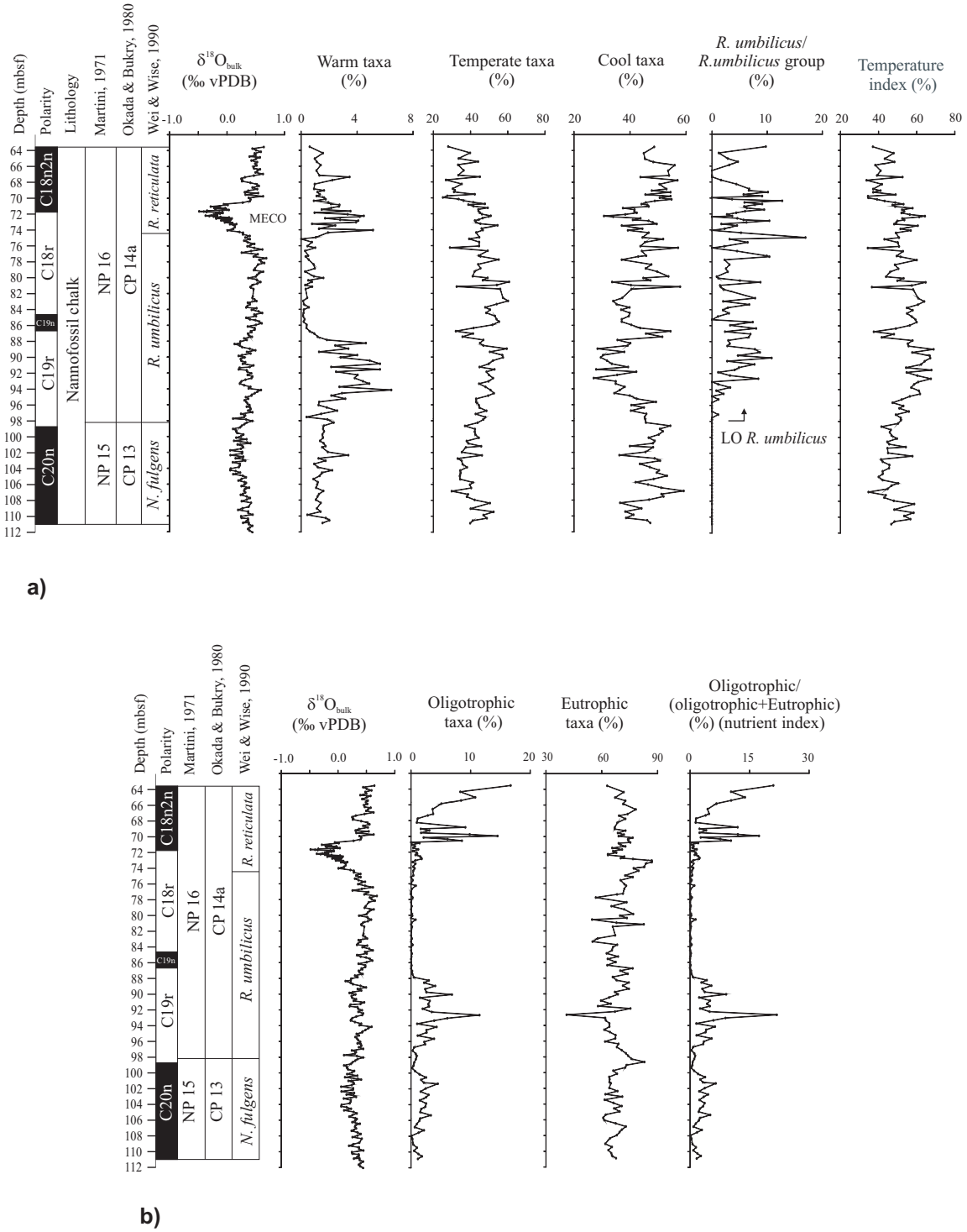

Figure 5: (a) Paleoecological group distribution (warm, cool and temperate water taxa), temperature index (see text for description) and oxygen isotope record, MECO: Middle Eocene Climatic Optimum, LO: Lowest Occurrence; (b) Relative abundance of oligotrophic and eutrophic taxa, and nutrient index (see text for discussion).

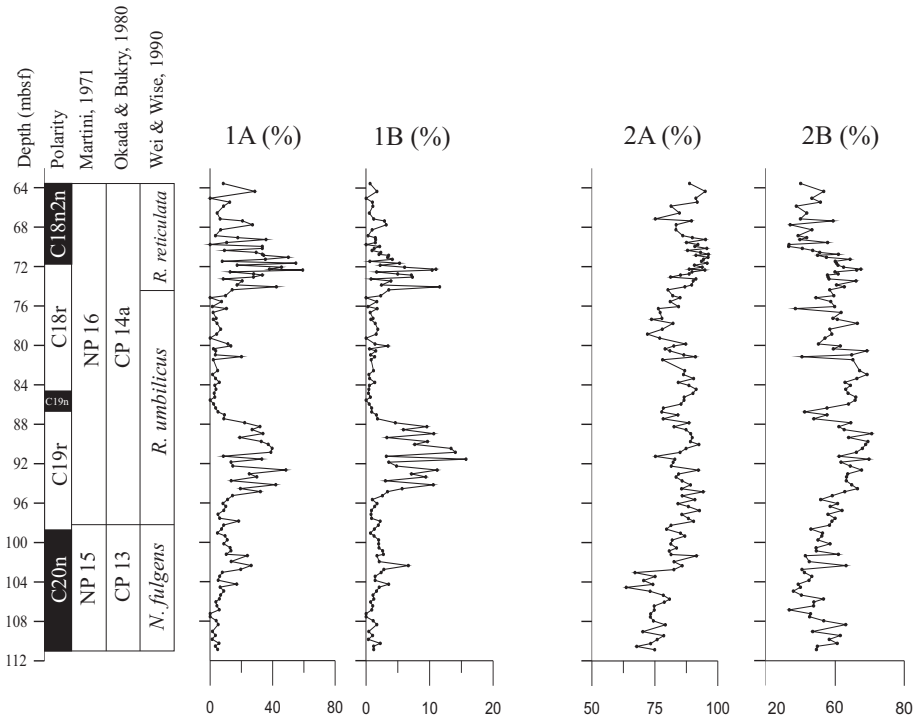

Figure 6: Indices used to verify that nannofossil assemblage characteristics are not biased by dissolution. 1A and 1B were calculated using taxa resistant to dissolution, 2A and 2B were calculated using both resistant and easily dissoluble taxa. Indices 1A and 1B represent a ratio betwenn warm taxa *vs* cool taxa, and 2A and 2B a ratio between temperate taxa *vs* cool taxa, and thus they can also be considered as temperature indices, with higher values corresponding to higher temperature. Indices 1A and 1B clearly show two warming phases, between 70 and 76 mcd and between 88 and 96 mcd.

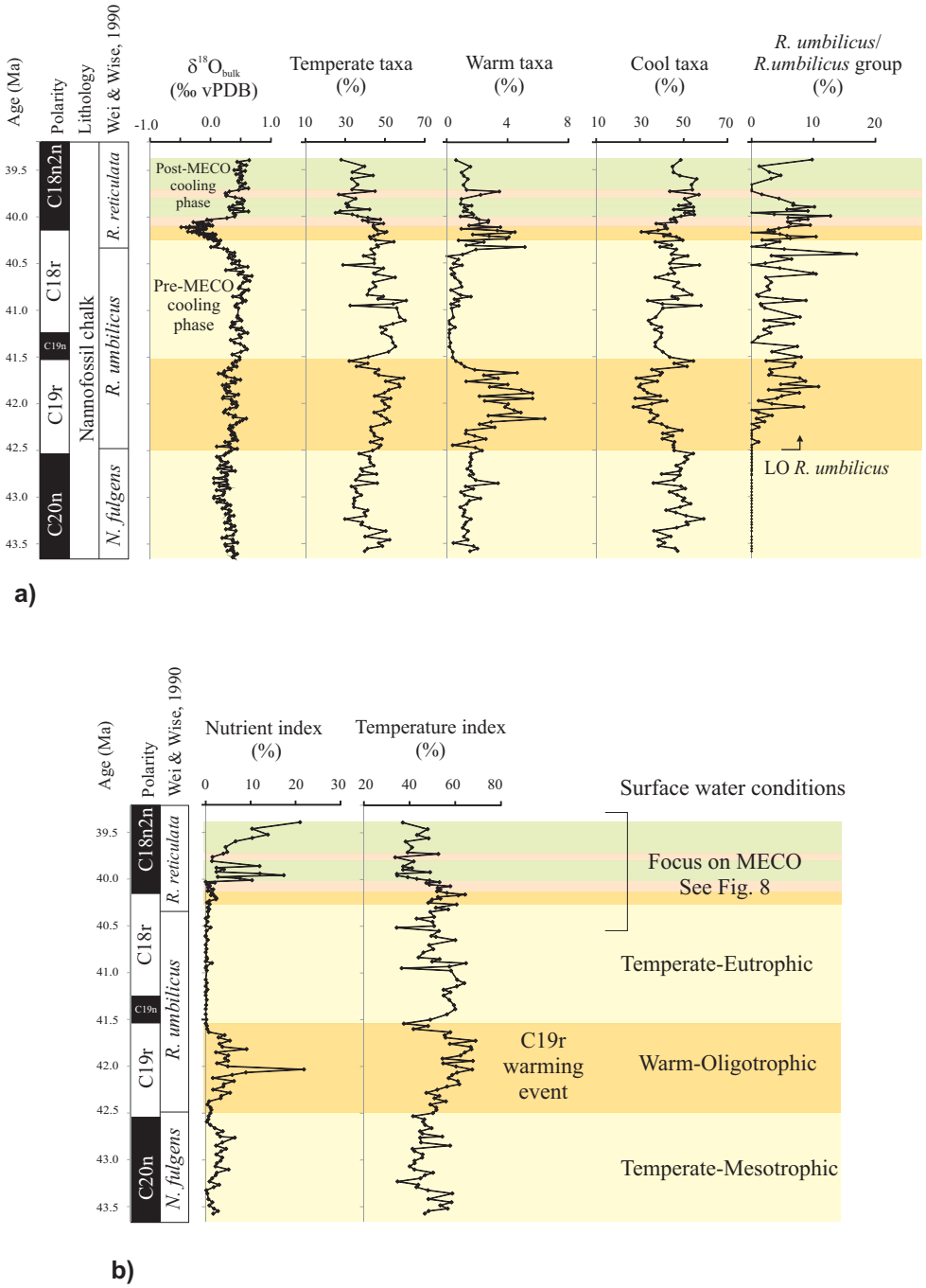

Figure 7: (a) paleoecological groups (warm, cool and temperate taxa) are shown next to the oxygen isotope record (the Pre-MECO and Post-MECO cooling phases of Bohaty et al. (2009) are indicated) and to the relative abundance of *R. umbilicus* vs *R. umbilicus* group; LO: Lowest Occurrence; (b) nutrient and temperature indices calculated using calcareous nannofossil assemblages. MECO: Middle Eocene Climatic Optimum. Coloured bands correspond to climatic phases identified using paleoecological group and index variations. The warming phase labelled *C19r warming event* (41.5 and 42.5 Ma) is indicated. A focus on the MECO event is shown in Fig. 8.

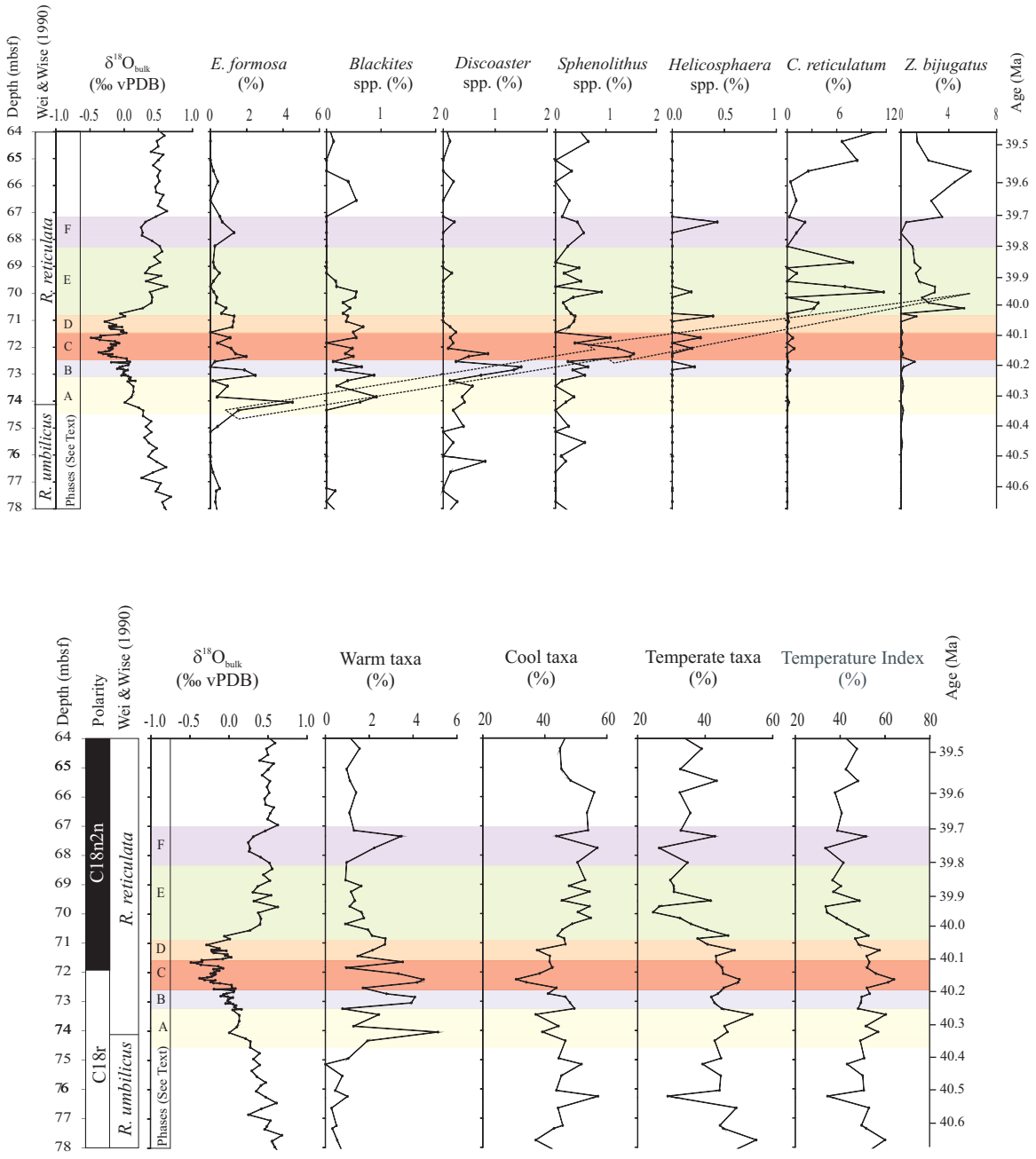

Figure 8: Focus on the Middle Eocene Climatic Optimum (MECO); (a) relative abundance of paleoecologically important taxa are shown next to the oxygen isotope record. The arrow indicates a switch in abundance between minor components; (b) paleoecological groups, temperature index and oxygen isotope record. Coloured bands, corresponding to phases A-F, represent climatic phases as recorded by nannofossils.

Event	Average depth (mbsf)	Sample interval (cm)	Age (Ma)	Chron
HCO *Discoaster* spp.	71.15	8X-6,25/8X-6,45	40.063	Lower C18n.2n
LO *D. bisectus*	73.15	9X-1,25/9X-1,45	40.241	Upper C18r
LO C. *reticulatum*	74.20	9X-1,125/9X-2,5	40.333	Upper C18r
HO *R. clatrata*	74.65	9X-2,5/9X-2,65	40.373	Upper C18r
LO *R. umbilicus*	98.05	11X-5,5/11X-5,45	42.482	Lower C19r

Table 1: Biostratigraphic events recognized at ODP Site 702. Ages were calculated using the Cande and Kent (1995) time scale.

Event	This work		Berggren et al. (1995)		Marino and Flores (2002)	Wei (2004)	Villa et al. (2008)
	Age	Chron	Age	Chron	Age	Age	Age
HCO *Discoaster* spp.	40.063	Lower C18n.2n					40.13
LCO *D. bisectus*	40.241	Upper C18r					
LO C. *reticulatum*	40.333	Upper C18r	42.0	C18n-C20	41.2	41.2	40.67
HO *R. clatrata*	40.373	Upper C18r					40.55
LO *D. bisectus*	40.475	Upper C18r	38	C17n.3n (diachronous)	38		37.55
LO *R. umbilicus*	42.482	Lower C19r	43.7 (Italian sections)	C20n/C20r		42.0	

Table 2: Ages of biostratigraphic events recognized at ODP Site 702, and comparison with ages assigned in other works. All ages are based on the Cande and Kent (1995) time scale.

Cool water taxa	Warm water taxa	Temperate water taxa	Mesotrophic-Eutrophic taxa	Oligotrophic taxa
Chiasmolithus spp.	*Discoaster* spp.	*R. umbilicus* group	*Sphenolithus* spp.	*Discoaster* spp.
R. daviesii group	*Sphenolithus* spp.	*C. pelagicus*	*E. formosa*	*Z. bijugatus*
	E. formosa	*Z. bijugatus*	*C. pelagicus*	*C. reticulatum*
	M. inversus	*N. dubius*	*Helicosphaera* spp.	*C. cf. reticulatum*
			Chiasmolithus spp.	
			R. daviesii group	
			M. inversus	
			R. umbilicus group	

Table 3: Taxa paleoecological interpretation adopted in this work.

Chapter 3

Late Eocene - Late Oligocene climate and biota at ODP Site 1090, South Atlantic Ocean: paleoecological and paleoceanographic reconstructions using Calcareous Nannofossils

Preface

Data presented in this chapter were collected by five people working within or in collaboration with the Micropaleontological Research Group (Calcareous Nannofossils) at the Earth Science Department of the University of Parma. These people are myself, Dr. Chiara Fioroni (University of Modena and Reggio Emilia), Dr. Davide Persico (University of Parma), Prof. Giuliana Villa (University of Parma), and Dr. Silvia Palandri (University of Pisa).

1. Introduction

In the late Paleogene, global climate dramatically changed. The most dramatic change, occurred in correspondence of the Eocene-Oligocene Transition (EOT) at ~34 Ma (Coxall and Pearson, 2007; Coxall et al., 2005; Pearson et al., 2008). The Eocene is characterized by generally warm conditions, and the Oligocene by a cooler climate, driven by the ice-sheet in East Antarctica (e.g. Zachos et al., 2001). The passage between the Eocene and the Oligocene has been associated with the transition from a "Greenhouse" to an "Icehouse" world (Miller et al., 1991). This climatic transition is characterized by a long and gradual cooling trend, as identified by marine oxygen stable isotope records (e.g. Miller et al., 1991; Zachos et al., 2001), which started right after the Early Oligocene Climatic Optimum (EECO) (Zachos et al., 2001). The early-middle

Eocene shows several short term warming events such as the Eocene Thermal Maximum 2 (~53.5 Ma) (ETM-2 or ELMO) (Lourens et al., 2005), the Early Eocene Climatic Optimum (~51-53 Ma) (Zachos et al., 2001) and the Middle Eocene Climatic Optimum (MECO) (~40 Ma) (Bohaty and Zachos, 2003; Bohaty et al., 2009) and is followed, in the late Eocene, by a period of high climatic instability (e.g. Villa et al., 2008; Zachos et al., 2001).

The most dramatic phase of the Paleogene transition, corresponding to cooling and Antarctic glaciation, occurs in the earliest Oligocene, at the Oi-1 event (~33.5 Ma) (Miller et al., 1991; Zachos et al., 2001). For clarity, we adopted in this work the terminology proposed by Coxall and Pearson (2007), considering as the *Eocene–Oligocene Transition* (EOT) the ~500 kyr climatic phase straddling the Eocene/Oligocene boundary (33.7 Ma), and during which two major 40 kyr shifts, labeled Step 1 and Step 2 by Coxall et al. (2005) of the oxygen and carbon isotope records occur. Step 2 corresponds to the Oi-1 event (Miller et al., 1991; Zachos et al., 2001). Step 1 is interpreted mainly as a temperature signal (Katz et al., 2008; Lear et al., 2008; Miller et al., 2008), Step 2 (Oi-1) is associated to both cooling and ice-growth (Coxall et al., 2005; Katz et al., 2008; Miller et al., 2009; Zachos et al., 1996). Step 2 (Oi-1) is the base of the Early Oligocene Glacial Maximum (EOGM) (e.g. Kennett and Shackleton, 1976; Liu et al., 2004; Miller et al., 1987).

The EOT is coupled with sea level fall (Kominz and Pekar, 2001; Pekar and Christie-Blick, 2008; Pekar et al., 2002), a strong deepening of the Calcite Compensation Depth (CCD) in all oceans (Coxall et al., 2005; Merico et al., 2008; Rea and Lyle, 2005; Van Andel, 1975) and a global increase in ocean productivity (e.g. Anderson and Delaney, 2005; Diester-Haass and Zachos, 2003; Diester-Haass and Zahn, 2001; Dunkley Jones et al., 2008; Salamy and Zachos, 1999; Zachos and Kump, 2005).

The EOT corresponds to the most pronounced faunal and floral turnover in the Cenozoic, involving both terrestrial (Francis, 1999; Hooker et al., 2004; Jaramillo et al., 2006; Leopold et al., 1992) and marine biota (Aubry, 1992; Keller et al., 1992; Nocchi et al., 1998). At this time all major groups of marine microfossils show changes in assemblage characteristics: radiolarian (Funakawa and Nishi, 2008; Funakawa et al., 2006; Lazarus and Caulet, 1993; Lazarus et al., 2004), diatoms (Baldauf, 1992; Suto, 2006), planktonic foraminifera (Keller et al., 1992; Molina et al., 2006; Wade and

Pearson, 2008), benthic foraminifera (Alegret et al., 2008; Molina et al., 2006; Pearson et al., 2008), and calcareous nannoplankton (Aubry, 1992; Bown et al., 2008; Dunkley Jones et al., 2008; Persico and Villa, 2004; Villa et al., 2008; Wei and Wise, 1990a).

As possible causes of the Paleogene cooling, different hypothesis have been proposed, including the thermal isolation of Antarctica following the opening of the circumpolar passages (Kennett, 1977; Lawver and Gahagan, 2003; Scher and Martin, 2006), atmospheric pCO_2 decline (DeConto et al., 2008; DeConto and Pollard, 2003; Pagani et al., 2005; Pearson and Palmer, 2000), a particular orbital configuration (eccentricity minimum and low-amplitude obliquity change) of the Earth favoring cool summers (Coxall et al., 2005; Liu et al., 2004; Pälike et al., 2006), and extraterrestrial impacts (e.g. Vonhof et al., 2000).

After the EOT, the Oligocene shows cool and relatively stable conditions (e.g. Miller et al., 1991; Zachos et al., 2001), interrupted by a warming event in the late Oligocene (Lagabrielle et al., 2009; Villa et al., 2008; Villa and Persico, 2006; Zachos et al., 2008; Zachos et al., 2001) which has been linked to a partial melting of the Antarctic ice-sheet (Zachos et al., 2001), to the effect of warmer deep waters affecting all ocean basins (Pekar et al., 2006) or to a temporary closure of the Drake Passage (Lagabrielle et al., 2009).

The Eocene/Oligocene boundary Global Stratotype Section and Point (GSSP) has been instituted at the Italian Massignano Section in the Umbria-Marche Basin (Italy), and is defined by the disappearance of the planktonic foraminifera family Hantkeninideae (Coccioni, 1988; Coccioni et al., 1988; Nocchi et al., 1988; Premoli Silva and Jenkins, 1993). Unfortunately, at southern high latitudes Hantkeninideae are absent and their last occurrence is not usually recorded.

The nannofossil bioevents that best approximate the Eocene/Oligocene boundary are the Highest Occurrence (HO) of *Discoaster saipanensis,* defining the NP20/NP21 boundary of Martini (1971) at 34.2 Ma according to Berggren et al. (1995), the HO *Discoaster barbadiensis*, and the HO of *Pemma papillatum* (Pearson et al., 2008). At high latitudes, where *Discoasters* are nearly absent, the Highest Occurrence of *Reticulofenestra oamaruensis*, at 33.7 Ma (Berggren et al., 1995), is used as the nannofossil bioevent that best approximates the E/O boundary (Wei and Thierstein, 1991; Wei and Wise, 1992).

In this study we carried out a quantitative analysis of calcareous nannofossil assemblages from Site 1090 Hole B (Agulhas Ridge, Atlantic sector of the Southern ocean) (Fig. 1) in the late Eocene- late Oligocene time interval (~35.5-26.5 Ma) (Cande and Kent, 1995). The goals of this study were: to carry out a high resolution biostratigraphic analysis in order to refine the position of the bioevents, previously identified in a lower resolution work by Marino and Flores (2002) and, based on assemblage composition variations, to reconstruct the characteristics of the sea surface waters in terms of temperature and fertility, with the final aim to obtain information about the paleoceanographic setting of South Atlantic in the studied time interval.
In the Eocene and Oligocene, Site 1090 was located very close to the CCD (Gersonde et al., 1999; Van Andel, 1975) and it therefore represents an ideal site to study the depth variations of this chemical oceanographic surface. Thus, we carried out a detailed study of nannofossil assemblage variations, in terms of composition and fragmentation, across the EOT at this Site. This theme is discussed in detail in Chapter 4 of this dissertation.
An unconformity was identified at ~221 mcd by seismic profiles (Wildeboer Shut et al., 2002) and it is represented by sediment disturbance in core 1090B-27X-6. This unconformity corresponds to a hiatus (Channell et al., 2003; Marino and Flores, 2002) lasting about 3.3 m.y.

2. Materials and methods

Site 1090 Hole B was drilled during Leg 177 and is located on the northern flank of the Agulhas Ridge in the Atlantic sector of the Southern Ocean (42° 54.81'S, 08° 53.98'E). The goal of Leg 177 was to reconstruct paleoclimatic changes of the Southern Ocean during the Cenozoic, focusing on Antarctic cryosphere evolution and on the role of the South Atlantic paleoceanographic changes in determining global climate evolution.
Site 1090 current water depth is 3702 m, and is located along the boundary between the North Atlantic Deep Water (NADW) and the Circumpolar Deep Water (CDW). It lies today above the CCD (Gersonde et al., 1999) but it was probably close or below it during the Eocene, until the CCD deepened at the Oi-1 event (Gersonde et al., 1999; Van Andel, 1975) and this may explain the presence of numerous samples barren of nannofossils seen along the section. Paleomagnetic data show that the latitudinal and

longitudinal position of this site changed as much as a few degrees (~ 5°) since the Eocene (Gersonde et al., 1999) and, therefore, its position in relation to continents, and with respect to ocean currents, has not changed.

The studied section belongs to Unit II (Gersonde et al., 1999) composed by mud-bearing diatom ooze, mud- and diatom-bearing nannofossil ooze, and chalk. Numerous samples are barren or almost barren of nannofossils and are distributed all along the section, but they were more common in cores 1090B-26X, 29X and 30X. Most of these samples correspond to the pale green diatom ooze intervals recognized by Gersonde et al. (1999). Also, Unit II shows high-amplitude and short-term fluctuations in carbonate content. This variability is linked to either carbonate dissolution or alternation between nannofossil ooze, opal-rich sediments and terrigenous mud.

The study section spans the late Eocene- late Oligocene, and it represents one of the best sections for this time interval thanks to the high sedimentation rates and to the excellent magnetostratigraphic signal (Channell et al., 2003). At this site, a short normal-polarity subchron ("cryptochron") within the C13r (Channell et al., 2003) was recognized for the first time, also thanks to late Eocene high sedimentation rates (15-40 m/Ma).

In this work, a quantitative analysis of calcareous nannofossil assemblages has been performed on 699 samples from IODP Hole 1090 B, on Cores 24 to 30 (182.91- 293.43 mcd), spanning the time interval from the late Eocene to the late Oligocene (~35.54-26.5 Ma). Samples were prepared using the settling technique proposed by de Kaenel and Villa (1996) and analyzed using a Zeiss Axioscope at 1250 magnification.

In each sample, 10 fields of view were analyzed, counting a total of at least 300 nannofossil specimens. In samples where nannofossil abundance was very low, up till 50 fields of view were examined. To find rare species, a further traverse was scanned in addition to the standard count. Data were acquired and collected using Bugwin software, and then plotted as abundances/mm^2 for the biostratigraphic analysis, and as percentages for the paleoecological interpretation. Sampling resolution applied in this work is 10 cm for most of the section, with some intervals analyzed every 20, 30, 40, 50 or 60 cm resolution. Standard nannofossil zonal schemes were adopted (Martini, 1971; Okada and Bukry, 1980) together the high latitude zonation of Wei and Thierstein (1991). The section spans from NP19/20 to NP23-NP24 *pars* (Martini, 1971), from

CP15b to CP17-CP19 *pars* (Okada and Bukry, 1980), from *Isthmolithus recurvus* Zone *pars* to *Chiasmolithus altus* Zone *pars* (Wei and Thierstein, 1991) (Fig. 2). Several additional events were identified and are shown in Figs. 2 and 3. A hiatus was identified at 221 mcd (This work, Channell et al., 2003; Marino and Flores, 2002).

A middle Eocene-early Oligocene (400-200 mcd) lower resolution (1-2 samples/ section) biostratigraphic study on Hole 1090 B was previously carried out by Marino and Flores (2002) and was used here as a reference.

Bulk stable carbon and oxygen isotopes and carbonate content (estimated from XRF analysis) from Site 1090 were provided by Bohaty and Palïke (unpublished data, 2010).

For the age-model, the time scale of Cande and Kent (1995), applied to the magnetostratigraphic signal of Channel et al. (2003), was used.

3. Results

Nannofossil assemblages at Site 1090 Hole B are highly variable in both abundance and preservation. Several interval within Hole 1090B are affected by intense carbonate dissolution. Two major dissolution events occur between ~201 and 213 mcd (28-28.8 Ma) (at the passage between Early and Late Oligocene) and between ~252 and 255 mcd (33.8-33.9 Ma) (latest Eocene). Despite the scarce preservation state observed in many samples/intervals, all nannofossil zonal markers of the adopted zonations were recognized (Fig. 2, Table 1), besides the top of Zone NP23 because of the lack of *S. pseudoradians*.

3.1. Nannofossil biostratigraphic events

The eleven nannofossil biostratigraphic events recognized at Site 1090 are summarized in Tables 1 and in Fig. 3, and are described hereinafter. In Table 2, age assignments of the recognized biostratigraphic events from some selected previous works, are given. Events are labeled as Lowest and Highest Occurrence (LO and HO, respectively), Base and Top Acme (BA, TA).

1) The **LO of *Reticulofenestra oamaruensis*** was found between Samples 1090B-30X-6-13 and 30X-6-44 (291.62-291.93 mcd) (average depth 291.77 mcd) with an estimated age of 35.455 Ma, slightly older than found by Marino and Flores (2002). *R. oamaruensis* is only present at high southern latitudes, where its HO and LO are considered useful events, which have been included in several high-latitude zonations (Edwards, 1971; Edwards and Perch-Nielsen, 1975; Fioroni et al., 2010; Wei and Wise, 1990b; Wise, 1988; Wise et al., 1983). The central area of *R. oamaruensis* is often missing, and the remaining rim can be easily confused with a *Chiasmolithus* rim. The great majority of *Chiasmolithus* at Site 1090 lack, as a matter of fact, their central crosses and, within *R. oamaruensis* distribution interval, it is possible that some specimens were not correctly identified. For this reason it is likely that both the LO and the HO of *R. oamaruensis* seen at this Site, might be slightly younger and older, respectively, than they are in reality. The LO of *R. oamaruensis* falls within Chron C16n1n, in agreement with Wei and Thierstein (1991) and Berrgren et al. (1995). This event marks the base of the *R. oamaruensis* Zone of Wei and Thierstein (1991).

2) The **HO of *Discoaster saipanensis*** is classically considered the best nannofossil event approximating the Eocene/Oligocene boundary but it is latitudinally diachronous (Berggren et al., 1995). The HO of *D. saipanensis* is used to define the NP21/NP20 zonal boundary (Martini, 1971) and the CP15b/CP16a zonal boundary (Okada and Bukry, 1980). At Site 1090, this event was seen in the middle part of Chron C13r, just above the short normal polarity Chron C13r.1n (Channell et al., 2003), between Samples 1090B-27X-5-82 and 27X-5-93 (261.71-261.82 mcd) (average depth 261.76 mcd) and it was dated at 34.067 Ma. At the same site, Marino and Flores (2002) found the HO of *D. saipanensis* in a slightly lower position, at 262.39 mcd.

   At low and middle latitudes, this event is found in the upper part of Chron C13r (Late Eocene) (e.g. Coccioni et al., 1988; McGonigal and Di Stefano, 2002) and, at higher latitudes, in Chron C16n-C18n (Late-Middle Eocene) (e.g. Arney and Wise, 2003; Villa et al., 2008; Wei and Thierstein, 1991; Wei et al., 1992). This diachronism is most likely linked to the paleoecological preference of

Discoasters toward warm and oligotrophic waters (e.g. Aubry, 1992; Wei and Wise, 1990a) and, as a consequence of the global cooling occurring starting from the Eocene (e.g. Zachos et al., 2001), at higher latitudes Discoasters experience an early extinction. This early extinction event has been proposed as a useful marker (Villa et al., 2008).

3) The **HO of *Reticulofenestra oamaruensis*** is another event used to define the Eocene/Oligocene boundary by using nannofossils. This event is particularly useful at high latitudes, where warm Discoasters are scarce. At Site 1090, the HO of *R. oamaruensis* was seen between Samples 1090B-27X-3-33 and 27X-3-43 (258.22-258.32 mcd) (average depth 258.27 mcd) and calibrated at 33.975 Ma. The HO of *R. oamaruensis* is used to define the top of *R. oamaruensis* Zone of Wei and Wise (1990b) and Wei and Thierstein (1991).
   At higher southern latitudes, the HO of *R. oamaruensis* was dated 33.7 Ma (Berggren et al., 1995; Wei and Thierstein, 1991; Wei et al., 1992; Wei, 2004) and 33.91-33.71 Ma (Persico and Villa, 2004).
   Based on the calculation of the sedimentation rates between Chron boundaries at Site 1090, the Eocene/Oligocene boundary (33.7 Ma) was placed at ~247.90 mcd, which falls within the plateau bracketed by the two steps, Step 1 (~251 mcd) and Step 2 (252 mcd), defined by oxygen isotope record (Coxall et al., 2005; Pearson et al., 2008).

4) The **Base of the Acme of *Clausicoccus*** was found between Samples 1090B-24X-1-14 and 24X-1-34 (245.33-245.53 mcd) (average depth 245.43 mcd) at 33.635 Ma. The acme of *Clausicoccus* occurs almost at the same stratigraphic level than the Acme of *Blackites*, the former starting about 10 m (mcd) below the latter. Also, the Acme of *Blackites* terminates at 226.18 mcd, differently from the top of the Acme of *Clausicoccus*, which occurs at 234.12 mcd.
   The classification at species level of *Clausicoccus* is difficult only by using a light microscope, being based on the number of holes in the central area. For this reason, specimens belonging to genus *Clausicoccus* were grouped together in

Clausicoccus spp. Several specimens of *C. fenestratus* were recognized in many samples, therefore we assume that most of *Clausicoccus* may be *C. fenestratus*.

5) The **Base of the Acme of *Blackites* spp.** was seen between Samples 1090B-25X-1-124 and 1090B-25X-1-134 (235.45-235.55 mcd) (average depth 235.50 mcd) and its estimated age is 33.369 Ma.

6) The **LO of *Reticulofenestra circus*** was seen between Samples 1090B-25X-1-104 and 25X-1-114 (235.25-235.35 mcd) (average depth 235.30 mcd) (33.363 Ma). At Site 1090, *R. circus* is present in low abundances. This event was previously seen at this Site at 234.81 mcd (Marino and Flores, 2002), so just slightly above the position found in this work. At Site 1090 this event occurs in the middle of Chron C13n, within nannofossil zone NP21. At lower latitudes, de Kaenel and Villa (1996) found (and erected) *R. circus* in early Oligocene sediments from the Iberia Abyssal Plain (Atlantic Ocean) and recognized its LO within zone NP22. Maiorano (2006) confirmed the stratigraphic position of this event within NP22 at North Atlantic DSDP Site 558.

7) **Top of the Acme of *Clausicoccus*** occurs at 234.12 mcd (average depth), between samples 1090B-24X-7-23 and 25X-1-4 (233.99-234.25 mcd) with an assigned age of 33.33 Ma, in agreement with Berggren et al. (1995) and Marino and Flores (2002). The TA was placed where *Clausicoccus* abundance drops from about 500 specimens/mm_2 to about 0. In Chapter 4, the use of *Clausicoccus* as dissolution proxy is given.

8) The **Top of the Acme of *Blackites*** was recognized between Samples 1090B-24X-1-137 and 24X-1-147 (226.13-226.23 mcd) (average depth 226.18 mcd) and dated at 33.117 Ma. The TA of *Blackites* is not as abrupt as the TA of *Clausicoccus*, and occurs after a gradual diminishing trend (Fig. 3). The TA of *Blackites* was picked at about mid-way of its decreasing trend. All *Blackites* seen at Site 1090 lack the base and thus cannot be recognized at species level, but the apical spine is similar to the spine of *B. spinonus*.

The acme of *Blackites* was found in the early Oligocene at several sites in the South Atlantic and South Pacific (Marino and Flores, 2002; McGonigal and Di Stefano, 2002; Wei and Wise, 1990a). A discussion about the potential of *Blackites* as dissolution indicator is given in Chapter 4 of this dissertation.

9) The **HO of *Ericsonia formosa*** occurs between Samples 1090B-23X-7-149 and 24X-1-7 (221.89-224.93 mcd), might fall within the hiatus, and either in the upper part of Chron C13n or in the lower part of Chron C12r.

   The HO of *E. formosa* is a diachronous event which was found in Chron C18 at southern high latitudes and in Chron C13n or C12 at middle and low latitudes (Berggren et al., 1995). At Site 1090, we consider reliable the age of 32.8 Ma assigned by Berggren et al. (1995), as plausible considering the age model adopted here.

10) and 11) The **HO of *Istmolithus recurvus*** and the **HO of *Reticulofenestra umbilicus*** both occur between Samples 1090B-23X-7-110 and 23X-7-130 (221.50-221.70 mcd), in Chron C12r or C11n, as also reported by Channell et al. (2003). The proximity of these three events marks the presence of a hiatus that cuts part of Chron C12r and C11n (Channell et al., 2003).

   The HO of *I. recurvus* is a diachronous event, found in either the upper part of Chron C13n (Coccioni et al., 1988; Poore et al., 1984), in the lower part of C12r (Lowrie et al., 1982; Miller et al., 1985; Parker et al., 1985; Poore et al., 1984; Villa et al., 2008; Wei and Wise, 1989) or in the middle part of Chron C12r (Wei and Thierstein, 1991; Wei and Wise, 1990b). Berggren et al. (1995) dated this event at 31.9-33.1 Ma.

   The HO of *R. umbilicus* is another diachronous event, found within the lower part of Chron C12r at low-mid latitudes (Berggren et al., 1995; Lowrie et al., 1982; Miller et al., 1985; Poore et al., 1984) and within the upper part of the same Chron at higher latitudes (Berggren et al., 1995).

   Based on biostratigraphic and magnetostratigraphic record interpretation, the hiatus, located at ~221 mcd, has an age comprised between ~29.6 Ma and ~32.9 Ma, with a total duration of ~3.3 Ma.

3.2. Taxa distribution

The most abundant taxa found at Site 1090 are *Cyclicargolithus floridanus*, *Reticulofenestra daviesii*, *Reticulofenestra* sp. (3-5 μm), *Coccolithus pelagicus*, *Chiasmolithus* spp., *Reticulofenestra umbilicus*, *Reticulofenestra samodurovi*, *Isthmolithus recurvus* and *Dictyococcites bisectus. Blackites* and *Clausicoccus* are present only in the lower Oligocene part of the section where they reach abundances up to 10% and 20%, respectively. Minor important components (≤5%) are Discoasters, *Sphenolithus* and *E. formosa.* Several other species in very low abundances were found but they are not shown because they do not have any biostratigraphic or paleoecological significance.

For the description of taxa distribution changes, stable oxygen isotope Step 1 (252-250 mcd, ~33.7 Ma) and step 2 (241-239 mcd, ~33.5 Ma) are used as marker levels, being such important phases in the global climatic evolution (Coxall et al., 2005; Dunkley Jones et al., 2008; Katz et al., 2008; Miller et al., 2009; Pearson et al., 2008).

Chiasmolithus

Representatives of genus *Chiasmolithus* found at Site 1090 are *C. expansus*, *C. grandis*, *C. modestus*, *C. oamaruensis*, *C. solitus* and *Chiasmolithus* sp. (specimens missing the central cross, the most abundant in the studied samples). From the base of the section up to 255 mcd (~33.9 Ma) *Chiasmolithus* relative abundance is generally lower than 10% (Fig. 4). A gradual increase occurs between Step 1 and Step 2. Higher values are reached just above Step 2 and are then maintained up to 221 mcd (hiatus). Above the hiatus, Chiasmoliths drop significantly in abundance. The succession is affected by an intense carbonate dissolution event from ~213 to 201 mcd, where samples are barren or almost barren of nannofossils. From 201 mcd up to the top of the section Chiasmoliths are highly variable in abundance.

Coccolithus

At Site 1090, genus *Coccolithus* is represented by *C. pelagicus* and *C. eopelagicus* (i.e. ≥14 μm). *Coccolithus* abundance is strongly variable along the section (Fig. 5). From the base of the section up to 264 mcd their abundance is generally lower than 10%. An

increase occurs between 264 and 257 mcd. At Step 1 and within the isotopic plateau (~250-241 mcd) values are quite constant (~10%). A well defined increase in abundance occurs in correspondence of Step 2, and, up to the hiatus, *Coccolithus* abundance is higher (15%) than in the Eocene part of the section. Above the hiatus, *C. pelagicus* abundance drops significantly. Similarly to *Chiasmolithus*, *Coccolithus* abundance is markedly variable in the upper part of the section (from ~201 mcd).

***Reticulofenestra daviesii* and *Reticulofenestra* sp. (3-5 µm)**

For the paleoecological interpretation, *R. daviesii* and *Reticulofenestra* sp. (3-5 µm) were grouped together in *R. daviesii* group because of their similar distribution and their supposed similar paleoecological preference. Hereinafter these two taxa are labeled *R. daviesii* group. This group is the most abundant component of the assemblages along most of the section. From the base of the section up to ~264 mcd, average values are around 50%; at this level, a marked decrease occurs, lowering the abundance to about 20% (Fig. 4). At Step 1 and within the isotopic plateau (~250-241 mcd), *R. daviesii* group shows a slight and gradual increase, that becomes much more pronounced in correspondence of the base of Step 2 (241-239 mcd). It fluctuates in abundance up to the hiatus and it drops to very low abundance above it.

Reticulofenestra umbilicus, R. samodurovi, R. hillae* and *R. dictyoda

For our paleoecological interpretation, all medium-sized and big *Reticulofenestra* were grouped together in *R. umbilicus* group, following an approach adopted previously (e.g. Villa et al., 2008), based on their similar distribution and deduced paleoecological preference. At Site 1090, *R. umbilicus* group shows high abundance variability, ranging between ~ 1% and ~58% from the base of the section up to 256 mcd, and with a subtle increase in abundance around 263 mcd (Fig. 4). At Step 1 values are low, followed by an increase within the isotopic plateau (~250-241 mcd), and a subsequent decrease at Step 2. From Step 2 up to 228 mcd, abundance values are comparable to those seen the Eocene part of the section. At 228 mcd, a gradual increase in abundance is shown by this group, similarly to *Chiasmolithus* trend. In the upper part of the section, from 201 mcd up to the top, *R. umbilicus* group is almost absent.

Cyclicargolithus floridanus

Cyclicargolithus floridanus is present in low abundances in the lower part of the section, up to 260 mcd, where its abundance increases (Fig. 5). At Step 1 and within the plateau (~250-241 mcd) values remain relatively high, similar to those reached below the dissolution level of the upper Eocene (below 256 mcd). From Step 2 up to the hiatus (221 mcd) *C. floridanus* has low abundances. Just above the hiatus, a striking increase in abundance of *C. floridanus* occurs, switching from about 1% to 80-100% abundance. Above the major dissolution level (from 201 mcd) this species still dominates within the assemblages, but shows a more pronounced variability compared to the interval below the dissolution level.

Dictyococcites bisectus

Dictyococcites bisectus shows wide abundance variations, ranging from 0 to 45% of the total abundance (Fig. 5). Eocene average values are around 15%, and they decrease within the isotopic plateau, reaching very low values at Step 2, values that are maintained up to the hiatus. A slight increase is shown between 230 mcd and the hiatus, at the same level where several other taxa, such as *R. daviesii* group, *Chiasmolithus* and *R. umbilicus* group, experience significant changes (Fig. 4 and 5). Above the hiatus, *D. bisectus* is quite changeable.

***Discoaster* spp.**

At Site 1090, *D. barbadiensis*, *D. saipanensis*, *D. adamanteus*, *D. nodosus*, *D. tani*, *D. tani nodifer*, *D. deflandrei* and *Discoaster* sp. were recognized and grouped together in *Discoaster* spp. for the paleoecological interpretation.

In the Eocene, *Discoaster* relative abundance is markedly variable (Fig. 5), with an average around 2%. Step 1 shows an almost complete absence of Discoasters and it is followed by a significant and short increase between 249 and 248 mcd. Within this phase of increased *Discoaster* abundance after Step 1, a few specimens of *D. saipanensis* were found and were interpreted as reworked. Reworking at this level is also indicated by the presence of some specimens of *R. oamaruensis* (Fig.3).

Ericsonia formosa

The relative abundance of *E. formosa* is quite stable and low along the studied section, being constantly lower than 5% (Fig. 5). An increase in abundance is recorded from 264 mcd to 255 mcd. No particular variations are shown at the EOT. However, Oligocene average abundances are clearly lower than those recorded in the Eocene. The HO of this species falls within the hiatus at 221 mcd (Table 1, Figs. 2, 3).

***Sphenolithus* spp.**

At Site 1090 Sphenoliths are scarce (≤1.5 %) and with a scattered distribution (Fig. 5). Representatives of genus *Sphenolithus* are at this site *S. moriformis* and *Sphenolithus* sp., and they were all grouped in *Sphenolithus* spp. for the paleoecological discussion. Only one specimen of *S. predistentus* was found in Sample 1090-29X-1-104 (275.33 mcd). Intervals of higher abundance are 294-280 mcd, 239-228 mcd and 194-190 mcd.

Isthmolithus recurvus

At Site 1090, *Istmolithus recurvus* is more abundant in the Eocene compared to the Oligocene, even if its distribution is strongly variable, especially in the lower part of the section, up to 255 mcd (Fig. 5). No particular variations are shown during the EOT.

***Clausicoccus* spp.**

Clausicoccus spp. show very low abundances from the base of the section up to 274 mcd (Fig. 6). From 274 to up to ~242 mcd they almost completely disappear. At 242 mcd, corresponding to the base of Step 2, *Clausicoccus* starts to significantly increase in abundance, determining the base of the Acme (Fig. 2, Table 1).

***Blackites* spp.**

Blackites are almost absent along the section, but two phases of increase can be distinguished between the base of the section up to 282 mcd, and between ~236 and 225 mcd. Our quantitative analysis of fragmentation within nannofossil assemblages across the EOT at Site 1090, discussed in Chapter 4 of this dissertation, revealed that *Blackites* and *Clausicoccus* can be used as reliable dissolution indicators.

Two general distribution patterns can be recognized within nannofossil distribution characterized by taxa *increasing* or *decreasing* in abundance across the EOT. Following an approach previously adopted by Dunkley Jones et al. (2008), we grouped together taxa showing the same general behavior, in a way to minimize the variations of the single species and to strengthen the general nannofossil assemblage fluctuations.

Taxa increasing across the EOT (Group 1) (Fig. 6-8) are *R. daviesii* group, *Chiasmolithus* spp., *C. pelagicus*, *Sphenolithus* spp., *Clausicoccus* spp. and *Blackites* spp.. Taxa decreasing at the EOT (Group 2) (Fig. 6-8) are *D. bisectus*, *E. formosa*, *Discoaster* spp. and *R. umbilicus* group. Group 1 is more abundant than Group 2 all along the section. Not all of the taxa are included within one of the two groups, so there is no closed-sum problem.

Group 1 has values around 60% from the base of the section up to 264 mcd, where a sudden drop occurs, lowering average abundances to 30% (Fig. 6-8). A marked increase is then showed at ~245 mcd. Very high values (~70%) are maintained up to the hiatus at ~221 mcd.

Group 2 relative abundance is around 30% from the base of the section up to 264 mcd, where values increase, reaching abundances of 50%. The variation in relative abundance shown by Group 1 is not as pronounced as the one recorded by Group 2.

Also, at 259 mcd, Group 2 abundances slightly decrease. Differently, at the same level, Group 1 shows more stable values, with no significant changes. A further significant change showed by Group 1 occurs at 245 mcd, where values decrease. Also in this case, Group 1 variation is not as marked as the one recorded at the same level by Group 2 but it is however well-defined.

Group 1 decrease in abundance at 245 mcd occurs within an interval of gradual declining values, that started at about 248 mcd. This represents another difference between records of Group 1 and Group 2 across the EOT (~240-251 mcd), where Group 1 shows gradually declining values started just above Step 1 and continues up to Step 2 (240 mcd). Differently, Group 2 shows more stepwise variations, with the major change occurring at 245 mcd. Above Step 2, Group 2 maintain abundances around 10% up to about 228 mcd, where abundances start gradually to decline up to the hiatus. Starting from 228 mcd, a similar but opposite trend can be also seen in Group 1 record, where a decrease in abundance occurs in the same interval.

Group 1 and 2 variations identify three major assemblage changes: at ~265 mcd (~34.1 Ma) (labeled N1), at ~244 mcd (~33.6 Ma) (labeled N2) and another one in correspondence of the hiatus (~221 mcd).

4. Discussion

4.1. Nannofossil paleoecological classification

For the paleoecological interpretation of the assemblages, only certain taxa were used. Our choice was based on interpretations available in previous works (described hereinafter), joined to the results obtained in this work. Among others, fundamental previous works on paleoecological and paleoecanographic reconstructions using calcareous nannofossil assemblages are Bukry (1973), Wei and Wise (1990a), Wei and Wise (1990b), Wei and Thierstein (1991), Aubry, (1992), Villa et al. (2008), Wei et al. (1992), Monechi et al. (2000), Dunkley Jones et al. (2008). Taxa paleoecological interpretation used in this work is shown in Table 2.

R. daviesii has been consistently interpreted as a cold water taxon (Monechi et al., 2000; Persico and Villa, 2004; Villa et al., 2008; Villa and Persico, 2006; Wei and Thierstein, 1991; Wei et al., 1992). *R. daviesii* group significantly increases in abundance in the early Oligocene of many Southern Ocean sites (e.g. Persico and Villa, 2004; Villa et al., 2008; Wei et al., 1992) and several works demonstrated an increase in fertility and productivity across the EOT at all latitudes (e.g. Diester-Haass and Zachos, 2003; Dunkley Jones et al., 2008; Zachos and Kump, 2005). For this reason *R. daviesii*, besides being considered cold/cool, is usually associated to nutrient-rich waters. In this work, we consider *R. daviesii* group as cold and eutrophic.

Chiasmolithus are considered cool/cold (this work, Bralower, 2002; Firth and Wise, 1992; Persico and Villa, 2004; Tremolada and Bralower, 2004; Villa et al., 2008; Villa and Persico, 2006; Wei and Wise, 1990a; Wei and Wise, 1990b).

C. pelagicus paleoecological interpretation was long debated and this species was seen as warm (Wei and Wise, 1990a; Wei and Wise, 1990b) or temperate (Persico et al., 2004; Villa et al., 2008; Villa and Persico, 2006). This species has changed its ecological preference through time as Pleistocene and living *C. pelagicus* prefer cold (Haq and Lohmann, 1976) or cold and mesotrophic (Holmes et al., 2004) and/or eutrophic waters (Cachao and Moita, 2000). In this work we assign to *C. pelagicus* a preference for temperate and eutrophic waters.

R. umbilicus and *R. samodurovi* have been considered temperate (together with *R. dictyoda*, forming the *R. umbilicus* group) (Persico and Villa, 2004; Villa et al., 2008; Wei and Wise, 1990b), warm- oligotrophic/mesotrophic (Aubry, 1992), and warm-mesotrophic (Monechi et al., 2000). Here we consider *R. umbilicus* group as temperate and mesotrophic/eutrophic.

E. formosa has been interpreted as warm (Monechi et al., 2000; Wei et al., 1992; Wei and Wise, 1990b), warm-oligotrophic (Bralower, 2002; Tremolada and Bralower, 2004; Villa et al., 2008) or warm-eutrophic (Agnini et al., 2009). We classify *E. formosa* as warm and mesotrophic.

Discoasters have been consistently thought as warm and oligotrophic (Bralower, 2002; Dunkley Jones et al., 2008; Kahn and Aubry, 2004; Kelly et al., 1996; Tremolada and Bralower, 2004; Villa et al., 2008), and this interpretation is followed in this work.

Sphenoliths have been considered warm and oligotrophic (Bralower, 2002; Gibbs et al., 2006b; Villa et al., 2008) or mesotrophic/eutrophic (Agnini et al., 2006; Dunkley Jones et al., 2008; Gibbs et al., 2006b; Wade and Palike, 2004). Based on our results, Sphenoliths are considered in this work as warm and mesotrophic.

C. floridanus has been interpreted as eutrophic (Aubry, 1992; Monechi et al., 2000) or temperate (Wei and Wise, 1990a) but a general consensus about the paleoecological preference of this species has not been reached yet, and results obtained in this work suggest the opportunistic character of this species.

D. bisectus has been considered warm/temperate (Wei and Wise, 1990a; Wei and Wise, 1990b), temperate (Persico and Villa, 2004; Villa et al., 2008; Villa and Persico, 2006; Wei et al., 1992) or warm (Monechi et al., 2000). Here we consider this species as temperate.

Nannofossil total abundance/mm^2 is shown, together with Group 1 and Group 2 distributions in Figs. 4 and 7.

4.2. Nannofossil assemblage changes

The first significant change (N1) experienced by nannofossil assemblages occur at ~34.12 Ma (264 mcd), before the EOT. This variation is recorded more intensely by Group 1 than by Group 2 (Figs. 6, 7) and corresponds with a decrease in nannofossil total abundance and with a short interval of low carbonate content (Figs. 4, 7), but it does not correspond to any particular fluctuation of stable oxygen and carbon isotopes (Figs. 4, 7). Carbonate content at Site 1090 is highly variable (Fig. 4) and dissolution is likely the most determinant factor in driving carbonate fluctuations (for a detailed discussion about nannofossil as dissolution proxies, see Chapter 4 of this dissertation). Site 1090 was, in the Eocene, very close to the CCD (Gersonde et al., 1999; Van Andel, 1975) and therefore it is in an ideal location to record also minor CCD depth variations. A major CCD deepening occurred at Step 2 (Oi-1) (~33.5 Ma) in all oceans (Coxall et al., 2005; Van Andel, 1975), as shown also at Site 1090 by the strong increase in carbonate content (Fig. 4).

It is possible that also nannofossil abundance decrease seen at N1 is partly controlled by dissolution. Nevertheless, our interpretation of nannofossil changes at N1 is not considered biased by dissolution. In fact, if nannofossil turnover occurring at N1 was determined by dissolution, the assemblage variations seen at that level, would have a limited duration, restricted to the low carbonate interval between about 263 and 264 mcd. Instead, the renovated nannofossil assemblage characteristics reached at N1 are maintained above the interval of low carbonate content, demonstrating that nannofossil assemblages experienced a long-term change, probably in response to a variation of the climatic conditions.

Among Group 1, assemblage change controlling N1 are a decrease in abundance of *R. daviesii* group and an increase of *C. pelagicus*. Within Group 2, a slight increase in abundance of *R. umbilicus* group and a quite pronounced increase in *E. formosa* are recorded.

Considering the paleoecological preference of taxa controlling N1 event, the paleoceanographic change occurring at this level could have been A) A warming event, shown by the decrease of *R. daviesii* group, the increase of *C. pelagicus* and the slight increase of *R. umbilicus* group; B) An increase in nutrient availability, shown by the increase in abundance of *C. pelagicus*, *R. umbilicus* group, *E. formosa* and *C. floridanus* (?); C) A warming with increasing nutrient availability.

The HO of *D. saipanensis* occurs slightly above N1, at 261.76 mcd (34.067 Ma); as said, Discoasters have been consistently described as warm and oligotrophic (Bralower, 2002; Dunkley Jones et al., 2008; Kahn and Aubry, 2004; Kelly et al., 1996; Tremolada and Bralower, 2004; Villa et al., 2008), so it seems plausible that at this site the HO of *D. saipanensis* may be linked to the climatic change recorded at N1. In fact, Discoasters marked paleoecological preference for warm and oligotrophic waters has been used to justify the diachrony of *D. saipanensis* HO at different latitudes (Berggren et al., 1995). Similarly, the HO of *R. oamaruensis* occurs just above the HO of *D. saipanensis*, very close to N1; it is therefore possible that both these events have been influenced by the same climatic change.

We think that the marked drop in abundance of cool-water *R. daviesii* at N1, from about 50% down to 20% must reflect a warming event, most likely accompanied by an increase in nutrient availability. This is in agreement with the increase in abundance of *C. pelagicus* (temperate and eutrophic), the increase of *C. floridanus* (if we consider reliable its interpretation as a eutrophic taxa) and the increase in abundance of *E. formosa* (warm and mesotrophic/eutrophic). This would be consistent with the climatic signal given by HO of oligotrophic *D. saipanensis*.

Differently from Site 1090, calcareous nannofossil EOT records from Tanzania (Dunkley Jones et al., 2008) show, at ~34 Ma a sea-surface temperature decrease (~2°C) (obtained from Mg/Ca measurements) and an increase in nutrient availability, as demonstrated by the decrease in oligotrophic taxa (holococcoliths and Discoasters).

Despite the opposite sea surface variation interpreted at these two far locations (South Atlantic Ocean and Tanzania), it is however significant that one of the major biotic changes recorded by nannofossils across the EOT occurs at the same time (~34 Ma). A possible link between these simultaneous events has not been established yet.
Radiolarian assemblage variations from the Southern Ocean (Site 689, Maud Rise) (Funakawa and Nishi, 2008) recorded, between 34.1 and 33.9 Ma, a warming phase that was interpreted as caused by the southward migration of the proto-Antarctic Polar Front, following either a global warming or an interglacial phase. Also, at the same site and in the same time interval, a warming phase was recorded by calcareous nannofossils (Persico and Villa, 2004). These records are in agreement with our nannofossils data, and considered the geographic/paleoceanographic vicinity between Site 689 (Maud Rise, 64°S) and Site 1090 (Agulhas Ridge, 42°S) the warming phase seen at both sites may be linked and driven by the same paleoceanographic processes.

Following N1 and up to the base of the dissolution interval at ~33.9 Ma (255 mcd) nannofossil assemblage characteristics are stable, not showing any marked variations (Fig. 7). Within this interval, a transient change is recorded at ~33.95 Ma (257 mcd), when Group 1 shows a peak in abundance. This peak is determined by a marked increase in abundance of cold *R. daviesii* group and by a decrease of temperate *C. pelagicus* (Figs. 4, 5) and may represent a short cooling event.

Between ~33.8 and 33.9 Ma (252-255 mcd) samples are almost barren of nannofossils (Fig. 7). This interval is affected by intense dissolution, as also indicated by low carbonate content (Fig. 4) and by nannofossil dissolution indices (Chapter 4 of this dissertation). As described there, major carbonate variations recorded at Site 1090 across the EOT are interpreted as CCD variations. The dissolution interval seen at Site 1090 between 33.8 and 33.9 Ma (252-255 mcd) (late Eocene) is a worldwide event that is considered integral of the climatic change occurring at EOT. This dissolution event has in fact been recorded at the same stratigraphic level, at the top of Chron C13r, at all latitudes (Coxall et al., 2005; Diester-Haass and Zachos, 2003; Lear et al., 2008; Liu et al., 2004; Zachos et al., 1996) and has been interpreted as a temporary shoaling of the CCD (e.g. Coxall and Pearson, 2007). Mechanisms driving CCD fluctuations are still

debated, as well as the relation between this and other oceanographic changes occurring at the EOT, such as the cooling, the sea-level drop, the reorganization of the carbon cycle, etc. This dissolution event affects the beginning of the oxygen isotope Step 1 (Figs. 4, 7), which, therefore, cannot be dated precisely. As a consequence, only part of Step 1 (~33.8-33.75 Ma) can be recognized in the isotopic record (Figs. 4, 7).

At Site 1090, isotopic Step 1 corresponds to stable abundance values of nannofossil Group 1, a subtle increase of Group 2 and a recover of the carbonate content (Figs. 4-7). No significant abundance changes are shown by single taxa, and not marked temperature/nutrient variations are recorded by nannofossils.
Step 1, or EOT1 as labeled by Katz et al. (2008) and Miller et al. (2009), has been associated with a cooling of about 2.5°C of tropical and high-latitude surface and bottom waters (Katz et al., 2008; Lear et al., 2008; Miller et al., 2009) and no (e.g. Miller et al., 2005) or limited (Miller et al., 2009) sea-level fall. Nevertheless, in these works, temperatures were estimated using Mg/Ca ratio, a method that suffers from significant limitations, therefore the results have to be considered with caution.
Step 1 corresponds to the extinction of some benthic (Pearson et al., 2008; Wade and Pearson, 2008) and planktonic foraminifera taxa (Miller et al., 2008; Pearson et al., 2008; Wade and Pearson, 2008). Radiolarian assemblages from the equatorial Pacific also experience pronounced assemblage changes at Step 1, with an increase in diversity and evenness, and an increased biotic turnover (Funakawa et al., 2006). No particular variations were seen in correspondence of Step 1 in radiolarian assemblages from Southern Ocean Site 689 (Funakawa and Nishi, 2008), similarly to what we found at Site 1090.

The other prominent nannofossil assemblage change (labeled here N2) occurs very close to the E/O boundary, at 33.6 Ma (~245 mcd), in the middle of the oxygen isotope plateau, and is characterized by a significant abundance increase of Group 1, and a less pronounced decrease of Group 2 (Figs. 6, 7). This turnover is driven by the increase of *R. daviesii* group, *Chiasmolithus* spp. and *Coccolithus*, and, less markedly, by the decrease of *D. bisectus* and *E. formosa*. Significantly, also warm water Discoasters

experience a drop in abundance at this level (Fig. 5), after which they become almost absent.

We interpret N2 as caused by a significant increase in fertility. Most of the taxa increasing in abundance at N2 are cool water taxa and it is possible that a transient cooling occurred at this level. Nevertheless, oxygen isotope record does not show any marked variation in correspondence of N2, and a major cooling event has to be ruled out. The increase in fertility at this level, and also across the EOT, is supported by the increase in abundance of temperate *Coccolithus*, which distribution is likely driven by its preference for nutrient-rich waters and not by temperature, otherwise an abundance decline would occur here. Also, at N2, warm and oligotrophic Discoasters, mainly represented around this interval by *D. deflandrei*, quickly decrease in abundance. In apparent disagreement with this interpretation, *C. floridanus*, another taxa with a proposed preference for eutrophic waters, do not show an increase, but rather a slight decrease. However, the ecological preference of this species is still debated.

Several other evidences of biological turnover have been found worldwide, involving both nannofossil and foraminifera communities. Marked nannofossil (Dunkley Jones et al., 2008) and foraminifera (Pearson et al., 2008; Wade and Pearson, 2008) assemblage changes were found at the same stratigraphic level (within the isotopic plateau). The foraminiferal turnover involves an extinction of five planktonic species, a dwarfing of one species (Molina et al., 2006; Wade and Pearson, 2008) and numerous large benthic biostratigraphic events (Pearson et al., 2008). The nannofossil assemblage turnover consists of a significant change in relative abundances, involving the decline in holococcoliths and Discoaster. This turnover was interpreted as a shift from oligotrophic to eutrophic conditions. Unfortunately, delicate holococcoliths (Wind and Wise, 1978) are not present at Site 1090, most likely because they went dissolved.

Several works spanning the EOT are available from the Southern Ocean (e.g. Persico and Villa, 2004; Villa et al., 2008; Wei et al., 1992; Wei and Wise, 1992; Wise et al., 1992) but sections are highly condensed and a close comparison between them and our records is not possible.

Katz et al. (2008) and Miller et al. (2009) recognized within the EOT a further oxygen isotope step, labeled EOT-2 and located at ~33.63 Ma, between the two Steps 1 and 2. EOT-2 was interpreted essentially as a temperature decrease (Miller et al., 2009),

possibly associated to a sea-level fall (Katz et al., 2008; Miller et al., 2009). EOT-2 is not present in Site 1090 isotopic record (Figs. 4, 7), probably because the resolution is not high enough, or because this it might be linked to a local event occurring at Saint Stephen Quarry (Alabama) where it was originally recorded (Katz et al., 2008). Even if the global character of EOT-2 has still to be verified, the co-occurrence of EOT-2 and cooling recorded at Site 1090 (N2) is considered significant.

The EOT has already shown to be a global event, even if it shows different characteristics (in terms of temperature and fertility changes, ice volume effect, water column stratification, sea level, etc.) at different latitudes and locations. It is therefore possible that global mechanisms (still debated) might have controlled also "minor" variations across the transition, which have still to be studied in detail, like the climatic meaning of the EOT-2 event.

After N2, group 1 abundance shows a gradual decrease that culminates at Step 2 (~33.5 Ma) (Figs. 4, 7); in an opposite way, group 2 shows, at Step 2, the lowest values ever reached along the section (Figs. 6-7). These extreme values are mainly determined by a peak in abundance of cold *R. daviesii* group, by a drop in abundance of temperate *Coccolithus* and by the base of the Acme of *Clausicoccus* (Figs. 4-6).

We interpret N2 as caused by an increase in nutrient availability, possibly accompanied by a cooling. Significantly, starting at Step 2, *Sphenolithus* show a slight increase, and the abundances reached at Step 2 are maintained in the early Oligocene, up to about 33.2 Ma (227 mcd). We think that this unexpected behavior of warm Sphenoliths is related to their preference for mesotrophic/eutrophic waters. *Sphenolithus* paleoecological interpretation is still matter of debate, having been considered as warm (Aubry, 1992; Monechi et al., 2000; Tremolada and Bralower, 2004; Villa and Persico, 2006; Wei et al., 1992), warm/oligotrophic (Agnini et al., 2006; Bralower, 2002; Gibbs et al., 2006a) or warm/eutrophic (Dunkley Jones et al., 2008; Wade and Bown, 2006; Wade and Palike, 2004). The persistence of *Sphenolithus* in the cold early Oligocene, certainly opens questions about the preference of this taxon for warm waters. It is possible, as suggested by Dunkley Jones et al. (2008), that paleoecological preferences are species-dependant and an interpretation of genus as a whole is misleading. In the Tanzania sections, an increase in abundance of *S. predistentus* occurs during the EOT,

while *S. moriformis* does not show significant variations (Dunkley Jones et al., 2008). Differently, at Site 1090, *S. moriformis* is the most abundant representative of the genus at this site and drives the signal of Sphenoliths increase in abundance across the EOT. Despite these uncertainties, it seems clear that at Site 1090 *S. moriformis* is quite tolerant toward cool waters, as shown by the relatively high abundances in the early Oligocene, and probably towards higher nutrient availability. Another indication of increased fertility after Step 2, comes from abundant *C. pelagicus* (Figs. 5).
The cool/nutrient rich conditions seen at Step 2 are maintained in the early Oligocene until ~33.2 Ma (~228 mcd). Our interpretation is in agreement with sedimentological evidence from Site 1090 (Anderson and Delaney, 2005; Diekmann et al., 2004) which indicate, for the early Oligocene, nutrient-rich waters driving diatom productivity.

At ~33.2 Ma (~228 mcd), another nannofossil assemblage change occurs: group 1 starts a gradual decrease in abundance that ends within the hiatus at ~221 mcd (~32.9 Ma) and, at the same time, group 2 gradually increase. This assemblage change is mainly controlled by the significant decrease of *R. daviesii* group and by the increase of temperate forms, such as *D. bisectus* and *R. umbilicus* group. This phase is interpreted a gradual warming phase, starting at 33.2 Ma (~228 mcd). The precise timing of its termination cannot be dated because is lost within the hiatus at ~221 mcd.
The origin of the unconformity at 221 mcd, seen also in seismic profiles (Wildeboer Shut et al., 2002) and of the hiatus associated to it, recognized thanks to nannofossil biostratigraphy (this work, Channell et al., 2003; Marino and Flores, 2002), is still debated. It has been linked to the Marshall Paraconformity (Marino and Flores, 2002), an early-mid Oligocene unconformity found in several sites in the Southern Pacific (Carter and Landis, 1972; Fulthorpe et al., 1996; McGonigal and Di Stefano, 2002) which, in turn, has been associated with either the early Oligocene eustatic lowstand of Haq et al. (1987) or the inception of the Antarctic Circumpolar Current (AACC) (Carter, 1985; Fulthorpe et al., 1996; Marino and Flores, 2002). There is no proved direct link between the early Oligocene unconformity in the South Atlantic Ocean and the Marshall Paraconformity, even if it possible that Southern Ocean unconformities spanning the same time interval are linked to the same paleoceanographic processes.

A further marked nannofossil assemblage change occurs in correspondence of the hiatus at ~221 mcd. Below the hiatus, *R. daviesii* group, *R. umbilicus* group, *C. pelagicus* are the major components of the assemblages, and several other taxa are minor components (Figs. 4, 5). Above the hiatus (Figs. 5, 7), *C. floridanus* becomes dominant, switching from less than 10%, below the hiatus, to almost 100% above the hiatus. This explosion in abundance of *C. floridanus*, and the strong decrease of all of the other components, marks a profound reorganization of nannofossil assemblages. This turnover is certainly linked to the paleoceanographic change that also determined the hiatus at 221 mcd. We suggest that the hiatus represents the inception of a new system of currents, that swept and eroded the ocean floor, creating the unconformity, and took nutrient-rich waters to the sea surface, favoring the dominance of *C. floridanus*. Again, the uncertain paleoecological interpretation of this species does not allow to better define the characteristics of the surface waters. Nevertheless, *C. floridanu*s behavior above the hiatus reveals its r-selective, opportunist character.

Correlated or not to the Marshall Paraconformity, linked or not to the global cooling and the formation of the ice-sheet in Antarctica, certainly surface waters characteristics dramatically changed at some time between about 32 and 29 Ma, and completely modified nannofossil assemblage composition.

An interval affected by carbonate dissolution is present between 28 and 28.8 Ma (~213-201 mcd) (Figs. 3-6,8), where most samples are barren of nannofossils. Also above the dissolution level, nannofossil total abundance is quite low.

Dissolution levels between the Early and the Late Oligocene were found at several Southern Ocean sites (Diester-Haass, 1996; Funakawa and Nishi, 2008; Kennett and Stott, 1990) and are interpreted as caused by a transient shoaling of the CCD (e.g. Diekmann et al., 2004), after the major deepening occurred at Step 2 (Oi-1) (33.5 Ma) (Coxall et al., 2005; Van Andel, 1975). This CCD shallowing might, in turn, be caused by a pulse of corrosive bottom waters produced around Antarctica as a consequence of glaciation (e.g. Diekmann et al., 2004; Kennett and Stott, 1990; Zachos et al., 1996).

To be able to estimate more precisely the degree of dissolution affecting nannofossil assemblages in the late Oligocene part of the section, within and after the dissolution interval, an analysis of fragmentation state of cocccoliths would be necessary.

4.3. Paleoceanography

Site 1090 is located in a strategic position for the understanding of the evolution of the Southern Ocean in the Paleogene, especially in relationship with the development of the Antarctic ice-sheet and its effect on global climate. In fact its location is optimal to record circulation changes following the opening of the Drake passage, the formation of the AACC and the evolution of the Proto-Agulhas Current.

4.3.1. Late Eocene cool-temperate phase (35.5-34.1 Ma)

Nannofossil assemblages at Site 1090 from 35.5 to 34.1 Ma identify cool and eutrophic surface waters. This indicates that cool conditions were present at Site 1090 in the late Eocene, well before the EOT, in correspondence of which the cooling became more pronounced. This is in agreement with sedimentological evidences that indicate high opal deposition during this time (Anderson and Delaney, 2005; Diekmann et al., 2004) which was caused by increased siliceous organism productivity and stronger upwelling (Diekmann et al., 2004), which was likely facilitated at this site by the location on a topographic high, on the flank of the Agulhas Ridge.

Several late Eocene sea surface warming and cooling phases have been recorded in other Southern Ocean sites (Persico and Villa, 2004; Villa et al., 2008) identifying a *late Eocene instability* (Villa et al., 2008), represented at Site 1090, by a cold/temperate phase (35.5-34.1 Ma) and a following warm phase (34.1-33.9 Ma). This periodicity may be linked to the northward and southward migration of the Antarctic polar front (AAPF), an oceanographic surface that today divides, as well as in the late Paleogene, the cold Antarctic surface water from the warmer subantarctic surface water. The AAPF is thought to be an important oceanographic boundary controlling paleoceanographic conditions and micropaleontological assemblages (Lazarus and Caulet, 1993). It is therefore possible that the AAPF, that today is located at about 50°S, slightly south of Site 1090, was located north of the Agulhas Ridge, determining the cool conditions recorded here between 35.5 and 34.1 Ma. The same process can explain the following warming event, recorded from 34.1 to 33.9 Ma, but in this case it would be explained by a southward migration of the polar front. However, temperate radiolarian (Funakawa

and Nishi, 2008) and nannofossil assemblages (Persico and Villa, 2004) suggest that, between 35.5 to 34.1 Ma, Site 689 (Maud Rise) was located northward with respect to the Polar Front. This means that the cool sea surface conditions recorded at Site 1090 in this time period probably have a different origin and are not related to the migration of the polar front.

According to the model proposed by Kennett and Stott (1990), the Eocene ocean was composed by two well-defined layers, the upper one composed of cold waters produced at high latitudes, the lower one composed of warm and saline waters (Warm Saline Deep Waters, WSDW) produced at low latitudes. The vertical movement of the boundary between these two water masses, determines the oceanographic characteristics at different locations. Following this model, the late Eocene periodicity of cool and warm phases at Site 1090, might be explained by the prevail of one of these water masses on the other one. Warming would occur with the movement of the WSDW up to the surface, maybe through upwelling, and cool periods would occur when the surface cold layer is thicker.

Our indication of cool surface between 35.5 and 34.1 Ma seem in disagreement with evidence obtained by TEX^{86} and U^{k}_{37} (Liu et al., 2009), that indicates, at Site 1090, warm temperatures (~20°C) between 37 and 34 Ma. However, the authors recognize that these values are probably overestimated because of the effect of diagenesis or seasonality. Also, their low resolution data (They dated the cooling at *about* 34 Ma) do not allow a precise correlation with our detailed paleontological record.

A large Iridium anomaly was found in Section in Core 30 of Site 1090 (Kyte, 2001). Peaks of Iridium and spherules of extraterrestrial origins were also found in the late Eocene at many other locations (Kyte, 2001; Liu et al., 2002; Montanari et al., 1993; Vonhof et al., 2000). This widespread distribution suggested that the late Eocene cooling may have been triggered or strengthened by extraterrestrial impacts (Vonhof et al., 2000). At Site 689 (Maud Rise) and at the Massignano section (Italy) Vonhof and co-authors proposed that cooling/increase in productivity was perhaps started by the impact and then maintained by some other factor (such as increased albedo from ice

build-up). No evidence of nannofossil assemblage variations were found in correspondence of the impact layer in Core 30 and therefore no significant changes in sea surface characteristics were recorded. Also, an extraterrestrial impact of moderate proportion would probably have a very time-limited influence on climate, and therefore cannot be claimed as a main factor in determining the late Eocene cool temperature at Site 1090.

An alternative explanation for the late Eocene cool phase comes from the influence of cold waters through the Drake Passage and the inception of a circumpolar circulation (Proto AACC). A long and unsolved debate is still underway about the timing of the opening of the Drake Passage, even if recent works date it back into the Eocene, at ~41 Ma (Scher and Martin, 2006) or at ~50 Ma (Livermore et al., 2007; Livermore et al., 2005). Such an early opening of the Drake Passage suggests that a circumpolar circulation started in the late Eocene-early Oligocene (Scher and Martin, 2006), when the Tasmanian gateway finally opened at 35.5-33.5 Ma (Stickley et al., 2004).

4.3.2. Late Eocene warm phase (34.1-33.9 Ma)

Nannofossil assemblages show at ~34.1 Ma (N2) a significant change, which marks the passage from cool to warmer and nutrient-enriched sea surface waters. It is possible that the warming phase recorded from 34.1 to 34.9 Ma was originated by the mechanism described in the previous section, i.e. by upwelling of warm and saline waters to the surface (Kennett and Stott, 1990), process favored by the presence of the Agulhas Ridge. Nevertheless, for these late Eocene warming event another possible interpretation is possible, described hereinafter.

In the Late Eocene, Site 1090 recorded a variation in terrigenous material composition, an increase in Al/Ti ratio, a proxy for sediment source rocks (Latimer and Filippelli, 2002) and an increase in illite content (Diekmann et al., 2004). These sedimentological variations were interpreted as caused by an increased terrigenous supply, and the source for this material was located in South Africa, where dry climate conditions existed (Diekmann et al., 2004; Latimer and Filippelli, 2002). Starting from the middle Eocene,

Site 1090 was affected by currents coming from the low latitudes and transporting heat, moisture and terrigenous material toward the Southern Ocean (Diekmann et al., 2004). These warm currents flowed from the Indian Ocean and along the tip of South Africa where part of it retroflexed, similarly to modern Agulhas Retroflection, and part of it flowed southward affecting the AACC, similarly to the Agulhas Current (Diekmann et al., 2004). It is therefore possible that the sea-surface warming and the shift in sediment composition have the same origin, deriving from the influence of the proto-Agulhas leakage flowing from the Indian ocean to the Atlantic Ocean, carrying warm and enriched waters on the Agulhas Ridge. The climatic shift recorded at 34.1 Ma can thus represent a consequence of either the diversion or the strengthening of the proto-Agulhas current or the effect of warm deep upwelled waters. The warm conditions recorded at Site 1090 coupled with the cool conditions recorded by radiolarian assemblages in the same time interval (34.1-33-9 Ma) at Maud Rise (Funakawa and Nishi, 2008) place the AAPF between 65°S and 42°S.

4.3.3. Event of increased fertility and cooling (?) at 33.6 Ma

Calcareous nannofossil assemblages record a marked increase in nutrient availability and cooling (?) at 33.6 Ma. Our data are in possible agreement with Liu et al. (2009) who estimated at Site 1090 a decrease of ~4.8°C in surface and deep water temperatures at ~33.5 Ma but their low resolution data do not allow a closer comparison with our results.

In the Eocene and Oligocene, Site 1090 was located very close to the Polar Front and therefore we suggest that nannofossil assemblage variations occurring during the EOT are a response to rapid northward and southward movements of this oceanographic boundary, whose latitudinal oscillations are plausibly caused by the formation of the ice-sheet in Antarctica.

Alternatively, it is possible that surface water characteristics at this site might indicate a full circumpolar circulation, allowed by the opening of both the Drake and Tasmanian Passages (Scher and Martin, 2006). This interpretation seems supported by the recorded increased fertility in the surface waters. A strengthened circumpolar circulation triggered vertical mixing and the formation of upwelling cells taking nutrients to the

surface. Again, the location of Site 1090 along the flank of a ridge, probably facilitated the recording of nutrient changes by phytoplankton assemblages.

4.3.4. Early Oligocene cold conditions (33.6-33.1 Ma) and the early Oligocene hiatus

As shown by calcareous nannofossil assemblages, stable and cool conditions are maintained in the surface waters from 34.1 to ~32.9 Ma, when a hiatus cuts the succession (Fig. 7). This period includes Step 2 (Oi-1) at ~33.5 Ma and the following EOGM, when the global CCD deepened (Coxall et al., 2005; Merico et al., 2008; Van Andel, 1975), a permanent ice-sheet formed in Antarctica (Miller et al., 1991; Zachos and Kump, 2005; Zachos et al., 2001), ocean temperatures globally decreased (Lear et al., 2008; Liu et al., 2009; Villa et al., 2008; Zachos et al., 2001) a reorganization of the carbon cycle occurred (Merico et al., 2008; Zachos and Kump, 2005), global marine productivity increased (e.g. Diester-Haass et al., 1996; Diester-Haass and Zachos, 2003; Dunkley Jones et al., 2008; Ehrmann and Mackensen, 1992; Salamy and Zachos, 1999) and sea level dropped (DeConto and Pollard, 2003; Katz et al., 2008; Miller et al., 2008; Miller et al., 1991; Pekar and Miller, 1996; Pekar et al., 2002).

During this period a decrease in sediment mass accumulation rates occurs at Site 1090 (Diekmann et al., 2004) and at other more southern locations in the South Atlantic (Diester-Haass and Zahn, 1996; Salamy and Zachos, 1999). Also, in the early Oligocene of Site 1090, the opal pulse that started in the late Eocene, terminates in correspondence of the hiatus (Diekmann et al., 2004). Hiatuses have been widely found near the E/O boundary and in the early Oligocene and have been interpreted as indicative of strengthened ocean circulation following the formation of the Antarctic ice sheet and the associated cooling and sea level fall (Kennett and Shackleton, 1976; Miller et al., 1991; Zachos et al., 1996). The same type of interpretation was given for the early Oligocene unconformity at Site 1090 by Diekmann et al. (2004) who linked it to a more vigorous circumpolar circulation, allowed by the complete opening of the Drake Passage.

The hiatus found at Site 1090 also represents a moment of marked nannofossil assemblage change with a complete reorganization of assemblage structure: above the hiatus nannofossil assemblages are mainly composed by *C. floridanus*, differently from

sediments below it, which show a much higher diversity. Such high abundances of *C. floridanus* might be related to more eutrophic waters. However, it has to be considered that 3 nannofossil extinctions fall within or very close to the hiatus (Figs. 2, 3) and therefore high abundance of *C. floridanus* might derive from the decrease in abundance of other species. Nevertheless, the strong increase in abundance of *C. floridanus* is real, even if probably slightly overestimated. Nevertheless, the hiatus certainly marks the transition between completely different surface waters, from colder and more stable waters before the hiatus, to more unstable and eutrophic (?) conditions after it. We think that the strengthened circumpolar circulation that originated the hiatus completely reorganized nannofossil assemblages and only the most opportunistic species, i.e. *C. floridanus*, promptly adapted to the new conditions.

Another possible interpretation is that the vertical depth of the three layers constituting the Proteus Paleogene ocean (Kennett and Stott, 1990), suddenly changed, moving cold and warm waters up and down the water column, destabilizing the water layers and dislocating the pycnocline depth. In the specific case of eutrophic conditions after the hiatus at Site 1090, the warm and saline deep waters composing the "middle layer" of the Oligocene oceans would have moved to the surface waters, maybe by upwelling, in turn favored by ocean current reorganization following the opening of the Drake Passage.

Marino and Flores (2002) associated the unconformity at Site 1090 to the Marshall Paraconformity (e.g. Fulthorpe et al., 1996), despite this name is usually used for the early, mid- Oligocene unconformities found in the Pacific Ocean and not in the Atlantic. A possible relationship between these unconformities cannot be neither confirmed nor ruled out at this stage, even if it seems plausible that they were formed by similar processes, maybe related to same triggering mechanisms, such as the strengthening of the AACC.

4.3.5. The Early/Late Oligocene carbonate dissolution level (28.8-28 Ma) and the Late Oligocene

Samples between ~213 and ~220 mcd are almost barren of nannofossils, indicating a period of intense carbonate dissolution interval between ~28 and 28.8 Ma. This dissolution interval might reflect a shoaling of the CCD. As said, the CCD deepened significantly in correspondence of Step 2 (Oi-1, 33.5 Ma) and was deep for all the Eocene and the Oligocene, except that during this phase located at the passage between the Early and Late Oligocene.

Intervals of carbonate dissolutions were also found in the early Oligocene at higher southern latitudes (Maud Rise and Kerguelen Plateau), corresponding to periods of low productivity (Diester-Haass, 1996; Diester-Haass et al., 1996) and they were interpreted as produced by a more intense action of the cold and old, and thus corrosive, Antarctic Bottom Waters (AABW), which formed by sinking of waters near Antarctica and then flowed northward affecting all oceans (Diester-Haass et al., 1996; Kennett and Stott, 1990).

The dissolution interval is followed by a period characterized, in terms of nannofossils, by assemblages transitional between those seen in the early Oligocene (below the hiatus) and those seen after the hiatus. In fact, *C. floridanus* is still very abundant in the Late Oligocene but shows a higher abundance variability, and other important taxa, such as *Chiasmolithus* and *C. pelagicus* are more abundant compared to below the hiatus. Nannofossil abundance/mm^2 is very variable and this might caused by dissolution, that biased relative taxa abundances.

5. Conclusions

A high resolution quantitative analysis of calcareous nannofossil assemblages was carried out at Site 1090 Hole B (Agulhas Ridge, 42°S, Atlantic sector of the Southern Ocean) in the time interval between ~35.5 and 26.5 Ma (Late Eocene-Late Oligocene). This work allowed to refine the position and the age assignment of biostratigraphic events previously recognized at lower resolution at the same site. Eleven calcareous nannofossil bioevents were found which, together with isotopic stratigraphy and magnetostratigraphy, provided a very good age control of the studied section.

Variation in relative abundances of paleoecologically significant species showed two moments of enhanced biotic change, reflecting fluctuations in sea surface temperature

and fertility: N1 (~34.1 Ma) (late Eocene) marking the passage from cold to warm and more eutrophic waters, and tentatively interpreted as produced by upward movement of waters belonging to the Warm Saline Deep Waters; N2 (33.6 Ma) (earliest Oligocene) represents an increase in fertility possibly coupled with a decrease in temperature, caused either by the northward movement of Polar Front or by a the effect of the AACC.

No marked temperature/nutrient variations are recorded by nannofossil in correspondence of isotopic Step 1 (~33.75). Isotope Step 2 represents the culmination of the nutrient increase started at N2 and is most likely associated to cooling. Starting from Step 2, relatively stable cool and eutrophic conditions are recorded in the early Oligocene. A marked nannofossil turnover occurs in correspondence of the early Oligocene hiatus (~29.6-32.9 Ma), after which opportunistic *C. floridanus* becomes dominant within the assemblages. The formation of the hiatus and the biotic turnover are indicative of a significant paleoceanographic change, which may be caused by the strengthening of the Antarctic Circumpolar Current.

An intense dissolution level, corresponding to samples almost barren of nannofossils, was identified between 28.0 and 28.8 Ma (at the boundary between the Early and Late Oligocene), and whose origin is plausibly linked to the effect of the cold and corrosive Antarctic Bottom Water.

References

Agnini, C. et al., 2006. Responses of calcareous nannofossil assemblages, mineralogy and geochemistry to the environmental perturbations across the Paleocene/Eocene boundary in the Venetian Pre-Alps. Marine Micropaleontology, 63: 19-38.

Agnini, C. et al., 2009. An Early Eocene carbon cycle perturbation at ~52.5 Ma in the Southern Alps: Chronology and Biotic Response Paleoceanography, 24.

Alegret, L. et al., 2008. Effects of the Oligocene climatic events on the foraminiferal record from Fuente Caldera section (Spain, western Tethys). Palaeogeography, Palaeoclimatology, Palaeoecology, 269: 94-102.

Anderson, L.D. and Delaney, M.L., 2005. Middle Eocene to early Oligocene paleoceanography from Agulhas Ridge, Southern Ocean (Ocean Drilling Program Leg 177, Site 1090). Paleoceanography, 20(1).

Arney, J.E. and Wise, S.W., 2003. Paleocene-Eocene nannofossil biostratigraphy of ODP Leg 183, Kerguelen Plateau. In: F.A. Frey, M.F. Coffin, P.J. Wallace and P.G.E. Quilty (Editors), Proc. ODP Sci. Results.

Aubry, M.P., 1992. Late Paleogene nannoplankton evolution: a tale of climatic deterioration. In: D.R. Prothero and W.A. Berggren (Editors), Eocene-Oligocene Climatic and Biotic Evolution. Princeton University Press, Princeton.

Baldauf, J.G., 1992. Middle Eocene through Early Miocene diatom floral turnover. In: D.R. Prothero and W.A. Berggren (Editors), Eocene-Oligocene Climatic and Biotic Evolution. Princeton University Press, Princeton, pp. 310-326.

Berggren, W.A., Kent, D.V., Swisher, C.C., III and Aubry, M.-P., 1995. A revised Cenozoic geochronology and chronostratigraphy. Special Publication - SEPM (Society for Sedimentary Geology), 54: 129-212.

Bohaty, S.M. and Zachos, J.C., 2003. Significant Southern Ocean warming event in the late middle Eocene. Geology, 31(11): 1017-1020.

Bohaty, S.M., Zachos, J.C., Florindo, F. and Delaney, M.L., 2009. Coupled greenhouse warming and deep sea acidification in the middle Eocene. Paleoceanography, 24(PA2207).

Bown, P.R. et al., 2008. A Paleogene calcareous microfossil Konservat-Lagerstatte from the Kilwa Group of coastal Tanzania. Geological Society of America Bulletin, 120: 3-12.

Bralower, T.J., 2002. Evidence of surface water oligotrophy during the Paleocene-Eocene thermal maximum: Nannofossil assemblage data from Ocean Drilling Program Site 690, Maud Rise, Weddell Sea (vol 17, pg 1023, 2002) - art. no. 1060. Paleoceanography, 17(4): 1060.

Bukry, D., 1973. Low-latitude coccolith biostratigraphic zonation. In: N.T. Edgar and J.B. Saunders (Editors), *Initial Reports* of the DSDP, pp. 685-704.

Cachao, M. and Moita, M.T., 2000. *Coccolithus pelagicus*, a prductivity proxy related to moderate fronts off Western Iberia. Marine Micropaleontology, 39: 131-155.

Cande, S.C. and Kent, D.V., 1995. Revised calibration of the geomagnetic polarity timescale for the Late Cretaceous and Cenozoic. Journal of Geophysical Research, 100(4): 6093-6095.

Carter, R.M., 1985. The mid-Oligocene Marshall Paraconformity, New Zealand: coincidence with global sea level fall or rise? *J. Geol.*, 93(3): 359-371.

Carter, R.M. and Landis, C.A., 1972. Correlative Oligocene unconformities in southern Australasia. Nature, Phys. Sci, 237: 12-13.

Channell, J.E.T. et al., 2003. Eocene to Miocene magnetostratigraphy, biostratigraphy, and chemostratigraphy at ODP Site 1090 (sub-Antarctic South Atlantic). Geological Society of America Bulletin, 115(5): 607-623.

Coccioni, R., Monaco, P., Monechi, S., Nocchi, M. and Parisi, G., 1988. Biostratigraphy of the Eocene/Oligocene boundary at Massignano (Ancona, Italy). In: I. Premoli Silva, R. Coccioni and A. Montanari (Editors), The Eocene/Oligocene Boundary in the Umbria-Marche Basin. Aniballi, Ancona, pp. 59-80.

Coxall, H.K. and Pearson, P.N., 2007. The Eocene-Oligocene Transition. In: M. Williams, A.M. Haywood, F.J. Gregory and D.N. Schmidt (Editors), Deep-time Perspectives on Climate Change: Marrying the Signal from Computer Models and Biological Proxies. The Micropalaeontological Society, Special Publications, The Geological Society, London, pp. 351-387.

Coxall, H.K., Wilson, P.A., Pälike, H., Lear, C.H. and Backman, J., 2005. Rapid stepwise onset of Antarctic glaciation and deeper calcite compensation in the Pacific Ocean. Nature, 433(7021): 53-57.

de Kaenel, E. and Villa, G., 1996. Oligocene/Miocene calcareous nannofossil biostratigraphy and paleoecology from the Iberia Abyssal Plain, Northeastern Atlantic., Whitmarsh, R.B., Sawyer, D.S., Klaus, A., Masson, D.G. (Eds.), Proc. ODP Sci. Results, pp. 79-145.

DeConto, R. et al., 2008. Thresholds for Cenozoic bipolar glaciation. Letters to Nature, 455.

DeConto, R.M. and Pollard, D., 2003. Rapid Cenozoic glaciation of Antarctica induced by declining atmospheric CO_2. Nature, 421(6920): 245-249.

Diekmann, B., Kuhn, G., Gersonde, R. and Mackensen, A., 2004. Middle Eocene to early Miocene environmental changes in the sub-Antarctic Southern Ocean: evidence from biogenic and terrigenous depositional patterns at ODP Site 1090. Global and Planetary Change, 40(3-4): 295-313.

Diester-Haass, L., 1996. Late Eocene-Oligocene paleoceanography in the southern Indian Ocean (ODP Site 744). Marine Geology, 130(1-2): 99-119.

Diester-Haass, L., Robert, C. and Chamley, H., 1996. The Eocene-Oligocene preglacial-glacial transition in the Atlantic sector of the Southern Ocean (ODP Site 690). Marine Geology, 131: 123-149.

Diester-Haass, L. and Zachos, J., 2003. The Eocene-Oligocene transition in the Equatorial Atlantic (ODP Site 925); paleoproductivity increase and positive delta (super 13) C excursion. In: D.R. Prothero, L.C. Ivany and E.A. Nesbitt (Editors). Columbia University Press, New York.

Diester-Haass, L. and Zahn, R., 1996. Eocene-Oligocene transition in the Southern Ocean: History of water mass circulation and biological productivity. Geology, 24(2): 163-166.

Diester-Haass, L. and Zahn, R., 2001. Paleoproductivity increase at the Eocene-Oligocene climatic transition; ODP/DSDP sites 763 and 592. Palaeogeography, Palaeoclimatology, Palaeoecology, 172(1-2): 153-170.

Dunkley Jones, T., Bown, P.R., Pearson, P.N., Wade, B.S. and Coxall, H.K., 2008. Major shifts in calcareous phytoplankton assemblages through the Eocene-Oligocene transition of Tanzania and their implications for low-latitude primary production. Paleoceanography, 23: PA4204.

Edwards, A.R., 1971. A calcareous nannoplankton zonation of the New Zealand Paleogene. In: A. Farinacci (Editor), *Proceedings 2nd Plank. Conf.* , Roma, pp. 381-419.

Edwards, A.R. and Perch-Nielsen, K., 1975. Calcareous nannofossils from the southern southwest Pacific. In: J.P. Kennett, R.E. Houtz and e. al. (Editors), Initial Reports DSDP, Leg 29. Deep Sea Drilling Project, Washington (U.S. Government Printing Office).

Ehrmann, W.U. and Mackensen, A., 1992. Sedimentological evidence for the formation of an East Antarctic ice sheet in Eocene/Oligocene time. Palaeogeography, Palaeoclimatology, Palaeoecology, 93(1-2): 85-112.

Fioroni, C., Villa, G., Persico, D., Wise, S.S. and Pea, L., 2010. Revised Eocene-Oligocene calcareous nannofossil biozonation for the Southern Ocean, 13th International Nannoplankton Association Conference, Yamagata.

Firth, J.V. and Wise, S.W., 1992. A preliminary study of the evolution of Chiasmolithus in the middle Eocene to Oligocene of Sites 647 and 748, Proceedings of the Ocean Drilling Program, Scientific Results.

Francis, J.E., 1999. Evidence from fossil plants for Antarctica paleoclimates over the past 100 million years. Terra Antartica, 3: 43-52.

Fulthorpe, C.S., Carter, R.M., Miller, K.G. and Wilson, G., 1996. Marshall Paraconformity: a mid-Oligocene record of inception of the Antarctic Circumpolar Current and coeval glacio-eustatic lowstand? Mar. Pet. Geol., 13: 61-77.

Funakawa, S. and Nishi, H., 2008. Radiolarian faunal changes during the Eocene-Oligocene transition in the Southern Ocean (Maud Rise, ODP Leg 113, Site 689) and its significance in paleoceanographic change. Micropaleontology, 54(1): 15-26.

Funakawa, S., Nishi, H., Moore, T.C. and Nigrini, C.A., 2006. Radiolarian faunal turnover and paleoceanographic change around Eocene/Oligocene boundary in the central equatorial Pacific, ODP Leg 199, Holes 1218A, 1219A and 1220A. Palaeogeography, Palaeoclimatology, Palaeoecology 230: 183-203.

Gersonde, R., Hodell, A., Blum, P. and Party, S.S., 1999. Leg 177 Summary, Proc. Ocean Drill. Program, Initial Rep., pp. 1-67.

Gibbs, S.J., Bown, P.R., Sessa, J.A., Bralower, T.J. and Wilson, P.A., 2006a. Nannoplankton extinction and origination across the Paleocene-Eocene Thermal Maximum. Science, 314(5806): 1770-1773.

Gibbs, S.J., Bralower, T.J., Bown, P.R., Zachos, J.C. and Bybell, L.M., 2006b. Shelf and open-ocean calcareous phytoplankton assemblages across the Paleocene-Eocene Thermal Maximum: implications for global productivity gradients. Geology, 34(4): 233-236.

Haq, B.U., Hardenbol, J. and Vail, P.R., 1987. Chronology of fluctuating sea levels since the Triassic. Science, 235(4793): 1156-1167.

Haq, B.U. and Lohmann, G.P., 1976. Early Cenozoic calcareous nannoplankton biogeography of the Atlantic Ocean. Marine Micropaleontology, 1: 119-194.

Holmes, M.A., Watkins, D.K. and Norris, R.D., 2004. Paleocene cyclic sedimentation in the Western North Atlantic, ODP Site 1051, Blake Nose. Marine Geology, 209: 31-43.

Hooker, J.J., Collinson, M.E. and Sille, N.P., 2004. Eocene-Oligocene mammalian faunal turnover in the Hampshire Basin, UK; calibration to the global time scale

and the global major event. Journal of the Geological Society of London, 161: 161-172.

Jaramillo, C., Rueda, M.J. and Mora, G., 2006. Cenozoic plant diversity in the Neotropics. Science, 311: 1893-1896.

Kahn, A. and Aubry, M.P., 2004. Provincialism associated with the Paleocene/Eocene Thermal maximum: temporal constrain. Marine Micropaleontology, 52: 117-131.

Katz, M.E. et al., 2008. Stepwise transition from the Eocene greenhouse to the Oligocene icehouse. Nature Geoscience, 1: 329-333.

Keller, G., Macleod, N. and Barrera, E., 1992. Eocene-Oligocene faunal turnover in planktonic foraminifera, and Antarctic Glaciation. In: D.R. Prothero and W.A. Berggren (Editors), Eocene and Oligocene Climatic and Biotic Evolution. Princeton University Press, Princeton, pp. 218-244.

Kelly, D.C., Bralower, T.J., Zachos, J.C., Premoli-Silva, I. and Thomas, E., 1996. Rapid diversification of planktonic foraminifera in the tropical Pacific (ODP Site 865) during the late Paleocene thermal maximum. Geology, 24(5): 423-426.

Kennett, J.P., 1977. Cenozoic evolution of Antarctic glaciation, circum-Antarctic ocean, and their impact on global paleoceanography. Journal of Geophysical Research-Oceans and Atmospheres, 82(27): 3843-3860.

Kennett, J.P. and Shackleton, N.J., 1976. Oxygen isotopic evidence for the development of the psychrosphere 38 Myr ago. Nature, 260(5551): 513-515.

Kennett, J.P. and Stott, L.D., 1990. Proteus and Proto-oceanus: Ancestral Paleogene oceans as revealed from Antarctic stable isotopic results; ODP Leg 113. Proc. ODP, Sci. Results, 113: 865-880.

Kominz, M.A. and Pekar, S.F., 2001. Oligocene eustasy from two-dimensional sequence stratigraphic backstripping. Geological Society of America Bulletin, 113(3): 291-304.

Kyte, F.T., 2001. Identification of late Eocene impact deposits at ODP Site 1090. Proc. ODP, Sci. Results, 177.

Lagabrielle, Y., Goddéris, Y., Donnadieu, Y., Malavieille, J. and Suarez, M., 2009. The tectonic history of Drake Passage and its possible impacts on global climate. Earth and Planetary Science Letters, 279: 197-211.

Latimer, J.C. and Filippelli, G.M., 2002. Eocene to Miocene terrigenous inputs and export production: Geochemical evidence from ODP Leg 177, Site 1090. Palaeogeography Palaeoclimatology Palaeoecology, 182(3-4): 151-164.

Lawver, L.A. and Gahagan, L.M., 2003. Evolution of Cenozoic seaways in the circum-Antarctic region. Palaeogeography, Palaeoclimatology, Palaeoecology, 198(1-2): 11-37.

Lazarus, D. and Caulet, J.P., 1993. Cenozoic Southern Ocean reconstructions from sedimentologic, radiolarian, and other microfossil data. In: J.P. Kennett and D.A. Warnke (Editors), The Antarctic Paleoenvironment: A Perspective on Global Change, Part Two. American Geophysical Union, pp. 145-174.

Lazarus, D., Hollis, C.J. and Apel, M., 2004. Radiolarian and sedimentologic evidence for Late Eocene origin of Southern Ocean Environments., AGU Meeting, San Francisco, California, pp. F1192.

Lear, C.H., Bailey, T.R., Pearson, P.N., Coxall, H.K. and Rosenthal, Y., 2008. Cooling and ice growth across the Eocene-Oligocene transition. Geology, 36(3): 251-254.

Leopold, E.B., Liu, G. and Clay-Poole, S., 1992. Low-biomass vegetation in the Oligocene? In: D.R. Prothero and W.A. Berggren (Editors), Eocene and Oligocene Climatic and Biotic Evolution. Princeton University Press, pp. 399-420.

Liu, S., Glass, B.P. and Anonymous, 2002. The distribution of unmelted impact ejecta associated with the upper Eocene clinopyroxene-bearing (cpx) spherule layer. Abstracts with Programs - Geological Society of America, 34(6): 402.

Liu, Z. et al., 2009. Global Cooling During the Eocene-Oligocene Climate Transition. Science, 323.

Liu, Z., Tuo, S., Zhao, Q., Cheng, X. and Huang, W., 2004. Deep-water earliest Oligocene glacial maximum (EOGM) in South Atlantic. Chinese Science Bulletin, 49(20): 2190-2197.

Livermore, R., Hillenbrand, C.-D., Meredith., M. and Eagles, G., 2007. Drake Passage and Cenozoic climate: An open and shut case? Geochem. Geophys. Geosyst., 8.

Livermore, R., Nankivell, A., Eagles, G. and Morris, P., 2005. Paleogene opening of Drake Passage. Earth and Planetary Science Letters, 236(1-2): 459-470.

Lourens, L.J. et al., 2005. Astronomical pacing of late Palaeocene to early Eocene global warming events. Nature, 435(7045): 1083-1087.

Lowrie, W. et al., 1982. Paleogene magnetic stratigraphy in Umbrian pelagic carbonate rocks: the Contessa sections, Gubbio. Geolo. Soc. Am. Bull., 93: 411-432.

Maiorano, P., 2006. *Reticulofenestra circus* var. *lata* n.var.: a large reticulofenestrid (Coccolithophoridae) from the Early Oligocene. Micropaleontology, 52(1): 81-86.

Marino, M. and Flores, J.A., 2002. Middle Eocene to Early Oligocene calcareous nannofossil stratigraphy at Leg 177 Site 1090. Marine Micropaleontology, 45: 383-398.

Martini, E., 1971. Standart Tertiary and Quaternary calcareous nannoplankton zonation. In: A. Farinacci (Editor), Second Planktonic Conference. Edizioni Tecnoscienza, Rome, pp. 739-785.

McGonigal, K. and Di Stefano, A., 2002. Calcareous Nannofossil Biostratigraphy of the Eocene-Oligocene Transition, ODP Sites 1123 and 1124. In: C. Richter (Editor), Proc. ODP, Sci. Results, pp. 1-22.

Merico, A., Tyrrell, T. and Wilson, P.A., 2008. Eocene/Oligocene ocean de-acidification linked to Antarctic glaciation by sea-level fall. Letters to Nature, 452: 979-982.

Miller, K.G. et al., 2008. Eocene-Oligocene global climate and sea-level change changes: St. Stephens Quarry, Alabama. Geological Society of America Bulletin, 120(1/2): 34-53.

Miller, K.G., Fairbanks, R.G. and Mountain, G.S., 1987. Tertiary oxygen isotope synthesis, sea level history, and continental margin erosion. Paleoceanography, 2(1): 1-19.

Miller, K.G. et al., 2005. The phanerozoic record of global sea-level change. Science, 310(5752): 1293-1298.

Miller, K.G., Wright, J.D. and Fairbanks, R.G., 1991. Unlocking the ice house: Oligocene-Miocene oxygen isotopes, eustasy, and margin erosion. Journal of Geophysical Research, B, Solid Earth and Planets, 96: 6829-6848.

Miller, K.G. et al., 2009. Climate threshold at the Eocene-Oligocene transition: Antarctic ice sheet influence on ocean circulation. In: C. Koeberl, and

Montanari, A., eds. (Editor), The Late Eocene Earth-Hothouse, Icehouse, and Impacts: Geological Society of America Special Paper, pp. 169-178.

Miller, K.J. et al., 1985. Oligocene-Miocene biostratigraphy, magnetostratigraphy, and isotopic stratigraphy of the western North Atlantic. Geology, 13: 257-261.

Molina, E., Gonzalvo, C., Ortiz, S. and Cruz, L.E., 2006. Foraminiferal turnover across the Eocene-Oligocene transition at Fuente Caldera, southern Spain: no cause-effect relationship between meteorite impacts and extinctions. Marine Micropaleontology, 58: 270-286.

Monechi, S., Buccianti, A. and Gardin, S., 2000. Biotic signals from nannoflora across the iridium anomaly in the upper Eocene of the Massignano section: evidence from statistical analysis. Marine Micropaleontology, 39: 219-237.

Montanari, A., Asaro, F., Michel, H.V. and Kennett, J.P., 1993. Iridium Anomalies of Late Eocene Age at Massignano (Italy), and ODP Site 689B (Maud-Rise, Antarctic). Palaios, 8(5): 420-437.

Nocchi, M., Monechi, S., Coccioni, R. and al., e., 1998. The extinction of Hantkeninidae as a marker for defining the Eocene-Oligocene boundary: A proposal. In: I. Premoli Silva, R. Coccioni and A. Montanari (Editors), International Union of Geological Science Commission on Stratigraphy, The international Subcommission of Paleogene Stratigraphy: The Eocene-Oligocene Boundary in the Marche-Umbria Basin (Italy), Ancona, Monte Cònero, pp. 249-252.

Okada, H. and Bukry, D., 1980. Supplementary modification and introduction of code numbers to the low-latitude coccolith biostratigraphic zonation (Bukry, 1973; 1975). Marine Micropaleontology, 5(3): 321-325.

Pagani, M., Zachos, J.C., Freeman, K.H., Tipple, B. and Bohaty, S., 2005. Marked decline in atmospheric carbon dioxide concentrations during the Paleogene. Science, 309(5734): 600-603.

Parker, M.E., Clark, M. and Wise, S.W.J., 1985. Calcareous nannofossils of Deep Sea Drilling Project Sites 558 and 563, Northe Atlantic Ocean: biostratigraphy and the distribution of Oligocene braarudosphaerids. In: H. Bougault, S.C. Cande and e. al. (Editors), *Init. Repts.* DSDP, Washington (U.S. Govt. Printing Office), pp. 559-589.

Pearson, P.N. et al., 2008. Extinction and environmental change across the Eocene-Oligocene boundary in Tanzania. Geology, 36(2): 179-182.

Pearson, P.N. and Palmer, M.R., 2000. Atmospheric carbon dioxide concentrations over the past 60 million years. Nature, 406(6797): 695-699.

Pekar, S. and Miller, K.G., 1996. New Jersey Oligocene "icehouse" sequences (ODP Leg 150X) correlated with global $\delta^{18}O$ and Exxon eustatic records. Geology, 24(6): 567-570.

Pekar, S.F. and Christie-Blick, N., 2008. Resolving apparent conflicts between oceanographic and Antarctic climate records and evidence for a decrease in pCO(2) during the Oligocene through early Miocene (34-16 Ma). Palaeogeography Palaeoclimatology Palaeoecology, 260(1-2): 41-49.

Pekar, S.F., Christie-Blick, N., Kominz, M.A. and Miller, K.G., 2002. Calibration between eustatic estimates from backstripping and oxygen isotopic records for the Oligocene. Geology, 30(10): 903-906.

Pekar, S.F., DeConto, R.M. and Harwood, D.M., 2006. Resolving a late Oligocene conundrum: Deep-sea warming and Antarctic glaciation. Palaeogeography, Palaeoclimatology, Palaeoecology, 231: 29-40.

Persico, D. and Villa, G., 2004. Eocene-Oligocene calcareous nannofossils from Maud Rise and Kerguelen Plateau (Antarctica): Paleoecological and paleoceanographic implications. Marine Micropaleontology, 52: 153-179.

Persico, D. et al., 2004. Nannofossil assemblage fluctuations during the Oligocene at Site 748 (Kerguelen Plateau, Antarctica); palaeoecological implications, Journal of Nannoplankton Research, pp. 85.

Poore, R.Z. et al., 1984. Late Cretaceous-Cenozoic Magnetostratigraphic and Biostratigraphic Correlations for the South Atlantic Ocean, Deep Sea Drilling Project Leg73. In: K.J. Hsu, J.L. LaBreque and *e. al.* (Editors), *Initial Reports* DSDP, Washington (U.S. Government Printing Office).

Pälike, H. et al., 2006. The heartbeat of the Oligocene climate system. Science, 314: 1894-1898.

Rea, D.K. and Lyle, M.W., 2005. Paleogene calcite compensation depth in the eastern subtropical Pacific: Answers and questions. Paleoceanography, 20.

Salamy, K.A. and Zachos, J.C., 1999. Latest Eocene-early Oligocene climate change and Southern Ocean fertility; inferences from sediment accumulation and stable isotope data. Palaeogeography, Palaeoclimatology, Palaeoecology, 145(1-3): 61-77.

Scher, H.D. and Martin, E.E., 2006. Timing and climatic consequences of the opening of Drake Passage. Science, 312(5772): 428-30.

Stickley, C.E. et al., 2004. Timing and nature of the deepening of the Tasmanian Gateway. Paleoceanography, 19(4).

Suto, I., 2006. The explosive diversification of the diatom genus Chaetoceros across the Eocene-Oligocene and Oligocene-Miocene boundaries in the Norwegian Sea. Marine Geology, 58: 259-269.

Tremolada, F. and Bralower, T.J., 2004. Nannofossil assemblage fluctuations during the Paleocene-Eocene Thermal Maximum at Site 213 (Indian Ocean) and 401 (North Atlantic Ocean): paleoceanographic implications. 52: 107-116.

Van Andel, T.H., 1975. Mesozoic/Cenozoic calcite compensation depth and the global distribution of calcareous sediments. Earth and Planetary Science Letters, 26(2): 187-194.

Villa, G., Fioroni, C., Pea, L., Bohaty, S. and Persico, D., 2008. Middle Eocene-late Oligocene climate variability: Calcareous nannofossil response at Kerguelen Plateau, Site 748. Marine Micropaleontology, 69: 173-192.

Villa, G. and Persico, D., 2006. Late Oligocene climatic changes: Evidence from calcareous nannofossils at Kerguelen Plateau Site 748 (Southern Ocean). Palaeogeography, Palaeoclimatology, Palaeoecology, 231: 110-119.

Vonhof, H.B., Smit, J., Brinkhuis, H., Montanari, A. and Nederbragt, A.J., 2000. Global cooling accelerated by early late Eocene impacts? Geology, 28(8): 687-690.

Wade, B.S. and Bown, P.R., 2006. Calcareous nannofossils in extreme environments: The Messinian Salinity Crisis, Polemi Basin, Cyprus. *Paleogeogr. Paleoclimatol. Palaeoecol.*, 233: 271-286.

Wade, B.S. and Palike, H., 2004. Oligocene climate dynamics. Paleoceanography, 19.

Wade, B.S. and Pearson, P.N., 2008. Planktonic foraminiferal turnover, diversity fluctuations and geochemical signals across the Eocene/Oligocene boundary in Tanzania. Marine Micropaleontology, 68: 244-255.

Wei, W. and Thierstein, H.R., 1991. Upper Cretaceous and Cenozoic calcareous nannofossils of the Kerguelen Plateau (southern Indian Ocean) and Prydz Bay (East Antarctica). Proc. ODP, Sci. Results, 119: 467-493.

Wei, W., Villa, G. and Wise, S.W., Jr., 1992. Paleoceanographic implications of Eocene-Oligocene calcareous nannofossils from sites 711 and 748 in the Indian Ocean. Proc. ODP, Sci. Results, 120: 979-999.

Wei, W. and Wise, S.W., Jr,, 1989. Paleogene calcareous nannofossil magnetobiochronology: results from South Atlantic DSDP Site 516. Marine Microplaeontology, 14: 119-152.

Wei, W. and Wise, S.W., Jr., 1990a. Biogeographic gradients of middle Eocene-Oligocene calcareous nannoplankton in the South Atlantic Ocean. Palaeogeography, Palaeoclimatology, Palaeoecology, 79(1-2): 29-61.

Wei, W. and Wise, S.W., Jr., 1990b. Middle Eocene to Pleistocene calcareous nannofossils recovered by Ocean Drilling Program Leg 113 in the Weddell Sea. Proc. ODP, Sci. Results, 113: 639-666.

Wei, W.C., 2004. Opening of the Australia-Antarctica gateway as dated by nannofossils. Marine Micropaleontology, 52(1-4): 133-152.

Wei, W.C. and Wise, S.W., 1992. Eocene-Oligocene calcareous nannofossils magnetobiochronology of the Southern Ocean. Newsl. Stratigr., 26: 119-132.

Wildeboer Shut, E., Uenzelmann-Neber, G. and Gersonde, R., 2002. Seismic evidence for bottom current activity at the Agulhas Ridge. Global and Planetary Change, 34: 185-198.

Wind, F.H. and Wise, S.W., 1978. Mesozoic holococcoliths. Geology, 6: 140-142.

Wise, 1988. Mesozoic-Cenozoic history of calcareous nannofossils in the region of the Southern Ocean. Paleogeography, Paleoecology, Paleoclimatology, 67: 157-179.

Wise, S.W., Jr., Breza, J.R., Harwood, D.M., Wei, W. and Zachos, J.C., 1992. Paleogene glacial history of Antarctica in light of Leg 120 drilling results. Proceedings of the Ocean Drilling Program, Scientific Results, 120: 1001-1030.

Wise, S.W., Jr. et al., 1983. Mesozoic and Cenozoic calcareous nannofossils recovered by Deep Sea Drilling Project Leg 71 in the Falkland Plateau region, Southwest Atlantic Ocean. Initial Reports of the Deep Sea Drilling Project, 71(2): 481-550.

Zachos, J.C., Dickens, G.R. and Zeebe, R.E., 2008. An early Cenozoic perspective on greenhouse warming and carbon-cycle dynamics. Nature, 45: 279-283.

Zachos, J.C. and Kump, L.R., 2005. Carbon cycle feedbacks and the initiation of Antarctic glaciation in the earliest Oligocene. Global and Planetary Change, 47(1): 51-66.

Zachos, J.C., Pagani, M., Sloan, L., Thomas, E. and Billups, K., 2001. Trends, rhythms, and aberrations in global climate 65 Ma to present. Science, 292(5517): 686-693.

Zachos, J.C., Quinn, T.M. and Salamy, K.A., 1996. High-resolution (10^4 years) deep-sea foraminiferal stable isotope records of the Eocene-Oligocene climate transition. Paleoceanography, 11(3): 251-266.

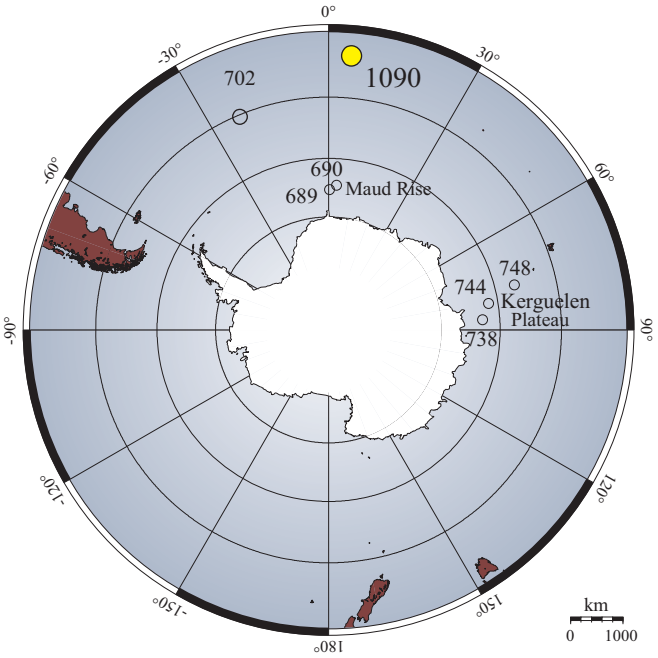

Figure 1: Location map of ODP Site 1090, South Atlantic Ocean (42°S).

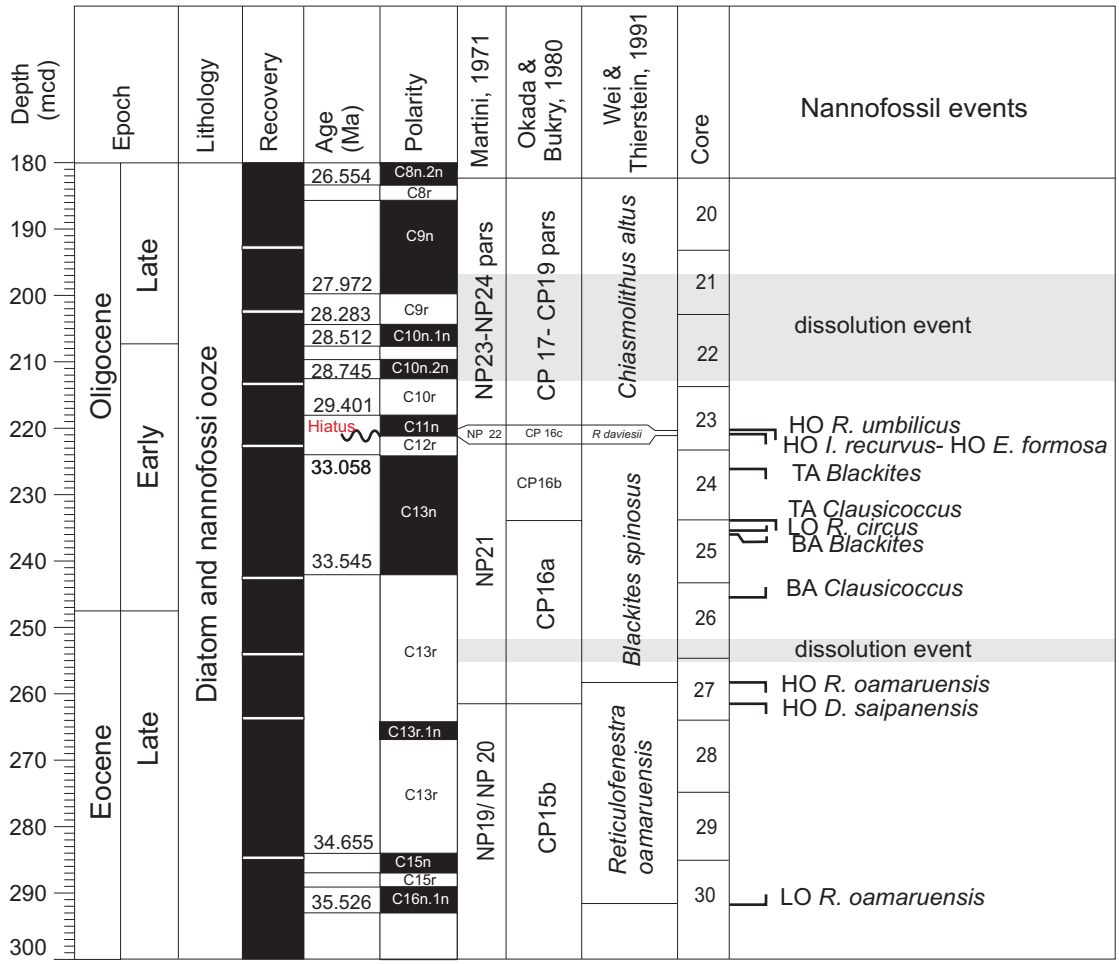

Figure 2: Biostratigraphic framework of the studied section. Eleven calcareous nannofossil events were found between the Late Eocene and the Late Oligocene. Polarity interpretation is from Channell et al. (2003) and the assignment of Chron boundary ages is based on the Cande and Kent (2005) time scale. A hiatus lasting about 3.3 m.y. was recognized at ~221 mcd. Two dissolution intervals were found and are indicated by grey bars, one in the late Eocene, and one at the boundary between the Early and the Late Oligocene. The Eocene/Oligocene boundary is placed at 247.90 mcd, based on the calculation of sedimentation rates between Chron boundaries.

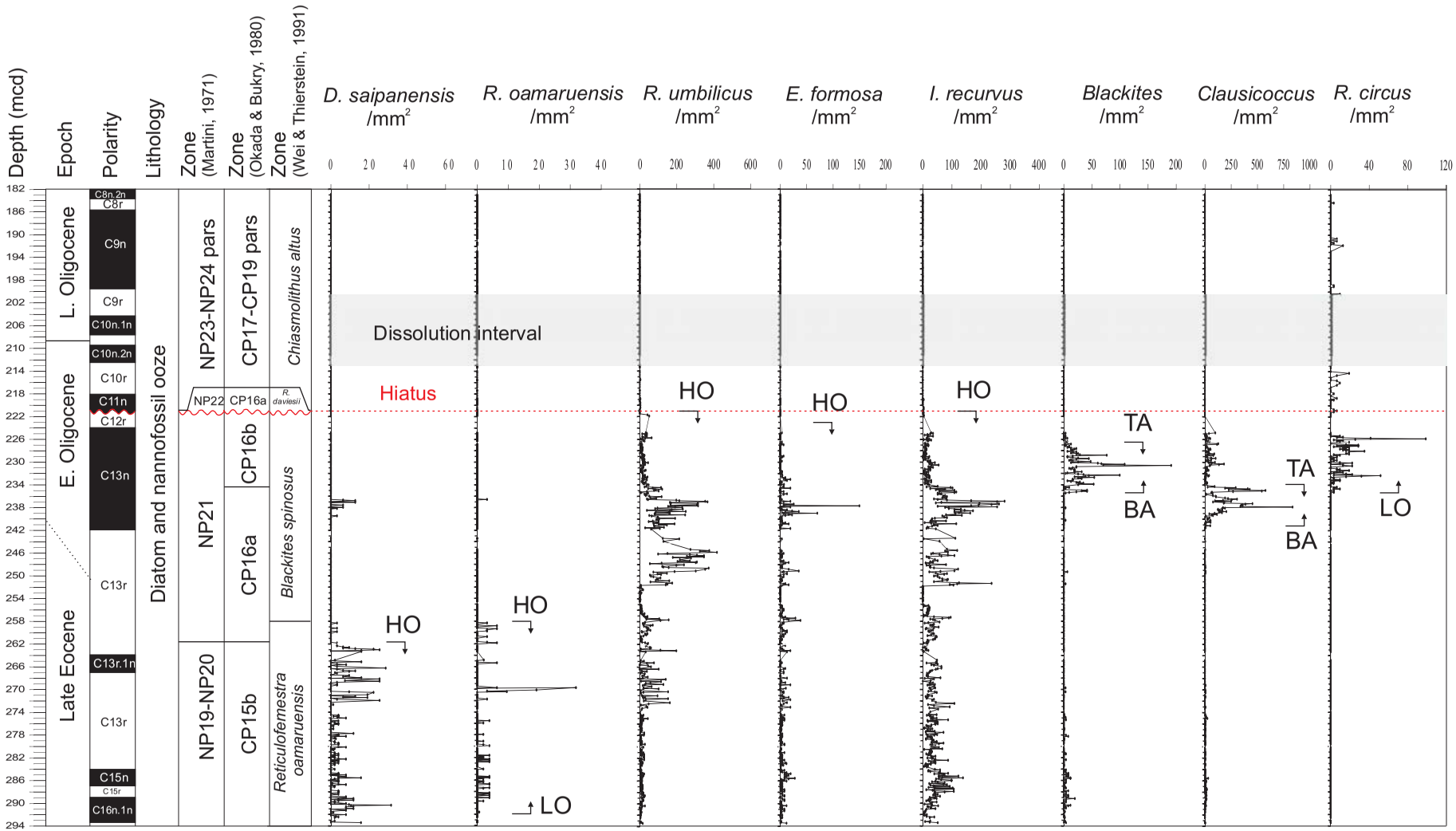

Figure 3: Stratigraphic position of the eleven biostratigraphic events recognized at Site 1090. LO: Lowest Occurrence, HO: Highest Occurrence, BA: Base Acme, TA: Top Acme. Abundances are expressed as number of specimens/mm^2. Two dissolution levels are indicated as grey bars and the hiatus found at 221 mcd is shown as a red dotted line.

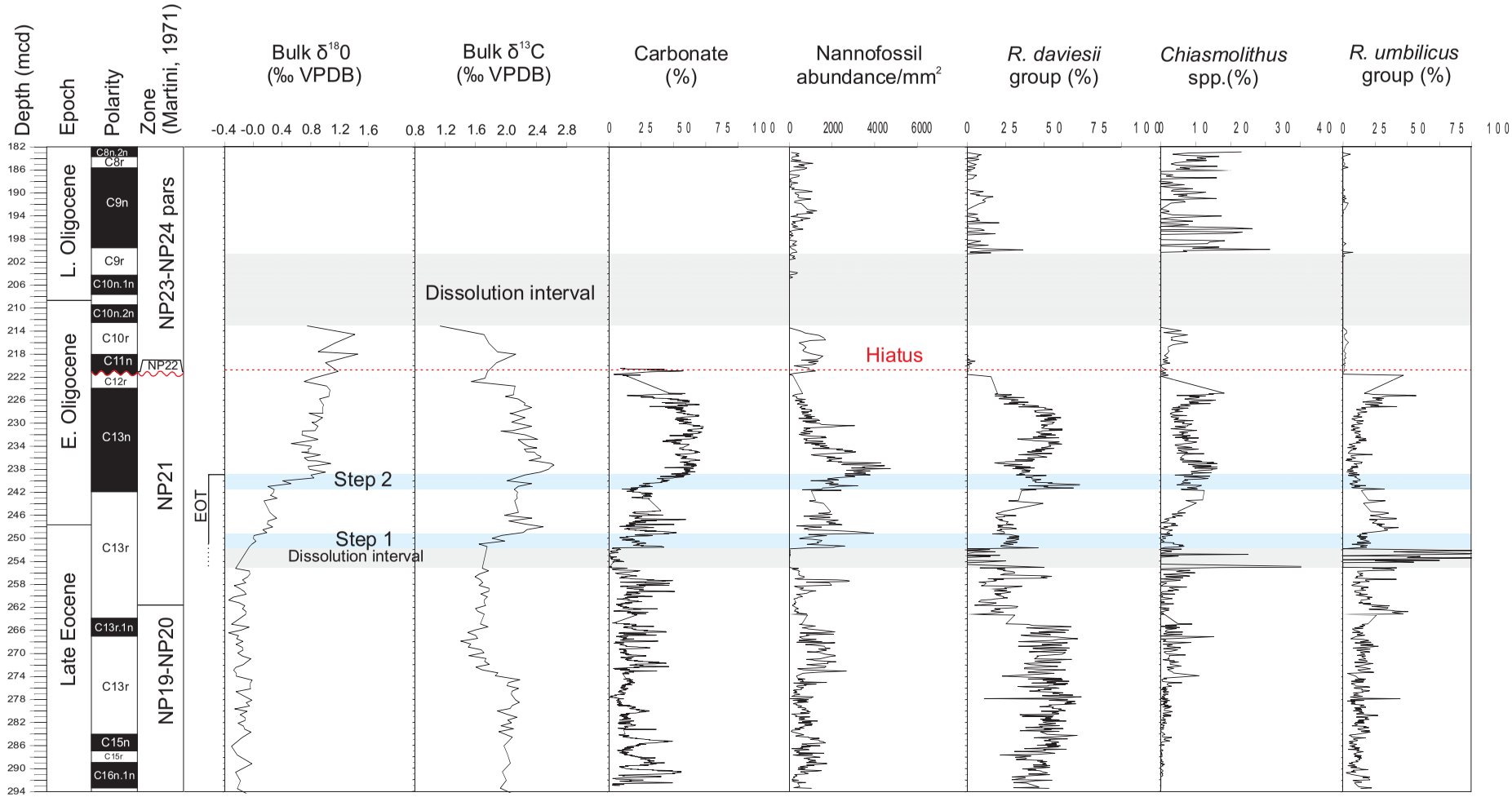

Figure 4: Taxa relative abundances are indicated as percentages (%) next to nannofossil total abundance/mm^2, bulk stable oxygen and carbon isotope, and carbonate records (Bohaty and Palïke, unpublished data, 2010). Two dissolution levels are indicated as grey bars. Oxygen isotope Steps 1 and 2 at the Eocene-Oligocene Transition (EOT) are remarked as blue bands. The hiatus found at 221 mcd is shown as a red dotted line.

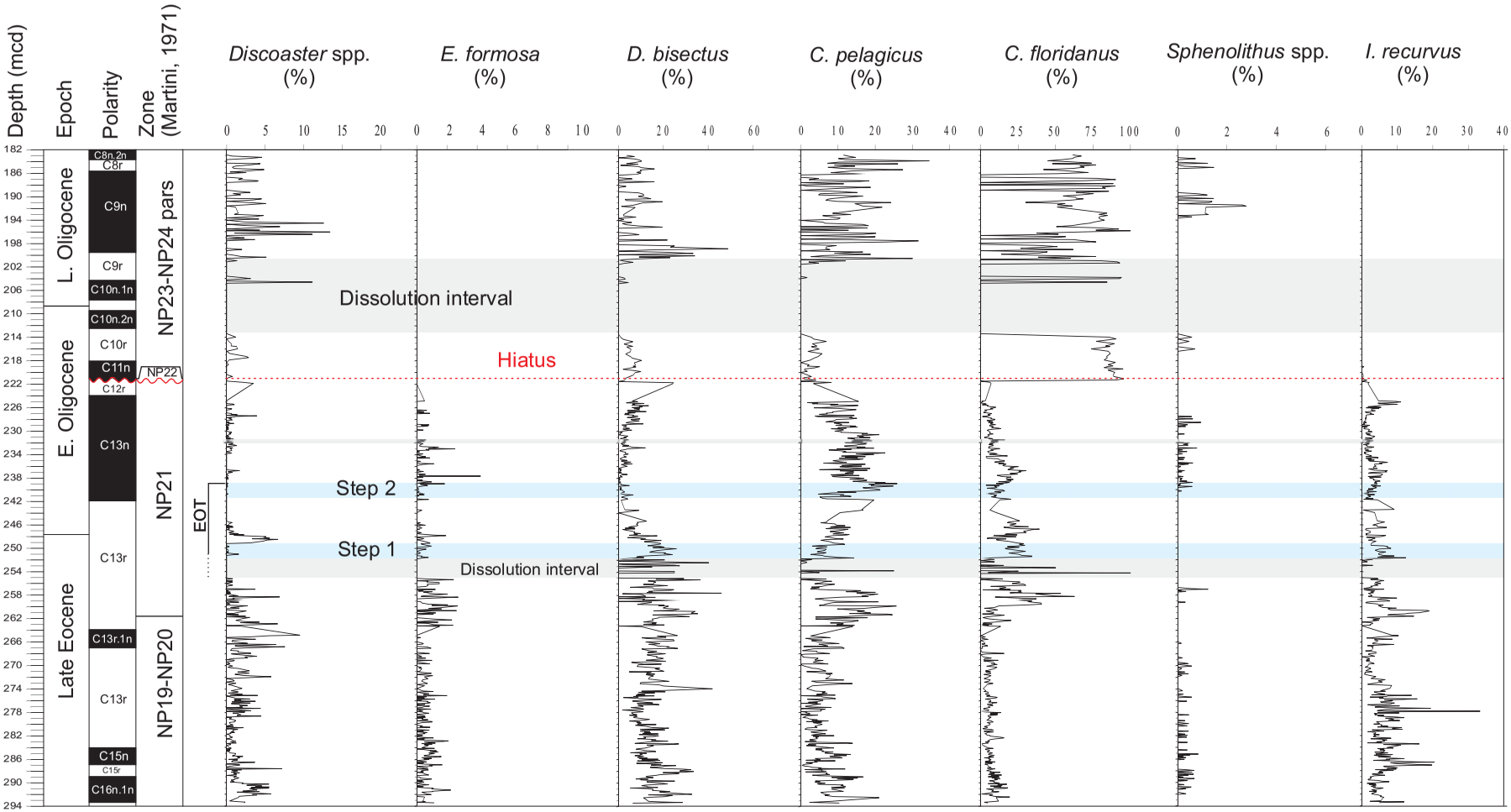

Figure 5: Taxa relative abundances are indicated as percentages (%). Two dissolution levels are indicated as grey bars. Oxygen isotope Steps 1 and 2 at the Eocene-Oligocene Transition (EOT) are remarked as blue bands. The hiatus found at 221 mcd is shown as a red dotted line.

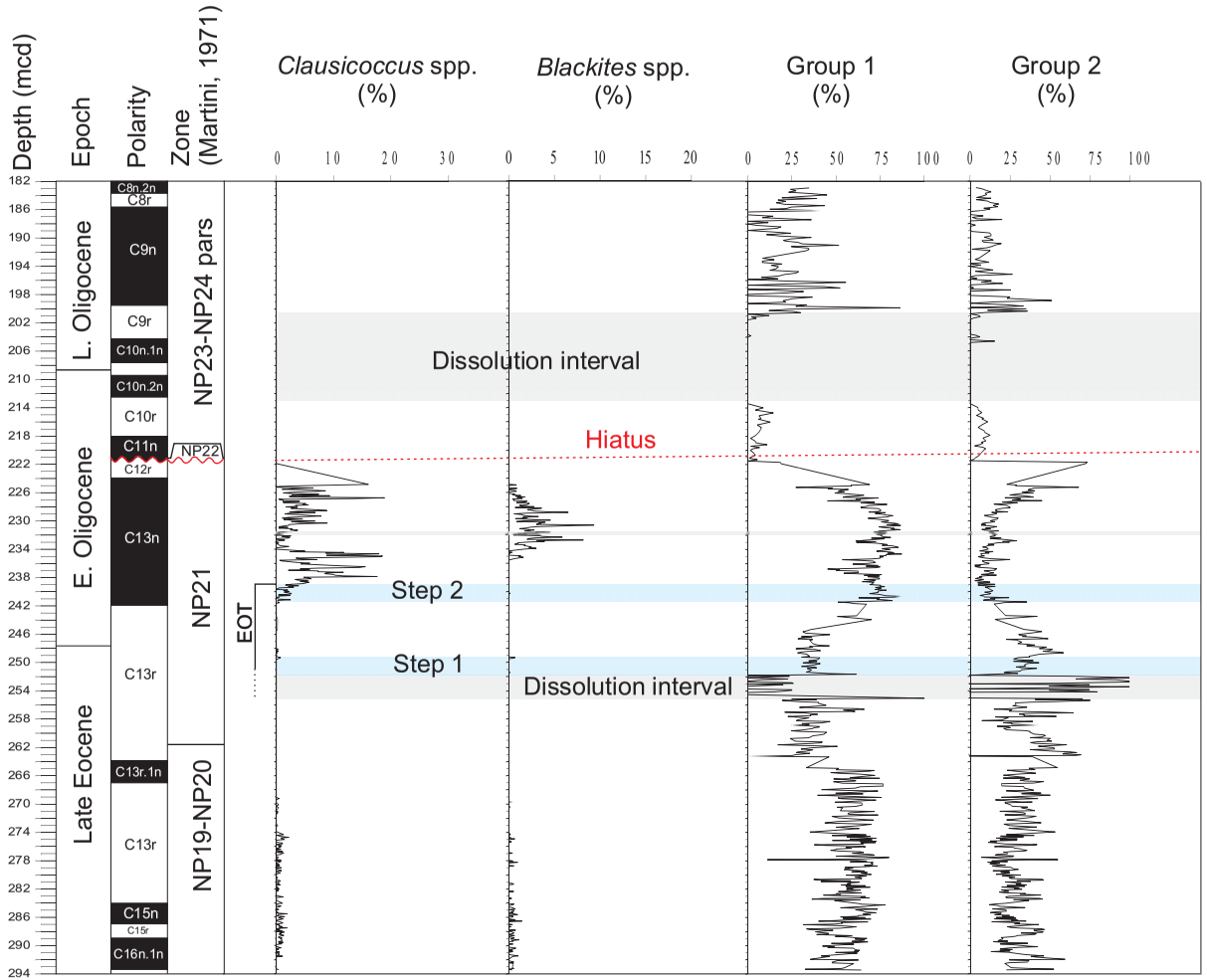

Figure 6: *Blackites* spp., *Clausicoccus* spp. relative abundance (%) and paleoecological Group 1 and Group 2 trends. EOT: Eocene-Oligocene Transition. Group 1 is composed by taxa increasing in abundance across the EOT, Group 2 is composed by taxa decreasing in abundance across the EOT (See text for description and discussion). Two dissolution levels are indicated as grey bars. Oxygen isotope Steps 1 and 2 at the EOT are remarked as blue bands. The hiatus found at ~221mcd is shown as a red dotted line.

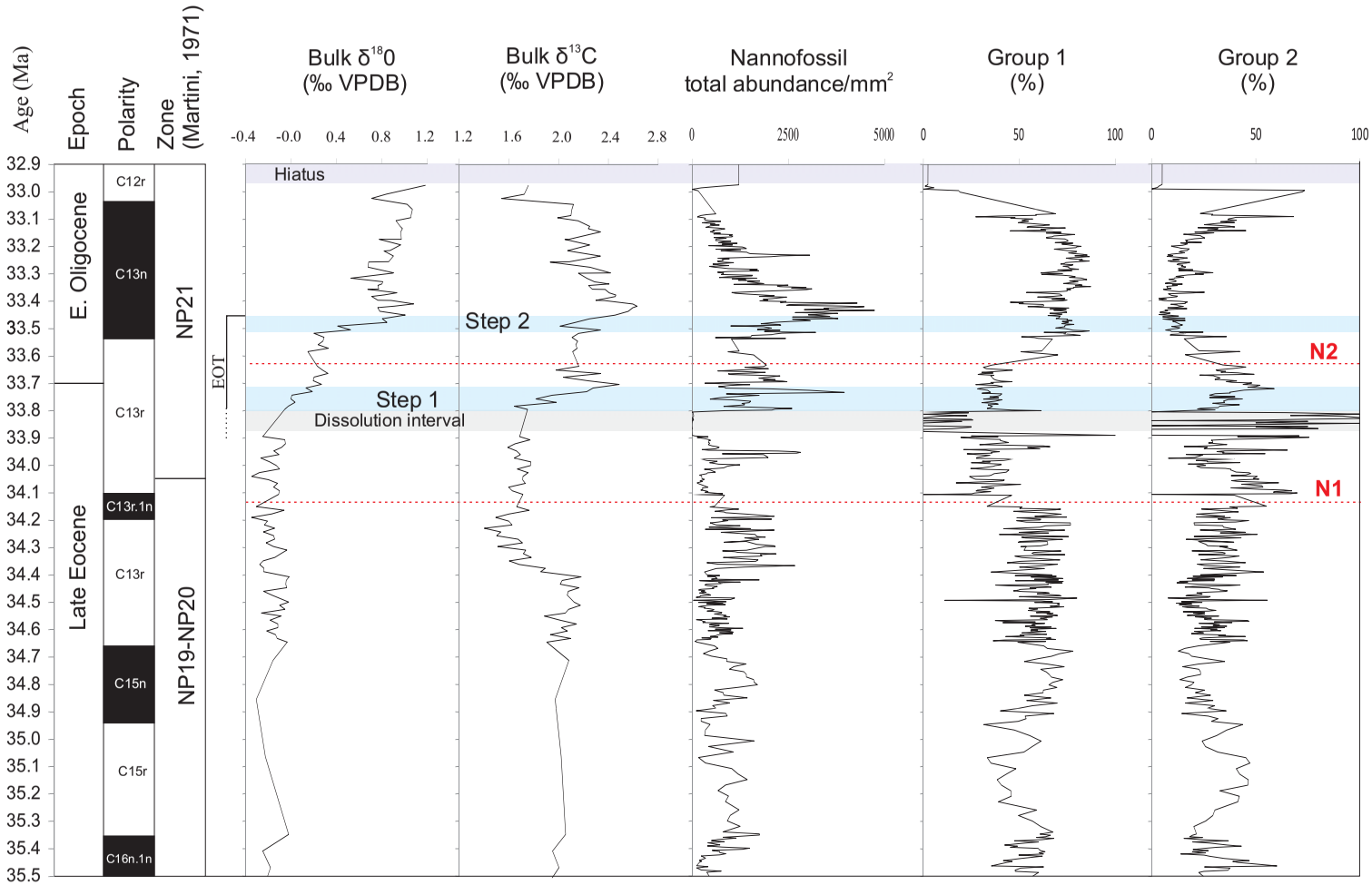

Figure 7: Group 1 and Group 2 variation trends (%) (See Fig. 6 for description), nannofossil total abundance (number of specimens per mm^2), and stable oxygen and carbon isotope records (Bohaty and Palïke, Unpublished data, 2010), plotted against age (Cande and Kent, 1995) from 35.5 Ma to the hiatus (~29.6-32.9 Ma). EOT: Eocene-Oligocene Transition. A dissolution level (grey bar), oxygen isotope Steps 1 and 2 at the EOT (blue bands) are indicated. N1 and N2 represent marked nannofossil assemblage changes.

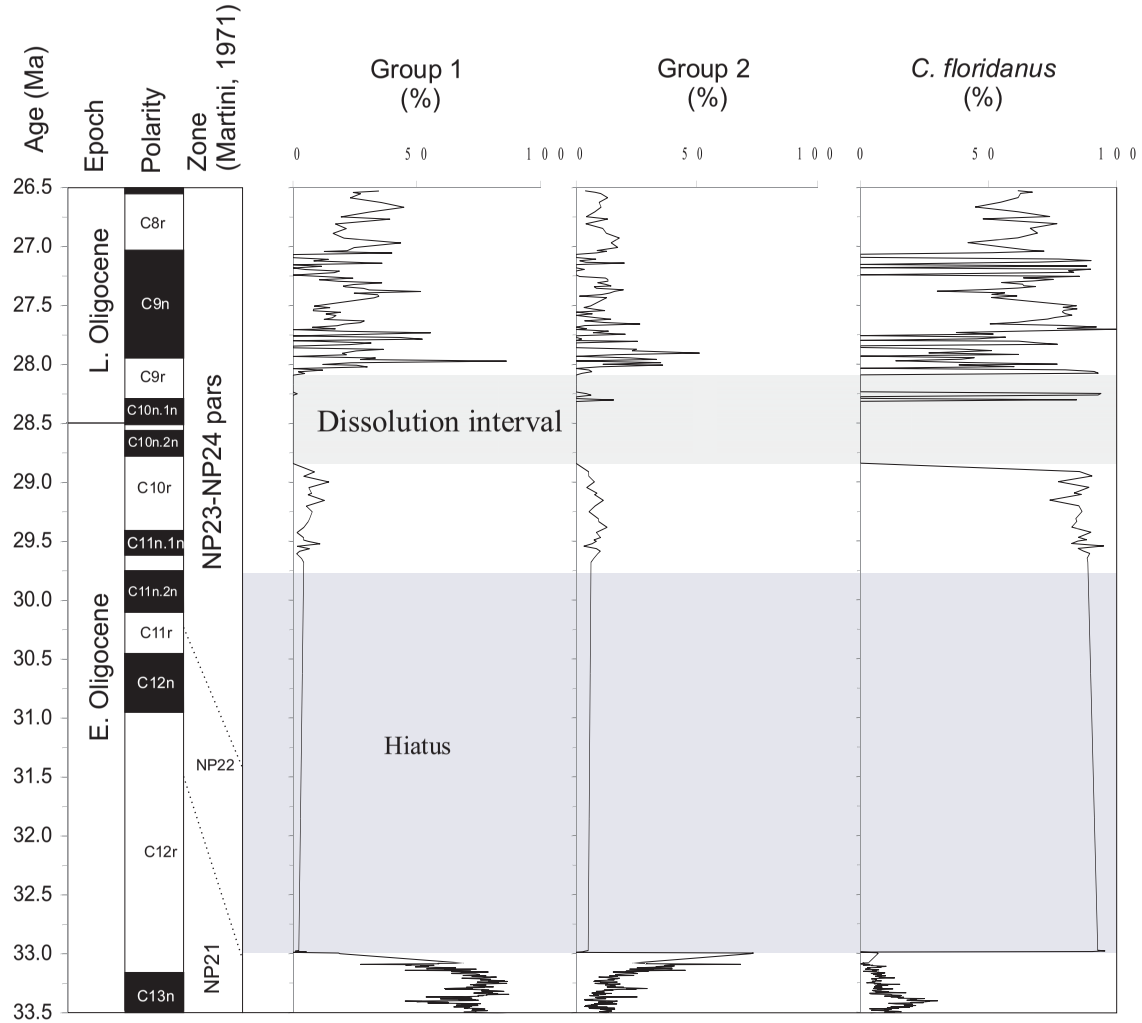

Figure 8: Group 1 and Group 2 variation trends (%) (See Fig. 6 for description), and *C. floridanus* relative abundance (%), plotted against ages from 33.5 to 26.5 Ma (Cande and Kent, 1995). A dissolution level (grey bar) and the early Oligocene hiatus (purple) are indicated. Nannofossil Zone NP22 (Martini, 1971) falls within the hiatus.

Event	Average depth (mcd)	Sample interval (cm)	Age (Ma)
HO *I. recurvus*	221.60	23X-7,110/23X-7,130	hiatus (29.6-32.9 Ma)
HO *R. umbilicus*	221.60	23X-7,110/23X-7,130	hiatus (29.6-32.9 Ma)
HO *E. formosa*	223.41	23X-7,149/24X-1,7	hiatus (29.6-32.9 Ma)
TA *Blackites*	226.18	24X-1,127/24X-1,147	33.117
TA *Clausicoccus*	234.12	24X-7,23/25X-1,4	33.331
LO *R. circus*	235.30	25X-1,104/25X-1,114	33.363
BA *Blackites*	235.50	25X-1,124/25X-1,134	33.369
BA *Clausicoccus*	245.43	24X-1,14/24X-1,34	33.635
HO *R. oamaruensis*	258.27	27X-3,33-27X-3,43	33.975
HO *D. saipanensis*	261.76	27X-5,82/27X-5,93	34.067
LO *R. oamaruensis*	291.77	30X-6,13/30X-6,44	35.455

Table 1: Depth, sample interval and ages of biostratigraphic events recognized at Site 1090. Ages are based on the Cande and Kent (1995) time scale.

Cool water taxa	Warm water taxa	Temperate water taxa	Mesotrophic-Eutrophic taxa	Oligotrophic taxa
R. daviesii group	*Discoaster* spp.	*R. umbilicus* group	*Sphenolithus* spp.	*Discoaster* spp.
Chiasmolithus spp.	*E. formosa*	*C. pelagicus*	*E. formosa*	
I. recurvus	*Sphenolithus* spp.	*D. bisectus*	*C. floridanus*	
			R. umbilicus group	
			C. pelagicus	

Table 3: Taxa paleoecological classification used in this work.

Event	This work		Berggren et al. (1995)		Wei and Thierstein (1991)	Wei and Wise (1992)	Marino and Flores (2002)	Wei (2004)	Persico and Villa (2004)	Villa et al. (2008)
	Age	Chron	Age	Chron	Age	Age	Age	Age	Age	Age
HO *I. recurvus*	hiatus (29.6-32.9 Ma)	C11n.1n	31.8-33.1	C12r diachronous	31.8	32.3	early C12r	32.3	32.34 (Site 689D), 32.55 (Site 744A)	32.46
HO *R. umbilicus*	hiatus (29.6-32.9 Ma)	C11n.1n	32.3 (mid-low lat) 31.3 (southern high)	early C12r (mid-low lat) late C12r (south high lat)	31.3	31.3	late C12r	31.3	31.4 (Site 689D), 32.55 (Site 744A)	31.52
HO *E. formosa*	hiatus (29.6-32.9 Ma)	C13n-C12r	32.8 (low-mid lat) 39.07 (south high lat)	C13n-C12r (low-mid lat) C18 (south high lat)			32.8			39.48
TA *Blackites*	33.117	C13n					C13n			
TA *Clausicoccus*	33.331	C13n	33.3	C13n			C13n			
LO *R. circus*	33.363	C13n					C13n			
BA *Blackites*	33.369	C13n					33.35			
BA *Clausicoccus*	33.635	C13n					C13n			
HO *R. oamaruensis*	33.975	C13r	33.7	C13n-C13r	33.7	33.7	34.0	33.7	33.91-33.71	33.75
HO *D. saipanensis*	34.067	C13r	34.2 (low lat) 35.4 (high lat)	C13r (low-mid lat) C16n .1n (south high lat)			34.09			
LO *R. oamaruensis*	35.455	C16n.1n	35.4	C16n.1n	35.4	35.4	35.36	33.7	35.78	35.51

Table 2: Ages from the literature of the biostratigraphic events recognized at Site 1090. All ages are converted to the Cande and Kent (1995) time scale.

Chapter 4

Calcareous Nannofossil preservation state as a dissolution and CCD proxy: a case study from the Eocene-Oligocene Transition at ODP Site 1090, South Atlantic Ocean

1. Introduction

The Eocene-Oligocene Transition (EOT) represents a global climatic change occurring near the passage between these two epochs and it is characterized by the Antarctic ice sheet development and by a global cooling recorded worldwide by planktic and benthic foraminiferal oxygen stable isotopes (Miller et al., 1991; Zachos et al., 2001).

The EOT is marked by two positive shifts of benthic oxygen isotope values ($\delta^{18}O$), Step 1 (0.5 ‰ increase, ~33.8 Ma) and Step 2 (1.0 ‰ increase, 33.54 Ma), separated by a ~200 kyr isotopic plateau (Coxall et al., 2005). Step 2 corresponds to the Oi-1 event (Miller et al., 1991; Zachos et al., 2001) and is located near the C13r/C13n boundary (Zachos et al., 1992). Shift associated to Step 2 culminates in the Early Oligocene Glacial Maximum (EOGM) (Coxall and Pearson, 2007; Zachos et al., 1996), with the formation of a permanent ice-sheet in Antarctica (Kennett and Shackleton, 1976; Miller et al., 1991). A further isotopic step (EOT2) was found at ~33.63 Ma (within the isotopic plateau) by Katz et al. (2008) but its global character is not certain. The EOT has a total duration of ~500 kyr, from ~33.5 to 34 Ma (Coxall and Pearson, 2007). Oxygen isotope record is paralleled by carbon stable isotope ($\delta^{13}C$) and carbonate records (Coxall et al., 2005), highlighting the tight relationship between cooling, carbon cycle reorganization and Carbonate Compensation Depth (CCD) deepening, all occurring at the EOT. This latter event was recorded worldwide by the increase of carbonate deposition in deep oceans, and it was more pronounced in the Pacific Ocean

(≥1 km) (Rea and Lyle, 2005; Van Andel, 1975), and less prominent in the Atlantic (Moore and et al., 1984) and in the Indian ocean (<700 m) (Peterson and Backman, 1990). In the South Atlantic, the CCD is interpreted to have deepened by ~1 km, but a detailed CCD history across the EOT has not been previously developed for this region. According to Rea and Lyle (2005), the worldwide deepening of the CCD increased of a factor of 2.25 the area of the ocean floor covered by carbonate deposits. Vertical movements of the CCD are influenced by several factors, such as marine productivity, sea level changes and water acidity, and therefore, CCD evolution is closely related to climate. Trigger mechanisms for the ice sheet formation and global cooling occurring in the Paleogene are still debated between the opening of circum-Antarctic gateways (e.g. Kennett, 1977; Lawver and Gahagan, 2003) and the decrease of CO_2 in the atmosphere (DeConto and Pollard, 2003a; Pagani et al., 2005).

The EOT is associated with a strong biotic turnover in the marine realm (e.g. Baldauf, 1992; Brinkhuis and Biffi, 1993; Dunkley Jones et al., 2008; Funakawa et al., 2006; Pearson et al., 2008; Wade and Pearson, 2008), with a significant variation in sedimentological properties (e.g. Anderson and Delaney, 2005; Diekmann et al., 2004; Diester-Haass and Zahn, 2001; Latimer and Filippelli, 2002; Nilsen et al., 2003) and with the reorganization of the carbon cycle (e.g. Merico et al., 2008; Zachos and Kump, 2005; Zachos et al., 1996).

This study wants to give a contribution to the understanding of the climatic changes occurring at the EOT in the Southern Ocean, with two specific goals: 1) to estimate the dissolution affecting nannofossil assemblages and to use the dissolution/preservation signal as a proxy for CCD variations; 2) to characterize the surface waters using the paleoecological/paleoceanographic information given by nannoplankton.

To do this, a quantitative analysis of nannofossil assemblages was carried out on sediments spanning the EOT from about 34.2 to 33.0 Ma (Cande and Kent, 1995) at Ocean Drilling Program (ODP) Hole 1090B (42°S, Agulhas Ridge, South Atlantic ocean) (Fig. 1). Today this site lies at 3700 m depth, above the CCD, but in the Eocene it was below of very close to it, and therefore has a great potential for studying even small variations of the CCD (Gersonde et al., 1999).

Traditional methods to evaluate carbonate dissolution are based on the fragmentation state of foraminifera (e.g. Berger, 1968). Only few works using nannofossils as dissolution indicators are available (Blaj et al., 2009) even if the effect of dissolution on nannofossil assemblages has been more widely studied (Gibbs et al., 2004; Jiang and Wise, 2009).

Several previous works on calcareous nannofossil assemblages at different latitudes gave a significant contribution in the comprehension of the climatic change occurring at the EOT (Dunkley Jones et al., 2008; Villa et al., 2008; Wei, 1991; Wei et al., 1992; Wei and Wise, 1990a; Wei, 2004).

2. Materials and methods

Sediments studied in this work were drilled at ODP Site 1090 Hole B (42°S, 8°E), located on a flank of the Agulhas Ridge, in the subantarctic sector of the Atlantic Ocean (Fig. 1). Samples, prepared using a settling technique (de Kaenel and Villa, 1996), were studied at 20 or 30 cm resolution by optical microscope (cross-polarized light and phase contrast) at 1250X magnification. Data were collected by BugWare software.

The standard nannofossil zonal schemes (Martini, 1971; Okada and Bukry, 1980) were used, together with a southern high latitude scheme (Wei and Wise, 1990b) .

The paleomagnetic signal is robust (Channell et al., 2003) and the ages of Chron boundaries were assigned using the GPTS of Cande and Kent (1995).

Considered the specific goal of our analysis, counts were carried out on entire specimens and fragments. In each sediment sample, at least 500 entire nannofossil specimens were counted. The count of fragments focused on pieces bigger than 3 μm, and two specific categories were distinguished: 1) fragments of *Coccolithus pelagicus*, easily recognisable in phase contrast, and 2) indistinct fragments, not recognizable at species level. Also, to obtain a more precise evaluation of assemblage preservation state, specimens belonging to *Reticulofenestra samodurovi* and *Reticulofenestra umbilicus* were split in *well preserved* and *partially dissolved* based on the preservation of the margin.

Within the carbonate dissolution level identified between ~255 and 251 mcd (Figs. 2, 3) nannofossils were counted by separating entire specimens and fragments (collecting

assemblage composition as metadata) on two traverses (~12.56 mm^2) at 40X magnification: the number of nannofossils (entire specimens+ fragments) varies from 0 to 278 (Fig. 6). Taxa relative abundance within this dissolution interval were not used for the paleoecological reconstruction because less than 300 entire specimens were counted.

Together with nannofossil assemblage analysis, bulk stable oxygen and carbon isotope records and carbonate content (Bohaty and Palïke, Unpublished data, 2010) are used as paleoceanographic proxies. Carbonate curve at the top left of Fig. 2 represents values estimated from XRF analysis. Carbonate records plotted in conjunction with nannofossil dissolution proxies in Figs. 2 and 3 represent the closest samples (selected from the Bohaty and Palike dataset) to the analysed micropaleontological samples. This way, similarities and differences between the two records are stressed.

For the paleoecological interpretation of the assemblages, samples not affected by dissolution were selected among all counted samples, based on results obtained from nannofossil dissolution indices. Obtained nannofossil relative abundances are plotted as percentages/mcd (meters composite depth) (Figs. 4, 5) and used to define paleoecological preferences. Taxa showing comparable behaviour (increasing or decreasing) across the EOT, were merged in groups, in a way to maximize nannofossil response to the climatic change. This response was then interpreted based on taxa paleoecological interpretations available from the literature.

3. Results

3.1. Biostratigraphic framework

The investigated time interval spans from ~34.2 to 33 Ma and nannofossil zones NP19/20-21 (Martini, 1971), CP15b-CP16b (Okada and Bukry, 1980) and the *Reticulofenestra oamaruensis* and *Blackites spinosus* Zones of Wei and Thierstein (1991), which correspond to *Reticulofenestra oamaruensis, Reticulonestra samodurovi,* and *Blackites spinosus* Zones of Fioroni et al. (2010).

The Eocene/Oligocene boundary is defined by the extinction of planktonic foraminifera family Hantkeninae (Nocchi et al., 1998; Premoli Silva and Jenkins, 1993). This

boundary cannot be defined at Site 1090 (Galeotti et al., 2002) because of the intense dissolution affecting foraminifera assemblages. Based on the calculation of sedimentation rates between Chron boundaries, the Eocene/Oligocene boundary was placed at 247.90 mcd.

Nannofossil biostratigraphic events identified at Site 1090 are described in detail and shown in Chapter 3 of this dissertation. Hereinafter, only the events identified in this work (Table 1) are described.

Two calcareous nannofossil events are thought to best approximate the Eocene/Oligocene boundary: the Highest Occurrence (HO) of *Reticulofenestra oamaruensis*, found at Site 1090 at 258.27 mcd (33.97 Ma) and the HO of *Discoaster saipanensis* seen at 261.76 mcd (34.06 Ma) (Table 1).

The position of the Eocene/Oligocene boundary can be determined using nannofossil biostratigraphy and and oxygen isotope stratigraphy, and it can be located within the plateau defined by the isotopic Steps 1 and Step 2 (Coxall et al., 2005), thus between about 251.8 and 241 mcd (Fig. 2), in a higher stratigraphic position than proposed by Marino and Flores (2002), who located the boundary between the LO of *D. saipanensis* and the LO of *R. oamaruensis* (262.39-258.69 mcd).

The base of the acme of *Clausicoccus* was seen at 245.43 mcd (33.63 Ma) and its top at 324.12 Ma (33.33 Ma). The base of the acme of *Blackites* was seen at 235.50 mcd (33.36 Ma) and its top at 226.18 mcd (33.11 Ma).

3.2. Nannofossil indices of dissolution

At ODP Site 702 (Chapter 2 of this dissertation) we used *Zygrablithus. bijugatus* as a reliable dissolution indicator and we suggested that the presence of this species within the assemblages ensured that no strong dissolution acted. Its absence, however, can be either caused by strong dissolution or paleoecological reasons. At Site 1090, *Z. bijugatus* is completely absent all along the studied section (35.5- 26.5 Ma, This Chapter and Chapter 3 of this dissertation). The reasons of this absence are unknown. It is possible that during the late Eocene, when waters were particularly aggressive, this species went dissolved. Nevertheless, it is not present either in the early and late Oligocene, when the CCD was much deeper and carbonate easily preserved. In fact,

Blackites, the other dissolution proxy we used at Site 702, is present at Site 1090 and, as explained hereinafter, the distribution of this taxon is tightly linked to carbonate content and CCD variations.

It is therefore possible that the complete absence of *Z. bijugatus* at Site 1090 is not caused by dissolution but by paleoecological/paleocenaographic reasons. If *Z. bijugatus* was strongly oligotrophic, as suggested in Chapter 2, then it is possible that the high nutrient availability characterizing both the Eocene and Oligocene at Site 1090, might have excluded this species. This hypothesis seems supported by the late Eocene opal pulse found at Site 1090, which undoubtedly indicates high fertility at the sea surface (see Chapter 3 of this dissertation). High nutrient availability is also suggested by nannofossil assemblage characteristics across and after the EOT. However, even if plausible, this consideration is purely speculative and the absence of *Z. bijugatus* remains unexplained. We therefore could not use the distribution of *Z. bijugatus* as a proxy for dissolution at Site 1090, but other quantitative indices were calculated.

Indices of dissolution were calculated by using nannofossil assemblage components. They are shown in Figure 2 and 3, next to the carbonate record (Bohaty and Palïke, Unpublished data, 2010).

Nannofossil preservation/dissolution indices are:

1) [(Total of entire specimens)/[Total assemblage (entire+ fragments)]*100 (Index 1, NI1);
2) [*R. umbilicus* group (entire specimens)]/[(*R. umbilicus* group (entire+ partially dissolved)]*100 (Index 2, NI2);
3) [*C. pelagicus* (entire specimens)]/[*C. pelagicus* (entire+ fragments)]*100 (Index 3, NI3);

These indices represent the preservation/dissolution state of nannofossil assemblages, and higher values correspond to a better preservation, lower values to a worse preservation/enhanced dissolution.

Within the category “Fragments”, only pieces bigger than 3 μm were considered. Fragments smaller than 3 μm were not counted.

The evaluation of the dissolution intensity affecting rims of *R. umbilicus* group (*R. umbilicus* and *R. samodurovi*) might have some character of subjectivity. As general

approach, specimens perfectly preserved or affected by very subtle etching were considered as w*ell preserved*; specimens with moderately to strongly dissolved rims were considered as *partially dissolved*.

When affected by dissolution, *C. pelagicus* does not show etched rims but breaks down in pieces. For this reason, we differentiated *entire specimens* of *C. pelagicus* from its *fragments*.

Also, *Blackites* and *Clausicoccus* distributions were used here as dissolution/ preservation indicators. This is based on a significant parallelism between *Blackites* and *Clausicoccus* distribution with respect to the carbonate record (Figs. 2, 3), which suggests that dissolution is the most important factor in driving their abundances. At Site 1090, these two taxa are essentially absent in the Eocene and they significantly increase in abundance at the EOT (Figs. 2, 3). Lower Oligocene acmes of *Clausicoccus* and *Blackites* were found at different locations (Marino and Flores, 2002; Mc Gonigal and Di Stefano, 2002; Wei and Wise, 1990a).

The general picture given by the calculated indices and by *Clausicoccus* and *Blackites* distributions (Figs. 2, 3), shows lower average values from the base of the section up to 242 mcd and higher values from ~242 to the top of the section. The upper part of the section, from 230 mcd shows a gradual trend of decrease.

NI1 shows the lowest variability compared to the other nannofossil dissolution indices NI2 and NI3. Its values span from 16 to 55% in the lower part of the section, and increase to 38-80 % in the upper part. Starting from about 230 mcd, a gradual trend of decrease can be noted, that can be seen in all dissolution indices (Figs. 2, 3).

NI2 shows a distribution very similar to NI1. Lower values are recorded from the base to about 245 mcd, and higher values are recorded from 241 mcd up to the top of the section. In the Oligocene part of the section, NI2 has the highest values (up to 94%), among all indices. In the Eocene, highest values are shown by NI1.

NI3 is strongly variable and has the lowest values among all indices. From the base of the section up to 244 mcd, its values spans between 0 to about 20%. From 244 mcd up to the top of the section, values are much higher, reaching almost 60%. A general trend of decrease can be seen starting from 230 mcd (Figs. 2, 3).

3.3. Taxa distribution

At Site 1090, the EOT corresponds to a considerable change within nannofossil assemblages and most species show marked abundance variations (Figs. 4, 5).
It is possible that these abundance variations might be caused by dissolution effect. Therefore, for the paleoecological interpretation of the assemblages, we only used "well-preserved" samples. To select suitable samples, nannofossil dissolution indices previously described were used (Figs. 1, 2), and only samples corresponding to higher values (positive peaks) of at least two nannofossil indices out of three were considered as pristine. This selection allowed to keep 50 samples out of 96 originally counted. This way, for the paleoecological interpretation, only unspoiled assemblages were used, and reliable nannofossil abundances were obtained, even if at lower resolution (Figs. 4, 5).

Chiasmolithus (Fig. 5) are mainly represented by *Chiasmolithus* sp. (lacking the central cross), *C. oamaruensis* and a very few specimens of *C. expansus*. Genus *Chiasmolithus* shows low abundances (0-3%) in the Eocene and a strong increase between 246 and 243 mcd, reaching in the early Oligocene much higher values (2-14%).

R. daviesii group, composed by *R. daviesii* and *Reticulofenestra* sp. (3-5 μm), has a similar trend to *Chiasmolithus*'s (Fig. 4), but with higher abundances. A significant increase is recorded between 246 and 244 mcd. Eocene abundances vary from 9 to 45%, Oligocene values from 18 to 58%.

R. umbilicus group decreases considerably in abundance across the EOT, being Eocene values around 30% and Oligocene values around 10%. Its abundance drops significantly between 244 and 246 mcd (Fig. 4).

C. pelagicus is quite variable in abundance all along the section (Fig. 4) and a marked increase is shown in correspondence of Step 2. High values reached at Step 2 are maintained upward, in the Oligocene part of the section, with minor oscillations.

Sphenolithus spp., *Ericsonia formosa* and *Discoaster* spp. are less abundant components of the assemblages. The few specimens of *Sphenolihus* found at Site 1090 are

represented by *S. moriformis*. This species has maximum abundance values lower than 1% and it s distribution is scattered across the EOT (Fig. 4).

Discoasters are present with abundances lower than 7% (Fig. 4). The lowest analysed sample is the only one showing a much higher value (about 15%). A peak in abundance is present just above Step 1. This peak is determined by an increase in abundance of *D. deflandrei*.

E. formosa shows a slightly more pronounced variability compared to *Sphenolithus* and *Discoaster*. Its abundances are low, constantly lower than 2% (Fig. 4).

Dictyococcites spp. (*D. bisectus* and *D. stavensis)* abundance pattern at Site 1090 shows higher values (3-27%) in the Eocene, a decreasing trend starting at ~250 mcd and much lower values in the Oligocene (0-10%).

At Site 1090, *Istmolithus recurvus* abundance varies from almost 0 to 8% (Fig. 5). Its distribution is markedly changeable and a precise trend across the EOT cannot be recognized.

Cyclicargolithus floridanus distribution (Fig. 4) is very variable and shows a slight decrease through the EOT, with abundances spanning from 0 to 46% in the Eocene and from 5 to 39% in the Oligocene.

Two general distribution patterns can be recognized, with species increasing (Group 1) or decreasing (Group 2) in abundance across the EOT (Fig. 5). We therefore follow the same approach adopted in Chapter 3 of this dissertation. *Chiasmolithus* spp., *R. daviesii* group, *Blackites* spp., *C. pelagicus* and *Clausicoccus* spp. increase in abundance through the EOT and were merged in Group 1; *Dictyococcites* spp., *R. umbilicus* group, *Discoaster* spp. and *E. formosa* decrease at the EOT and were merged in Group 2 (Figs. 4, 5). *I. recurvus* and *C. floridanus* do not significantly change their abundance across the EOT and therefore they were not considered in any group.

4. Discussion

4.1. Dissolution effect on nannofossils

The influence of dissolution on nannofossils is of particular interest when assemblages are used for paleoecological/paleoceanographic studies. Dissolution, in fact, can drastically impoverish the assemblages, favouring more resistant taxa, and providing fake relative abundances. Several recent works pointed out as dissolution is a fundamental factor in determining the characteristics of nannofossil assemblages (Blaj et al., 2009; Gibbs et al., 2004; Jiang and Wise, 2009).

Dissolution of coccolitophores can occur in either the water column or within the sediment, as a consequence of diagenetic processes. Distinguishing the role of these two processes is difficult because the final effect is the same. Usually, dissolution acting within the sediment is accompanied by re-deposition of calcite, disguised as re-crystallisation/overgrowth on more robust nannofossil taxa (e.g. Discoasters, Neococcolithes). Nevertheless, dissolution acting on coccoliths does not only represents a disturbance factor in the study of assemblages, but can also be a tool for paleoceanographic studies. In this work, we tested the potential of nannofossils as proxies for carbonate water under-saturation through the EOT, a time interval very critical for the evolution of the global CCD (e.g Coxall et al., 2005).

Carbonate dissolution is also used to estimate primary productivity in the sea surface water (e.g. Diester-Haass et al., 1993; Diester-Haass et al., 1996). In fact, carbonate dissolution can be produced either by changes in water chemistry or by change of organic matter supply to sea floor. Organic matter produced at the sea surface sinks in the water column and it is progressively oxidized by bacterial activity. This process produces CO_2 that goes dissolved into the water, increasing water acidity and finally causing carbonate dissolution. Therefore, when productivity is higher at the sea surface, carbonate dissolution is more intense, as well. Classical methods to evaluate dissolution are based on fragmentation and etching of foraminifera tests (Berger, 1973; Berger, 1977; Diester-Haass and Zahn, 1996). The use of nannofossils as dissolution proxies can provide further details compared to foraminifera; in fact, coccolith lysocline (Berger, 1973) is deeper than foraminifera lysocline (Bramlette, 1961), because

nannoplankton has a low-magnesium calcite, which is more resistant than calcite of foraminifera (e.g. Bukry, 1991).

4.1.1. Nannofossil preservation state as a dissolution proxy

As shown in Figs. 2 and 3, the marked similarity between all nannofossil indices, and between nannofossil indices and carbonate content, elect calcareous nannofossils as powerful indicators of dissolution intensity. Carbonate abundance alone is not a dissolution proxy because the amount of carbonate within the sediment depends on 1) carbonate productivity in the surface waters 2) dissolution (along the water column or within the sediment, 3) dilution by siliceous or terrrigenous material. Nannofossils can help to distinguish these factors: results obtained in this work confirm that nannofossils are independent and reliable dissolution indicators, as previously suggested by Blaj et al. (2009).

Our data show that, in most cases, higher/lower values of carbonate correspond to better/worse nannofossil preservation and this is clearly shown by parallelism between nannofossil indices and carbonate record (Figs. 2, 3). This means that carbonate deposition at this site is mainly controlled by dissolution and not by other factors. This implies that low carbonate content is caused by dissolution and not, for example, by decreased nannofossil/ foraminifera productivity at the surface water.

Only the interval in the upper part of the isotopic plateau (~241-244 mcd) reveals a different pattern, with high values of NI1 and NI2, moderate values of NI3 and low carbonate content (Figs. 2, 3). This highlights that within this interval, low carbonate content is not caused by dissolution, otherwise NI1 and NI2 would have low values as well. Here, low $CaCO_3$ content can result from lower carbonate productivity with respect to siliceous productivity or dilution by siliceous material. This last hypothesis seems in agreement with the increasing SiO_2 content recognized within the same interval by Diekmann et al. (2004).

4.1.2. Ranking of nannofossil sensitivity toward dissolution

Nannofossil dissolution indices allow to define a ranking of sensitivity toward dissolution among taxa used for their calculation (*C. pelagicus*, *R. umbilicus* group). The general picture shows distinctly that a strong variation in dissolution intensity occur between 241 and 239 mcd (Figs. 2, 3), which corresponds to the strong CCD deepening recorded worldwide at Step 2 (Coxall et al., 2005).

Nannofossil index patterns are described hereinafter. For simplicity, we refer to *part A* for samples below ~244 mcd, and to *part B* for samples above this depth (Fig. 2, 3). The limit between these two parts was picked in correspondence of the carbonate dilution level, which marks the boundary between different nannofossil dissolution index pattern. Approximately (because the E/O boundary is located at 247.90 mcd), *part A* corresponds to the latest Eocene, and *part B* to the earliest Oligocene.

In *part A*, NI1 reaches the highest values, ranging from ~16 to ~54% , followed by NI2 with similar values but slightly lower (~7- 63%). NI3 shows the lowest values, ranging from 0 to ~22% (Fig. 2, 3). This pattern indicates that, in similar conditions of water under-saturation, *R. umbilicus* group (NI2) is more resistant compared to *C. pelagicus* (NI3), and that the fracture of *C. pelagicus* occurs more easily than the corrosion of the margin of *R. umbilicus* group.

Looking carefully at indices in *part A* (Figs. 2, 3), NI2 is highly variable, with minimum values around 10% and maximum values around 60%. On the contrary, NI3 is much more constant, with average values ranging from about 0 to 25%. NI2 is similar to NI3, with the same positive and negative peaks, but NI3 shows less pronounced variations than NI2. This difference in behaviour between NI2 and NI3 reveals that *R. umbilicus* group dissolution signal is significantly strengthened between higher (negative peaks) and lower (positive peaks) dissolution intensity periods. On the contrary, *C. pelagicus* response to water acidity variations is minimized and flattened, as shown by NI3, where only smaller amplitude oscillations are recorded.

Within *part B*, all proxies show higher values compared to *part A* (Figs. 2, 3). Notably, a switch in relative position, with respect to *part A*, occurs between NI1 and NI2: NI1 values span ~39-79%, NI2 spans ~18 ~93%, and NI3 spans values ~10- ~59%.

Higher values of all indices in *part B* compared to *part A* indicate that a much weaker dissolution acted here compared to the previous phase. This interpretation is in

agreement with the carbonate content and with the numerous previous works that showed the CCD deepening at the EOT (Coxall et al., 2005; Van Andel, 1975).

At the passage between *parts A* and *B*, NI1 shows a less pronounced change compared to NI2 and NI3, and average values switch from ~30 to 60%. NI 2 and NI3 switch from ~25 to 75 % and from ~10 to 40%, respectively.

The weakened change recorded by NI1 can be explained by the fact that this index (indicative of total entire versus fragmented specimens) also includes a great number of *entire* specimens of cool taxa, such as *Chiasmolithus* spp. and *R. daviesii* group, which are more abundant in the Oligocene compared to the Eocene. For this reason, their higher abundances in the Oligocene affect the numerator of the ratio we used to calculate NI1, increasing the final value of the ratio.

Within *part B*, a much wider gap between NI3 and the carbonate record is shown, compared to *part A*. A possible explanation for this behaviour can be found in the evaluation of the number of *C. pelagicus* fragments. As said, only fragments bigger than 3 μm were counted and considered within NI3. It is likely that during periods of more intense dissolution, such as *part A*, *C. pelagicus* broke down in very small pieces that were not considered in our counts. If they were, they would increase the denominator of NI1 and decrease the total ratio, allowing a much greater difference between NI2 and NI3, comparable to the gap seen in *part B*. Only considering fragments bigger than 3μm, NI3 might be slightly under-estimated.

Also, NI3 shows wider amplitude oscillations in *part B* compared to *part A*. This can be explained by a generally weaker dissolution in *part B* that allowed *C. pelagicus* to record even small variations in water characteristics and not to undergo the flattening dissolution effect seen in *part A*, and also by the missing information given by fragments smaller than 3 μm. Differently, this flattening is not shown by NI2, which displays wide amplitude variations in both *parts A* and *B*.

In general, in conditions of weak-moderate water aggressiveness (*part B*, Oligocene) *C. pelagicus* is more sensitive in recording water acidity variations compared to periods of stronger acidity (*part A*, Eocene). This conclusion may be checked by counting all *C. pelagicus* fragments. It is possible that considering all fragment, more pronounced oscillations would be shown by NI3, similarly to variations of NI2. If this was true, a

very similar response of *C. pelagicus* and *R. umbilicus* group toward dissolution, would be proved.

R. umbilicus group index (NI2) has a more constant behaviour in both *parts A* and *B,* and the high-frequency and wide amplitude variations corresponding to carbonate content oscillations are present all along the section.

All this allows several considerations:

1) The perfect matching between nannofossil dissolution proxies and the carbonate curve indicates manifestly that coccoliths are extremely sensitive to water acidity and nannofossil fragmentation state is a powerful proxy for dissolution, comparable or even better than proxies based on foraminifera fragmentation. In fact, being the coccolith lysocline (Berger, 1973) deeper than the foraminifera lysocline (Berger, 1968; Bramlette, 1961), a generally better preservation would be shown at all depths by coccoliths compared to foraminifera, allowing a more detailed evaluation of the degree of carbonate under-saturation.
2) Carbonate sedimentation at Site 1090 is mainly driven by dissolution and not by other factors such as primary productivity changes at the surface water or dilution.
3) Nannofossil assemblages were significantly more affected by dissolution within *part A* (Eocene) than *part B* (Oligocene), as shown by all indices. This means that in the Eocene, dissolution was much more pronounced that in the Oligocene.
4) *R. umbilicus* group is more resistant to dissolution than *C. pelagicus*, as shown by constantly higher values of NI2 compared NI3.
5) In conditions of marked carbonate under-saturation, *C. pelagicus* breaks extremely easily and its signal as a dissolution proxy is smoothened and underestimated (remember the question about very small fragments). In these conditions, as well as when waters are weakly aggressive, *R. umbilicus* group is very sensitive in recording even small acidity changes, and as a consequence, NI2 is considered here the best dissolution/ preservation indicator.

6) In conditions of moderate-weak acidity, *C. pelagicus* and *R. umbilicus* group respond in a very similar way and their associated NI3 and NI2 indices are equally reliable.

4.1.3. CCD variations

The CCD is the depth in ocean waters at which there is a balance between $CaCO_3$ saturation and dissolution. This depth varied in geological time in response to paleoceanographic/paleoclimatic changes. A strong deepening of the CCD occurred during the EOT (Coxall et al., 2005; Van Andel, 1975), and it affected all oceans. The most marked deepening occurred in the Pacific Ocean (~1.2 Km), followed by the Atlantic Ocean (~1 km) and by the Indian Ocean (~700 m) (Berger, 1973; Peterson and Backman, 1990).

CCD variations are usually interpreted from carbonate content within sediments. A close correspondence between carbonate content variations and oxygen and carbon isotope records was found at the EOT, emphasizing the connection between cooling/ice growth (oxygen isotopes), carbon cycle perturbation (carbon isotopes), sea level variations and the deepening of the CCD (carbonate content) (Coxall et al., 2005; Wade and Pearson, 2008). (Coxall et al., 2005) observed that the carbon isotope record at the EOT does not match perfectly the oxygen isotope and carbonate record but is slightly successive (~8-10 kyr) (as also shown in our record in Fig. 2), remarking that the carbon cycle perturbation did not act as a trigger mechanism for the climate change at the EOT, even if it might have acted as a positive feedback for the cooling. Nevertheless, the cause/effect relation among all climatic components across the EOT is little known.

Today, Site 1090 is above the CCD; in the late Eocene, it was very close or just below it (Gersonde et al., 1999) and, starting from the early Oligocene it was well above it (Gersonde et al., 1999; Van Andel, 1975). Thanks to its privileged position, this Site is optimal to study CCD variations. The major CCD deepening occurring worldwide at Step 2, is interpreted as related to changes in ocean chemistry (e.g. Coxall et al., 2005), following the sea level drop (e.g. Kominz et al., 1998) and the discharge of carbonate from the shelves to the deep ocean (shelf-basin fractionation) (e.g. Merico et al., 2008). Differently, Miller et al. (2009) suggest that the CCD deepening was triggered by

increased thermoaline circulation and deep-water ventilation which caused a decrease of oceanic water residence time and a decrease in deep-water acidity, allowing carbonate to be preserved at deeper depth.
It is possible that high-frequency oscillations of carbonate content and dissolution intensity seen at Site 1090 might be caused by productivity changes or by both oceanographic and biological processes. Enhanced dissolution is induced by surface water productivity variations (Diester-Haass, 1992; Diester-Haass et al., 1996) which controls the amount of organic matter sinking to the sea floor. When the organic matter is decomposed by bacterial activity, CO_2 is produced and released into the water causing carbonate dissolution.

Along most of the studied section, the calculated dissolution indices match perfectly the carbonate record (Figs. 2, 3), indicating that carbonate content was controlled by dissolution and not by dilution or other factors. At Site 1090, changes in carbonate water saturation are thought to be linked to CCD oscillations, because of the position of the Site, very close, in the late Eocene, to the CCD (Gersonde et al., 1999). Mean values of nannofossil indices in *part A* (Eocene) are much lower than in *part B* (Oligocene) (Figs. 2, 3). This indicates that, independently from different taxa behaviour, dissolution was stronger in the Eocene than in the Oligocene. Also, a higher-resolution variability is over-imposed on this general trend, along all the section.

The interval between 251.5 to 255.5 mcd represents a dissolution event found worldwide (Coxall et al., 2005; Diester-Haass and Zachos, 2003; Liu et al., 2004; Peck et al., in press; Zachos et al., 1996) in the upper part of Chron C13r, and it is interpreted as a temporary shoaling of the CCD (Coxall et al., 2005; Van Andel, 1975). It is therefore considered an important element characterizing the climatic change occurring at the EOT. At Site 1090, this interval shows carbonate content from 0 to ~12%. To test if nannofossil dissolution indices are reliable even in conditions of very intense water acidity, we carried out an analysis with a different method, compared to the rest of the section, which is described in Section 2. Among the 19 samples counted within this interval, only one (1090B-26X-5-63; 251.82 mcd) was completely barren of nannofossils. Ratio between the number of entire specimens relatively to the total

assemblage shows very high values (28-83%) (Fig. 6) and was not used neither to estimate dissolution intensity nor for the paleoecological interpretation of assemblages, for two reasons: 1) nannofossils are too rare and counts involved less than 300 entire specimens and thus taxa relative abundances are not statistically valid; 2) within this interval, dissolution is so strong that the most delicate taxa went completely dissolved, and only very robust specimens (e.g. *Dictyococcites bisectus*, *R. samodurovi*, *R. umbilicus*) were left behind. Nevertheless, nannofossil total abundance (number of counted entire specimens summed to fragments, on two traverses) roughly parallels the carbonate record (Fig. 6), and only one sample has a mismatching behaviour (252.5 mcd). Assuming that water acidity did not change within this interval, and that the most delicate species went completely dissolved, then, even in conditions of marked carbonate under-saturation, nannofossil assemblages (in this case, the abundance of entire specimens summed to fragments) represent a valuable proxy for carbonate preservation/dissolution. A higher resolution study involving at least 300 entire specimens would be necessary to better establish the link between nannofossil assemblage characteristics relatively to carbonate content in sediments so strongly affected by dissolution.

This highly dissolved interval (251.5-255.5 mcd) corresponds to very high opal content (maximum values: 78%) and Total Organic Carbon (TOC) (maximum value 0.148 %) (Diekmann et al., 2004) and represents a moment of higher siliceous productivity. This indicates that the silica pulse is coupled with an increase of organic carbon *burial*, a process that allows CO_2 sequestration from ocean waters (Diekmann et al., 2004). This might seem in contrast with the intense carbonate dissolution occurring at the same level but actually it is not because, as said, this late Eocene dissolution event is global in character (Coxall et al., 2005; Diester-Haass and Zachos, 2003; Liu et al., 2004; Peck et al., in press; Zachos et al., 1996) and, also at Site 1090, is driven by CCD changes and not productivity changes.

Part A (late Eocene- earliest Oligocene) shows repeated, high frequency variations in carbonate content, which correspond to variations in the nannofossil preservation/dissolution proxies (Figs. 2, 3). Dissolution driving these variations can derive from: 1) CCD rapid fluctuations, as seen for the intense dissolution interval from 251.5 to 255.5 mcd. Further comparison and high resolution data from other locations

are needed to prove a larger scale/global character of these oscillations. Also, if all these variations represented global CCD variations, what would the driving mechanism/s be? If the CCD is responsible for this dissolution pattern, this would mean that the CCD started to oscillate significantly well before Step 1, at least from 34 Ma, i.e. from the base of our study section; 2) another possible cause of the late Eocene dissolution high variability might be related to high frequency variations in the organic carbon burial (and the associated sequestration/release of CO_2) (Diekmann et al., 2004) but to verify this hypothesis high resolution TOC records are necessary, which are not currently available: if TOC variations corresponded to higher carbonate content and higher nannofossil indices values, this could be an indication that late Eocene dissolution changes are linked to organic burial rates.

Because, in the late Eocene, Site 1090 was very close to the CCD, we support the first hypothesis and we interpret carbonate/nannofossil indices variations as CCD oscillations. At this stage we do not know if these variations were only occurring at Site 1090 (local event) or globally, and further analyses would be needed at other sites located close to the paleo CCD depth.

From 263 to ~255.4 mcd, CCD strongly varied (Figs. 2, 3) and then experienced a 60 kyr shoaling event, identified by the dissolution interval. This dissolution event is then followed (~251.5-245.5 mcd) by several, high frequency CCD variations (Figs. 2, 3), very similar in amplitude and duration to those seen below the dissolution level.

As explained in Section 4.4.1., relatively low carbonate content between 245.5 and 242 mcd (Fig. 2, 3) is not interpreted as a consequence of dissolution, but it is caused by dilution with siliceous material, In fact nannofossil indices show high values, indicating well-preserved coccoliths. Above this dilution interval, between 241 and 239 mcd, a major change in carbonate content, nannofossil indices and oxygen stable isotope occur. This corresponds to the Oi-1 event of Miller et al. (1991) and to Step 2 of Coxall et al. (2005), during which an enduring deepening of the CCD occurs.

Above the marked deepening occurring at Step 2, the CCD is much deeper but not yet stable, showing repeated oscillations that seems to have a pattern similar to those shown in part A (Fig. 2, 3).

A rough calculation of a possible ciclicity of CCD oscillations was carried out on the upper Eocene part of the section and a 20 kyr periodicity was found, identifying precessional cycle print, but a higher resolution analysis is needed to assess the correct timing/ciclicity.
A CCD shoaling starts at 232 mcd as indicated by a gradual and stepwise decrease of both nannofossil dissolution indices and carbonate content. Again, this perfect parallelism confirms that dissolution/CCD variations are driving carbonate content changes at the EOT at Site 1090.

4.2. Climatic change at the EOT

Temperature and nutrient availability are deemed as the most important factors in determining nannofossil distribution, also in the modern oceans. We therefore classified taxa based on temperature and fertility preferences, based on interpretations given in the literature (Aubry, 1992; Bralower, 2002; Monechi et al., 2000; Persico and Villa, 2004; Tremolada and Bralower, 2004; Villa et al., 2008; Wei and Wise, 1990b) and on indications provided by our micropaleontological and geochemical records.
Paleoecological and paleoceanographic inferences primarily derive from comparison of single species distribution with taxa with a well-defined paleoecological preference, and with comparison with oxygen and carbon stable isotopes.

4.2.1. Taxa paleoecological classification

Chiasmolithus have been considered cool/cold (Bralower, 2002; Firth and Wise, 1992; Tremolada and Bralower, 2004; Villa et al., 2008; Villa and Persico, 2006; Wei and Wise, 1990a; Wei and Wise, 1990b) or mesotrophic/eutrophic (Aubry, 1992; Bralower, 2002) or as r-mode specialists (Bralower, 2002). We consider this genus as cold and eutrophic.

R. daviesii has been interpreted as cold (Wei and Thierstein, 1991) or cool (Monechi et al., 2000; Persico and Villa, 2004; Villa et al., 2008; Villa and Persico, 2006; Wei et al., 1992). For the paleoecological interpretation, *R. daviesii* and *Reticulofenestra* sp. (3-5

μm) were considered together within the *R. daviesii* group because these two taxa show a comparable distribution pattern at Site 1090, and a similar paleoecological preference is inferred (Villa et al., 2008). At this Site, *R. daviesii* group has a similar trend to Chiasmolithus's (Figs. 4, 5), even if the former is present in much higher abundance than the latter.

R. umbilicus and *R. samodurovi* have been considered temperate (Persico and Villa, 2004; Wei and Wise, 1990b), warm and oligotrophic-mesotrophic (Aubry, 1992) or warm and mesotrophic (Monechi et al., 2000). The interpretation as temperate forms is confirmed at Site 1090 and these two species are grouped here to form *R. umbilicus* group (Fig. 4), as previously done by Villa et al. (2008).

C. pelagicus has been considered warm (Wei and Wise, 1990a; Wei and Wise, 1990b) or temperate (Villa et al., 2008). This species has changed its ecological preference through time because the Pleistocene and living *C. pelagicus* prefer cold (Haq and Lohmann, 1976) or cold and mesotrophic (Holmes et al., 2004) and/or eutrophic waters (Cachao and Moita, 2000). We think that *C. pelagicus* is an indicator of temperate and mesotrophic/eutrophic waters. At Site 1090 this species is highly variable all along the section, and within the interval of major nannofossil assemblage changes, between 246 and 243 mcd, it increases its abundance (Fig. 4). Being *C. pelagicus* a temperate form, we think that its increase in abundance at the EOT is a response to a nutrient availability increase, in agreement with several previous studies recognizing an increase in fertility and productivity at the EOT (Anderson and Delaney, 2005; Diester-Haass and Zachos, 2003; Diester-Haass and Zahn, 2001; Dunkley Jones et al., 2008; Nilsen et al., 2003).

C. floridanus has been regarded as eutrophic by Aubry et al. (1992) and Monechi et al. (2000) and as temperate by Wei and Wise (1990a). The distribution pattern of this species at Site 1090 does not show any particular characteristic with respect to oxygen stable isotopes but it displays a trend parallel to *R. umbilicus* in the Oligocene part of the section, and opposite to it in the Eocene (Fig. 4). Because its interpretation is uncertain, no paleoecological preference was assigned to *C. floridanus*. This species is considered here opportunistic.

A well-established paleoecological interpretation is available for Discoasters, which have been considered as warm (Wei et al., 1992), warm and oligotrophic (Aubry, 1992; Bralower, 2002; Gibbs et al., 2006; Kahn and Aubry, 2004; Kelly et al., 1996; Tremolada and Bralower, 2004; Villa et al., 2008). We consider Discoasters as warm and oligotrophic. Their distribution is shown in Fig. 4.

Sphenolithus have been considered warm and oligotrophic (Bralower, 2002; Gibbs et al., 2006; Villa et al., 2008) or mesotrophic (Agnini et al., 2006; Dunkley Jones et al., 2008; Gibbs et al., 2006). *Sphenolithus* are scarce at Site 1090 and the few specimens found are represented by *S. moriformis*. The theme described in Chapter 3 of this dissertation shows how Sphenoliths experience an increase in the lower Oligocene of Site 1090, and we confirm the interpretation of a preference for eutrophic waters and with a good tolerance for different temperatures.

E. formosa has been interpreted as a warm (Monechi et al., 2000; Villa et al., 2008; Wei et al., 1992; Wei and Wise, 1990b) and oligotrophic (Bralower, 2002; Tremolada and Bralower, 2004; Villa et al., 2008) or eutrophic (Agnini et al., 2009) species. At Site 1090 this species is present in very low abundances. The long-term trend of *E. formosa* (See Chapter 3 of this dissertation) shows a gradual decrease from the late Eocene to the early Oligocene, confirming its preference for warm waters. We interpret *E. formosa* as a warm and mesotrophic/eutrophic species. Its permanence in the early Oligocene suggests it is tolerant to cold temperatures, similarly to *Sphenolithus*.

Dictyococcites bisectus is either warm (Monechi et al., 2000), warm-temperate (Wei and Wise, 1990a) or temperate (Villa et al., 2008; Villa and Persico, 2006; Wei et al., 1992). For the paleoecological interpretation, we grouped this species together with *D. stavensis* (defined as bigger than 10 μm) to form *Dictyococcites* spp.. *Dictyococcites* spp. abundance pattern at Site 1090 shows higher values in the Eocene, a decreasing trend starting between 246 and 243 mcd, and much lower values in the Oligocene (Fig. 4).

There are no paleoecological interpretations of *Blackites spinosus* available in the literature but its acme found in the lower Oligocene in many southern high latitude locations (Marino and Flores, 2002; Mc Gonigal and Di Stefano, 2002; Wei and Wise, 1990a) supports a preference for this species toward cold waters. According to Wei and Wise (1990a), *B. spinosus* and *C. fenestratus* distribution is not controlled by temperature because both of these species do not show particular latitudinal changes but, having an acme in the lower Oligocene at southern high latitudes (Marino and Flores, 2002; Mc Gonigal and Di Stefano, 2002; Wei and Wise, 1990a), they certainly do not dislike cold waters, and their distribution may be controlled by other ecological factors other than temperature. As discussed in a previous section, we infer that *Blackites* and *Clausicoccus* spp. distribution at Site 1090 is significantly controlled by dissolution intensity (Fig. 2, 3). *Blackites* have also been used as dissolution indicators in the analysis of dissolution intensity during the Middle Eocene Climatic Optimum at ODP Site 702, as described in Chapter 2 of this dissertation.

Isthmolithus recurvus prefers cool (Monechi et al., 2000; Wei et al., 1992; Wei and Wise, 1990a) or temperate (Persico et al., 2004) waters. At site 1090 its abundance ranges from almost 0 to 8% and does not show any significant similarity with oxygen isotope records or other species distribution (Fig. 5).

4.2.2. Paleoecological groups

As said, taxa were grouped based on their behaviour across the EOT, i.e. taxa increasing or decreasing in relative abundance. This is the same approach used in Chapter 3 of this dissertation to interpret nannofossil assemblage changes from the late Eocene to the late Oligocene at Site 1090. Group 1 is composed by taxa increasing at the EOT, i.e. *Chiasmolithus*, *R. daviesii* group, *C. pelagicus, Sphenolithus* spp., *Blackites* spp. and *Clausicoccus* spp.. Group 2 is composed by taxa decreasing across the EOT, i.e. *R. umbilicus* group, *Dyictyococcites* spp., *E. formosa* and *Discoaster* spp.. Not showing significant variations across the EOT, *C. floridanus* and *I. recurvus* were not considered in any group, as well as several other minor components. Groups 1 and 2 variations are shown, against age, in Fig. 5.

In correspondence of Step 1 (~33.75-33.8 Ma), nannofossil assemblages do not record any particular variations, and temperate, cool and warm forms vary only slightly compared to values seen below (Figs. 4, 5). The low sample resolution shown at Step 1 (as well as all along the studied section) is caused by the sample selection we applied for the paleoecological interpretation, based on dissolution effect. Our selection guarantees that nannofossil assemblages are pristine, but, as a consequence, the lower resolution does not allow to recognize possible rapid and transient shifts within the assemblages. Because of this low resolution, we cannot exclude that nannofossil assemblage variations related to cooling occur during Step 1.

Step 1 (Coxall et al., 2005; Pearson et al., 2008) or EOT1 (Katz et al., 2008; Miller et al., 2009) has been associated to a temperature decrease (Katz et al., 2008; Lear et al., 2008; Miller et al., 2009) of 2-2.5 °C (Katz et al., 2008; Lear et al., 2008) or 1-2°C (Miller et al., 2009). (For a wider discussion about the interpretation of Step 1, see Chapter 3 of this dissertation).

A possible slight warming phase occurs right after Step 1 (~33.7 Ma) (Figs. 4, 5) as shown by the increase in abundance of *Discoaster* spp. (mainly *D. deflandrei*), the decrease of cold *I. recurvus* and the increase of *R. umbilicus* group. We interpret this period as characterized by warm and oligotrophic waters, based on the well-established and reliable paleoecological preference of genus *Discoaster* (Aubry, 1992; Bralower, 2002; Gibbs et al., 2006; Kahn and Aubry, 2004; Kelly et al., 1996; Tremolada and Bralower, 2004; Villa et al., 2008). At this level, some reworking occurred, indicated by the presence within the assemblages of *D. saipanensis* and *R. oamaruensis*.

The major change experienced by nannofossil assemblages is recorded between 36.65 and 36.6 Ma, as shown by significant variation of both Group 1 and 2. As already discussed in Chapter 3 of this dissertation, this event is interpreted as a significant increase in sea surface fertility. No marked oxygen isotope variation corresponds to this nannofossil shift, occurring in the middle of the isotopic plateau (Coxall et al., 2005; Pearson et al., 2008). The fact that oxygen stable isotope record does not show any marked variation where nannofossil assemblages experience their most prominent change, may imply that the isotopic signal within the plateau is mainly determined by ice volume and not temperature (Katz et al., 2008; Lear et al., 2008; Miller et al., 2009);

as a consequence, we interpret the nannofossil turnover as mainly driven by an increase in nutrient availability accompanied by a weak or null temperature decrease.

Katz et al. (2008) and Miller et al. (2009) recognized *three* main benthic oxygen isotope steps (positive shifts) during the EOT, labelled 1) EOT1 (33.8 Ma), 2) Oi-1 (33.55 Ma), corresponding, respectively, to Step 1 and Step 2 of Coxall et al. (2005), and 3) a further intermediate event labelled EOT2 at 33.63 Ma, just after the Eocene/Oligocene boundary (33.7 Ma), i.e. within the isotopic plateau of Coxall et al. (2005).
Other micropaleontological evidence (Dunkley Jones et al., 2008; Funakawa et al., 2006; Wade and Pearson, 2008) show that significant paleoeceanographic changes occurred *before* the major isotopic event at 33.55 Ma (Step 2 or Oi-1): a profound foraminifera turnover was recognized in Tanzania sections, with the extinction of 5 species of *Hantkenina* (used to define the Eocene/Oligocene boundary) and 3 species of *Turborotalia*, and the dwarfing of *Pseudohastigerina micra* (Wade and Pearson, 2008). This biotic turnover was interpreted as a consequence of changes in the thermal structure of the ocean. Also, at the same stratigraphic position, the extinction of large benthic foraminifera was recorded and interpreted as caused by a decrease in shelf carbonate production (Pearson et al., 2008) following the sea level fall associated to ice build in Antarctica (Merico et al., 2008; Miller et al., 1991). Radiolarian communities recorded a marked change just below isotopic Step 2, in both the equatorial Pacific (Funakawa et al., 2006) and the Southern Ocean (Funakawa and Nishi, 2008). A further confirmation of the paleoceanographic change occurring very close to the E/O boundary is given by nannofossil records from Tanzania, where marked assemblage changes gave evidence of increased productivity and sea level fall (Dunkley Jones et al., 2008). Therefore, the major nannofossil assemblage change recorded at Site 1090 is most likely related to an increase in fertility of the surface waters and occurs at the same time at different locations where several other micropaleontological records give evidence of paleoceanographic change.

Group 1 and 2 records show the highest and the lowest values, respectively, between 33.5 and 33.4 Ma, in correspondence of Step 2 and of the EOGM (Fig. 5). These abundances are controlled mainly by the increase in abundance of *C. pelagicus*, *R.*

daviesii group and *Chiasmolithus* spp., accompanied by a decrease of *R. umbilicus* group and *Dictyococcites* spp.. Also, Step 2 is the base of *Blackites* and *Clausicoccus* acmes. All these taxa (besides *Blackites* and *Clausicoccus*) vary significantly around 33.6 Ma, when a major nannofossil change is recorded. This shift is followed by a gradual increase or decrease in abundance of single taxa, most likely responding to the ongoing climatic change. The last phase of the transition, as experienced by nannofossils, occurs during Step 2, where taxa find their equilibrium with the new climatic conditions. Also, nannofossil event N2, within the plateau, is probably driven by enhanced fertility, plausibly associated to some cooling. We think that starting from N2, nutrient availability increase is accompanied by gradual cooling that becomes more intense at Step 2, but, at this point, nannofossil assemblages already gained a certain balance with new sea surface water conditions, and this is the reason why the general picture of nannofossil assemblage behaviour at Step 2 is not as extreme as maybe expected. The strong increase of *C. pelagicus* reveals that the cooling occurring at Step 2 is most likely accompanied by a further increase in nutrient availability.

4.2.3. Productivity changes across the EOT

One main characteristic of the EOT is a worldwide benthic foraminifera positive carbon isotope excursion, almost coincident (10 kyr delayed) with oxygen isotope record, that indicates a reorganization of the carbon cycle (e.g. Coxall et al., 2005; Zachos et al., 2001) (Figs. 2, 4). The origin of this shift involves sea level fall, changes in carbonate deposition settings and in water chemical equilibrium. A 30-90 m (Miller et al., 1991) or 70 m (Pekar et al., 2002) or 40-50 m (DeConto and Pollard, 2003b) sea level fall caused the exposure of continental shelves, and carbonate deposition moved from shelves to deep sea (shelf-basin fractionation) (Berger and Winterer, 1974; Coxall et al., 2005; Merico et al., 2008; Rea and Lyle, 2005), causing an increase in $\delta^{13}C$ in the ocean waters and the deepening of the CCD (Coxall et al., 2005; Merico et al., 2008). All these processes were accompanied by CO_2 drawdown (Pagani et al., 2005). Miller et al. (2009) question whether the shelf-basin fractionation mechanism caused the CCD deepening and the $\delta^{13}C$ increase, and suggest that the strengthened thermoaline circulation reduced the water residence time in the oceans, supporting a decrease in

water acidity, and allowing a deeper carbonate deposition and the CCD deepening. Furthermore, the same authors claim that the $\delta^{13}C$ increase associated with the EOT is not linked to the CCD deepening (Coxall et al., 2005; Merico et al., 2008), but it is controlled by a change in the ratio of the organic carbon burial relative to carbonate in a million year time-scale pattern that dominates in the Oligocene and in the Miocene. Despite factors controlling benthic carbon isotope records are still debated, certainly the reorganization of the carbon cycle occurring at the EOT included paleoproductivity changes at all latitudes, as shown by several works (e.g. Diester-Haass et al., 1996; Diester-Haass and Zachos, 2003; Dunkley Jones et al., 2008; Salamy and Zachos, 1999).

An increase in fertility across the EOT is recorded at Site 1090 by calcareous nannofossil assemblage changes, and the passage to more eutrophic conditions occurred in two phases, at ~33.6 Ma (N2) and at Step 2 (Oi-1) (33.5 Ma). This increase in nutrient availability in the surface waters can be a response to the strengthened ocean mixing, upwelling and circulation occurring through the EOT (e.g. Diester-Haass, 1996; Diester-Haass and Zahn, 1996; Hay et al., 2005). The reorganization of the oceanic circulation across the EOT affected the position of the Polar Front (PF) that moved northward and southward in response to ice formation in Antarctica and to cooling. Periods during which the PF moved northward were characterized by nutrient rich waters over Site 1090 (which still today is located very close to the PF) and, during other periods, the front moved southward. This latter process can explain the transient warming phase seen just above Step 1, at about 33.75 Ma.

5. Conclusions

A quantitative analysis of composition and fragmentation state of calcareous nannofossil assemblages was carried out on sediments spanning the Eocene-Oligocene Transition at Site 1090 Hole B (Agulhas Ridge, South Atlantic), in the time interval between ~33.0 and 34.2 Ma. Three major indices of dissolution were calculated by using nannofossil assemblage composition based on dissolution pattern and fragmentation state of two abundant taxa, *C. pelagicus* and *R. umbilicus* group. A third

index was calculated using the characteristics of the whole assemblages, including a large amount of unidentified fragments (≥ 3μm).

Also, two nannofossil taxa experiencing acmes in the early Oligocene (*Blackites* and *Clausicoccus*) are good dissolution indicators, as shown by the strong similarity between these taxa distribution and carbonate content.

The comparison between carbonate content and calculated indices showed a striking parallelism, indicating that 1) here carbonate sedimentation is controlled by dissolution; 2) nannofossil assemblage characteristic can be used as independent dissolution/ preservation proxies. The comparison between the three calculated indices revealed that, in the same conditions of water acidity, *R. umbilicus* group is more resistant than *C. pelagicus*. *R. umbilicus* group is elected as the best dissolution indicator within the assemblages seen at Site 1090, acting as a robust and reliable proxy for dissolution in all conditions of water acidity. Differently, *C. pelagicus* is reliable in conditions of weak/moderate dissolution but not as detailed as *R. umbilicus* in case of intense dissolution.

Variations shown by nannofossil indices and carbonate content were interpreted as CCD fluctuations, seen that Site 1090 was, in the late Eocene, very close to the CCD, and therefore most likely very sensitive to its even subtle CCD shoaling/deepening. Our data show that the CCD markedly varied all along the studied section, that it was shallow in the Eocene and that deepened significantly at Step 2.

One intense dissolution interval was found in the late Eocene. Within this interval, only one sample is barren of nannofossils and the total nannofossil abundance roughly varies in association with carbonate content. Nannofossil dissolution/preservation indices also allowed to better define an interval of dilution of carbonate within siliceous material in the middle of the EOT just before Step 2.

A selection of well-preserved samples was used for the paleoecological interpretation of nannofossil assemblages across the EOT. A major nannofossil assemblage change was found near the Eocene/Oligocene boundary (N2) (~33.6 Ma), and was interpreted as caused by an increase in sea surface nutrient availability, possibly associated to some cooling. N2 was followed by a gradual increase in fertility associated to cooling, which culminated at Step 2. The early Oligocene is characterized by nutrient-enriched cold waters.

References

Agnini, C. et al., 2006. Responses of calcareous nannofossil assemblages, mineralogy and geochemistry to the environmental perturbations across the Paleocene/Eocene boundary in the Venetian Pre-Alps. Marine Micropaleontology, 63: 19-38.

Agnini, C. et al., 2009. An Early Eocene carbon cycle perturbation at ~52.5 Ma in the Southern Alps: Chronology and Biotic Response Paleoceanography, 24.

Anderson, L.D. and Delaney, M.L., 2005. Middle Eocene to early Oligocene paleoceanography from Agulhas Ridge, Southern Ocean (Ocean Drilling Program Leg 177, Site 1090). Paleoceanography, 20(1).

Aubry, M.P., 1992. Late Paleogene nannoplankton evolution: a tale of climatic deterioration. In: D.R. Prothero and W.A. Berggren (Editors), Eocene-Oligocene Climatic and Biotic Evolution. Princeton University Press, Princeton.

Baldauf, J.G., 1992. Middle Eocene through Early Miocene diatom floral turnover. In: D.R. Prothero and W.A. Berggren (Editors), Eocene-Oligocene Climatic and Biotic Evolution. Princeton University Press, Princeton, pp. 310-326.

Berger, W.H., 1968. Planktonic foraminifera: Selective solution and paleoclimatic interpretation. Deep-sea research, 15: 31-43.

Berger, W.H., 1973. Deep-sea carbonates: evidence for a coccolith lysocline. Deep-Sea Research, 20: 917-921.

Berger, W.H., 1977. Carbon dioxide excursions and the deep-sea record: Aspects of the problem. In: N.R. Andersen and A. Malahoff (Editors), The Fate of Fossil Fuel CO2 in the Oceans. Plenum Press, New York, pp. 505-542.

Berger, W.H. and Winterer, E.L., 1974. Plate stratigraphy and the fluctuating carbonate line. In: K.J. Hsü and H.C. Jenkyns (Editors), Plate Stratigraphy and the Fluctuating Carbonate line in Pelagic Sediments: On Land and Under the Sea. Special Publication of the International Association of Sedimentologists, No. 1. Blackwell Science, Oxford, pp. 11-48.

Blaj, T., Backman, J. and Raffi, I., 2009. Late Eocene to Oligocene preservation history and biochronology of calcareous nannofossils from paleo-equatorial Pacific Ocean sediments. Rivista Italiana di Paleontologia e Stratigrafia, 115(1): 67-85.

Bralower, T.J., 2002. Evidence of surface water oligotrophy during the Paleocene-Eocene thermal maximum: Nannofossil assemblage data from Ocean Drilling Program Site 690, Maud Rise, Weddell Sea (vol 17, pg 1023, 2002) - art. no. 1060. Paleoceanography, 17(4): 1060.

Bramlette, M.N., 1961. Pelagic sediments. In: S. M. (Editor), Oceanography. AAAS Publication, New York, pp. 345-366.

Brinkhuis, H. and Biffi, U., 1993. Dinoflagellate cysts strattigraphy of the Eocene-Oligocene transition in central Italy. Marine Micropaleontology, 22: 131-183.

Bukry, D., 1991. Cenozoic calcareous nannofossils from the Pacific ocean. Trans. San Diego Soc. Nat. Hist., 16: 303-327.

Cachao, M. and Moita, M.T., 2000. *Coccolithus pelagicus*, a prductivity proxy related to moderate fronts off Western Iberia. Marine Micropaleontology, 39: 131-155.

Cande, S.C. and Kent, D.V., 1995. Revised calibration of the geomagnetic polarity timescale for the Late Cretaceous and Cenozoic. Journal of Geophysical Research, 100(4): 6093-6095.

Channell, J.E.T. et al., 2003. Eocene to Miocene magnetostratigraphy, biostratigraphy, and chemostratigraphy at ODP Site 1090 (sub-Antarctic South Atlantic). Geological Society of America Bulletin, 115(5): 607-623.

Coxall, H.K. and Pearson, P.N., 2007. The Eocene-Oligocene Transition. In: M. Williams, A.M. Haywood, F.J. Gregory and D.N. Schmidt (Editors), Deep-time Perspectives on Climate Change: Marrying the Signal from Computer Models and Biological Proxies. The Micropalaeontological Society, Special Publications, The Geological Society, London, pp. 351-387.

Coxall, H.K., Wilson, P.A., Pälike, H., Lear, C.H. and Backman, J., 2005. Rapid stepwise onset of Antarctic glaciation and deeper calcite compensation in the Pacific Ocean. Nature, 433(7021): 53-57.

de Kaenel, E. and Villa, G., 1996. Oligocene/Miocene calcareous nannofossil biostratigraphy and paleoecology from the Iberia Abyssal Plain, Northeastern Atlantic., Whitmarsh, R.B., Sawyer, D.S., Klaus, A., Masson, D.G. (Eds.), Proc. ODP Sci. Results, pp. 79-145.

DeConto, R.M. and Pollard, D., 2003a. A coupled climate-ice sheet modeling approach to the early Cenozoic history of the Antarctic ice sheet. Palaeogeography, Palaeoclimatology, Palaeoecology, 198(1-2): 39-52.

DeConto, R.M. and Pollard, D., 2003b. Rapid Cenozoic glaciation of Antarctica induced by declining atmospheric CO_2. Nature, 421(6920): 245-249.

Diekmann, B., Kuhn, G., Gersonde, R. and Mackensen, A., 2004. Middle Eocene to early Miocene environmental changes in the sub-Antarctic Southern Ocean: evidence from biogenic and terrigenous depositional patterns at ODP Site 1090. Global and Planetary Change, 40(3-4): 295-313.

Diester-Haass, 1992. Late Eocene-Oligocene sedimentation in the Antarctic ocean, Atlanctic sector (Maud Rise, ODP Leg 113, Site 689): development of surface and bottom water circulation. In: J.P. Kennett and D.A. Warnke (Editors), The Antarctic paleoenvironment: a perspective on global change, pp. 185-202.

Diester-Haass, L., 1996. Late Eocene-Oligocene paleoceanography in the southern Indian Ocean (ODP Site 744). Marine Geology, 130(1-2): 99-119.

Diester-Haass, L., Robert, C. and Chamley, H., 1993. Paleoceanographic and paleoclimatic evolution in the Weddell Sea (Antarctica) during the middle Eocene-late Oligocene, from a coarse sediment fraction and clay mineral data (ODP Site 689). Marine Geology, 114(3-4): 233-250.

Diester-Haass, L., Robert, C. and Chamley, H., 1996. The Eocene-Oligocene preglacial-glacial transition in the Atlantic sector of the Southern Ocean (ODP Site 690). Marine Geology, 131: 123-149.

Diester-Haass, L. and Zachos, J., 2003. The Eocene-Oligocene transition in the Equatorial Atlantic (ODP Site 925); paleoproductivity increase and positive delta (super 13) C excursion. In: D.R. Prothero, L.C. Ivany and E.A. Nesbitt (Editors). Columbia University Press, New York.

Diester-Haass, L. and Zahn, R., 1996. Eocene-Oligocene transition in the Southern Ocean: History of water mass circulation and biological productivity. Geology, 24(2): 163-166.

Diester-Haass, L. and Zahn, R., 2001. Paleoproductivity increase at the Eocene-Oligocene climatic transition; ODP/DSDP sites 763 and 592. Palaeogeography, Palaeoclimatology, Palaeoecology, 172(1-2): 153-170.

Dunkley Jones, T., Bown, P.R., Pearson, P.N., Wade, B.S. and Coxall, H.K., 2008. Major shifts in calcareous phytoplankton assemblages through the Eocene-Oligocene transition of Tanzania and their implications for low-latitude primary production. Paleoceanography, 23: PA4204.

Fioroni, C., Villa, G., Persico, D., Wise, S.S. and Pea, L., 2010. Revised Eocene-Oligocene calcareous nannofossil biozonation for the Southern Ocean, 13th International Nannoplankton Association Conference, Yamagata.

Firth, J.V. and Wise, S.W., 1992. A preliminary study of the evolution of Chiasmolithus in the middle Eocene to Oligocene of Sites 647 and 748, Proceedings of the Ocean Drilling Program, Scientific Results.

Funakawa, S. and Nishi, H., 2008. Radiolarian faunal changes during the Eocene-Oligocene transition in the Southern Ocean (Maud Rise, ODP Leg 113, Site 689) and its significance in paleoceanographic change. Micropaleontology, 54(1): 15-26.

Funakawa, S., Nishi, H., Moore, T.C. and Nigrini, C.A., 2006. Radiolarian faunal turnover and paleoceanographic change around Eocene/Oligocene boundary in the central equatorial Pacific, ODP Leg 199, Holes 1218A, 1219A and 1220A. Palaeogeography, Palaeoclimatology, Palaeoecology 230: 183-203.

Galeotti, S., Coccioni, R. and Gersonde, R., 2002. Middle Eocene–early Pliocene planktic foraminiferal biostratigraphy of ODP Leg 177, Site 1090, Agulhas Ridge:. Marine Micropaleontology,, 45: 357-381.

Gersonde, R., Hodell, A., Blum, P. and Party, S.S., 1999. Leg 177 Summary, Proc. Ocean Drill. Program, Initial Rep., pp. 1-67.

Gibbs, S.J., Bralower, T.J., Bown, P.R., Zachos, J.C. and Bybell, L.M., 2006. Shelf and open-ocean calcareous phytoplankton assemblages across the Paleocene-Eocene Thermal Maximum: implications for global productivity gradients. Geology, 34(4): 233-236.

Gibbs, S.J., Shackleton, N.J. and Young, J.R., 2004. Identification of dissolution pattern in nannofossil assemblages: A high resolution comparison of synchronous records from Ceara Rise, ODP Leg 154. Paleoceanography, 19: PA1029.

Haq, B.U. and Lohmann, G.P., 1976. Early Cenozoic calcareous nannoplankton biogeography of the Atlantic Ocean. Marine Micropaleontology, 1: 119-194.

Hay, W.W., Floegel, S. and Soding, E., 2005. Is the initiation of glaciation on Antarctica related to a change in the structure of the ocean? Global and Planetary Change, 45(1-3): 23-33.

Holmes, M.A., Watkins, D.K. and Norris, R.D., 2004. Paleocene cyclic sedimentation in the Western North Atlantic, ODP Site 1051, Blake Nose. Marine Geology, 209: 31-43.

Jiang, S. and Wise, S.W., 2009. Distinguishing the influence of diagenesis on the paleoecological reconstruction of nannoplankton across the Paleocene/Eocene Thermal Maximum: An example from the Kerguelen Plateau, southern Indian Ocean. Marine Micropaleontology, 72: 49-59.

Kahn, A. and Aubry, M.P., 2004. Provincialism associated with the Paleocene/Eocene Thermal maximum: temporal constrain. Marine Micropaleontology, 52: 117-131.

Katz, M.E. et al., 2008. Stepwise transition from the Eocene greenhouse to the Oligocene icehouse. Nature Geoscience, 1: 329-333.

Kelly, D.C., Bralower, T.J., Zachos, J.C., Premoli-Silva, I. and Thomas, E., 1996. Rapid diversification of planktonic foraminifera in the tropical Pacific (ODP Site 865) during the late Paleocene thermal maximum. Geology, 24(5): 423-426.

Kennett, J.P., 1977. Cenozoic evolution of Antarctic glaciation, circum-Antarctic ocean, and their impact on global paleoceanography. Journal of Geophysical Research-Oceans and Atmospheres, 82(27): 3843-3860.

Kennett, J.P. and Shackleton, N.J., 1976. Oxygen isotopic evidence for the development of the psychrosphere 38 Myr ago. Nature, 260(5551): 513-515.

Kominz, M.A., Miller, K.G. and Browning, J.V., 1998. Long-term and short-term global Cenozoic sea-level estimates. Geology, 26(4): 311-314.

Latimer, J.C. and Filippelli, G.M., 2002. Eocene to Miocene terrigenous inputs and export production: Geochemical evidence from ODP Leg 177, Site 1090. Palaeogeography Palaeoclimatology Palaeoecology, 182(3-4): 151-164.

Lawver, L.A. and Gahagan, L.M., 2003. Evolution of Cenozoic seaways in the circum-Antarctic region. Palaeogeography, Palaeoclimatology, Palaeoecology, 198(1-2): 11-37.

Lear, C.H., Bailey, T.R., Pearson, P.N., Coxall, H.K. and Rosenthal, Y., 2008. Cooling and ice growth across the Eocene-Oligocene transition. Geology, 36(3): 251-254.

Liu, Z., Tuo, S., Zhao, Q., Cheng, X. and Huang, W., 2004. Deep-water earliest Oligocene glacial maximum (EOGM) in South Atlantic. Chinese Science Bulletin, 49(20): 2190-2197.

Marino, M. and Flores, J.A., 2002. Middle Eocene to Early Oligocene calcareous nannofossil stratigraphy at Leg 177 Site 1090. Marine Micropaleontology, 45: 383-398.

Martini, E., 1971. Standart Tertiary and Quaternary calcareous nannoplankton zonation. In: A. Farinacci (Editor), Second Planktonic Conference. Edizioni Tecnoscienza, Rome, pp. 739-785.

Mc Gonigal, K. and Di Stefano, A., 2002. Calcareous Nannofossil Biostratigraphy of the Eocene- Oligocene transition, ODP Sites 1123 and 1124., Proc. ODP, Sci. Results, pp. 1-22.

Merico, A., Tyrrell, T. and Wilson, P.A., 2008. Eocene/Oligocene ocean de-acidification linked to Antarctic glaciation by sea-level fall. Letters to Nature, 452: 979-982.

Miller, K.G., Wright, J.D. and Fairbanks, R.G., 1991. Unlocking the ice house: Oligocene-Miocene oxygen isotopes, eustasy, and margin erosion. Journal of Geophysical Research, B, Solid Earth and Planets, 96: 6829-6848.

Miller, K.G. et al., 2009. Climate threshold at the Eocene-Oligocene transition: Antarctic ice sheet influence on ocean circulation. In: C. Koeberl, and Montanari, A., eds. (Editor), The Late Eocene Earth-Hothouse, Icehouse, and Impacts: Geological Society of America Special Paper, pp. 169-178.

Monechi, S., Buccianti, A. and Gardin, S., 2000. Biotic signals from nannoflora across the iridium anomaly in the upper Eocene of the Massignano section: evidence from statistical analysis. Marine Micropaleontology, 39: 219-237.

Moore, T.C.J., Rabinowitz, P.D., . and et al. (Editors), 1984. Leg 74. Init. Repts. DSDP, 74. U.S. Govt. Printing Office, Washington.

Nilsen, E., Anderson, J.B. and Delaney, M.I., 2003. Paleoproductivity, nutrient burial, climate change and carbon cycle in the western equatorial Atlantic across the Eocene/Oligocene boundary. Paleoceanography, 18.

Nocchi, M., Monechi, S., Coccioni, R. and al., e., 1998. The extinction of Hantkeninidae as a marker for defining the Eocene-Oligocene boundary: A proposal. In: I. Premoli Silva, R. Coccioni and A. Montanari (Editors), International Union of Geological Science Commission on Stratigraphy, The international Subcommission of Paleogene Stratigraphy: The Eocene-Oligocene Boundary in the Marche-Umbria Basin (Italy), Ancona, Monte Cònero, pp. 249-252.

Okada, H. and Bukry, D., 1980. Supplementary modification and introduction of code numbers to the low-latitude coccolith biostratigraphic zonation (Bukry, 1973; 1975). Marine Micropaleontology, 5(3): 321-325.

Pagani, M., Zachos, J.C., Freeman, K.H., Tipple, B. and Bohaty, S., 2005. Marked decline in atmospheric carbon dioxide concentrations during the Paleogene. Science, 309(5734): 600-603.

Pearson, P.N. et al., 2008. Extinction and environmental change across the Eocene-Oligocene boundary in Tanzania. Geology, 36(2): 179-182.

Peck, V.L., Yu, J., Kender, S. and Riesselman, C.R., in press. Shifting ocean carbonate chemistry during the Eocene-Oligocene climate transition: implications for deep ocean Ma/Ca-paleotermometry. Paleoceanography.

Pekar, S.F., Christie-Blick, N., Kominz, M.A. and Miller, K.G., 2002. Calibration between eustatic estimates from backstripping and oxygen isotopic records for the Oligocene. Geology, 30(10): 903-906.

Persico, D. and Villa, G., 2004. Eocene-Oligocene calcareous nannofossils from Maud Rise and Kerguelen Plateau (Antarctica): Paleoecological and paleoceanographic implications. Marine Micropaleontology, 52: 153-179.

Persico, D. et al., 2004. Nannofossil assemblage fluctuations during the Oligocene at Site 748 (Kerguelen Plateau, Antarctica); palaeoecological implications, Journal of Nannoplankton Research, pp. 85.

Peterson, L.C. and Backman, J., 1990. Late Cenozoic carbonate accumulation and the history of the carbonate compensation depth in the western equatorial Indian Ocean. Proc. ODP, Sci. Results, 115: 467-507.

Premoli Silva, I. and Jenkins, D.J., 1993. Decision on the Eocene-Oligocene boundary stratotype. Episodes, 16: 379-381.

Rea, D.K. and Lyle, M.W., 2005. Paleogene calcite compensation depth in the eastern subtropical Pacific: Answers and questions. Paleoceanography, 20.

Salamy, K.A. and Zachos, J.C., 1999. Latest Eocene-early Oligocene climate change and Southern Ocean fertility; inferences from sediment accumulation and stable isotope data. Palaeogeography, Palaeoclimatology, Palaeoecology, 145(1-3): 61-77.

Tremolada, F. and Bralower, T.J., 2004. Nannofossil assemblage fluctuations during the Paleocene-Eocene Thermal Maximum at Site 213 (Indian Ocean) and 401 (North Atlantic Ocean): paleoceanographic implications. 52: 107-116.

Van Andel, T.H., 1975. Mesozoic/Cenozoic calcite compensation depth and the global distribution of calcareous sediments. Earth and Planetary Science Letters, 26(2): 187-194.

Villa, G., Fioroni, C., Pea, L., Bohaty, S. and Persico, D., 2008. Middle Eocene-late Oligocene climate variability: Calcareous nannofossil response at Kerguelen Plateau, Site 748. Marine Micropaleontology, 69: 173-192.

Villa, G. and Persico, D., 2006. Late Oligocene climatic changes: Evidence from calcareous nannofossils at Kerguelen Plateau Site 748 (Southern Ocean). Palaeogeography, Palaeoclimatology, Palaeoecology, 231: 110-119.

Wade, B.S. and Pearson, P.N., 2008. Planktonic foraminiferal turnover, diversity fluctuations and geochemical signals across the Eocene/Oligocene boundary in Tanzania. Marine Micropaleontology, 68: 244-255.

Wei, W., 1991. Evidence for an earliest Oligocene abrupt cooling in the surface waters of the Southern Ocean. Geology, 19(8): 780-783.

Wei, W. and Thierstein, H.R., 1991. Upper Cretaceous and Cenozoic calcareous nannofossils of the Kerguelen Plateau (southern Indian Ocean) and Prydz Bay (East Antarctica). Proc. ODP, Sci. Results, 119: 467-493.

Wei, W., Villa, G. and Wise, S.W., Jr., 1992. Paleoceanographic implications of Eocene-Oligocene calcareous nannofossils from sites 711 and 748 in the Indian Ocean. Proc. ODP, Sci. Results, 120: 979-999.

Wei, W. and Wise, S.W., Jr., 1990a. Biogeographic gradients of middle Eocene-Oligocene calcareous nannoplankton in the South Atlantic Ocean. Palaeogeography, Palaeoclimatology, Palaeoecology, 79(1-2): 29-61.

Wei, W. and Wise, S.W., Jr., 1990b. Middle Eocene to Pleistocene calcareous nannofossils recovered by Ocean Drilling Program Leg 113 in the Weddell Sea. Proc. ODP, Sci. Results, 113: 639-666.

Wei, W.C., 2004. Opening of the Australia-Antarctica gateway as dated by nannofossils. Marine Micropaleontology, 52(1-4): 133-152.

Zachos, J.C., Breza, J.R. and Wise, S.W., 1992. Early Oligocene ice-sheet expansion on Antarctica: Stable isotope and sedimentological evidence from Kerguelen Plateau, southern Indian Ocean. Geology, 20(6): 569-573.

Zachos, J.C. and Kump, L.R., 2005. Carbon cycle feedbacks and the initiation of Antarctic glaciation in the earliest Oligocene. Global and Planetary Change, 47(1): 51-66.

Zachos, J.C., Pagani, M., Sloan, L., Thomas, E. and Billups, K., 2001. Trends, rhythms, and aberrations in global climate 65 Ma to present. Science, 292(5517): 686-693.

Zachos, J.C., Quinn, T.M. and Salamy, K.A., 1996. High-resolution (10^4 years) deep-sea foraminiferal stable isotope records of the Eocene-Oligocene climate transition. Paleoceanography, 11(3): 251-266.

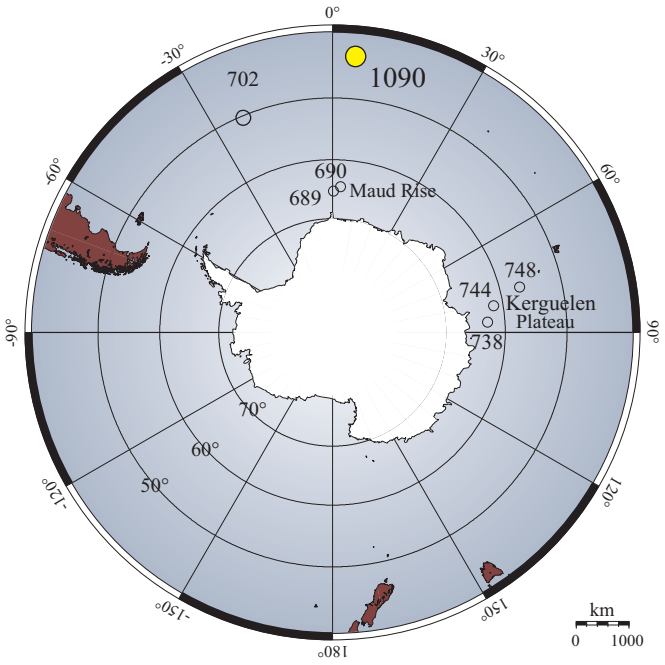

Figure 1: Location map of ODP Site 1090 (42°S, 8°E) , Agulhas Ridge, South Atlanctic Ocean.

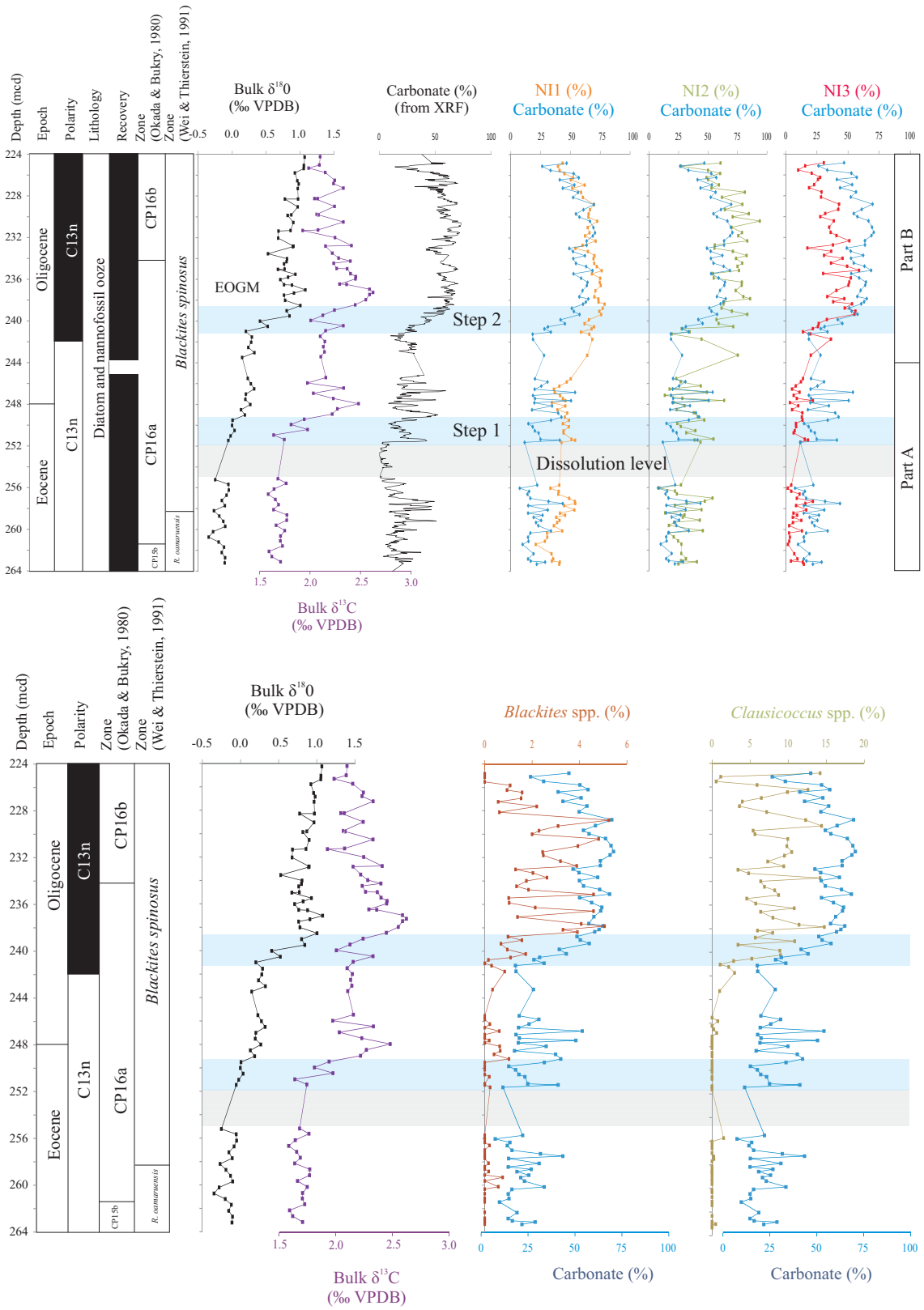

Figure 2: Nannofossil dissolution indices (NI1, NI2, NI3) and relative abundance of *Blackites* and *Clausicoccus* are plotted versus carbonate content estimated by XRF (closest samples, blu lines) and bulk oxygen and carbon stable isotopes (Bohaty and Palike, Unpublished data, 2010). Isotopic Steps 1 and 2 are indicated by blue bars, and the dissolution level by a grey bar. A marked parallelism is shown between all nannofossil indices and carbonate records. See text for description of *Parts A* and *B*. EOGM: Early Oligocene Glacial Maximum.

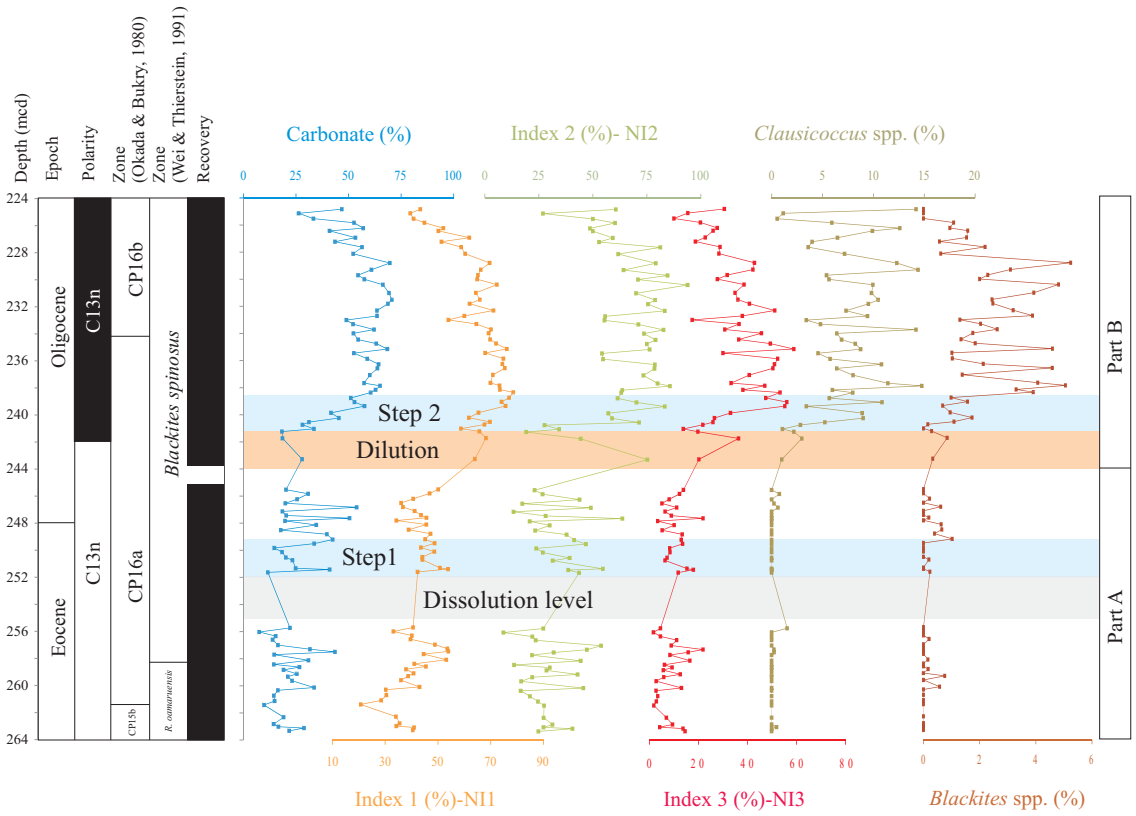

Figure 3: Comparison between distribution of all nannofossil dissolution indices (NI1, NI2, NI3, *Blackites* and *Clausicoccus* relative abundance) used in this work, and carbonate content (closest samples, blue lines) (Bohaty and Palike, Unpublished data, 2010). Isotopic Steps 1 and 2 are indicated by a blue bar, the late Eocene dissolution level by a grey bar, and the dilution interval by an orange bar. See text for description of *Parts A* and *B* and for discussion.

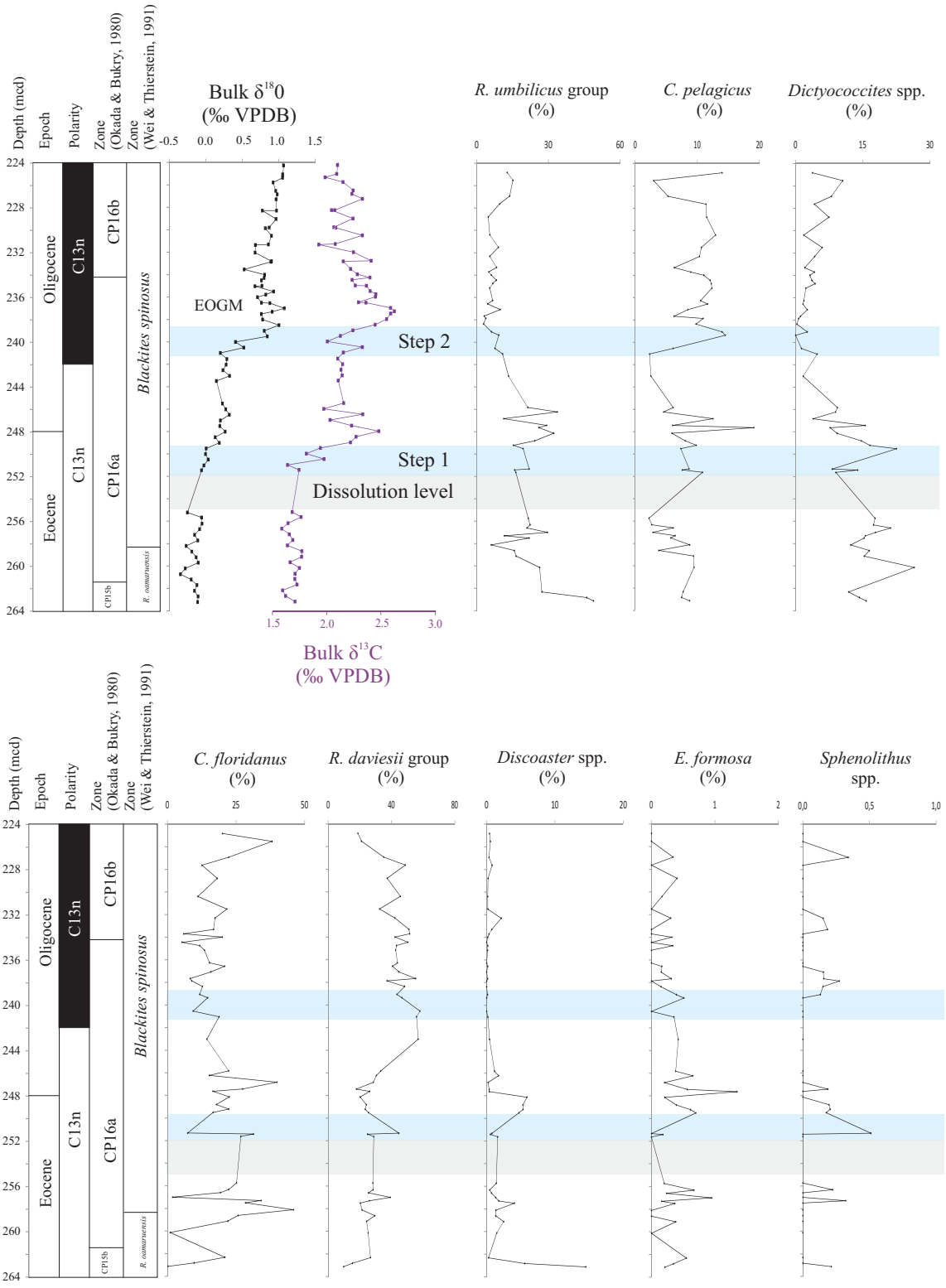

Figure 4: Relative abundance (%) of some nannofossil taxa. Samples used for the paleoecological reconstruction were selected from the original dataset based on the preservation state indicated by nannofossil dissolution indices shown in Figure 3. Bulk oxygen and carbon stable isotopes are shown at the top left (Bohaty and Palike, Unpublished data, 2010). Isotopic Steps 1 and 2 are indicated by a blue bar and the dissolution level by a grey bar. EOGM: Early Oligocene Glacial Maximum.

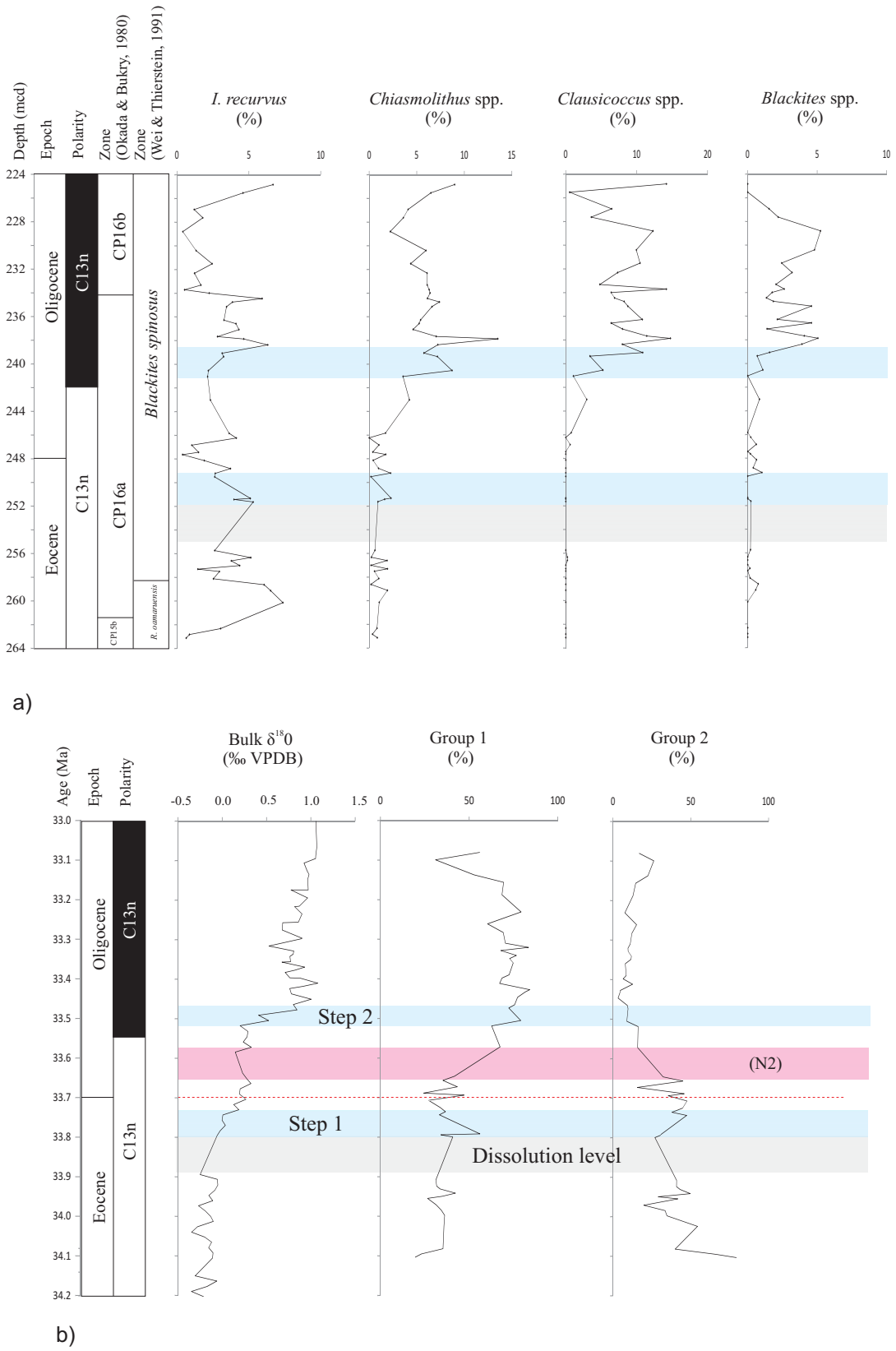

Figure 5: (a) Relative abundance (%) of some nannofossil taxa. *Blackites* and *Clausicoccus* have an acme in the early Oligocene; (b) Oxygen and carbon stable isotopes (Bohaty and Palike, Unpublished data, 2010) are shown together with nannofossil paleoecological groups 1 (taxa increasing at the EOT) and 2 (taxa decreasing at the EOT). Data are plotted against age (Cande and Kent, 1995).
Isotopic Steps 1 and 2 are indicated by blue bars, and major nannofossil change event (N2) by a pink bar. The red line represents the Eocene/Oligocene boundary (33.7 Ma).

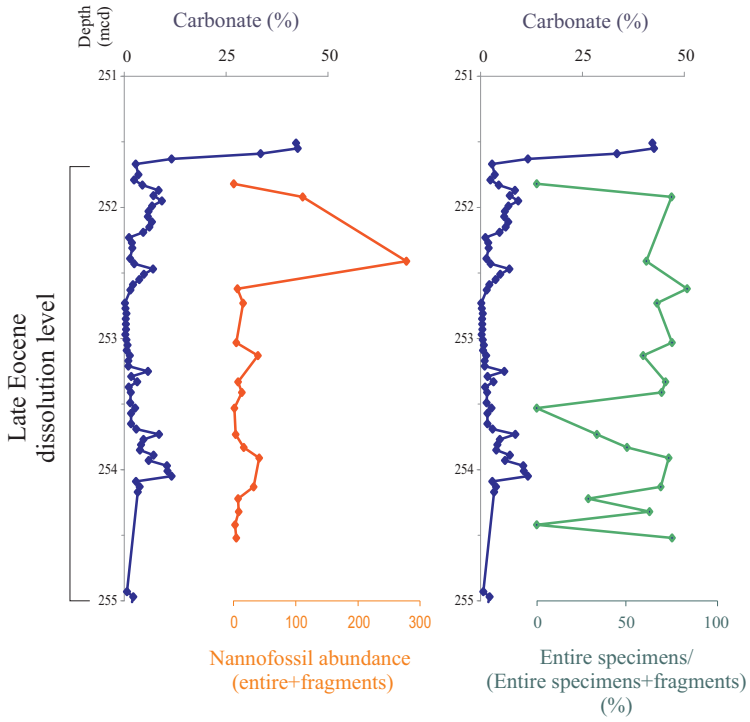

Figure 6: Focus on the late Eocene dissolution level. Within this highly dissolved interval, nannofossil assemblage analysis was carried out on 2 traverses at 40 X magnification, and entire specimens and fragments were counted. Carbonate content (blue lines) (Bohaty and Palike, Unpublished data, 2010) is compared to (on the left) nannofossil total abundance (entire+fragments) and (on the right) to the ratio (entire specimens)/(entire specimen+fragments)*100. A general correspondence between the two records can be seen in the plot on the left, with only one sample at 252.5 mcd showing a mismatching pattern. No correspondence is shown in the plot on the right.

Event	Average depth (mcd)	Sample interval (cm)	Age (Ma)
TA *Blackites*	226.18	24X-1,127/24X-1,147	33.117
TA *Clausicoccus*	234.12	24X-7,23/25X-1,4	33.331
LO *R. circus*	235.30	25X-1,104/25X-1,114	33.363
BA *Blackites*	235.50	25X-1,124/25X-1,134	33.369
BA *Clausicoccus*	245.43	24X-1,14/24X-1,34	33.635
HO *R. oamaruensis*	258.27	27X-3,33-27X-3,43	33.975
HO *D. saipanensis*	261.76	27X-5,82/27X-5,93	34.067

Table 1: Depth, sample interval and ages of nannofossil biostratigraphic events recognized at Site 1090. Ages are assigned using the time scale of Cande and Kent (1995).

Chapter 5

IODP Expedition 317, Canterbury Basin Sea Level (New Zealand), Global and local controls on continental margin stratigraphy (4 November 2009- 3 January 2010)

Laura Pea and IODP Expedition 317 Shipboard Scientists

1. Introduction

Between November 2009 and January 2010 I participated as a Nannnofossil Micropaleontologist in the Integrated Ocean Drilling Program (IODP) Expedition 317 in the Canterbury Basin, offshore New Zealand (Fig. 1). My post-cruise work on sediments recovered will start at the beginning of 2011 and therefore my post-cruise projects are not included in my Ph.D. dissertation. Nevertheless, considerable time was dedicated to the preparation to the cruise and two months were spent out at sea onboard research vessel *Joides Resolution* (Fig. 2). As a consequence, I decided to include in this dissertation a short description of the activities undertaken before the Expedition, and the preliminary results obtained. Also, the participation in this IODP Expedition was an extremely positive, useful and formative experience that I would like to share, and that I would suggest to everyone, especially to young researchers like me.

This Chapter does not cover all preliminary results obtained from the cruise, but it is only a brief description of what Expedition 317 aimed to do and how, as shipboard nannofossil micropaleontologist, I tried to give my contribution to the cruise goals. The participation on the cruise was a fantastic experience in every aspect, personal and

professional, and thus I also mentioned, here and there, events, mood, thought that are integral part of this peerless experience.
General preliminary results obtained by my group (Micropaleontology group) are described hereinafter. A wider description of the preliminary results obtained by all disciplines can be found in the Preliminary Report (Expedition 317 Scientists, 2010) and in the recently published *Proceedings* (Fulthorpe et al., 2011).

The Integrated Ocean Drilling Program (IODP) (2003-present) (http://www.iodp.org/) is an international research program supported by 24 countries that explores the history and structure of the earth by monitoring, drilling, sampling, and analyzing sub-seafloor environments. IODP is supported by two lead agencies, the U.S. National Science Foundation (NSF) and Japan's Ministry of Education, Culture, Sports, Science, and Technology. IODP is the heir of the Deep Sea Drilling Project (DSDP) (1968-1983) and the Ocean Drilling Program (ODP) (1983-2004). The Deep Sea Drilling Project (DSDP) (1968-1983) was the first of three international scientific ocean drilling programs that have operated over more than 40 years. DSDP used R/V *Glomar Challenger* from 1968 to 1983. The R/V *JOIDES Resolution* (Fig. 2) began to operate in 1978 as an oil exploration vessel; in 1985, after being converted for scientific research, the vessel began working for ODP. The same vessel was used by IODP from 2004. The vessel is named after the *HMS Resolution,* commanded by Captain James Cook over 200 years ago, who explored the Pacific Ocean and the subantarctic region. In 2007, the vessel underwent a complete refurbishment in Singapore, where the living quarters and laboratory structures were replaced.

Expedition 317 embraces a series of IODP transects, drilled to investigate global sea-level changes during the Neogene, when eustatic changes are driven by Antarctic ice sheet variations. The strategy consists in drilling multiple margins worldwide in a way to determine inter- and extra- basinal correlations to evaluate global synchroneity. The drilling involved different tectonic and depositional geological settings, both carbonate and siliciclastic. Previous ODP/IODP drillings belonging to this sea-level Expeditions array involved the silicoclastic New Jersey margin (Legs 150, 150X, 174A, and 174AX), and carbonatic margins at Bahamas (Leg 166) and Marion Plateau (Leg 194).

2. Activities in preparation to Expedition 317

For my Master thesis and for my Ph.D. projects I worked mainly on Paleogene sediments. The target of the Expedition 317 was to drill section spanning from the Eocene to Recent, and therefore I needed to impove my knowledge on Neogene taxonomy and biostratigraphy. To do that, I planned a stay in the Unites States of about two months. March 2009 was spent in Houston (Texas) where I did an intense training on Neogene calcareous nannofossil taxonomy, under the guidance of micropaleontologist Jim Bergen and Eric de Kaenel, both biostratigraphers at British Petroleum (BP) Oil Company. Training was organized in side-by-side classes on the microscope with one or both my tutors. We discussed numerous biostratigraphic markers not included in the two most important and used nannofossil zonation schemes (Martini, 1971; Okada and Bukry, 1980). .

The following month, I moved to the Florida State University in Tallahassee (Florida, U.S.A.), where I worked, at he Mannofossil Lab of Prof. Sherwood Wise, for about one month, with Stacie Blair, the other nannofossil specialist onboard *Joides Resolution* on Expedition 317. Together, we analyzed samples coming from Neogene sections, cleared doubts about taxonomic classification of some problematic species and arranged work strategies for the ship-board and post-cruise work.

3. The Science Party

The shipboard Science Party was composed by 33 people (Fig. 2), coming from 12 different countries. One teacher (Julie Pollard) was also onboard and was responsible for educational activities such as blogging, social networking, organizing video conferences to classrooms, museums, etc. Among the Science Party, Craig Fulthorpe (University of Texas, Austin, Texas) and Koichi Hoyanagy (Shinsu University, Japan) were our Co-chiefs, and Peter Blum (Texas A&M University, College Station Texas) was the Staff Scientist. The other Italian Scientist onboard, besides me, was Jaume Dinarès-Turell, from the Istituto Nazionale di Geofisica and Vulcanologia (INGV) in Rome.

The crew was composed by 92 people (Fig. 2) and included technicians, curators, cooks, people operating the ship and the drilling processes.

Work never stopped. Both the Science Party and the ship crew were split in two work shifts, the day shift (midday-midnight) and the night-shift (midnight-midday) in a way to cover the 24 hours. I was assigned to the day-shift. To be able to cover the 24 hour shifts, two specialists for every discipline were enrolled.

4. Canterbury Basin Geological Setting

The rifting of New Zealand from Antarctica began in the Cretaceous, at about 80 Ma. From the Cretaceous to the Eocene, New Zealand was a passive margin; in the early Eocene, at about 55 Ma, the active margin between Australian and Pacific plates, along which New Zealand currently lies, originated. The Alpine fault represents part of plate boundary that cuts the continent. Starting from the Cretaceous, the passive margin was affected by tectonically-controlled, transgressive-regressive cycles. Cretaceous and Paleogene experienced a transgressive phase, followed by high-stand in the Oligocene, most likely caused by enhanced subsidence and limited sediment supply from the continent. During this period limestones were deposited in the Canterbury Basin (Amuri Formation). This transgressive sequence is cut near the Early-Late Oligocene boundary by the Marshall Paraconformity, a regional unconformity that may represent the proto-Antarctic Circumpolar Current initiation following the opening of Tasmanian Gateway (~33.7 Ma). A regressive phase started in the early Miocene, most likely in response to an increase in sediment supply derived by the formation of the Alpine Fault at about 23 Ma. Subsequently, from about 8-5 Ma or 10-8 Ma (Late Miocene) uplift of Southern Alps accelerated, indicating an enhanced convergence along the Alpine Fault. This new transpressive phase led to an increase in the rate of sediment supply to the basin, sediments that were deposited in the Canterbuty Basin disguised as clinoforms and constituing the Otakou Group.

Sedimentation on the margin is also influenced by ocean currents. Still now, new Zealand coast is affected by a current flowing north-ward. The presence of large sediment drifts within the regressive sequence shows that currects were already flowing from the Early Miocene. Eleven sediments drifts are present withing the Canterbury

Basin margin and were deposited from the Early Miocene until the Pliocene (about 3.6 Ma). The termination of the formation of these large sedimentay bodies has been releated to the initiation of Pliocene to Pleistocene high-amplitude sea-level changes.
The geological evolution of New Zealand is very nicely described in the book *A continent on the move* (2009).

5. Objectives of Expedition 317

Expedition 317 aimed to give a contribution to the understanding of the relative importance of global sea level variations (eustasy) versus local tectonic, sedimentary and oceanographic processes in determining continental margin depositional pattern and cyclicity. With this goals, IODP Expedition 317 drilled on the Canterbury Basin, on the eastern margin of the South Island of New Zealand (Fig. 1).
Continental margins are ideal geological locations to try to evaluate the timing and rate of eustatic variations and their effect on depositional processes. The study of sea level changes and their stratigraphic response are nowadays particularly important considering that the current global warming is driving sea level rise. Past sea level changes recorded in marginal depositional sequences can be used to predict future sea level variations. The interpretation of stratigraphic sequences is, however, very difficult as it is necessary to distinguish between local effects, such as subsidence and sediment supply coming from the continent, and global effect given by eustacy. The comparison between stratigraphic sequences coming from several continental margin locations pointed out a similar pattern of sedimentary cyclicity, suggesting and eustatic control on sedimentary deposition and taking to the compilation of eustatic charts (Haq et al., 1987).

The Canterbury Basin is characterized by high rates of Neogene sediment supply (0.1-0.5 m.y.) that allowed to record seismically resolvable high-frequency depositional cyclicity (Lu and Fulthorpe, 2004). The Canterbury Basin belongs to the Eastern New Zealand Oceanic Sedimentary System (ENZOSS), whose distal part was drilled during Ocean Drilling Program Leg 181. Expedition 317 represents a sequel of Leg 181 and drilled the proximal part of that sedimentary system.

More detailedly, Expedition 317 aimed to

1) understand the relative importance among factors determining sedimentation along the margin, i.e. eustatic variations, local tectonic and oceanographic processes. This means to evaluate the timing and modalities of these processes;
2) drill the Marshall Paraconformity (MP), whose formation has been linked to the intensification of oceanic currents following the opening of the Tasmanian gateway. Drilling the MP in the offshore Canterbury Basin gave information about its age and distribution;
3) understand the erosion history of the Southern Alps. The sedimentary prism lying on the continental margin is constituted by material eroded from the mountain chain and preserve information about both 1) periods of more/less intense erosion; 2) provenance;
4) determine sediment drift depositional history. These drifts were deposited parallel to the coast by a current flowing northward. A slope contour current alone is not sufficient to build these bodies, as shown by the fact that drifts are not being formed today.

6. Drilling strategies

During Expedition 317, four Sites were drilled, located along a transect perpendicular to the coast (Fig. 3), in a way to define the age of the sequence boundaries, to see facies and lithologies changes and to obtain paleo-water depth information from benthic facies. Three Sites were drilled on the shelf (U1351, U1353 and U1354) and one on the slope (U1352) (Fig. 3).

Drilling operations on the shelf are challenging for the *Joides Resolution* for two main reasons: firstly, for the type of sediments, mainly sand and gravels, which are problematic to recover with currently available technologies. This type of sediment, in fact, tends to be washed away from the core-barrels; secondly, during drilling operations, the ship has to maintain its position only by using a dynamic positioning system, with any anchorage at the ocean floor. In shallow water, the movement allowed to the ship is minimum and keeping the ship in position is a challenging process, but absolutely necessary to avoid pipes and barrel bending.

7. Role of shipboard micropaleontologists

The micropaleontology group was composed by 7 people, 2 nannofossil specialists (Stacie Blair and myself), 2 planktonic foraminifera specialists (Martin Crundwell and Shungo Kawagata), 2 benthic foraminifera specialists (Takeshi Ohi and Xuang Ding) and 1 diatom specialist (Itsuki Suto). As all Science Party and crew, micropaleontologist were split into 2 groups, each working 12 houls/day, the day shift (midday-midnight) and the night shift (midnight-midday).

The role of the micropaleontology group was to provide robust and paleo-depth inputs to help constrain the timing and magnitude of global sea level perturbations. Ages were assigned based upon core-catcher samples, using calcareous nannofossil, planktic and benthic foraminifer and diatom biostratigraphy. Unfortunately, almost no diatoms were found. The work flow was divided between the sample preparation laboratory and the microscopy laboratory. When a new core was carried onto the catwalk, a core catcher sample was taken from the bottom of the core, brought into the preparation lab, where it was prepared to be studied on the microscope. For nannofossil assemblage analysis, smear slides were prepared. At the microscope, the major goal was to date the sample. providing the most detailed possible description of assemblage composition and relative abundance of single taxa. Also, a general estimate of preservation state was given.

As said, drilling in shallow waters is not easy not only because the ship has to be maintained in position, but because drilling and coring are much faster than in deep waters, and the scientists struggle to catch up on with coming up cores. This is particularly true for the micropaleontologists. We were supposed to date samples as soon as possible, in a way to maintain a good age control of the sequences during drilling and coring. Coring was very fast when we were drilling in the first hundreds of meters, and cores came up every 40-50 minutes. During this time, we had to prepare the core-catcher sample, analyze it on the microscope and, as said, describe the assemblage and date it. The Pleistocene was very well represented at all sites, and samples were quite easy to zone. Things became more complicated from the Pliocene to the middle Miocene, where nannofossil marker species were almost completely absent. The situation improved in the early Miocene down to the Eocene. Fortunately, when deeper sediments were being drilled, new cores were taken to the surface every 2-3 hours, so

we had a little more time to try to date our samples, hunting for markers that sometimes we never found. All of us, 7 people of the biostratigraphy group, spent a long time together, out of our respective shifts (therefore working 14-15 hours/day) when it was time to write, near the end of drilling at each site, the Site Summaries and the Site Chapters. There was just a little time available before starting drilling at a new site, and so we had to sit down and write to be able to finish the reports; we knew that after a couple of days, new Pleistocene cores would have started to come up again, and fast, and there wouldn't be time to do anything else.

Participating in an IODP expedition was a fantastic opportunity. I think it is not comparable with any other experience I have had. I have travelled a lot during my Ph.D. for courses, meetings and workshops and each one of these experiences was interesting, useful and involving. But being onboard the JR was different. I will always remember when the first core was taken onto the catwalk. We heard from the first time on the speaker, the voice announcing: "*Core on deck, core on deck*". The first core, at site U1352 was drilled during the afternoon, and I was on shift. I was really excited. This was my first time on a scientific cruise so I didn't know precisely how the work flow was. I got a plastic beaker and I went on the catwalk (hard hat and safety glasses on) to get the first core catcher. It was exciting to think that I was the first person handling that sample and I was going to be one of the first one to look extremely close to it. No one before us studied those sediments from the Canterbury Basin, and only seismic profiles were available from this area. Doing frontline research, is like being pioneers in a new land. I hope I will be able, in the future, to sail again onboard the JR, maybe in a paleoceanographic expedition.

8. Preliminary Results: biostratigraphy

Sediments recovered during the Expedition were of Holocene to Eocene Age (0-36 Ma) (Fig. 4). Age assignment was based on results provided by all shipboard micropaleontologist. Here, for brevity, only general observations and preliminary results obtained by using nannofossil assemblages are described, and they focus on the age assignement of the drilled sequences.

The preliminary shipboard analysis revealed that sequence stratigraphy processes significantly influenced, in terms of composition, abundance and preservation, nannofossil and foraminifera assemblages, and the variations of one of more of these factors showed a close relation with lithology changes. Factors influencing the characteristics of the assemblages can be several and the most important are climatic changes (local or global), oceanographic processes (such as ocean currents, fronts), sea level changes (local or eustatic) and tectonic processes (influencing amount of terrigenous, preservation state of microfossils, presence of reworked material, etc.).

Ages were assigned by using nannofossils from the Recent to the middle Pliocene, and on planktonic foraminifera from the early Pliocene to late Miocene. Both groups were used to date sediments from the middle Miocene to Eocene.

The base of the Holocene could not be defined biostratigraphically. Mudline samples taken from three of the four drilled sites showed temperate planktonic foraminifera assemblages, consistent with the current high-stand.

Nannofossil biostratigraphy provided a very good age control of the Pleistocene sequences and the recognition of several unconformities and associated hiatuses. Nannofossil assemblage variations showed a clear pattern of variation, with higher abundance during highstands, and lower abundances during lowstands. Calcareous nannofossils were more abundant in greenish gray sandy marls where the characteristics of the assemblages indicate warm waters. Differently, low nannofossil abundances and cool water assemblages were found in gray sandy muds.

At all four sites, the Pliocene/Pleistocene boundary falls within an unconformity and most of all of the upper Pliocene is missing. Standard nannofossil zonations could not be used and no zonal markers were found. This lack is probably caused by the oceanographic setting of the Canterbury Basin and the effect of cold currents. Both standard zonations have been, in fact, compiled at low-mid latitudes and are based on events involving warm and temperate taxa (mainly Discoasters), which might have been completely absent in this area. The age assignment of the Pliocene sediments was made more complicated by the presence of Miocene reworked nannofossils, especially at the most distal shelf site (Site 1351). The amount and timing of pulses of reworked material was different between the three shelf sites, most likely depending on the intensity,

direction and origin of the currents affecting the three different locations. The age control of the lower Pliocene was mainly provided by planktonic foraminifera.

Upper Miocene sediments were recovered at two shelf sites and at the slope site, where coring went down to the Eocene. At these sites, the Miocene/Pliocene boundary does not fall within an unconformity. Sediments from Site 1351 showed a persistent reworking of nannofossils from the Oligocene to the lower Miocene. Standard zonal boundary markers were almost completely absent in the Miocene sections. Nevertheless, approximated calcareous ages could be assigned using the *Reticulofenestra* lineage. Nannofossil assemblages in the Miocene section of slope Site U1352 include pulses of reworked sediment, but the total amount of reworked material is less than at Site 1351.

A significant hiatus was noted between the middle and the upper Miocene at Site U1352, where at least 1.3 m.y was missing. A marked change to warmer planktonic foraminifera and calcareous nannofossil assemblages occurs in the lower Miocene, below the level of the hiatus. This coincides with the return of standard nannofossil zonal markers in the lower Miocene.

Oligocene and Eocene sediments were only recovered at slope Site U1352 and are relatively thin. Microfossil preservation is generally poor in the Oligocene sediments, and moderate in the Eocene. A good age control was possible using calcareous nannofossils and planktonic foraminifera. The MP, one of the target of the Expedition, was reached at Site U1352 and corresponds to a hiatus lasting from the lower Miocene (18-19 Ma) to the lower Oligocene (30.1-32.0 Ma) with a total duration of ~12 Ma (Fig. 4). The Oligocene/Miocene boundary falls within the MP. The MP is interpreted as produced by current erosion related to the inception of the Proto-Antarctic Circumpolar Current (e.g. Fulthorpe et al., 1996).
Another hiatus was found at the same site, lasting from the lower Oligocene (32.5-32.9 Ma) to the upper Eocene (35.2-36.0 Ma). The Eocene/Oligocene boundary falls within this unconformity. Both these hiatuses were dated thanks to calcareous nannofossil biostratigraphy. The age of the bottom of the site U1352 is 35.2-36.0 Ma.

Expedition 317 set several records:

1) Deepest hole drilled by the JR on the continental shelf (1030 meters)

2) Deepest hole drilled on a single expedition in the history of scientific ocean drilling (1927 meters)

3) Deepest sample taken by scientific ocean drilling for microbiological studies (1925 meters)

4) Shallowest water site (85 meters) ever drilled for science by the JR

9. Post-cruise work

In the post-cruise research phase, I planned to carry out a detailed biostratigraphic study of the Middle Miocene section recovered at slope Site U1352. Additionally, using the same sample set, I would like to develop high-resolution nannofossil occurrence and assemblage records for the purpose of paleoecologic interpretation. These results will be used to reveal major changes in sedimentary facies and paleo-water depth (perhaps due to sea-level variation), temperature variations, and/or other paleoceanographic changes. I am interested in interpreting paleoceanographic changes that occurred on the New Zealand margin during this critical period, at a time when the Southern Ocean cooled significantly and major ice-sheet expansion took place in East Antarctica.

Furthermore, I will focus on the Pleistocene part of the recovered sections in order to assess the calcareous nannofossil distribution of the basin and compare it with southernmost locations such as Andrill core (Ross Sea) and Prydz Bay areas. In particular, I planned to focus on the behavior of the assemblages during the Marine Isotope Stage 31, recovered at Site U1352, an interglacial, recently recognized in the Southern Ocean as one of the most distinct obliquity driven warm stages (Scherer et al., 2008; Villa et al., 2008). In November 2011, results obtained from this first works will be presented at the second post-cruise meeting in Oamaru (New Zealand).

References

A.A., 2009. A Continent on the move: New Zealand Geoscience into the 21th Century. Craig Potton Publishing.

Expedition 317 Scientists, 2010. Canterbury Basin Sea Level: Global and local controls on continental margin stratigraphy. IODP Prel. Rept., 317.

Fulthorpe, C.S., Carter, R.M., Miller, K.G. and Wilson, G., 1996. Marshall Paraconformity: a mid-Oligocene record of inception of the Antarctic Circumpolar Current and coeval glacio-eustatic lowstand? Mar. Pet. Geol., 13: 61-77.

Fulthorpe, C.S., Hoyanagi, K., Blum, P. and Scientists, E., 2011. *Proc. IODP, 317*. Integrated Ocean Drilling Program Management International, Inc., Tokyo.

Haq, B.U., Hardenbol, J. and Vail, P.R., 1987. Chronology of fluctuating sea levels since the Triassic. Science, 235(4793): 1156-1167.

Lu, H.B. and Fulthorpe, C.S., 2004. Controls on sequence stratigraphy of a middle Miocene-Holocene, current-swept, passive margin: Offshore Canterbury Basin, New Zealand. Geological Society of America Bulletin, 116(11-12): 1345-1366.

Martini, E., 1971. Standard Tertiary and Quaternary calcareous nannoplankton zonation. In: A. Farinacci (Editor), Second Planktonic Conference. Edizioni Tecnoscienza, Rome, pp. 739-785.

Okada, H. and Bukry, D., 1980. Supplementary modification and introduction of code numbers to the low-latitude coccolith biostratigraphic zonation (Bukry, 1973; 1975). Marine Micropaleontology, 5(3): 321-325.

Scherer, R.P. et al., 2008. Antarctic records of precession-paced insolation-driven warming during early Pleistocene Marine Isotope Stage 31. Geophysical Research Letters, 35(3).

Villa, G., Lupi, C., Cobianchi, M., Florindo, F. and Pekar, S.F., 2008. A Pleistocene warming event at 1 Ma in Prydz Bay, East Antarctica: Evidence from ODP site 1165. Palaeogeography Palaeoclimatology Palaeoecology, 260(1-2): 230-244.

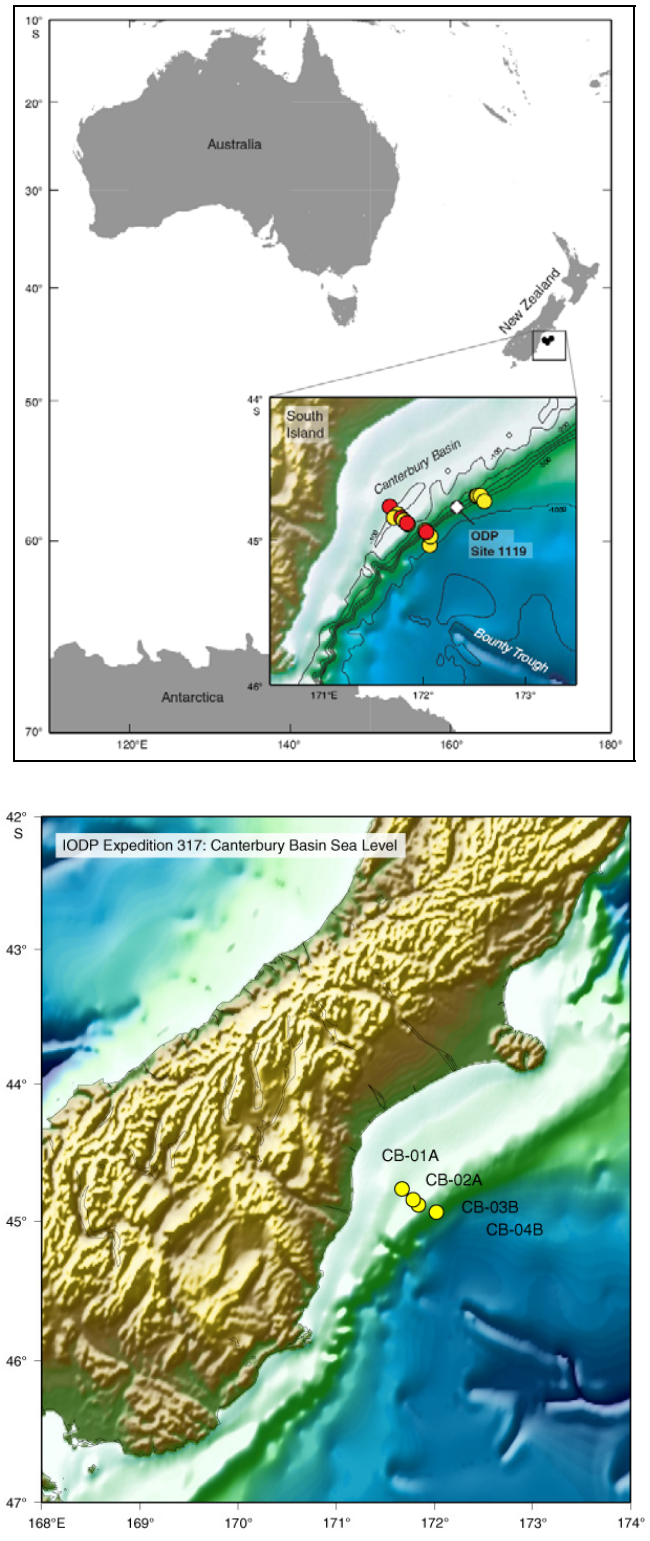

Figure 1: (Top and Bottom) Location map of the Canterbury Basin, on the eastern margin of New Zealand South Island. Yellow dots: proposed sites. Red dots: drilled sites. Site 1119 was drilled during ODP Leg 181.

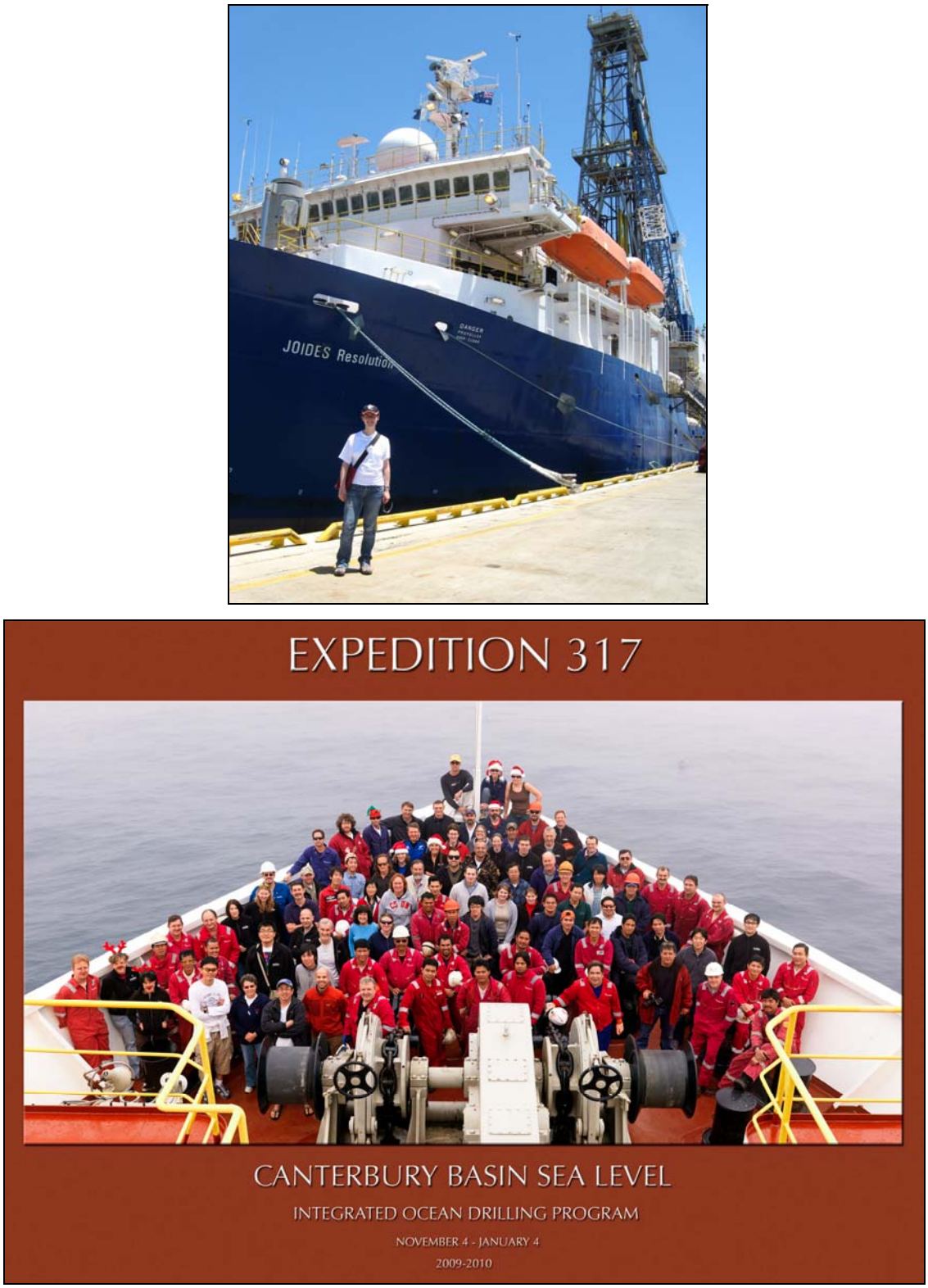

Figure 2: (Top) Research Vessel *Joides Resolution* in Townsville, November 2009, before leaving on Expedition 317; (Bottom) Exp. 317 Science Party and part of the crew.

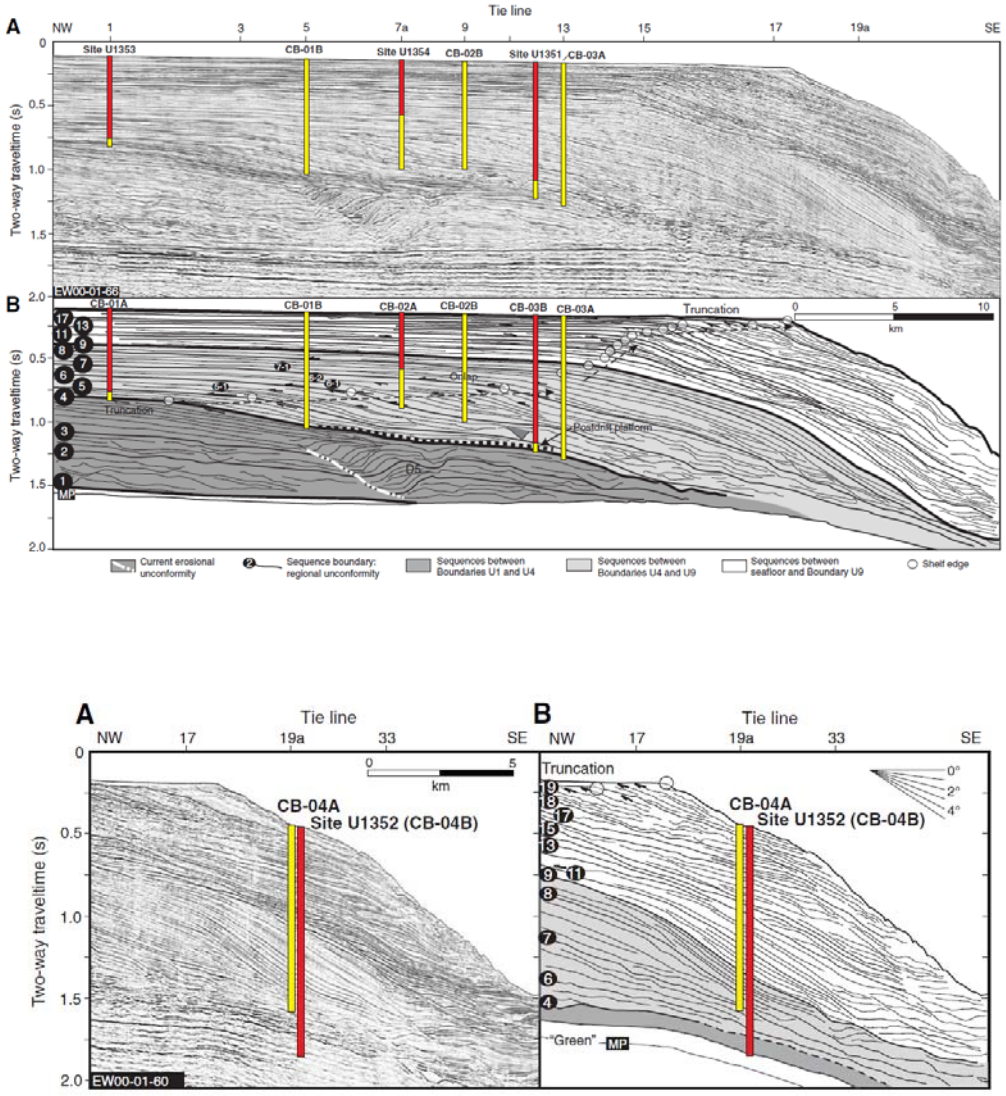

Figure 3: Uninterpreted (A) and interpreted (B) multichannel seismic profiles showing the locations of Sites U1351, U1353, and U1354 (top), and U1352 (bottom). Red = actual penetrations, yellow = proposed penetrations. Proposed al-ternate Sites CB-01B, CB-02B, and CB-03A (yellow) are also shown. For a detailed description of the features shown, see Expedition 317 Scientists (2010).

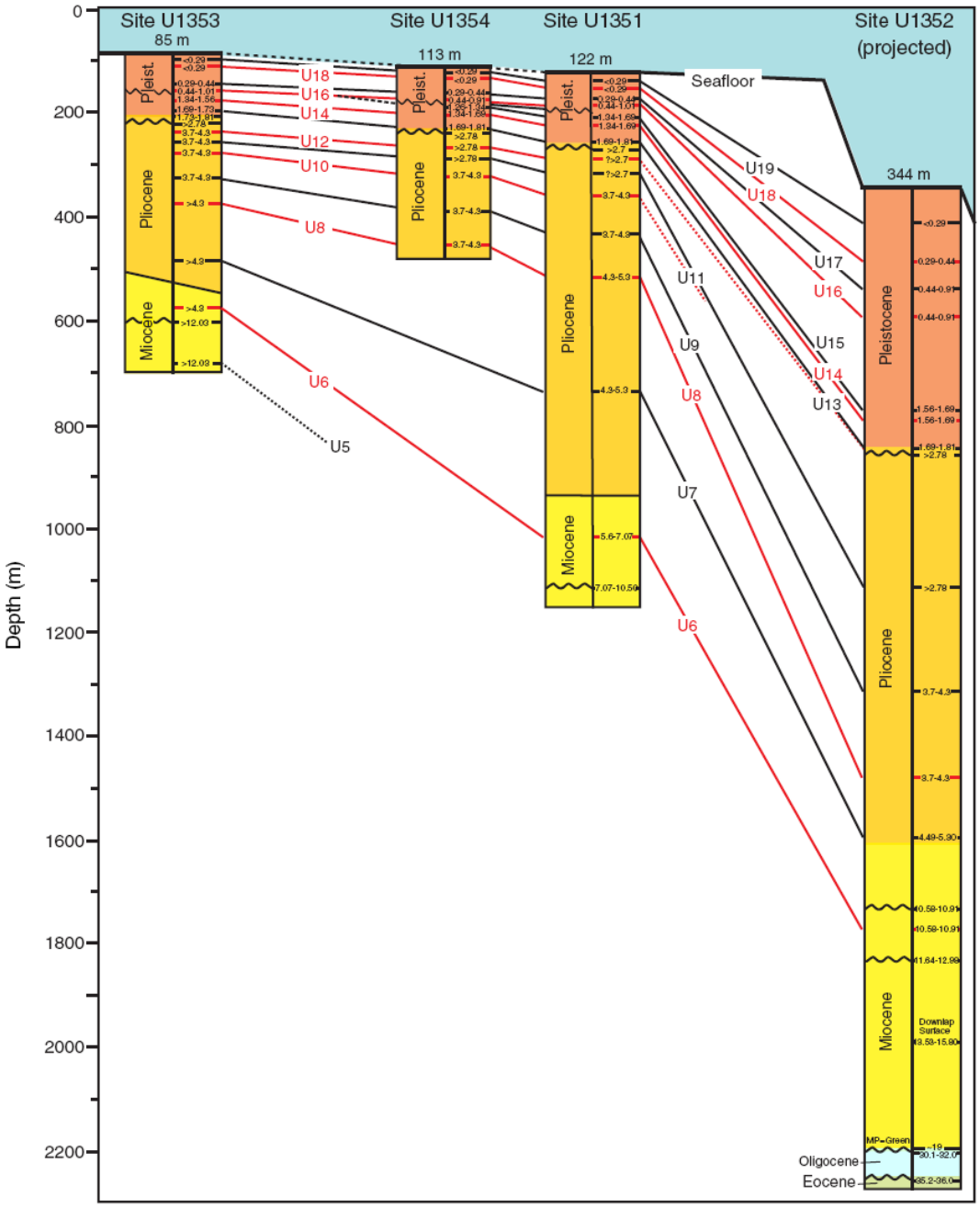

Figure 4: Chronostratigraphic framework and biostratigraphic ages of predicted seismic sequence boundary units across the Expedition 317 drilling transect. Major hiatuses indicated by microfossil biostratigraphy are displayed in the epoch (lefthand) column for each site. Righthand columns provide ages (in Ma) at the predicted depths of seismic sequence boundaries. The Marshall Paraconformity (MP) is found at Site U1352 as the unconformable boundary between the early Miocene and early Oligocene.

Chapter 6

Conclusions

Projects developed during this doctoral program had, as a general theme, the study of paleoclimatic variations during the Eocene and the Oligocene in the southern South Atlantic Ocean as recorded by calcareous nannofossil assemblages.

During the Paleogene, the global climatic transition from the Greenhouse world to the Icehouse occurs, and marks the passage from a warmer to cooler global climate, controlled by the presence of a continental ice-sheet in Antarctica. This long-term transition is interrupted by several climatic events which represent transient warming or cooling phases over-imposed on the general decrease in global temperatures (e.g. Zachos et al., 2001). The major representatives of these warming events are the early and middle Eocene *hyperthermals* (e.g. Zachos et al., 2006). The last Paleogene hyperthermal, the Middle Eocene Climatic Optimum (MECO) (Bohaty and Zachos, 2003; Bohaty et al., 2009), occurs at ~40 Ma and is followed by a gradual cooling. Several cooling and warming events characterize the *Late Eocene Climatic Variability* (e.g. Villa et al., 2008) which leads to a major cooling and glaciation at the Eocene-Oligocene Transition (EOT) (~34 Ma) (e.g. Coxall and Pearson, 2007). During the Oligocene, global climate is generally cooler and more stable compared to the Eocene, and only one major late Oligocene warming phase (26.5 Ma) (e.g. Zachos et al., 2001) is recognized globally.

The Southern Ocean has nowadays, and also had in the past, a major role in determining the global climate, as there deep water formation occurs, which affects global current system, heat distribution and climate. The characteristics of the Southern Ocean are strictly linked to the evolution of the Antarctic ice sheet and the arrangement of the continents. Thus, studying sedimentary records from the Southern Ocean during critical past climatic phases, when continental ice sheet started to form and widen, can provide

valuable clues in the understanding of the global climatic evolution. The two oceanic sites studied during this Ph.D. program are both located in the Atlantic sector of the Southern Ocean.

This dissertation focused on two phases considered critical within the global climatic evolution from the Greenhouse to the Icehouse: the MECO (~40 Ma) (Bohaty and Zachos, 2003; Bohaty et al., 2009), and the EOT (~34 Ma) (Coxall and Pearson, 2007). With the final goal of better characterizing these two climatic phases, sediments from ODP Sites 702 and 1090, both located in Atlantic sector of the Southern Ocean (~50° and 42°S, respectively) were studied. The MECO was studied at Site 702 (Islas Orcadas Rise) (Chapter 2), and the EOT at Site 1090 (Agulhas Ridge) (Chapters 3 and 4). More precisely, Chapter 3 pertained the micropaleontological analysis of sediments spanning the late Eocene to the late Oligocene (35.5-26.5 Ma) at Site 1090. Chapter 4 focused on the EOT (~34 Ma) at the same site, but the analysis was aimed to test and use calcareous nannofossil fragmentation as a dissolution and CCD proxy.
Chapter 5 is about the Preliminary Results of *IODP Expedition 317- Canterbury Basin Sea Level (New Zealand), Global and Local Controls on Continental Margin Stratigraphy*, in which I participated as a shipboard calcareous nannofossil micropaleontologist and biostratigrapher. Despite the IODP cruise was not planned to be part of Ph.D. program, its objectives had several points in common with the themes discussed in this dissertation, i.e. the climatic evolution from the Paleogene at southern high latitudes, the related global sea level oscillations, and paleoceanographic changes occurred at the onset of the thermoaline circulation in the lower Oligocene.
Hereinafter, more detailed conclusions derived from results obtained in Chapters 2, 3 and 4 are given.

Chapter 2

The quantitative calcareous nannofossil analysis carried out at Site 702 (Islas Orcadas Rise, 50°S, South Atlantic) (Chapter 2) involved sediments dated 43.5- 39.3 Ma, and aimed to reconstruct the characteristics of the surface waters during this time interval. In addition, it was verified whether nannofossil assemblages were affected by dissolution.

To try to evaluate if nannofossil assemblages were biased by dissolution, indices of dissolution were calculated by using calcareous nannofossil assemblage components, and were based either on ratios between preserved/dissolved specimens (relative abundance of *Chiasmolithus* sp. versus Total Chiasmoliths, and relative abundance of unidentified small *Reticulofenestra* remains versus *R. daviesii* group) or on the distribution of easily dissolved taxa (*Blackites* spp. and holococcolith *Z. bijugatus*). The comparison between all indices allowed to establish a ranking of reliability, electing *Blackites* and *Z. bijugatus* as the most reliable proxies. The dissolution index based on *Chiasmolithus* sp. relative abundance is unreliable, as *Chiasmolithus* central crosses are extremely easily dissoluble. This analysis allowed to recognize several phases where assemblages were differently affected by dissolution but, certainly, no strong dissolution affected Site 702 anywhere within the studied period. As a consequence, taxa relative abundances were judged suitable for paleoecological and paleoceanographic studies. This approach to the dissolution subject represented the first step, still qualitative, in the process of understanding the effect of carbonate under-saturated waters on nannofossil assemblages. A quantitative approach to the same problem was subsequently utilized across the EOT at Site 1090 (Chapter 4).

Within the studied section, 5 nannofossil biostratigraphic event were recognized, 4 of them (Lowest occurrence of *Cribocentrum reticulatum* and *Dictyococcites bisectus*, Highest Occurrence of *Reticulofenestra clatrata* and the Highest Common Occurrence of *Discoaster* spp.) were found in the time interval included between 40.06 and 40.47 Ma, in correspondence of the isotopic MECO, indicating that a biotic turnover is associated to this climatic event. Another biostratigraphic event, i.e. the Lowest Occurrence of *R. umbilicus* was found at 42.48 Ma, at the beginning of an intense warming phase (labeled *C19r warming event*; ~42.5-41.5 Ma) identified by calcareous nannofossil assemblage changes, but not recorded by bulk oxygen stable isotopes from the same site. The mismatching between the two paleoclimatic proxies (calcareous nannofossil paleoecology and oxygen isotope records) can be explained by mechanisms (See Chapter 2) which, at this stage, can only be hypothesized but not confirmed. Trusting the strong paleoecological preferences of some of the taxa used for the interpretation of the assemblages (i.e., among others, warm and oligotrophic Discoasters

and cool *R. daviesii* group and *Chiasmolithus*), we think that isotopic dataset in the lower part of the studied section might be biased by cementation and diagenenis. The acquired micropaleontological record highlights how the climatic evolution of the middle Eocene at southern high latitudes has still a lot to reveal. The *C19r warming event* is followed by a cool/eutrophic phase that lasts until ~40.5 Ma, when a gradual warming starts, as recorded by both nannofossil assemblages and oxygen isotope record (MECO event). A detailed analysis of nannofossils assemblage variations across the MECO revealed that this event was characterized by an alternation of sea surface waters with different nutrient properties, and a transient switch from oligotrophic to more eutrophic conditions occurred in correspondence of the peak of the isotopic MECO, between 40.2 and 40.1 Ma. The termination of the warming at the MECO is recorded by all paleoecological groups, especially by temperate and warm taxa. The decrease in temperature is accompanied by a return to oligotrophic conditions, as shown by the marked increase in abundance of *Z. bijugatus* and *C. reticulatum*. The post-MECO cooling phase lasts at least until 39.4 Ma, top of the studied section, but it is interrupted between 39.8 and 39.7 Ma by a warm/oligotrophic phase, in agreement with the oxygen isotope record.

The causes of the two major warming events found at Site 702 are still uncertain. The global character of the MECO warming event suggests that atmospheric CO_2 increase can have act as a major cause, which would explain both the warming and the CCD shallowing (Bohaty and Zachos, 2003; Bohaty et al., 2009).

So far, a warming event occurring during Chron C19r was only found at Site 702 (this work) and in the equatorial Atlantic (Edgar et al., 2007), and other middle Eocene records are needed to understand the local or global character of this climatic event and its possible origin.

Chapter 3

A late Eocene-late Oligocene record (35.5-26.5 Ma) of nannofossil assemblage changes was obtained at Site 1090, located on the Agulhas Ridge, in the South Atlantic ocean, at 42°S. A very good age control of the studied section was provided by 11 biostratigraphic nannofossil events and by the good magnetostratigraphic signal

(Channell et al., 2003). The acquired micropaleontological dataset was analyzed together with bulk oxygen and carbon isotope records, and carbonate content provided by Bohaty and Palïke (Unpublished data, 2010). Two major dissolution levels were found, one in the late Eocene (33.8-33.9 Ma), and one near the boundary between the Early and the Late Oligocene (28.1-28.8 Ma).

Nannofossil assemblage characteristic shows that sea surface waters were cool/cold from 35.5 to 34.15 Ma. At 34.15 (N1 event, late Eocene), a warm phase, associated to an increase in nutrient availability, starts and lasts until ~33.8 Ma. The major nannofossil turnover within the studied section is recorded at ~33.6 Ma (N2) (earliest Oligocene), i.e. between oxygen isotope Steps 1 and 2, and represents a passage to more eutrophic conditions, possibly coupled with a decrease in temperature. Starting from N2 (~33.6 Ma), nannofossil assemblages do not show any strong variation until ~33 Ma, when a hiatus of ~3.3 m.y. (29.6-32.9 Ma) cuts the succession. The hiatus corresponds to the third major nannofossil turnover recorded at Site 1090: assemblages before and after it are noticeably different in terms of total abundance and composition, suggesting that the hiatus was associated to a reorganization of the water masses and, certainly, by a significant change in sea-surface characteristics. From 29.6 Ma to 26.5 Ma (late Early Oligocene-Late Oligocene), nannofossil assemblages are dominated by *Cyclicargolithus floridanus*, a species with a supposed, but highly debated, preference for eutrophic waters.

The alternation between warmer and cooler waters at this site gave clues about the characteristics and the origins of the oceanic currents affecting the south Atlantic from the late Eocene to the late Oligocene. Changes in sea surface water characteristics are interpreted as caused by the effect of different ocean currents or oceanic fronts, such as the Agulhas current coming from the equatorial Indian Ocean, the latitudinal oscillation of the Polar Front, or the Antarctic Circumpolar current triggered by the opening of the Drake Passage. Most likely, upwelling also affected nannoplankton assemblages at Site 1090 as located on a flank of a topographic high.

The late Eocene warming phase (N1, ~34.15-33.8 Ma) is interpreted as caused by warm waters flowing from the equatorial Indian Ocean (Proto Agulhas Current). This seems supported by sedimentological evidence indicating increased terrigenous sediment,

whose source is most likely southern Africa (Diekmann et al., 2004). Differently, the early Oligocene nannofossil turnover N2 (~33.6 Ma) is interpreted as caused by the effect of the northward movement of the Polar front. The third nannofossil turnover occurs in conjunction with an early Oligocene unconformity/hiatus, which suggests that a significant current reorganization occurred at that time and markedly affected phytoplankton assemblages. It is plausible that the oceanographic current sweeping Site 1090, also responsible for the hiatus, was the AACC following the opening of the Drake Passage to deep waters.

Chapter 4

In Chapter 4, I discussed the use of calcareous nannofossil fragmentation as a proxy for dissolution/CCD variations across the EOT (~34.2-33.0 Ma) at ODP Site 1090 (42°S, South Atlantic Ocean). Also, a paleoecological analysis of assemblage composition was carried out to characterize the surface waters in the studied period.
One of the events characterizing the EOT is the global deepening of the CCD (≥ 1 km in the Atlantic) (Rea and Lyle, 2005) which has been related to a shelf-basin fractionation process (Merico et al., 2008) or to a shortened oceanic water residence time following strengthened oceanic circulation (Miller et al., 2009). This event was preceded in the late Eocene by a transient CCD shallowing which originated a carbonate dissolution level at numerous locations. Nevertheless, the functioning of the CCD and its link to other climatic factors is still poorly understood.
Today Site 1090 lies at 3700 m depth, above the CCD, but in the Eocene it was below of very close to it, and has a great potential for studying even small CCD oscillations (Gersonde et al., 1999).

This work focused on two major topics: 1) the quantitative assessment of dissolution affecting calcareous nannofossils and its use for CCD reconstruction; 2) the reconstruction of sea surface water characteristic (temperature and fertility) changes.
Data interpretation was based on acquired micropaleontological data compared to the carbonate content record of Bohaty and Palïke (unpublished data, 2010).

Traditional methods to evaluate carbonate dissolution are based on the preservation state of foraminifera (e.g. Berger, 1968) and only few works proposed nannofossil fragmentation as a proxy for dissolution (Blaj et al., 2009). Therefore, to try to accomplish the first task, a quantitative analysis of nannofossil assemblages, including entire specimens and fragments was carried out at the studied site. Counts included at least 500 entire specimens and all fragments bigger than 3 μm. Fragments were classified as *Coccolithus pelagicus fragments*, easily recognizable in phase contrast analysis, and *unidentified fragments.* Furthermore, *Reticulofenestra umbilicus* and *R. samodurovi* specimens were classified as *well preserved* and *partially dissolved*, based on the preservation state of the margins. Using collected data, three major dissolution indices were calculated, based on the preservation state of *C. pelagicus*, *R. umbilicus* group and of the assemblage considered as a whole. The striking matching between these independent indices with the carbonate record clearly indicates that 1) calcareous nannofossils preservation state is a powerful tool for dissolution intensity variations, 2) dissolution is the major factor in controlling carbonate content at Site 1090. Furthermore, we noticed that *Blackites* spp. and *Clausicoccus* spp. distribution shows a strong correspondence to the carbonate record, indicating that the abundance pattern of these two taxa, both having an acme in the lower Oligocene, is substantially controlled by dissolution and not only by paleoecological factors. Considered the vicinity of Site 1090 to the CCD in the Paleogene, the oscillations shown by the indices and by the carbonate content are interpreted as CCD variations. Based on this assumption, the CCD varied significantly in the late Eocene and early Oligocene, highlighting the instability of the CCD well before its major deepening at Step 2. This instability is also represented by the transient late Eocene CCD shallowing event which originated the dissolution level seen at Site 1090 just before Step 1. Nannofossil indices and carbonate content indicate that CCD dropped significantly at Step 2, and, afterwards, it remained significantly deeper than in the late Eocene. A dilution interval was recognized in the early Oligocene before Step 2.

Furthermore, the comparison between the three calculated indices revealed that, in the same conditions of water acidity, *R. umbilicus* group is more resistant than *C. pelagicus*. *R. umbilicus* group is elected as the best dissolution indicator within the assemblages seen at Site 1090, acting as a reliable proxy for dissolution in all conditions of water

acidity. Differently, *C. pelagicus* is reliable in conditions of weak/moderate dissolution but its signal is not as detailed as *R. umbilicus*'s in case of intense dissolution.
Standard nannofossil assemblage counts were not possible within the late Eocene dissolution interval because of the very low abundance of nannofossils. Therefore, within this interval, nannofossil assemblage component counts (splitting entire specimens and fragments) were carried out at 40X magnification on two traverses. Results from this analysis showed that the total nannofossil abundance (entire specimens+ fragments) roughly mirrors the carbonate content, confirming that nannofossils are very good dissolution proxies even in conditions of extremely strong dissolution.
The new approach described in this work in using calcareous nannofossils as dissolution proxies sheds a new light on the potential of this group of algae as dissolution and CCD indicators, similarly to the classical use of foraminifera fragmentation state.

Moreover, a selection of "well-preserved" samples was used for the paleoecological reconstruction of the assemblage changes across the EOT. The paleoecolgical and paleoceanographic interpretation of Site 1090 across the EOT was also given is Chapter 3, where relative abundances were based on all counted samples, with no distinction between badly and well preserved samples. Differently, in Chapter 4, thanks to the assessment of dissolution intensity obtained by calculated indices, only samples with better preserved assemblages were used, guaranteeing that obtained data reflected pristine relative abundances. Taxa relative abundance and the derived paleoecological interpretations are similar using the two different approaches, and both indicate, as described above, that the major nannofossil turnover across the EOT occurs within the isotopic plateau between Step 1 and 2, and is interpreted as a marked nutrient availability increase. This indicates that, despite dissolution strongly affected nannofossil assemblages at Site 1090, especially in the Eocene, the paleoecological signal interpreted from the whole assemblages (Chapter 3) is anyway reliable. However, despite the general paleoecological frame provided by the two different approaches (taking into account or not the dissolution effect), for future works I would rely on quantitative analysis which also consider coccolith fragmentation state, especially when analysis is finalized to paleoecological reconstruction.

The general paleoclimatic frame obtained in the late middle Eocene and in the Eocene and Oligocene from both studied sites (702 and 1090), as reconstructed by calcareous nannofossil assemblages and oxygen and carbon isotope records, identify a marked variability in the characteristics of the ocean surface waters. Generally, variability recorded by nannofossil is higher than isotope records, which can be ascribed to the sensitivity of phytoplankton to manifold factors, besides temperature, in determining assemblage composition.

Projects developed during this doctoral program confirmed the high potential and usefulness of calcareous nannofossil as biostratigraphic and paleoceanographic proxies. Their biostratigraphic value has been widely recognized for decades (see Haq, 1984 for a compilation of nannofossil biostratigraphy works); their utility as paleoceanographic proxies, mainly as temperature indicators, keeps being confirmed year by year, also at southern high latitudes (Bralower, 2002; e.g. Villa et al., 2008; Villa and Persico, 2006; Wei et al., 1992; Wei and Wise, 1990; Wise, 1988; Wise et al., 1985). The detailed quantitative analysis of fragmentation state of calcareous nannofossils used to estimate carbonate dissolution (this work and Blaj et al., 2009) demonstrates the great potential of nannoplankton in paleoceanographic reconstructions, well beyond temperature and fertility assessments. Calcareous nannofossil fragmentation was used in this work to estimate CCD variations but, in combination with absolute abundance calculation of single taxa and total abundance, it would help to distinguish the relative effect of dissolution, paleoecological response to changes in water characteristics, and productivity variations.

References

Berger, W.H., 1968. Planktonic foraminifera: Selective solution and paleoclimatic interpretation. Deep-sea research, 15: 31-43.

Blaj, T., Backman, J. and Raffi, I., 2009. Late Eocene to Oligocene preservation history and biochronology of calcareous nannofossils from paleo-equatorial Pacific Ocean sediments. Rivista Italiana di Paleontologia e Stratigrafia, 115(1): 67-85.

Bohaty, S.M. and Zachos, J.C., 2003. Significant Southern Ocean warming event in the late middle Eocene. Geology, 31(11): 1017-1020.

Bohaty, S.M., Zachos, J.C., Florindo, F. and Delaney, M.L., 2009. Coupled greenhouse warming and deep sea acidification in the middle Eocene. Paleoceanography, 24(PA2207).

Bralower, T.J., 2002. Evidence of surface water oligotrophy during the Paleocene-Eocene thermal maximum: Nannofossil assemblage data from Ocean Drilling Program Site 690, Maud Rise, Weddell Sea (vol 17, pg 1023, 2002) - art. no. 1060. Paleoceanography, 17(4): 1060.

Channell, J.E.T. et al., 2003. Eocene to Miocene magnetostratigraphy, biostratigraphy, and chemostratigraphy at ODP Site 1090 (sub-Antarctic South Atlantic). Geological Society of America Bulletin, 115(5): 607-623.

Coxall, H.K. and Pearson, P.N., 2007. The Eocene-Oligocene Transition. In: M. Williams, A.M. Haywood, F.J. Gregory and D.N. Schmidt (Editors), Deep-time Perspectives on Climate Change: Marrying the Signal from Computer Models and Biological Proxies. Special Publication. The Micropaleontological Society, London, pp. 351-387.

Diekmann, B., Kuhn, G., Gersonde, R. and Mackensen, A., 2004. Middle Eocene to early Miocene environmental changes in the sub-Antarctic Southern Ocean: evidence from biogenic and terrigenous depositional patterns at ODP Site 1090. Global and Planetary Change, 40(3-4): 295-313.

Edgar, K.M., Wilson, P.A., Sexton, P.F. and Suganuma, Y., 2007. No extreme bipolar glaciation during the main Eocene calcite compensation shift. Nature, 448: 908-911.

Gersonde, R., Hodell, A., Blum, P. and Party, S.S., 1999. Leg 177 Summary, Proc. Ocean Drill. Program, Initial Rep., pp. 1-67.

Haq, B.U., 1984. Nannofossil Biostratigraphy. Benchmark Papers in Geology. Hutchinson Ross Publishing Company, Stroudsburg, Pennsylvania.

Merico, A., Tyrrell, T. and Wilson, P.A., 2008. Eocene/Oligocene ocean de-acidification linked to Antarctic glaciation by sea-level fall. Letters to Nature, 452: 979-982.

Miller, K.G. et al., 2009. Climate threshold at the Eocene-Oligocene transition: Antarctic ice sheet influence on ocean circulation. In: C. Koeberl, and Montanari, A., eds. (Editor), The Late Eocene Earth-Hothouse, Icehouse, and Impacts: Geological Society of America Special Paper, pp. 169-178.

Rea, D.K. and Lyle, M.W., 2005. Paleogene calcite compensation depth in the eastern subtropical Pacific: Answers and questions. Paleoceanography, 20.

Villa, G., Fioroni, C., Pea, L., Bohaty, S. and Persico, D., 2008. Middle Eocene-late Oligocene climate variability: Calcareous nannofossil response at Kerguelen Plateau, Site 748. Marine Micropaleontology, 69: 173-192.

Villa, G. and Persico, D., 2006. Late Oligocene climatic changes: Evidence from calcareous nannofossils at Kerguelen Plateau Site 748 (Southern Ocean). Palaeogeography, Palaeoclimatology, Palaeoecology, 231: 110-119.

Wei, W., Villa, G. and Wise, S.W., Jr., 1992. Paleoceanographic implications of Eocene-Oligocene calcareous nannofossils from sites 711 and 748 in the Indian Ocean. Proc. ODP, Sci. Results, 120: 979-999.

Wei, W. and Wise, S.W., Jr., 1990. Biogeographic gradients of middle Eocene-Oligocene calcareous nannoplankton in the South Atlantic Ocean. Palaeogeography, Palaeoclimatology, Palaeoecology, 79(1-2): 29-61.

Wise, 1988. Mesozoic-Cenozoic history of calcareous nannofossils in the region of the Southern Ocean. Paleogeography, Paleoecology, Paleoclimatology, 67: 157-179.

Wise, S.W., Gombos, A.M. and Muza, J.P., 1985. Cenozoic evolution of polar water masses, southwest Atlantic Ocean. In: K.J. Hsü and H.J. Weissert (Editors), South Atlantic Paleoceanography. Cambridge University Press, pp. 283-324.

Zachos, J.C., Pagani, M., Sloan, L., Thomas, E. and Billups, K., 2001. Trends, rhythms, and aberrations in global climate 65 Ma to present. Science, 292(5517): 686-693.

Zachos, J.C. et al., 2006. Extreme warming of mid-latitude coastal ocean during the Paleocene-Eocene Thermal Maximum; inferences from TEX86 and isotope data. Geology, 34(9): 737-740.

Acknowledgments

I would like to sincerely thank my supervisor, Prof. Giuliana Villa, for her support, encouragement, and confidence in me. I am grateful for all of the wonderful opportunities she has given me during my Ph.D. studies.

I am also indebted to Dr. Chiara Fioroni for her guidance and making time for our many discussions over the past three years. Her support provided much needed encouragement during difficult periods.

I am tremendously grateful to Prof. Sherwood Wise for hosting me as a visiting student at Florida State University in 2008 and 2009. My visit to Florida was a great work and life experience, and Woody's kindness and hospitality made me feel at home.

I would also like to extend my sincere thanks to Dr. Eric de Kaenel and Dr. Jim Bergen for the in-depth training I received in Neogene nannofossil taxonomy and biostratigraphy during my stay in Texas in 2009. Their time and patience is much appreciated.

I owe much gratitude to Dr. Peter Blum, staff scientist for IODP Expedition 317. Participating in Exp. 317 was a great opportunity and an amazing experience for me, and Peter's help was fundamental in enabling me to carry out my research on the cruise.

I am also grateful to Tom Dunkley Jones, Paul Bown, Shijun Jiang, Jorijntje Henderiks, Tim Bralower, Antonio Longinelli, Jean Self-Trail, Mike Styzen, Bridget Wade, Jens Herrle and several instructors of the Urbino Summer School in Paleoclimatology (USSP; 2008) for many useful discussions throughout my Ph.D. studies. I would also like to thank all of the people who participated in the International Nannoplankton Association meetings in Lyon (2008) and Yamagata (2010); both conferences were fantastic opportunities for meeting other scientists in the field and discussing my research.

Ringrazio di cuore i miei genitori che mi hanno aiutato, incoraggiato e sopportato durante questo dottorato. Un ringraziamento particolare va a mia nonna Teresa, mia grande sostenitrice, per avermi sempre ricordato che esistono il senso del dovere e le responsabilità, ma anche le gioie della giovinezza.

Many thanks to my former housemates Anna Bianchi, Elisa Fontanesi, Laura Ragazzi, Alessia Gadaleta, Matteo Gerelli, Davide Derni and Marcello Olivari and to my current housemate and close friend Carla Cogliati for tolerating my crazy lifestyle.

I would like to thank my Ph.D. buddy and long-time friend Claudia Grillenzoni for sharing good and bad moments in the last three years. Also, a heartfelt thanks to my old friends Davide Bonfanti, Lorenzo Buratti, Viola Piccinelli and Mariateresa Guainazzi; their presence in my life has been extremely precious!

Also, I would like to thank Giovanna Gianelli, Rocco Gennari, Brunello Manfredini and Gaetano Taranto for cheering me up, especially during the final hectic months of my Ph.D.

And finally, a special thanks to Steve Bohaty for sharing his geochemical records, for his support, his encouragement and extreme patience, and for his effort in trying to teach me English idioms and how to write proper paragraphs, but, above all, for his love.